frontiers | Research Topics

Neurobiological underpinnings of neurodegenerative and neuropsychiatric disorders: from models to therapy

Edited by
Ferdinando Di Cunto, Maria Vincenza Catania and Nicola Simola

Coordinated by
Jessica Mingardi, Marcello Serra and Federica Campanelli

Published in
Frontiers in Neuroscience
Frontiers in Molecular Neuroscience

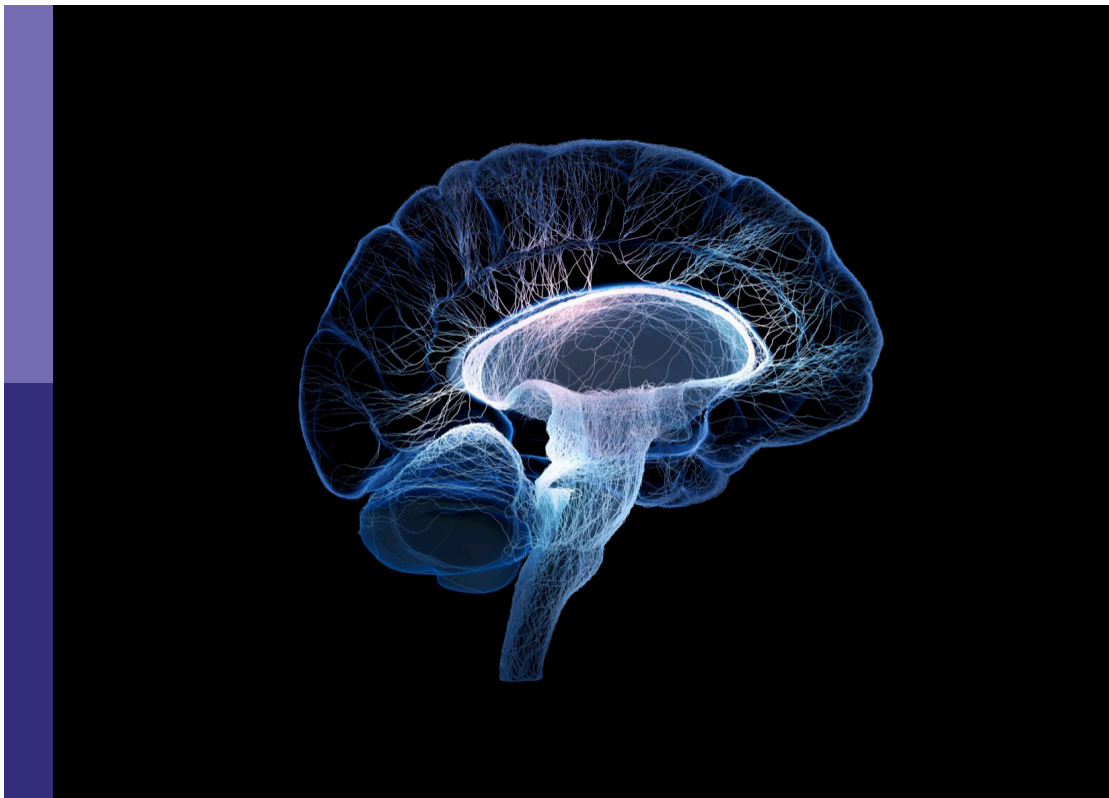

ISSN 1664-8714
ISBN 978-2-8325-6480-6
DOI 10.3389/978-2-8325-6480-6

Generative AI statement
Any alternative text (Alt text) provided alongside figures in the articles in this ebook has been generated by Frontiers with the support of artificial intelligence and reasonable efforts have been made to ensure accuracy, including review by the authors wherever possible. If you identify any issues, please contact us.

About Frontiers

Frontiers is more than just an open access publisher of scholarly articles: it is a pioneering approach to the world of academia, radically improving the way scholarly research is managed. The grand vision of Frontiers is a world where all people have an equal opportunity to seek, share and generate knowledge. Frontiers provides immediate and permanent online open access to all its publications, but this alone is not enough to realize our grand goals.

Frontiers journal series

The Frontiers journal series is a multi-tier and interdisciplinary set of open-access, online journals, promising a paradigm shift from the current review, selection and dissemination processes in academic publishing. All Frontiers journals are driven by researchers for researchers; therefore, they constitute a service to the scholarly community. At the same time, the *Frontiers journal series* operates on a revolutionary invention, the tiered publishing system, initially addressing specific communities of scholars, and gradually climbing up to broader public understanding, thus serving the interests of the lay society, too.

Dedication to quality

Each Frontiers article is a landmark of the highest quality, thanks to genuinely collaborative interactions between authors and review editors, who include some of the world's best academicians. Research must be certified by peers before entering a stream of knowledge that may eventually reach the public - and shape society; therefore, Frontiers only applies the most rigorous and unbiased reviews. Frontiers revolutionizes research publishing by freely delivering the most outstanding research, evaluated with no bias from both the academic and social point of view. By applying the most advanced information technologies, Frontiers is catapulting scholarly publishing into a new generation.

What are Frontiers Research Topics?

Frontiers Research Topics are very popular trademarks of the *Frontiers journals series*: they are collections of at least ten articles, all centered on a particular subject. With their unique mix of varied contributions from Original Research to Review Articles, Frontiers Research Topics unify the most influential researchers, the latest key findings and historical advances in a hot research area.

Find out more on how to host your own Frontiers Research Topic or contribute to one as an author by contacting the Frontiers editorial office: frontiersin.org/about/contact

Neurobiological underpinnings of neurodegenerative and neuropsychiatric disorders: from models to therapy

Topic editors
Ferdinando Di Cunto — University of Turin, Italy
Maria Vincenza Catania — Institute for Biomedical Research and Innovation, National Research Council (CNR), Italy
Nicola Simola — University of Cagliari, Italy

Topic coordinators
Jessica Mingardi — University of Milano-Bicocca, Italy
Marcello Serra — University of Cagliari, Italy
Federica Campanelli — Catholic University of the Sacred Heart, Rome, Italy

Citation
Di Cunto, F., Catania, M. V., Simola, N., Mingardi, J., Serra, M., Campanelli, F., eds. (2025). *Neurobiological underpinnings of neurodegenerative and neuropsychiatric disorders: from models to therapy*. Lausanne: Frontiers Media SA. doi: 10.3389/978-2-8325-6480-6

Table of contents

frontiers | Frontiers in Neuroscience

TYPE Editorial
PUBLISHED 09 June 2025
DOI 10.3389/fnins.2025.1627262

OPEN ACCESS

EDITED AND REVIEWED BY
Einar M. Sigurdsson,
New York University, United States

*CORRESPONDENCE
Ferdinando Di Cunto
✉ ferdinando.dicunto@unito.it
Maria Vincenza Catania
✉ mariavincenza.catania@cnr.it
Nicola Simola
✉ nicola.simola@unica.it

RECEIVED 12 May 2025
ACCEPTED 22 May 2025
PUBLISHED 09 June 2025

CITATION
Di Cunto F, Catania MV, Simola N, Mingardi J, Serra M and Campanelli F (2025) Editorial: Neurobiological underpinnings of neurodegenerative and neuropsychiatric disorders: from models to therapy. *Front. Neurosci.* 19:1627262. doi: 10.3389/fnins.2025.1627262

Editorial: Neurobiological underpinnings of neurodegenerative and neuropsychiatric disorders: from models to therapy

Ferdinando Di Cunto[1]*, Maria Vincenza Catania[2]*, Nicola Simola[3]*, Jessica Mingardi[4], Marcello Serra[3] and Federica Campanelli[5]

[1]Department of Neuroscience 'Rita Levi Montalcini', University of Turin, Turin, Italy, [2]Institute for Biomedical Research and Innovation, National Research Council (IRIB-CNR), Catania, Italy, [3]Department of Biomedical Sciences, University of Cagliari, Cagliari, Italy, [4]School of Medicine and Surgery, University of Milano-Bicocca, Monza, Italy, [5]Department of Neuroscience, Università Cattolica del Sacro Cuore, Rome, Italy

KEYWORDS

brain disease mechanisms, neurodegeneration, animal models, neurodevelopmental disorders, acute brain injury

Editorial on the Research Topic
Neurobiological underpinnings of neurodegenerative and neuropsychiatric disorders: from models to therapy

During the last two decades, seminal advances in different areas of Neurosciences have clearly highlighted the complex nature of neuropsychiatric and neurodegenerative disorders. The proper assembly, maturation, and maintenance of neuronal circuits underlying physiological functioning of the nervous system require the execution of specific genetic programs, finely tuned in space and time.

The widespread detection of genes, mRNAs, proteins, and metabolites has shed much light on relevant missteps in these delicate processes that may cause detrimental consequences for brain wiring and function. A clear role of cell-autonomous alterations, involving cell adhesion molecules, ion channels, and intracellular pathways impinging on synaptic function is well established in neuropsychiatric diseases. Similarly, modifications in protein sequence and structure resulting in the accumulation of insoluble aggregates are widely acknowledged as culprits of most neurodegenerative disorders. On the other hand, the careful study of pathophysiological mechanisms that may translate genetic predisposition into fully manifested disease phenotypes has revealed the involvement of non-genetic and non-neuronal factors in establishment and propagation of the damage from cell to network level. Indeed, current research is emphasizing the crucial role of epigenetic modifications, metabolic rewiring, brain-immune system cross-talk, glial cell functions, gut-to-brain axis, and blood-brain barrier, both in neuropsychiatric and neurodegenerative disorders. Importantly, these additional layers of complexity represent a rich interface between genetic variants and environmental stressors, whose nature and relevance are also being elucidated.

A critical factor in advancing the translation of this knowledge into enhanced diagnostic and therapeutic strategies lies in the accurate modeling of human disease pathogenesis. This necessitates comprehensively considering the complexity of cellular

and molecular interactions, as well as species-specific characteristics that drive the disease processes. Traditional cellular and animal models have so far been of utmost importance for understanding the molecular mechanisms underlying brain disorders. However, their actual translational value has also been questioned, due to the failure of several clinical trials resulting from pharmacological findings in animal models. Different cutting-edge strategies, including bioprinting, microfluidics 3D cell co-culture, human organoids, single-cell multi-omics, *in vivo* functional imaging, and multidimensional data integration have great potential to help filling the gap between *in vitro* and *in vivo* molecular-cellular-network responses, as well as to reduce the attrition rate between preclinical research and clinical applications. The complexity of these research tools also poses major challenges in terms of reliability and reproducibility.

This Research Topic, proposed on the occasion of the XX meeting of the Italian Society for Neuroscience (SINS) was aimed at advancing the understanding of state-of-the-art techniques and methodologies for modeling neuropsychiatric and neurodegenerative disorders. Specific focus was on critical aspects of the complex genetic, molecular, and cellular mechanisms underlying these conditions, and on novel avenues in brain disease modeling.

The selection and peer review process resulted in the publication of 10 papers, including four original research contributions and six review or mini-review articles, covering a wide range of congenital and acquired neurological conditions and employing diverse modeling strategies.

In vivo modeling of neurological disorders

The majority of the studies included in the Research Topic are focused on the usage of mouse or zebrafish as disease models.

The research report by Chen Z. et al. explored the lifespan progression of dysfunction, oxidative stress, and neuroinflammation in a mouse model of moderate Traumatic Brain Injury (TBI). The findings reveal persistent cognitive and emotional deficits in middle-aged mice. These behavioral changes were linked to increased neuronal cell death, elevated oxidative stress, and chronic neuroinflammation in the hippocampus, suggesting that persistent oxidative stress and neuroinflammation play a significant role in the long-term neurological decline following TBI, providing potential therapeutic targets for TBI-induced late-phase neurological dysfunction.

The brief report by Tanaka et al. presents a new mouse model carrying the Bassoon (Bsn) p.P3882A mutation, analogous to the human BSN p.P3866A mutation found in a family with progressive supranuclear palsy-like syndrome (PSP-like syndrome). Although no significant structural brain abnormalities were observed, this model exhibits impaired working memory and decreased locomotor activity, providing a valuable tool for investigating the relationship between Bsn mutations, tauopathy, and the development of PSP-like syndrome.

The transgenic mouse model provided in the Research Report by Chen L. et al. is characterized by mTORC1 pathway hyperactivation in striatal inhibitory neurons. This model shows disrupted dopamine receptor expression and behavioral abnormalities such as impaired motor learning and altered olfactory preference. These findings offer a molecular basis for understanding the deficits seen in neurodegenerative disorders such as Parkinson's (PD) and Huntington's diseases, as well as neuropsychiatric disorders such as autism-spectrum disorder (ASD).

The mini review contributed by Bossini and Sessa highlights the importance of using diverse and complementary approaches when developing mouse models for neurological diseases. The authors argue that relying on single-approach models may contribute to the high failure rates of clinical trials by providing incomplete or misleading data. Focusing on neurodevelopmental disorders, they advocate for incorporating strategies such as cell-specific gene manipulation, temporal control of gene expression, and molecular reversibility to create more robust and translatable models.

In their research report, Naderi et al. utilized CRISPR-Cas9 technology in zebrafish larvae to investigate the socio-cognitive consequences of KCC2 disruption, a protein involved in excitatory/inhibitory (E/I) balance. This model demonstrates impaired social interactions and memory deficits, along with molecular changes in GABAergic, glutamatergic, oxytocin, and BDNF systems, highlighting the role of KCC2 in these functions and suggesting potential therapeutic avenues.

The growing utility of zebrafish models is further underscored by the mini-review contributed by Bagwell and Larsen, who discussed the mechanisms of MPTP toxicity and highlighted the advantages of zebrafish for high-throughput screening and their ability to recapitulate biochemical mechanisms and symptoms of human PD, addressing limitations of larval models for age-related conditions.

Investigating molecular and cellular pathogenesis of neurological disorders

Two papers of the Research Topic delve into the molecular and cellular underpinnings of acquired brain disorders or into the conditions that may prevent them.

In particular, the research report by Yao et al. investigated how a perioperative enriched environment (EE) attenuates postoperative cognitive dysfunction (POCD) in a mouse model of ischemic stroke. The authors found that an EE improved neurological function and reduced neuroinflammation in mice subjected to stroke and surgery. This protective effect is mediated by the upregulation of microglia TREM2, via the PI3K/Akt pathway, underscoring the potential of targeting TREM2 and utilizing EE for managing POCD in stroke patients.

In addition, the review by Cong et al. examines the role of the mitochondrial permeability transition pore (mPTP) in the pathogenesis of Intracerebral Hemorrhage (ICH). The authors discuss how mPTP opening leads to mitochondrial dysfunction and contributes to various pathological processes, including oxidative stress, apoptosis, necrosis, autophagy, and ferroptosis. While ICH is a stroke subtype, the mechanisms discussed are highly relevant to neurodegenerative processes and the authors advocate for further investigation into the role of mPTP as a potential therapeutic target for managing ICH-induced secondary injury.

On the front of neurodegenerative disorders of genetic origin, the review by Cui et al. summarizes the pathogenesis of Spinocerebellar Ataxias (SCAs), discussing how various genetic mutations disrupt cellular processes leading to neuronal dysfunction and loss. Although not a modeling paper, it synthesizes knowledge crucial for designing relevant models and developing therapies for SCAs.

Finally, a systematic review by Tesfaye et al. explores brain functional connectivity changes in hyperthyroid patients, a condition that can cause mood and cognitive impairments. It suggests that altered connectivity, particularly involving the hippocampus, may influence cognitive and emotional processing in the framework of hyperthyroidism.

In conclusion, the accepted manuscripts contributed significantly to the Research Topic by presenting original research using diverse *in vivo* animal models (mice, zebrafish) and genetic tools to study the molecular, cellular, and behavioral aspects of various neurodegenerative and neuropsychiatric disorders. Additionally, review articles synthesized existing knowledge on disease mechanisms, modeling challenges, and therapeutic avenues, reinforcing the topic's goal of advancing modeling and understanding pathogenesis of brain diseases.

Author contributions

FD: Writing – original draft, Writing – review & editing. MVC: Writing – review & editing. NS: Writing – review & editing. JM: Writing – review & editing. MS: Writing – review & editing. FC: Writing – review & editing.

Conflict of interest

The authors declare that the research was conducted in the absence of any commercial or financial relationships that could be construed as a potential conflict of interest.

The author(s) declared that they were an editorial board member of Frontiers, at the time of submission. This had no impact on the peer review process and the final decision.

Generative AI statement

The author(s) declare that Gen AI was used in the creation of this manuscript. Notebook LM was used for the creation of this manuscript.

Publisher's note

frontiers | Frontiers in Neuroscience

TYPE Original Research
PUBLISHED 25 October 2023
DOI 10.3389/fnins.2023.1292014

OPEN ACCESS

EDITED BY
Ferdinando Di Cunto,
University of Turin, Italy

REVIEWED BY
Sukanya Saha,
National Institute of Environmental Health Sciences (NIH), United States
Luz Navarro,
National Autonomous University of Mexico, Mexico

*CORRESPONDENCE
Linlin Wang
✉ wangll@cmu.edu.cn
Rui Zhao
✉ rzhao@cmu.edu.cn

†These authors have contributed equally to this work

RECEIVED 10 September 2023
ACCEPTED 13 October 2023
PUBLISHED 25 October 2023

CITATION
Chen Z, Wang P, Cheng H, Wang N, Wu M, Wang Z, Wang Z, Dong W, Guan D, Wang L and Zhao R (2023) Adolescent traumatic brain injury leads to incremental neural impairment in middle-aged mice: role of persistent oxidative stress and neuroinflammation. *Front. Neurosci.* 17:1292014. doi: 10.3389/fnins.2023.1292014

Adolescent traumatic brain injury leads to incremental neural impairment in middle-aged mice: role of persistent oxidative stress and neuroinflammation

Ziyuan Chen[1†], Pengfei Wang[1†], Hao Cheng[1], Ning Wang[1], Mingzhe Wu[1], Ziwei Wang[1], Zhi Wang[1], Wenwen Dong[1], Dawei Guan[1], Linlin Wang[1*] and Rui Zhao[1,2,3*]

[1]Department of Forensic Pathology, School of Forensic Medicine, China Medical University, Shenyang, Liaoning, China, [2]Key Laboratory of Environmental Stress and Chronic Disease Control and Prevention, Ministry of Education, China Medical University, Shenyang, Liaoning, China, [3]Liaoning Province Key Laboratory of Forensic Bio-Evidence Sciences, Shenyang, China

Background: Traumatic brain injury (TBI) increases the risk of mental disorders and neurodegenerative diseases in the chronic phase. However, there is limited neuropathological or molecular data on the long-term neural dysfunction and its potential mechanism following adolescent TBI.

Methods: A total of 160 male mice aged 8 weeks were used to mimic moderate TBI by controlled cortical impact. At 1, 3, 6 and 12 months post-injury (mpi), different neurological functions were evaluated by elevated plus maze, forced swimming test, sucrose preference test and Morris water maze. The levels of oxidative stress, antioxidant response, reactive astrocytes and microglia, and expression of inflammatory cytokines were subsequently assessed in the ipsilateral hippocampus, followed by neuronal apoptosis detection. Additionally, the morphological complexity of hippocampal astrocytes was evaluated by Sholl analysis.

Results: The adolescent mice exhibited persistent and incremental deficits in memory and anxiety-like behavior after TBI, which were sharply exacerbated at 12 mpi. Depression-like behaviors were observed in TBI mice at 6 mpi and 12 mpi. Compared with the age-matched control mice, apoptotic neurons were observed in the ipsilateral hippocampus during the chronic phase of TBI, which were accompanied by enhanced oxidative stress, and expression of inflammatory cytokines (IL-1β and TNF-α). Moreover, the reactive astrogliosis and microgliosis in the ipsilateral hippocampus were observed in the late phase of TBI, especially at 12 mpi.

Conclusion: Adolescent TBI leads to incremental cognitive dysfunction, and depression- and anxiety-like behaviors in middle-aged mice. The chronic persistent neuroinflammation and oxidative stress account for the neuronal loss and neural dysfunction in the ipsilateral hippocampus. Our results provide evidence for the pathogenesis of chronic neural damage following TBI and shed new light on the treatment of TBI-induced late-phase neurological dysfunction.

KEYWORDS

traumatic brain injury, anxiety and depression, cognitive dysfunction, neuroinflammation, oxidative stress

Introduction

Traumatic brain injury (TBI) is the leading cause of disability and death in both children and young adults (Maas et al., 2017; Quaglio et al., 2017). Accumulated evidence in the past decades demonstrates that young adults and adolescent survivors after TBI may present cognitive, behavioral, or mental symptoms in their adulthood or late life (Moretti et al., 2012; Richmond and Rogol, 2014; Sun et al., 2017; Rodgin et al., 2021; Xu et al., 2021; Bourke et al., 2022; Max et al., 2022; Sanchez et al., 2022). Thereafter, TBI has been commonly recognized as a risk factor for many neurodegenerative diseases, such as Alzheimer's disease, Parkinson's disease, dementia, and chronic traumatic encephalopathy (VanItallie, 2019; Vázquez-Rosa et al., 2020; Brett et al., 2022). However, the underlying mechanisms of late-life neural dysfunction post TBI remains unclear.

Both primary and secondary injuries contribute to neuronal damage in the acute and subacute phase of TBI. Intracranial hemorrhage and brain destruction are caused by the initial external force (Maegele et al., 2017), followed by the reactive microglia and astrocytes that alter their transcriptional and morphological profiles and exert pro-or anti-inflammatory effects (Karve et al., 2016), which promotes the clearance of damaged tissue and neural regeneration after TBI (Corps et al., 2015). In the chronic phase, damage-associated molecular patterns, such as excitotoxicity, mitochondrial dysfunction, oxidative stress, and neuroinflammation, trigger secondary injuries (Braun et al., 2017). Chronic neuroinflammation, supported by the persisting reactive astrocytes and microglia in the injured animal and human brain (Smith et al., 1997; Ramlackhansingh et al., 2011; Faden et al., 2016; Pischiutta et al., 2018; van Vliet et al., 2020), can last for an extended period and contribute to the chronic neurological disorder post-injury (Faden et al., 2016; van Vliet et al., 2020). In addition, oxidative stress has been well recognized as a common denominator of both brain injury and TBI-related neurodegenerative disease (Mackay et al., 2006; Ma et al., 2017; Dong et al., 2018; Cheng et al., 2022). Excessive reactive oxygen species (ROS) and reactive nitrogen species are generated and cause neurotoxicity by increasing intracellular free Ca^{2+} and releasing excitatory amino acids (Khatri et al., 2021) or directly inducing peroxidation of lipid, protein, and DNA in the acute phase of TBI (Ma et al., 2017). These findings provide evidence to link chronic inflammation and oxidative stress with TBI-related neurodegenerative pathology.

Nuclear factor erythroid-derived 2-related factor 2 (NRF2), is widely recognized as a key transcription factor that regulates both the antioxidant responses and neuroinflammation (Buendia et al., 2016). Our previous study presented that NRF2 is widely expressed in neurons and glia post TBI (Dong et al., 2019). Many evidence has demonstrated that NRF2 plays neuroprotective roles against TBI-induced brain injury (Li et al., 2014; Lu et al., 2015; Dong et al., 2018; Sigfridsson et al., 2020; Wang et al., 2020; Cui et al., 2021) and neurodegenerative diseases (Rojo et al., 2010, 2018; Osama et al., 2020; Ren et al., 2020; Zgorzynska et al., 2021). Considering the critical role of NRF2 in TBI and numerous neurodegenerative diseases, it is necessary to explore the expression pattern of NRF2 during the late phase of TBI.

In this study, to reveal the underlying mechanisms of long-lasting neurological dysfunction following TBI in mice, we explored the lifespan change of neurological dysfunction, oxidative stress and neuroinflammation in ipsilateral hippocampus from young age to late life of TBI mice.

Materials and methods

Animals and controlled cortical impact models

A total of 160 male C57BL/6 mice (8 weeks old, 20–26 g) were used in our study. Mice were randomly divided into TBI and age-matched control groups. Then mice were subdivided into four subgroups as the indicated timepoints (1, 3, 6 and 12 mpi, $n = 20$ in each subgroup). All the mice were housed under constant temperature (23 ± 1°C), humidity (60%) and a 12-h light–dark cycle, with free access to food and water. In the TBI group, CCI was used to mimic the stable moderate TBI model (considerable cortical tissue loss without hippocampal injury) as in our previous studies (Siebold et al., 2018; Ma et al., 2019; Cheng et al., 2023). Briefly, the mice were placed on a stereotaxic apparatus after being anesthetized. A scalp incision was subsequently made at the midline to expose the skull. A 4 mm craniotomy was performed in the left hemisphere between the bregma and lambda to expose the dura mater. The craniocerebral strike apparatus (PinPoint™ PCI3000, Hatteras instruments, America) was used to perform a vertical impact on the cortex (3 mm diameter impactor, velocity 1.5 m/s, residence time 50 ms, depth 1 mm), followed by sutured scalped. The comatose mice were then placed on a 37°C heating pad and returned to the cages until the vital signs were stable. The mice in the sham group underwent the same surgical procedure without any cortical impact. No mice died after the surgery or during feeding. All the experiments were approved by the Animal Ethics Committee of China Medical University.

Behavior tests

The following behavioral tests were conducted at the indicated timepoints post injury. Mice were tested by sucrose preference test (SPT) and elevated plus maze (EPM) first, and followed by the force swimming test (FST) and Morris water maze (MWM). To avoid the effects among different behavior tests, mice were kept in the cages for 1 day to recover before the next test.

SPT

The SPT was adapted from a previous protocol (Leng et al., 2018; Browne et al., 2022). Briefly, each mouse was allowed free access to 1% sucrose solution and tap water for 16 h, and the placement of the two bottles was changed every 12 h to avoid side preference at the training stage. After 12 h of food deprivation, the mice were allowed free access to tap water and 1% sucrose solution for the next 24 h. Sucrose preference was calculated as the percentage of the consumed sucrose solution from the total consumed fluid (sucrose + water).

FST

The FST was performed as previously described (Li et al., 2021). Briefly, the mice were placed in a cylindrical glass filled with no less than three quarters of water for 6 min, and their activity was recorded for the last 5 min at a temperature of 23 ± 1°C. SMART™ tracking software (San Diego Instruments, San Diego, CA, USA) was used to record the time of immobility.

EPM

To measure anxiety-like behavior post-injury, the EPM test was performed as previously described (Toshkezi et al., 2018). The EPM was consisted of two opened arms and two closed arms. Mice were placed at the center of the junction of the maze facing one open arm and allowed to explore freely for 5 min. The spent time and number of entries into the open arms were recorded using SMART™ tracking software for further analysis.

MWM

To evaluate the spatial memory of mice post injury, we performed the MWM test at 1, 3, 6 and 12 mpi as previously described (Ren et al., 2020). Briefly, the mice were trained to find a platform that relied on distal cues from four different starting positions in an open circular tank. Mice that failed to find the platform within 60 s were guided and remained on the platform for 30 s before being returned to their cages. On the first day, mice were trained to find the platform 0.5 cm above the water. Then, the mice were trained for four more days to find the platform below the opaque water. On the sixth day, mice were placed at the starting quadrant opposite to the quadrant with removed platform and several variables were recorded and measured for 60 s: the distance in the platform quadrant, time spent in the platform quadrant, and number of crossings between the platform and platform quadrant, using SMART™ tracking software (San Diego Instruments, San Diego, CA, United States).

Animal selection and sample collection

TBI mice with abnormal behavior were selected for the subsequent biological experiments ($n \geq 12$ in each time point) according to the method proposed by Rodney M Ritzel with a slight modification (Ritzel et al., 2022). Briefly, we established a baseline according to the means of behavioral parameters (SPT, EPM, MWM and FST) from age-matched control mice, and then evaluate the neurological dysfunction of TBI mice. The mice with behavioral parameters exceeding the baseline were selected for the followed experiments. The proportion of TBI mice meeting these criteria was presented in Supplementary Table S3. Brain samples were collected as previously described (Dong et al., 2018). For immunoblotting, malondialdehyde (MDA) detection and quantitative real time polymerase chain reaction (RT-qPCR), mice were perfused with cold phosphate buffered saline. The ipsilateral hippocampus was dissected on ice and placed in liquid nitrogen for use. For immunohistochemical or immunofluorescence staining, the mice were perfused with cold 4% paraformaldehyde. The brains were embedded in paraffin and 5 μm sections were prepared for histological staining.

MDA

MDA was detected using the commercial kit (Nanjing Jiancheng Bioengineering Institute, Nanjing, China). The total protein concentration was quantified with the bicinchoninic acid assay kit (Beyotime, P0009) according to the manufacturer's instructions. The MDA content was expressed in nmol/mg protein.

Immunofluorescence and immunohistochemistry

Immunofluorescence and immunohistochemical staining were performed as previously described (Dong et al., 2018). Breifly, tissue sections were deparaffinized and hydrated, followed by antigen retrieval in citrate buffer at 95°C for 5 min. Then sections were incubated by primary and secondary antibodies, which were listed in the Supplementary Table S1. Three animals per group were used for immunofluorescence or immunohistochemical staining, and the definite fields of two sections per animal were evaluated ($n = 6$). The number of positive cells in the ipsilateral hippocampal CA1 and hilus was counted at ×200 magnification. The average optical density and positive area were quantified using ImageJ, version 6.0 (National Institutes of Health).

Fluoro-Jade C staining

Fluoro-Jade C (FJC; Millipore, AG325–30MG) was used to assess the number of degenerating neurons following injury. As previously described (Dong et al., 2018), the sections of ipsilateral hippocampus were incubated with 0.06% potassium permanganate solution and then incubated in 0.01% FJC solution for 10 min.

Western blot

The ipsilateral hippocampus was collected for protein extraction as previously described (Dong et al., 2018). Protein concentration was measured using a BCA kit (P0012; Beyotime Biotechnology, Shanghai, China). The primary and secondary antibodies used in this study are listed in Supplementary Table S1. Relative band density was quantified using ImageJ software (National Institutes of Health).

RT-qPCR

RNA extraction, and RT-qPCR were performed as previously described (Dong et al., 2018). The housekeeping gene *Gapdh* was amplified to ensure the addition of equal amounts of cDNA to the PCR reactions. ΔΔCT was used to quantify the target gene expression, with *Gapdh* as the reference gene. Primers used in this study were listed in Supplementary Table S2.

Morphological data collection and Sholl analysis

Fluorescence images were captured using Zeiss Axio Scan.Z1 under ×200 magnification. Morphological reconstruction of glial fibrillary acidic protein (GFAP) positive astrocytes was performed using ImageJ (version 6.0; National Institutes of Health), as previously described (Bondi et al., 2021). Briefly, images of the ipsilateral hippocampal hilus were converted to an 8-bit format. Two sections were taken from each animal, and two GFAP-positive cells ($n = 12$) were randomly selected from the hilus region of each section. Then the total and maximum lengths of the process and the number of intersections were measured with circles of different diameters increasing by 4 μm from the center of the cell body.

Statistical analysis

Data are expressed as mean ± standard deviation. All the data were analyzed using Prism software (version 8.0; GraphPad Software, Inc.). Two-way ANOVA was used to measure the differences between Sham and TBI groups of different time points, and multi-group comparisons were performed using Tukey's *post hoc* test. Mann–Whitney U test was

used for comparison between two groups with non-normal distributed data. Statistical significance was set at $p < 0.05$.

Results

Adolescent TBI causes exacerbated neural impairment in the middle-aged mice

To explore neural function impairment during the late phase of TBI, we conducted the SPT, FST, EPM, and MWM to evaluate depression-like and anxiety-like behaviors and memory deficits at 1, 3, 6 and 12 mpi (Figure 1A). As shown in Figures 1B,C, the mice in the TBI group demonstrated a significant decrease in the sucrose consumption and increase in the immobility time compared with sham mice from 6 mpi, which was exacerbated sharply at 12 mpi, suggesting that injured mice exhibited depression-like behaviors at 6 mpi and beyond. Furthermore, the decrease of the number and the time of entries in the open arms were worsened at 12 mpi in EPM (Figures 1D–F), demonstrating a prolonged anxiety-like behavior in injured mice. In MWM test (Figure 1G), the path length, the time in the platform quadrant (Figures 1H,I), the number of platform quadrants (Figure 1J) and the number of platform in the probe test (Figure 1K) decreased in the TBI mice compared with the age-matched mice; all of them were significantly decreased at 12 mpi (Figures 1H–K), indicating a persistent and incremental spatial memory impairment post-injury. In summary, these behavioral observations revealed that TBI in adolescent mice resulted in the deterioration of neurological function in the late phase of their life (6 mpi and 12 mpi).

Apoptosis contributes to chronic neuron loss in ipsilateral hippocampus following TBI

Since the hippocampal neurons play the key roles of both processing memory storage and regulating depression/anxiety-like behaviors (Tunc-Ozcan et al., 2019; Takahashi et al., 2021), we explored the relationship between neural dysfunction and ipsilateral hippocampal neuron loss. A progressive neuronal decrease in ipsilateral hippocampal CA1 (Figure 2A; Supplementary Figure S1) and hilus (Figure 2B; Supplementary Figure S1) was revealed by the NeuN-positive staining from 3 mpi, which was not affected by the ageing of the mice (Figures 2A,B). In addition, as shown in Figures 2C,D,G,H, FJC-positive cells remained at a constant low level within 6 months post-injury and increased sharply at 12 mpi both in CA1 and hilus. In line with this, immunohistochemical staining of cleaved caspase 3 demonstrated the same pattern (Figures 2E,F,I,J). Although the objective number of apoptotic cells gradually increased with ageing, no statistical difference was observed among the mice with different age in the sham group (Figures 2G–J), demonstrating ageing-related neuron apoptosis in the hippocampus could not account for the neural dysfunction in middle-aged mice. Furthermore, the protein band of cleaved-caspase 3 in the TBI hippocampus was densified at 12 mpi compared with the age-matched mice (Figures 2K,L), which accounted for the exacerbated neural dysfunction in the middle-aged mice. Our data revealed that neuronal apoptosis in the ipsilateral hippocampus contributes to chronic neural dysfunction following TBI.

Chronic persistent oxidative stress is associated with robust neuronal damage in middle-aged mice

To explore whether neuronal damage is associated with chronic oxidative stress during the pathological process following TBI, we first evaluated the protein level of 4-hydroxynonenal (4-HNE), a marker of lipid peroxidation. As shown in Figures 3A,B, the level of 4-HNE in the TBI groups was elevated compared with the corresponding sham mice at all indicated timepoints, which was increased sharply at 12 mpi (fold change = 2.05 ± 0.43). Then, 4-HNE was further confirmed by immunostaining, and the average optical density of 4-HNE in the CA1 and hilus increased following injury (Figures 3C,D; Supplementary Figures S2A,B). To further evaluate oxidative stress alteration, MDA was detected in the ipsilateral hippocampus. As shown in Figure 3E, MDA was elevated with the same trend as 4-HNE at all intervals post-injury. Unexpectedly, no difference was observed on 4-HNE and MDA in the hippocampus of the sham mice (Figures 3B–E). To assess endogenous protective capability, we subsequently determined the level of the antioxidant response. NRF2 and its regulated antioxidant enzymes, heme oxygenase-1 (HMOX-1) and quinone oxidoreductase-1(NQO-1), were upregulated at both protein and mRNA levels following TBI within 6 mpi (Figures 3F–L) and significantly decreased at 12 mpi both in the TBI and its age-matched mice (Figures 3F–L). Whereas, ccompared with the age-matched sham mice, the protein level of glutamate-cysteine ligase catalytic subunit (GCLC) and its modifier subunit (GCLM) were only decreased at 12 mpi, with no significant changes at 1, 3, and 6 mpi (Supplementary Figures S3A–D). Our data indicated that persistent oxidative stress contributes to neuronal damage following TBI, which was also related to the ageing.

Persistent inflammation induced by TBI is exacerbated in middle-aged mice

To explore the changes in neuroinflammation in the ipsilateral hippocampus at different intervals post-injury, we tested the protein and mRNA levels of interleukin (IL)-1β, IL-6, and tumor necrosis factor-alpha (TNF-α). As shown in Figure 4, the protein and mRNA levels of IL-1β and TNF-α were elevated following TBI compared with the age-matched sham mice at each indicated time point. However, IL-6 expression was only increased at 12 mpi (fold change = 1.56 ± 0.20) and revealed no significant difference at 1, 3, and 6 mpi (Figures 4B–E). Our data demonstrated that long-lasting neuroinflammation in the ipsilateral hippocampus was present following TBI, which was aggravated in middle-aged mice (12 mpi).

Alteration of hippocampal astrocytes during the chronic phase of TBI

To assess the reactive astroglia, we detected GFAP expression by immunofluorescence, a marker of astrocytes. As shown in

10.3389/fnins.2023.1292014

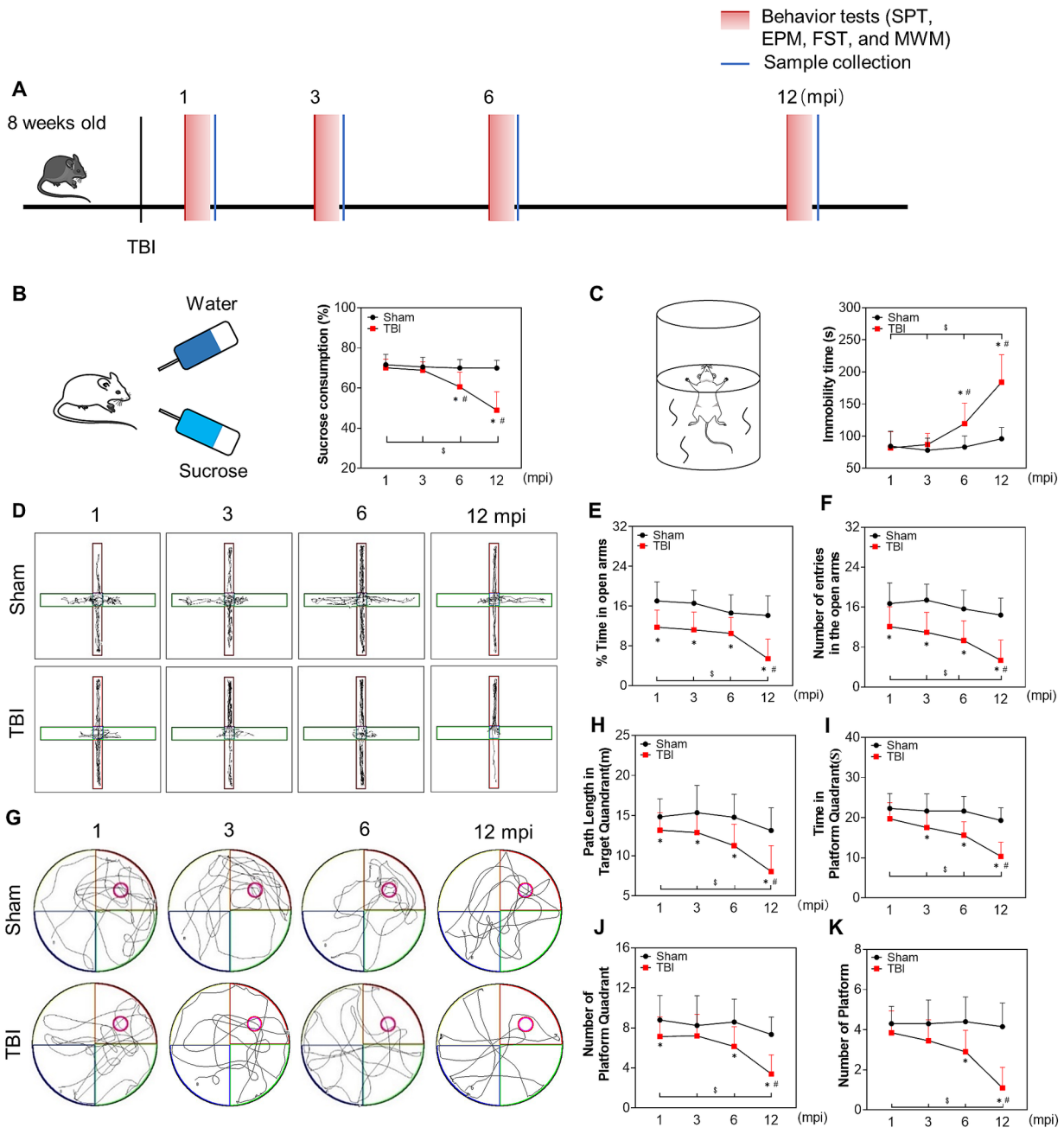

FIGURE 1
The late phase changes on neurological function post injury. **(A)** Schematic diagram of the experimental design. **(B)** Schematic diagram of the SPT (left panel) and the percentage of sucrose consumption over total fluid volume of mice at 1, 3, 6 and 12 mpi (right panel). **(C)** Schematic diagram of the FST (left panel) and the statistical analysis of immobility time at each indicated timepoints (right panel). **(D)** The representative moving path of mice in EPM test at 1, 3, 6 and 12 mpi. **(E)** The percentage of time in the open arm. **(F)** The number of entries in the open arm. **(G)** The representative moving path of MWM in probe test at 1, 3, 6 and 12 mpi. **(H)** The path length in the platform quadrant. **(I)** The time in the platform quadrant. **(J)** The number of platform quadrant. **(K)** The number of platform. $n = 20$, $^*p < 0.05$ compared with the age-matched sham (Mann–Whitney U Test); $\$p < 0.05$ 1, 3, 6 mpi versus 12 mpi (Tukey's *post hoc* test); $\#p < 0.05$ compared with the preceding adjacent TBI group (Tukey's *post hoc* test).

Figures 5A,B, the immunoreactivity of GFAP and the percentage of GFAP+ area in the ipsilateral hippocampus were higher than those in sham mice at each time point, especially at 12 mpi (Figure 5C). In line with these, the protein levels of GFAP were also upregulated upon Western blot (Figures 5D,E). Our data proved that TBI led to astrogliosis in the hippocampus, and the astrocytic response was intensified in the hippocampus of middle-aged mice. It has been known that A1 astrocytes contribute to the pathogenesis of TBI and neurodegenerative diseases (Diaz-Castro et al., 2019; Song et al., 2020; Taylor et al., 2020). We explored the A1 astrocytes by C3d and GFAP double immunostaining. Several C3d + astrocytes signal colocalized with GFAP+ cells in the ipsilateral hippocampus post injury (Supplementary Figure S4A, lower panel). Whereas, no double-positive astrocyte was found in the hippocampus of sham mice from

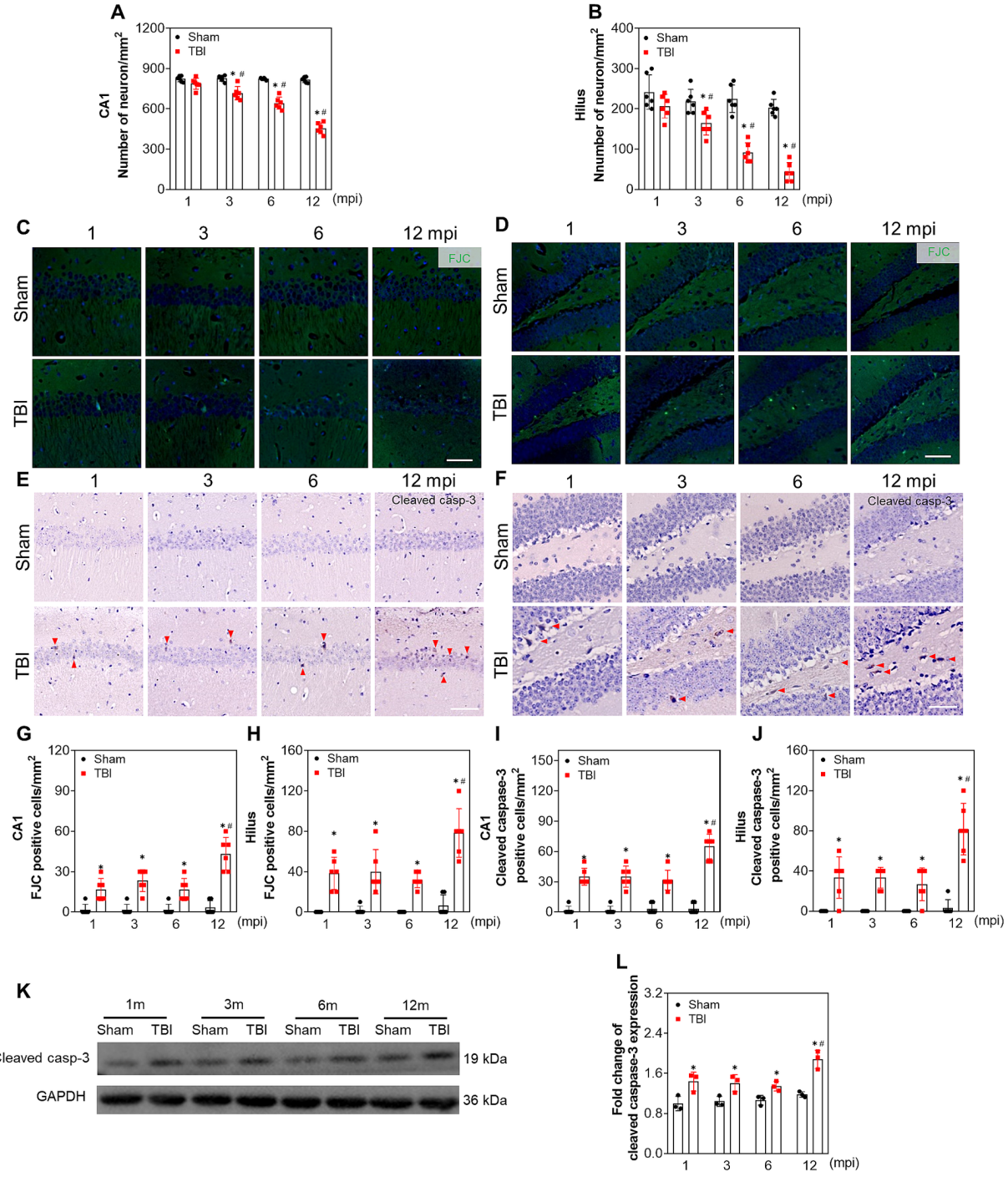

FIGURE 2
Apoptosis contributes to chronic neuron loss in ipsilateral hippocampus following TBI. **(A,B)** The quantitative analysis of the number of NeuN positive cells in CA1 and hilus at different indicated time points post injury, $n = 6$. **(C,D)** Representative images of FJC staining in CA1 and hilus of ipsilateral hippocampus at different time post injury. **(E,F)** Representative immunostaining images of cleaved caspase-3 in CA1 and hilus of ipsilateral hippocampus at different time post injury. **(G–J)** The quantitative analysis of the number of FJC and cleaved caspase-3 positive cells in CA1 and hilus at different time post injury, $n = 6$. **(K,L)** The representative immunoblots and relative densities of cleaved caspase-3 in the ipsilateral hippocampus of each group; $n = 3$. Scale bar, 20 μm. $*p < 0.05$ compared with the age-matched sham mice (Mann–Whitney U Test); $\#p < 0.05$ compared with the TBI mice of preceding adjacent group (Tukey's *post hoc* test).

adolescence to middle age (Supplementary Figures S4A,B). Then the complexity of the reactive astrocytes was evaluated in the ipsilateral hippocampus by Sholl analysis. The representative astrocytes and their reconstructed skeleton in each group were shown in Figure 5F. A significant difference in the morphological complexity of astrocytes in sham mice was observed only in middle-aged mice (12 mpi) (Figure 5G). However, in TBI mice, the reactive astrocytes sustained the complex morphology post injury, which was presented by the total

10.3389/fnins.2023.1292014

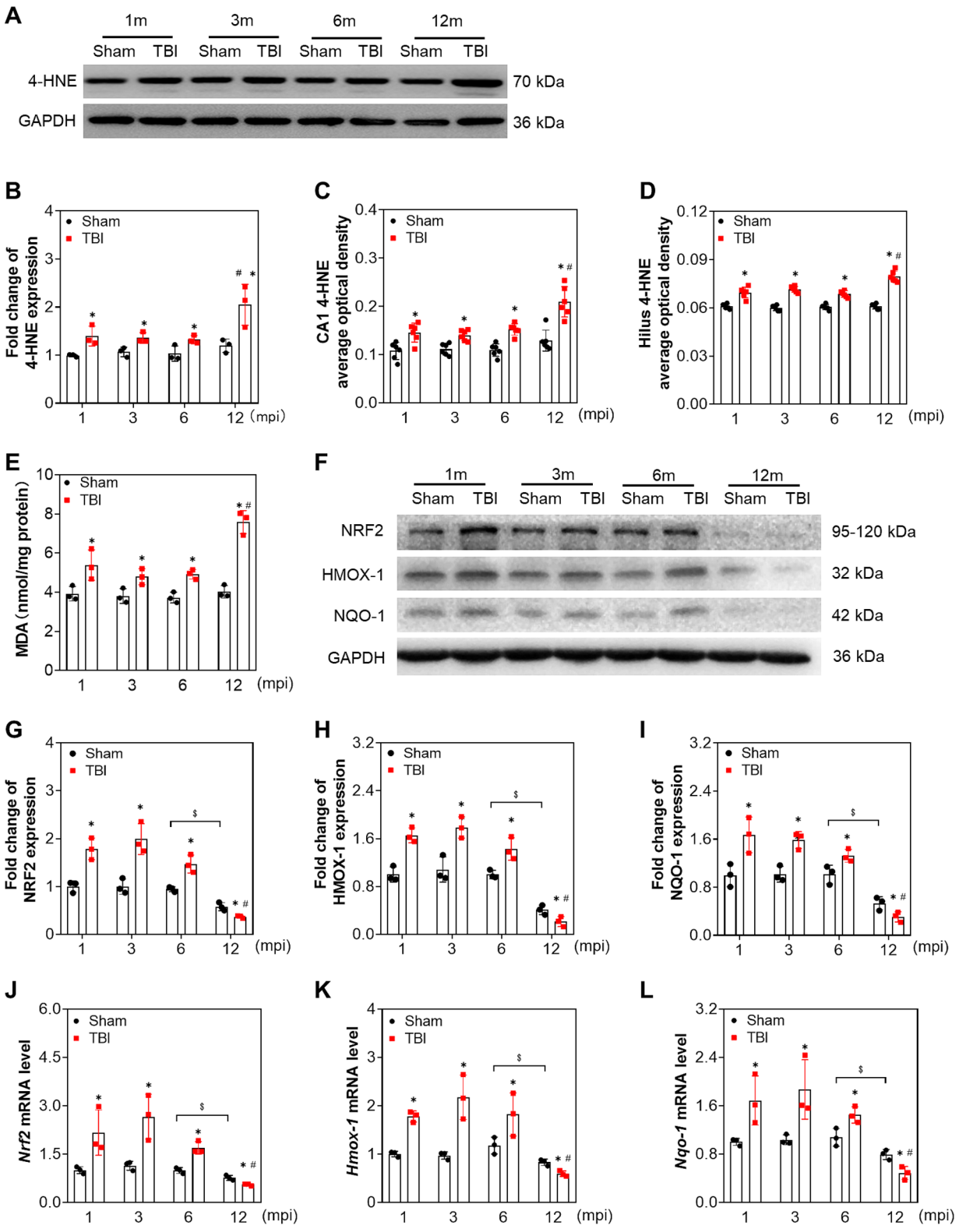

FIGURE 3
Adolescent TBI-induced persistent oxidative stress is enhanced in middle-aged mice. **(A,B)** Representative immunoblots and relative densities of 4-HNE in the ipsilateral hippocampus at 1, 3, 6 and 12 mpi, $n = 3$. **(C,D)** The quantitative analysis of the average optical density of 4-HNE immunohistochemical staining in CA1 and Hilus, $n = 6$. **(E)** The quantitative analysis of MDA content, $n = 3$. **(F)** Representative immunoblots of NRF2, HMOX-1, NQO-1 of the ipsilateral hippocampus at 1, 3, 6 and 12 mpi. **(G–I)** Relative densities of NRF2, HMOX-1, NQO-1, $n = 3$. **(J–L)** The mRNA levels *Nrf2*, *Hmox-1*, *Nqo-1* of the ipsilateral hippocampus at 1, 3, 6 and 12 mpi, $n = 3$. $^*p < 0.05$ compared with age-matched sham (Mann–Whitney U Test); $\$p < 0.05$ comparison between sham groups (Tukey's *post hoc* test); $\#p < 0.05$ compared with the TBI mice of preceding adjacent group (Tukey's *post hoc* test).

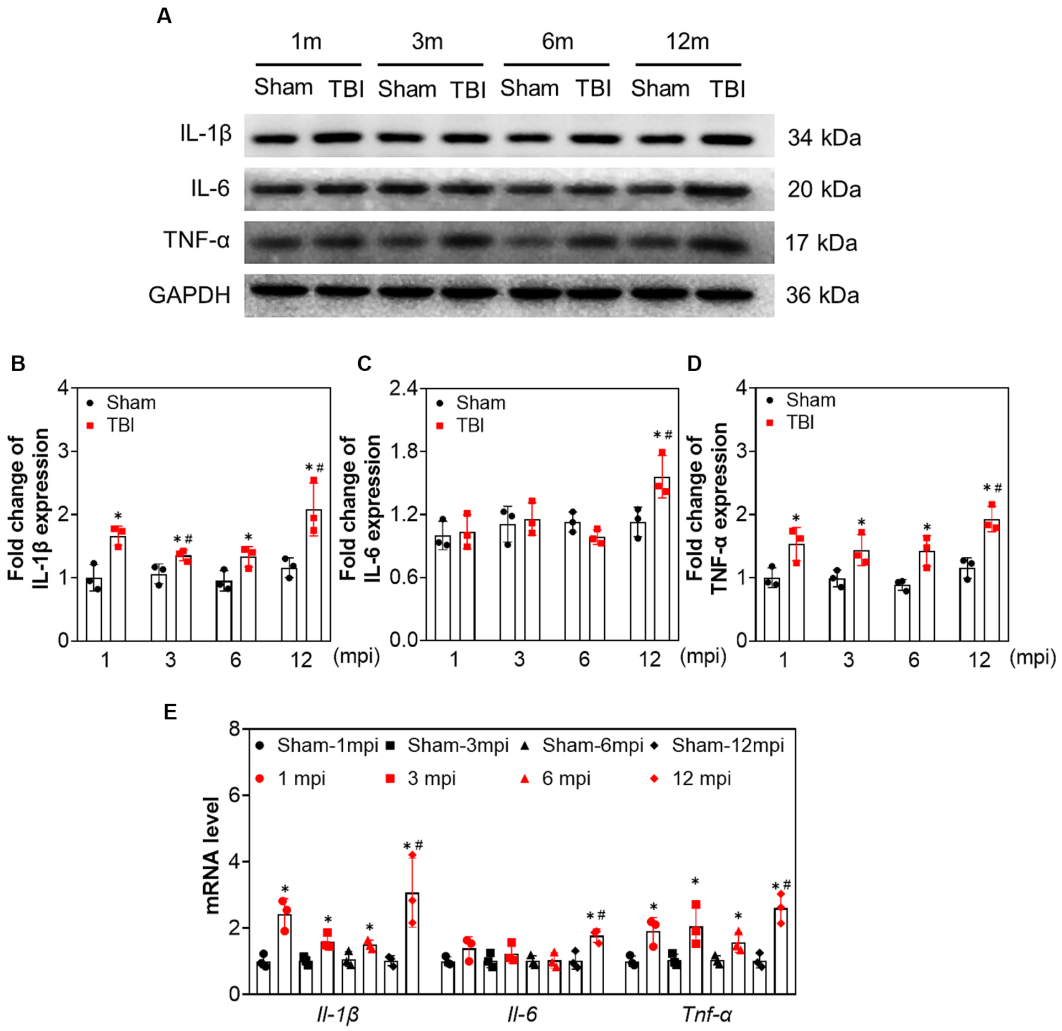

FIGURE 4
The increased expression of proinflammatory cytokines in ipsilateral hippocampus induced by adolescent TBI. **(A–D)** Representative immunoblots and relative densities of IL-1β, IL-6 and TNF-α of the ipsilateral hippocampus, $n = 3$. **(E)** The mRNA levels of *Il-1β*, *Il-6* and *Tnf-α* of the ipsilateral hippocampus, $n = 3$. $^{*}p < 0.05$ compared age-matched sham (Mann–Whitney U Test); $^{\#}p < 0.05$ compared with the TBI mice of preceding adjacent group (Tukey's *post hoc* test).

and maximum process length in Figures 5H,I. Our data revealed the alternation of reactive astrocytes and their morphological complexity in the ipsilateral hippocampus after TBI.

Reactive microglia is aggravated in the late phase of TBI

To evaluate the reactive microgliosis during the chronic phase of TBI, we measured the protein levels of ionized calcium binding adaptor molecule 1 (IBA1), CD16/32, and Arginase 1 (ARG-1). As shown in Figures 6A–C, the protein levels of IBA1 and CD16/32 were increased in the hippocampus of TBI mice at each indicated time point compared with that of sham mice. However, the ARG-1 level only increased slightly at 1 mpi in TBI mice (Figures 6A,D). Moreover, double immunofluorescence staining of IBA1 + CD16/32 and IBA1 + ARG-1 (Figures 6E,G) supported M1 polarization of microglia in TBI mice. The ratio of CD16/32+ microglia in the hilus at 1, 3, 6 mpi were 31.5 ± 3.8%, 30.7 ± 5.2% and 32.8 ± 3.9% separately, which increased sharply to 64.8 ± 10.8% at 12 mpi (Figure 6F). While ARG-1+ microglia accounted for approximately 13.7 ± 5.0% of the microglia at 1 mpi and 1.1 ± 2.7%, 1.0 ± 2.6%, 1.3 ± 3.1% at 3–12 mpi in hilus (Figure 6H). These data indicated that persistent reactive microglia could contributed to neuronal damage following TBI, especially in middle-aged mice.

Discussion

Chronic pathophysiological changes post-TBI are responsible for neurological dysfunction and neurodegenerative diseases. Despite growing awareness of the chronic progressive nature of TBI (Tomaszczyk et al., 2014), there is still a need to characterize the pathogenesis of long-term neurological function post-injury. In this study, we described that adolescent TBI led to chronic neurological dysfunction, which was aggravated in middle-aged mice. Chronic oxidative stress, sustained reactive astrocyte and microgliosis contribute to the pathogenesis of neurological dysfunction and

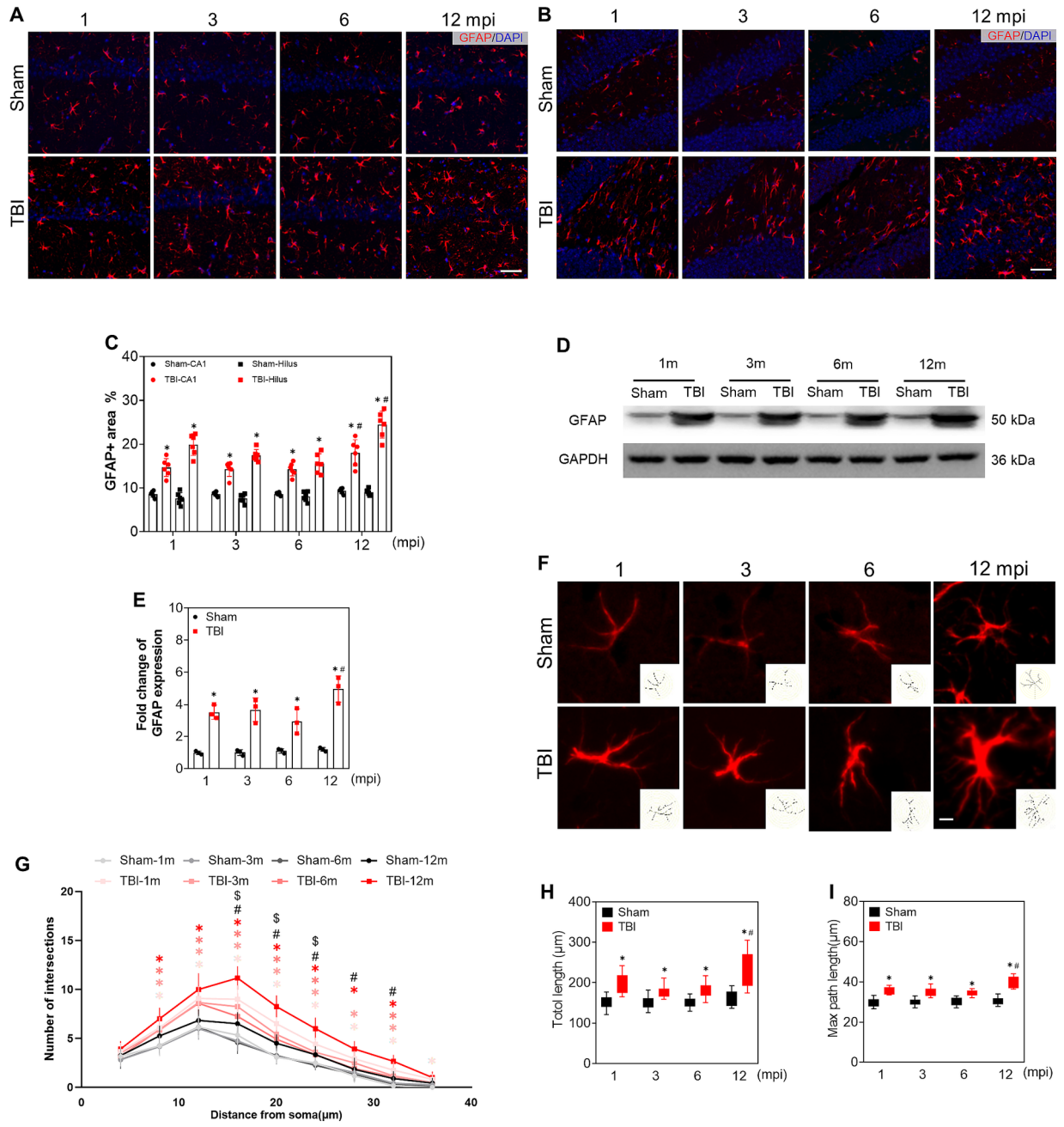

FIGURE 5
The alteration of reactive astrocytes during the chronic phase of adolescent TBI. **(A,B)** Representative images of GFAP (red) immunofluorescent staining of CA1 and hilus of ipsilateral hippocampus; scale bar, 20 μm; $n = 6$. **(C)** The quantitative analysis of GFAP positive area of CA1 and hilus, $n = 6$. **(D,E)** Representative immunoblots and relative densities of GFAP of the ipsilateral hippocampus at 1, 3, 6 and 12 mpi, $n = 3$. **(F)** Representative image of GFAP+ astrocytes in hilus at 1, 3, 6 and 12 mpi, the reconstructed skeleton of representative astrocytes was present in the lower right corner of the image; scale bar, 5 μm. **(G)** Intersection profile of astrocytes in hilus at 1, 3, 6 and 12 mpi, $n = 12$. **(H)** The quantitative analysis of total length of astrocytic process. **(I)** The quantitative analysis of the max length of astrocytic process; $n = 12$. $^{*}p < 0.05$ comparison between TBI and age-matched Sham groups (Mann–Whitney U Test); $\#p < 0.05$ comparison between 6 and 12 mpi groups (Tukey's *post hoc* test); $\$p < 0.05$, comparison between Sham mice of 6 and 12 mpi groups (Tukey's *post hoc* test).

hippocampal neuron loss following TBI. Moreover, the aggravated neurological dysfunction in middle-aged TBI mice was partly due to the decrease of NRF2-mediated antioxidant response. Our present study suggests that ageing might be a contributory factor for long-term neural damage following TBI. The potential mechanism of long-term neural dysfunction after TBI is schematically illustrated in Figure 7.

Brain injuries trigger various neurological complications, including epilepsy, depression, and dementia (Burke et al., 2021; Stopa et al., 2021; Wang et al., 2021). Our observations revealed that adolescent traumatic brain injury results in spatial memory impairment and anxiety/depression-like behavior in middle-aged mice, which is consistent with the previous study (Mao et al., 2020). Although epidemiological study has revealed no obvious correlation

10.3389/fnins.2023.1292014

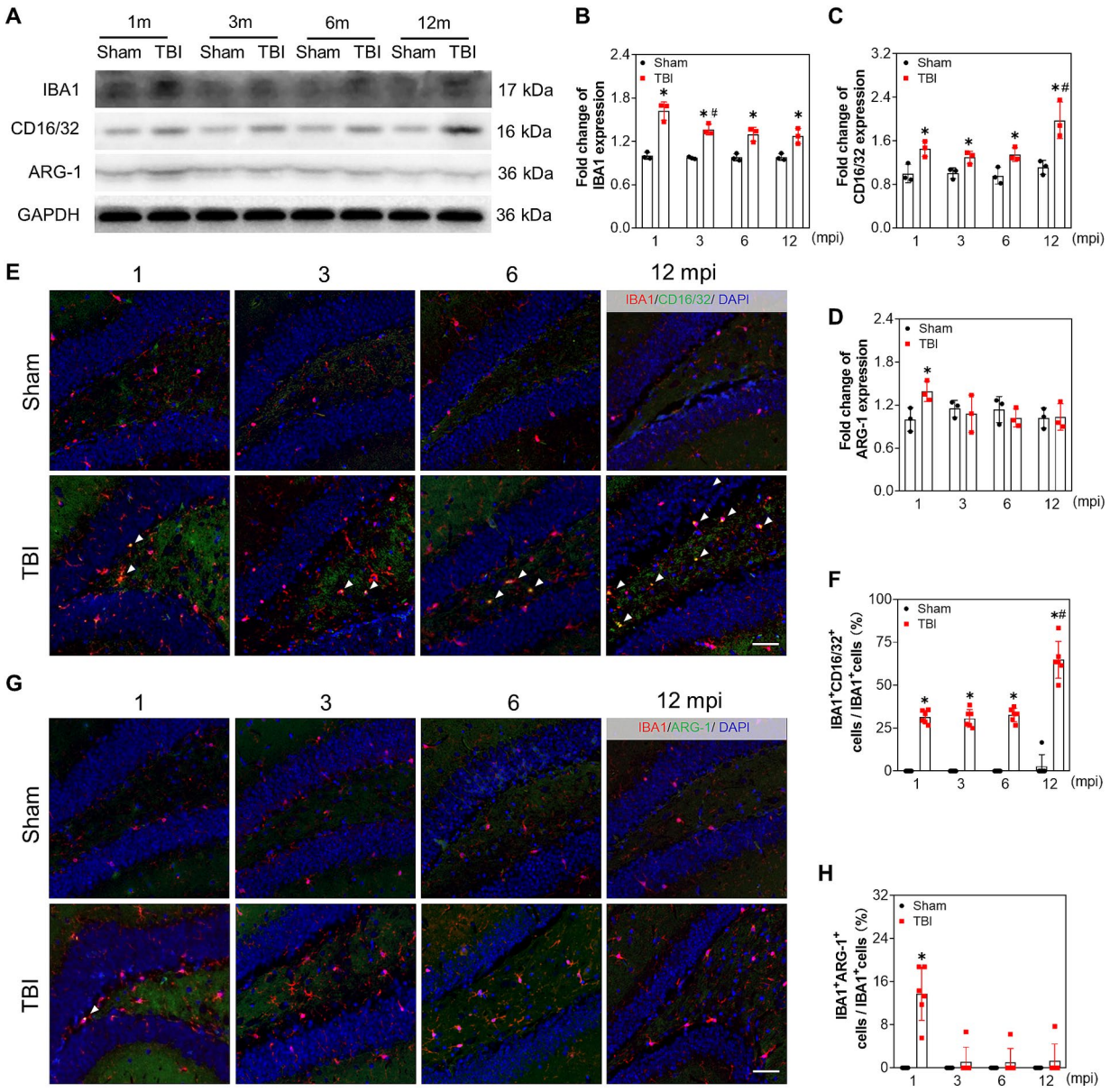

FIGURE 6
Reactive microglia is aggravated in the late phase of adolescent TBI. **(A–D)** Representative immunoblots and relative densities of IBA1, CD16/32, ARG-1 of the ipsilateral hippocampus at 1, 3, 6 and 12 mpi, $n = 3$. **(E)** Representative images of immunofluorescent double staining of IBA1 (red) and CD16/32 (green) of the ipsilateral hippocampal hilus; white arrows, IBA1 and CD16/32 double positive cells. **(F)** The quantitative analysis of the percentage of IBA1 and CD16/32 double positive cells, $n = 6$. **(G)** Representative images of immunofluorescent double staining of IBA1 (red) and ARG-1 (green) of the ipsilateral hippocampal hilus; white arrows, IBA1 and ARG-1 double positive cells. **(H)** The quantitative analysis of the percentage of IBA1 and ARG-1 double positive cells, $n = 6$. $*p < 0.05$ compared with age-matched sham (Mann–Whitney U Test), $\#p < 0.05$ compared with the TBI mice of preceding adjacent group (Tukey's *post hoc* test); scale bar, 20 μm.

between injury severity and depression occurrence (Vadlamani and Albrecht, 2020), previous study observed that mice underwent severe TBI showed depression-like behavior at 3 months post-injury (Mao et al., 2020), while this neural dysfunction was observed at 6 months post moderate TBI in our present study, the time delay of depression-like behavior post injury may be associated with the severity of TBI model.

In addition, local TBI could promote the secondary damage of certain remote brain regions in the late phase, resulting in a diverse range of neurological disorders. Numerous studies reported that chronic atrophy and degenerative disease of white matter post brain trauma aggravate cognitive dysfunction, depression, and apathy (Filley and Fields, 2016; Cole et al., 2018; Bartnik-Olson et al., 2021; Mohamed et al., 2021; Navarro-Main et al., 2021; Medeiros et al., 2022). Demyelination, blood–brain barrier impairment, and increased neuroinflammation are revealed in the thalamus of late stage TBI, which is accompanied by the appearance of sleep spindles and epilepsy[64,65]. Given that the hippocampus is a fundamental region in regulating mood and memory (Tartt et al., 2022) and is particularly vulnerable to brain injury, even to mild TBI (Obenaus et al., 2023), our present study provided evidence that the neurological dysfunction after TBI in mice is associated with the exacerbation of inflammation and oxidative stress in hippocampus, demonstrating that hippocampus would be a crucial brain region for preventing and ameliorating the

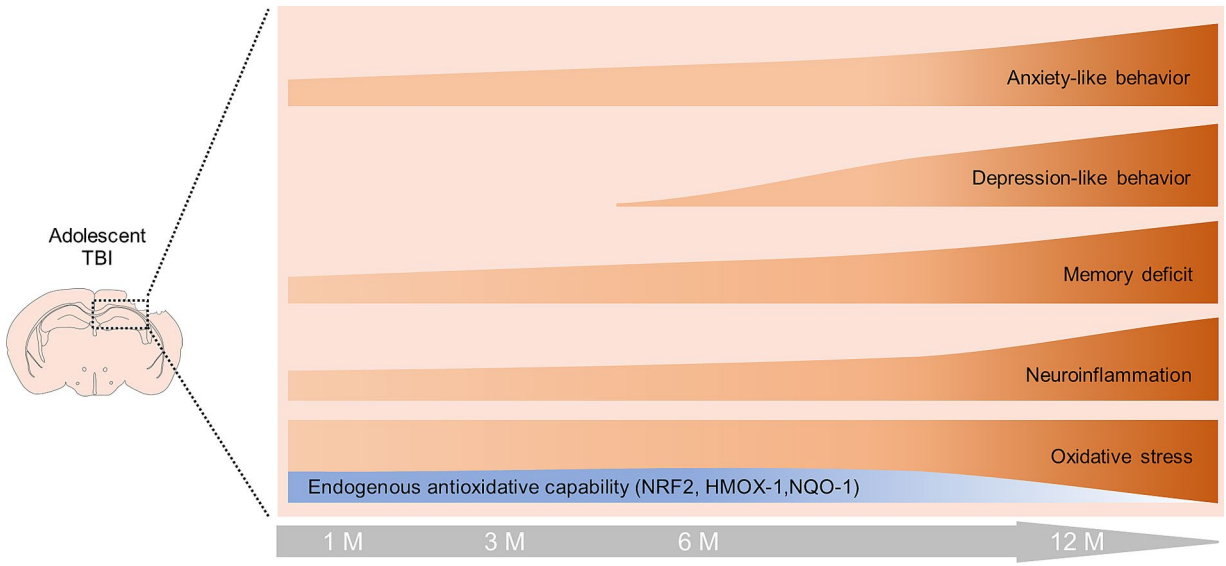

FIGURE 7
Schematic diagram of changes in neurological function, oxidative stress and neuroinflammation during the late phase of TBI. Oxidative stress and neuroinflammation occur in the hippocampus of adolescent TBI mice within 6 mpi, accompanied by increased expression of NRF2, HMOX-1, and NQO-1. TBI mice developed persistent memory impairment and anxiety behavior within 6 mpi, and began to develop depression-like behavior at 6 mpi. At 12 mpi, the expression of NRF2, HMOX-1, and NQO-1 was significantly decreased, leading to aggravated oxidative stress and neuroinflammation, as well as exacerbated memory impairment, anxiety-and depression-like behaviors.

secondary neurological dysfunctions at the late stage of TBI. Future studies are still needed to explore the link between the damage of neurological functions and the pathophysiological changes in different brain regions in the late stage of TBI.

Different mechanisms of neuronal death have been reported during the acute phase of TBI, including apoptosis, autophagy, necrosis, and ferroptosis (Dong et al., 2018; Liu et al., 2018; Xie et al., 2019; Akamatsu and Hanafy, 2020; Sarkar et al., 2020; Cheng et al., 2023). Abnormal autophagy is detected in the perilesional cortex after 12 weeks following TBI (Ritzel et al., 2022). However, few studies have focused on the pattern of cell death in the ipsilateral hippocampus during chronic phase of TBI. In the present study, we disclosed that apoptosis accounted for the long-term chronic neuronal loss in the ipsilateral hippocampus following TBI, which is consistent with the previous study that elevated cleaved-caspase-3 in the ipsilateral thalamus resulted in chronic myelin pathology following TBI (Glushakov et al., 2018). Further studies on the manner of neuronal impairment in different regions during the late phase of TBI are warranted.

During the early stage of TBI, excessive ROS are generated by granulocytes and macrophages rather than activated or resting microglia, leading to extensive oxidative stress at the lesion site (Abe et al., 2018; Wu et al., 2022). In the chronic phase of TBI, microglia or macrophages contribute more to ROS generation and oxidative stress in the injured brain, which is supported by the increased NADPH oxidase (NOX2) in the microglia or macrophages at 1 year post injury (Loane et al., 2014). Although we did not explore the source of ROS in the late phase of adolescent TBI, the aggravated oxidative stress in the ipsilateral hippocampus may contribute to the neurological dysfunction in middle-aged mice. Our present data is consistent with the previous study that oxidative stress is one of the etiologies of various neurodegenerative diseases (George et al., 2022).

It has been reported that astrocytes and microglia/macrophages play important roles in the initiation and persistence of inflammatory responses following TBI (Mira et al., 2021). Our present study revealed that the persistent reactive astrocytes undergo morphological changes in the ipsilateral hippocampus during the whole observed chronic phase, which is consistent with the previous study that reactive gliosis is maintained for up to 60 days following injury in the CCI model (Villapol et al., 2014). The reactive astrogliosis may secrete various cytokines/chemokines and transform into A1 neurotoxic astrocytes to influence the local inflammatory microenvironment, which is supported by the evidence that astrocytic complement C3 is linked to various neurological diseases (Yun et al., 2018; Clark et al., 2019; Li et al., 2022; Stym-Popper et al., 2023). In line with the intricate spatial morphological structure of reactive astrogliosis post injury, we observed that certain astrocytes in the hippocampal hilus underwent morphological complexity, which might contribute to the neuronal damage in the chronic phase of TBI.

Microglia is recognized as the most important contributor to inflammation following TBI. Reactive microglia are found in multiple brain regions in the early and late stages of TBI (Loane et al., 2014). In our study, M1 subtype of the microglia was demonstrated to be a chronic and possibly lifelong event in the ipsilateral hippocampus post injury, which is also consistent with the previous opinion that microglia maintains a prolonged proinflammatory state after brain trauma (Loane et al., 2014). Some studies have reported that the reactivate microglia and the proinflammatory subtype of microglia may enhance the phagocytosis of degenerative axons and synapsis in mouse models of multiple neurodegenerative diseases (Alawieh et al., 2021; Guo et al., 2022). Though we did not test the phagocytotic capability of reactive microglia in hippocampus, the reactive microglia in the late stage of TBI may partly account for the neurological dysfunction in the late life of TBI mice.

Considering that NRF2 is the most important element for mediating antioxidant and anti-inflammatory response in both human and rodent TBI models (Dong et al., 2018, 2019; Guo et al., 2019; He et al., 2019), our previous study reveals that NRF2 is ubiquitously activated in neurons, astrocytes, microglia, and

oligodendrocytes in the early stages of TBI in a spatial and temporal pattern (Dong et al., 2018, 2019; Guo et al., 2019; He et al., 2019). In our present study, persistent NRF2, and its regulated genes, HMOX-1 and NQO-1 were triggered by TBI within 6 mpi. However, it is not sufficient to antagonize the chronic oxidative stress. In addition, NRF2-mediated antioxidative response decreased sharply in the middle-aged mice (12 mpi), which is consistent with the previous studies that downregulation of NRF2 results in increased oxidative stress in aged mice (Zhang et al., 2015; Schmidlin et al., 2019) and neurodegenerative diseases (Osama et al., 2020; Zgorzynska et al., 2021). The lack of NRF2 in the late life of TBI mice may also account for the enhanced inflammation and neural dysfunction, which is supported by the evidence that NRF2 ablation leads to the increase of proinflammatory cytokines and modulation of microglial dynamics (Rojo et al., 2010; Chen et al., 2018). Thus, chronic oxidative stress and neuroinflammation in the hippocampus may be linked with the physical deficiency of NRF2 in the late life of TBI mice, which also needs further investigation.

Conclusion

Our study describes the dynamic neurological dysfunction in the chronic late phase of TBI. The persistent neuroinflammation and oxidative stress contribute to the neuronal apoptosis and neural dysfunction in the late life of adolescent TBI mice. The aggravated neurological dysfunction in middle-age of the TBI mice may be partly associated with the physical deficiency of NRF2. Our present study provides significant insights into the mechanism underlying the long-term neurological decline post-injury in adolescent individuals and the detrimental effects of TBI in the late life of the victims.

Data availability statement

The raw data supporting the conclusions of this article will be made available by the authors, without undue reservation.

Ethics statement

The animal study was approved by Animal Ethics Committee of China Medical University. The study was conducted in accordance with the local legislation and institutional requirements.

Author contributions

ZC: Writing – original draft. PW: Formal analysis, Writing – review & editing. HC: Methodology, Writing – review & editing. NW: Writing – review & editing. MW: Writing – review & editing. ZiW: Writing – review & editing. ZhW: Writing – review & editing. WD: Writing – review & editing. DG: Writing – review & editing. LW: Writing – review & editing. RZ: Funding acquisition, Project administration, Supervision, Writing – review & editing.

Funding

The author(s) declare financial support was received for the research, authorship, and/or publication of this article. This work was supported by grant from the National Natural Science Foundation of China (81971793, 82002003, 82371894), and Liaoning Natural Science Foundation (2022-YGJC-74, 20180550722), Shenyang science and technology innovation support plan for young and middle-age talent (RC200412).

Conflict of interest

The authors declare that the research was conducted in the absence of any commercial or financial relationships that could be construed as a potential conflict of interest.

Publisher's note

Supplementary material

The Supplementary material for this article can be found online at: https://www.frontiersin.org/articles/10.3389/fnins.2023.1292014/full#supplementary-material

References

Abe, N., Choudhury, M. E., Watanabe, M., Kawasaki, S., Nishihara, T., Yano, H., et al. (2018). Comparison of the detrimental features of microglia and infiltrated macrophages in traumatic brain injury: a study using a hypnotic bromovalerylurea. *Glia* 66, 2158–2173. doi: 10.1002/glia.23469

Akamatsu, Y., and Hanafy, K. A. (2020). Cell death and recovery in traumatic brain injury. *Neurotherapeutics* 17, 446–456. doi: 10.1007/s13311-020-00840-7

Alawieh, A., Chalhoub, R. M., Mallah, K., Langley, E. F., York, M., Broome, H., et al. (2021). Complement drives synaptic degeneration and progressive cognitive decline in the chronic phase after traumatic brain injury. *J. Neurosci.* 41, 1830–1843. doi: 10.1523/JNEUROSCI.1734-20.2020

Bartnik-Olson, B., Holshouser, B., Ghosh, N., Oyoyo, U. E., Nichols, J. G., Pivonka-Jones, J., et al. (2021). Evolving white matter injury following pediatric traumatic brain injury. *J. Neurotrauma* 38, 111–121. doi: 10.1089/neu.2019.6574

Bondi, H., Bortolotto, V., Canonico, P. L., and Grilli, M. (2021). Complex and regional-specific changes in the morphological complexity of GFAP(+) astrocytes in middle-aged mice. *Neurobiol. Aging* 100, 59–71. doi: 10.1016/j.neurobiolaging.2020.12.018

Bourke, N. J., Demarchi, C., De Simoni, S., Samra, R., Patel, M. C., Kuczynski, A., et al. (2022). Brain volume abnormalities and clinical outcomes following paediatric traumatic brain injury. *Brain* 145, 2920–2934. doi: 10.1093/brain/awac130

Braun, M., Vaibhav, K., Saad, N. M., Fatima, S., Vender, J. R., Baban, B., et al. (2017). White matter damage after traumatic brain injury: a role for damage associated molecular patterns. *Biochim Biophys Acta Mol Basis Dis* 1863, 2614–2626. doi: 10.1016/j.bbadis.2017.05.020

Brett, B. L., Gardner, R. C., Godbout, J., Dams-O'Connor, K., and Keene, C. D. (2022). Traumatic brain injury and risk of neurodegenerative disorder. *Biol. Psychiatry* 91, 498–507. doi: 10.1016/j.biopsych.2021.05.025

Browne, C. A., Wulf, H. A., Jacobson, M. L., Oyola, M. G., Wu, T. J., and Lucki, I. (2022). Long-term increase in sensitivity to ketamine's behavioral effects in mice exposed to mild blast induced traumatic brain injury. *Exp. Neurol.* 350:113963. doi: 10.1016/j.expneurol.2021.113963

Buendia, I., Michalska, P., Navarro, E., Gameiro, I., Egea, J., and León, R. (2016). Nrf2-ARE pathway: an emerging target against oxidative stress and neuroinflammation in neurodegenerative diseases. *Pharmacol. Ther.* 157, 84–104. doi: 10.1016/j.pharmthera.2015.11.003

Burke, J., Gugger, J., Ding, K., Kim, J. A., Foreman, B., Yue, J. K., et al. (2021). Association of Posttraumatic Epilepsy with 1-year outcomes after traumatic brain injury. *JAMA Netw. Open* 4:e2140191. doi: 10.1001/jamanetworkopen.2021.40191

Chen, X., Liu, S., Zhang, W., Wu, C., Liu, H., Zhang, F., et al. (2018). Nrf2 deficiency exacerbates PM(2.5)-induced olfactory bulb injury. *Biochem. Biophys. Res. Commun.* 505, 1154–1160. doi: 10.1016/j.bbrc.2018.10.057

Cheng, H., Wang, N., Ma, X., Wang, P., Dong, W., Chen, Z., et al. (2022). Spatial-temporal changes of iron deposition and iron metabolism after traumatic brain injury in mice. *Front. Mol. Neurosci.* 15:949573. doi: 10.3389/fnmol.2022.949573

Cheng, H., Wang, P., Wang, N., Dong, W., Chen, Z., Wu, M., et al. (2023). Neuroprotection of NRF2 against Ferroptosis after traumatic brain injury in mice. *Antioxidants (Basel).* 12:3. doi: 10.3390/antiox12030731

Clark, D. P. Q., Perreau, V. M., Shultz, S. R., Brady, R. D., Lei, E., Dixit, S., et al. (2019). Inflammation in traumatic brain injury: roles for toxic A1 astrocytes and microglial-astrocytic crosstalk. *Neurochem. Res.* 44, 1410–1424. doi: 10.1007/s11064-019-02721-8

Cole, J. H., Jolly, A., de Simoni, S., Bourke, N., Patel, M. C., Scott, G., et al. (2018). Spatial patterns of progressive brain volume loss after moderate-severe traumatic brain injury. *Brain* 141, 822–836. doi: 10.1093/brain/awx354

Corps, K. N., Roth, T. L., and McGavern, D. B. (2015). Inflammation and neuroprotection in traumatic brain injury. *JAMA Neurol.* 72, 355–362. doi: 10.1001/jamaneurol.2014.3558

Cui, C., Wang, C., Jin, F., Yang, M., Kong, L., Han, W., et al. (2021). Calcitriol confers neuroprotective effects in traumatic brain injury by activating Nrf2 signaling through an autophagy-mediated mechanism. *Mol. Med.* 27:118. doi: 10.1186/s10020-021-00377-1

Diaz-Castro, B., Gangwani, M. R., Yu, X., Coppola, G., and Khakh, B. S. (2019). Astrocyte molecular signatures in Huntington's disease. *Sci. Transl. Med.* 11:8546. doi: 10.1126/scitranslmed.aaw8546

Dong, W., Sun, Y., Cheng, H., Yang, B., Wang, L., Jiang, Z., et al. (2019). Dynamic cell type-specific expression of Nrf2 after traumatic brain injury in mice. *Eur. J. Neurosci.* 50, 1981–1993. doi: 10.1111/ejn.14399

Dong, W., Yang, B., Wang, L., Li, B., Guo, X., Zhang, M., et al. (2018). Curcumin plays neuroprotective roles against traumatic brain injury partly via Nrf2 signaling. *Toxicol. Appl. Pharmacol.* 346, 28–36. doi: 10.1016/j.taap.2018.03.020

Faden, A. I., Wu, J., Stoica, B. A., and Loane, D. J. (2016). Progressive inflammation-mediated neurodegeneration after traumatic brain or spinal cord injury. *Br. J. Pharmacol.* 173, 681–691. doi: 10.1111/bph.13179

Filley, C. M., and Fields, R. D. (2016). White matter and cognition: making the connection. *J. Neurophysiol.* 116, 2093–2104. doi: 10.1152/jn.00221.2016

George, M., Tharakan, M., Culberson, J., Reddy, A. P., and Reddy, P. H. (2022). Role of Nrf2 in aging, Alzheimer's and other neurodegenerative diseases. *Ageing Res. Rev.* 82:101756. doi: 10.1016/j.arr.2022.101756

Glushakov, A. O., Glushakova, O. Y., Korol, T. Y., Acosta, S. A., Borlongan, C. V., Valadka, A. B., et al. (2018). Chronic upregulation of cleaved-Caspase-3 associated with chronic myelin pathology and microvascular reorganization in the thalamus after traumatic brain injury in rats. *Int. J. Mol. Sci.* 19:3151. doi: 10.3390/ijms19103151

Guo, S., Wang, H., and Yin, Y. (2022). Microglia polarization from M1 to M2 in neurodegenerative diseases. *Front. Aging Neurosci.* 14:815347. doi: 10.3389/fnagi.2022.815347

Guo, X. S., Wen, S. H., Dong, W. W., Li, B. X., Chen, Z. Y., Wang, L. L., et al. (2019). Expression of Nrf2 in different cells after human cerebral cortex contusion. *Fa Yi Xue Za Zhi* 35, 273–279. doi: 10.12116/j.issn.1004-5619.2019.03.002

He, Y., Yan, H., Ni, H., Liang, W., and Jin, W. (2019). Expression of nuclear factor erythroid 2-related factor 2 following traumatic brain injury in the human brain. *Neuroreport* 30, 344–349. doi: 10.1097/WNR.0000000000001205

Karve, I. P., Taylor, J. M., and Crack, P. J. (2016). The contribution of astrocytes and microglia to traumatic brain injury. *Br. J. Pharmacol.* 173, 692–702. doi: 10.1111/bph.13125

Khatri, N., Sumadhura, B., Kumar, S., Kaundal, R. K., Sharma, S., and Datusalia, A. K. (2021). The complexity of secondary Cascade consequent to traumatic brain injury: pathobiology and potential treatments. *Curr. Neuropharmacol.* 19, 1984–2011. doi: 10.2174/1570159X19666210215123914

Leng, L., Zhuang, K., Liu, Z., Huang, C., Gao, Y., Chen, G., et al. (2018). Menin deficiency leads to depressive-like behaviors in mice by modulating astrocyte-mediated Neuroinflammation. *Neuron* 100, 551–563.e7. doi: 10.1016/j.neuron.2018.08.031

Li, W., Ali, T., He, K., Liu, Z., Shah, F. A., Ren, Q., et al. (2021). Ibrutinib alleviates LPS-induced neuroinflammation and synaptic defects in a mouse model of depression. *Brain Behav. Immun.* 92, 10–24. doi: 10.1016/j.bbi.2020.11.008

Li, S., Fang, Y., Zhang, Y., Song, M., Zhang, X., Ding, X., et al. (2022). Microglial NLRP3 inflammasome activates neurotoxic astrocytes in depression-like mice. *Cell Rep.* 41:111532. doi: 10.1016/j.celrep.2022.111532

Li, T., Wang, H., Ding, Y., Zhou, M., Zhou, X., Zhang, X., et al. (2014). Genetic elimination of Nrf2 aggravates secondary complications except for vasospasm after experimental subarachnoid hemorrhage in mice. *Brain Res.* 1558, 90–99. doi: 10.1016/j.brainres.2014.02.036

Liu, Z. M., Chen, Q. X., Chen, Z. B., Tian, D. F., Li, M. C., Wang, J. M., et al. (2018). RIP3 deficiency protects against traumatic brain injury (TBI) through suppressing oxidative stress, inflammation and apoptosis: dependent on AMPK pathway. *Biochem. Biophys. Res. Commun.* 499, 112–119. doi: 10.1016/j.bbrc.2018.02.150

Loane, D. J., Kumar, A., Stoica, B. A., Cabatbat, R., and Faden, A. I. (2014). Progressive neurodegeneration after experimental brain trauma: association with chronic microglial activation. *J. Neuropathol. Exp. Neurol.* 73, 14–29. doi: 10.1097/NEN.0000000000000021

Lu, X. Y., Wang, H. D., Xu, J. G., Ding, K., and Li, T. (2015). Deletion of Nrf2 exacerbates oxidative stress after traumatic brain injury in mice. *Cell. Mol. Neurobiol.* 35, 713–721. doi: 10.1007/s10571-015-0167-9

Ma, X., Aravind, A., Pfister, B. J., Chandra, N., and Haorah, J. (2019). Animal models of traumatic brain injury and assessment of injury severity. *Mol. Neurobiol.* 56, 5332–5345. doi: 10.1007/s12035-018-1454-5

Ma, M. W., Wang, J., Zhang, Q., Wang, R., Dhandapani, K. M., Vadlamudi, R. K., et al. (2017). NADPH oxidase in brain injury and neurodegenerative disorders. *Mol. Neurodegener.* 12:7. doi: 10.1186/s13024-017-0150-7

Maas, A. I. R., Menon, D. K., Adelson, P. D., Andelic, N., Bell, M. J., Belli, A., et al. (2017). Traumatic brain injury: integrated approaches to improve prevention, clinical care, and research. *Lancet Neurol.* 16, 987–1048. doi: 10.1016/S1474-4422(17)30371-X

Mackay, G. M., Forrest, C. M., Stoy, N., Christofides, J., Egerton, M., Stone, T. W., et al. (2006). Tryptophan metabolism and oxidative stress in patients with chronic brain injury. *Eur. J. Neurol.* 13, 30–42. doi: 10.1111/j.1468-1331.2006.01220.x

Maegele, M., Schöchl, H., Menovsky, T., Maréchal, H., Marklund, N., Buki, A., et al. (2017). Coagulopathy and haemorrhagic progression in traumatic brain injury: advances in mechanisms, diagnosis, and management. *Lancet Neurol.* 16, 630–647. doi: 10.1016/S1474-4422(17)30197-7

Mao, X., Terpolilli, N. A., Wehn, A., Cheng, S., Hellal, F., Liu, B., et al. (2020). Progressive histopathological damage occurring up to one year after experimental traumatic brain injury is associated with cognitive decline and depression-like behavior. *J. Neurotrauma* 37, 1331–1341. doi: 10.1089/neu.2019.6510

Max, J. E., Troyer, E. A., Arif, H., Vaida, F., Wilde, E. A., Bigler, E. D., et al. (2022). Traumatic brain injury in children and adolescents: psychiatric disorders 24 years later. *J. Neuropsychiatry Clin. Neurosci.* 34, 60–67. doi: 10.1176/appi.neuropsych.20050104

Medeiros, G. C., Twose, C., Weller, A., Dougherty, J. W. 3rd, Goes, F. S., Sair, H. I., et al. (2022). Neuroimaging correlates of depression after traumatic brain injury: a systematic review. *J. Neurotrauma* 39, 755–772. doi: 10.1089/neu.2021.0374

Mira, R. G., Lira, M., and Cerpa, W. (2021). Traumatic brain injury: mechanisms of glial response. *Front. Physiol.* 12:740939. doi: 10.3389/fphys.2021.740939

Mohamed, A. Z., Cumming, P., and Nasrallah, F. A. (2021). White matter alterations are associated with cognitive dysfunction decades after moderate-to-severe traumatic brain injury and/or posttraumatic stress disorder. *Biol Psychiatry Cogn Neurosci Neuroimaging.* 6, 1100–1109. doi: 10.1016/j.bpsc.2021.04.014

Moretti, L., Cristofori, I., Weaver, S. M., Chau, A., Portelli, J. N., and Grafman, J. (2012). Cognitive decline in older adults with a history of traumatic brain injury. *Lancet Neurol.* 11, 1103–1112. doi: 10.1016/S1474-4422(12)70226-0

Navarro-Main, B., Castaño-León, A. M., Hilario, A., Lagares, A., Rubio, G., Periañez, J. A., et al. (2021). Apathetic symptoms and white matter integrity after traumatic brain injury. *Brain Inj.* 35, 1043–1053. doi: 10.1080/02699052.2021.1953145

Obenaus, A., Rodriguez-Grande, B., Lee, J. B., Dubois, C. J., Fournier, M. L., Cador, M., et al. (2023). A single mild juvenile TBI in male mice leads to regional brain tissue abnormalities at 12 months of age that correlate with cognitive impairment at the middle age. *Acta Neuropathol. Commun.* 11:32. doi: 10.1186/s40478-023-01515-y

Osama, A., Zhang, J., Yao, J., Yao, X., and Fang, J. (2020). Nrf2: a dark horse in Alzheimer's disease treatment. *Ageing Res. Rev.* 64:101206. doi: 10.1016/j.arr.2020.101206

Pischiutta, F., Micotti, E., Hay, J. R., Marongiu, I., Sammali, E., Tolomeo, D., et al. (2018). Single severe traumatic brain injury produces progressive pathology with ongoing contralateral white matter damage one year after injury. *Exp. Neurol.* 300, 167–178. doi: 10.1016/j.expneurol.2017.11.003

Quaglio, G., Gallucci, M., Brand, H., Dawood, A., and Cobello, F. (2017). Traumatic brain injury: a priority for public health policy. *Lancet Neurol.* 16, 951–952. doi: 10.1016/s1474-4422(17)30370-8

Ramlackhansingh, A. F., Brooks, D. J., Greenwood, R. J., Bose, S. K., Turkheimer, F. E., Kinnunen, K. M., et al. (2011). Inflammation after trauma: microglial activation and traumatic brain injury. *Ann. Neurol.* 70, 374–383. doi: 10.1002/ana.22455

Ren, P., Chen, J., Li, B., Zhang, M., Yang, B., Guo, X., et al. (2020). Nrf2 ablation promotes Alzheimer's disease-like pathology in APP/PS1 transgenic mice: the role of neuroinflammation and oxidative stress. *Oxidative Med. Cell. Longev.* 2020:3050971. doi: 10.1155/2020/3050971

Richmond, E., and Rogol, A. D. (2014). Traumatic brain injury: endocrine consequences in children and adults. *Endocrine* 45, 3–8. doi: 10.1007/s12020-013-0049-1

Ritzel, R. M., Li, Y., Lei, Z., Carter, J., He, J., Choi, H. M. C., et al. (2022). Functional and transcriptional profiling of microglial activation during the chronic phase of TBI identifies an age-related driver of poor outcome in old mice. *Geroscience.* 44, 1407–1440. doi: 10.1007/s11357-022-00562-y

Rodgin, S., Suskauer, S. J., Chen, J., Katz, E., Davis, K. C., and Slomine, B. S. (2021). Very long-term outcomes in children admitted in a disorder of consciousness after severe traumatic brain injury. *Arch. Phys. Med. Rehabil.* 102, 1507–1513. doi: 10.1016/j.apmr.2021.01.084

Rojo, A. I., Innamorato, N. G., Martín-Moreno, A. M., De Ceballos, M. L., Yamamoto, M., and Cuadrado, A. (2010). Nrf2 regulates microglial dynamics and neuroinflammation in experimental Parkinson's disease. *Glia* 58, 588–598. doi: 10.1002/glia.20947

Rojo, A. I., Pajares, M., García-Yagüe, A. J., Buendia, I., Van Leuven, F., Yamamoto, M., et al. (2018). Deficiency in the transcription factor NRF2 worsens inflammatory parameters in a mouse model with combined tauopathy and amyloidopathy. *Redox Biol.* 18, 173–180. doi: 10.1016/j.redox.2018.07.006

Sanchez, E., Blais, H., Duclos, C., Arbour, C., Van Der Maren, S., El-Khatib, H., et al. (2022). Sleep from acute to chronic traumatic brain injury and cognitive outcomes. *Sleep* 45:zsac123. doi: 10.1093/sleep/zsac123

Sarkar, C., Jones, J. W., Hegdekar, N., Thayer, J. A., Kumar, A., Faden, A. I., et al. (2020). PLA2G4A/cPLA2-mediated lysosomal membrane damage leads to inhibition of autophagy and neurodegeneration after brain trauma. *Autophagy* 16, 466–485. doi: 10.1080/15548627.2019.1628538

Schmidlin, C. J., Dodson, M. B., Madhavan, L., and Zhang, D. D. (2019). Redox regulation by NRF2 in aging and disease. *Free Radic. Biol. Med.* 134, 702–707. doi: 10.1016/j.freeradbiomed.2019.01.016

Siebold, L., Obenaus, A., and Goyal, R. (2018). Criteria to define mild, moderate, and severe traumatic brain injury in the mouse controlled cortical impact model. *Exp. Neurol.* 310, 48–57. doi: 10.1016/j.expneurol.2018.07.004

Sigfridsson, E., Marangoni, M., Hardingham, G. E., Horsburgh, K., and Fowler, J. H. (2020). Deficiency of Nrf2 exacerbates white matter damage and microglia/macrophage levels in a mouse model of vascular cognitive impairment. *J. Neuroinflammation* 17:367. doi: 10.1186/s12974-020-02038-2

Smith, D. H., Chen, X. H., Pierce, J. E., Wolf, J. A., Trojanowski, J. Q., Graham, D. I., et al. (1997). Progressive atrophy and neuron death for one year following brain trauma in the rat. *J. Neurotrauma* 14, 715–727. doi: 10.1089/neu.1997.14.715

Song, N., Zhu, H., Xu, R., Liu, J., Fang, Y., Zhang, J., et al. (2020). Induced expression of kir6.2 in A1 astrocytes propagates inflammatory neurodegeneration via Drp1-dependent mitochondrial fission. *Front. Pharmacol.* 11:618992. doi: 10.3389/fphar.2020.618992

Stopa, B. M., Tahir, Z., Mezzalira, E., Boaro, A., Khawaja, A., Grashow, R., et al. (2021). The impact of age and severity on dementia after traumatic brain injury: a comparison study. *Neurosurgery* 89, 810–818. doi: 10.1093/neuros/nyab297

Stym-Popper, G., Matta, K., Chaigneau, T., Rupra, R., Demetriou, A., Fouquet, S., et al. (2023). Regulatory T cells decrease C3-positive reactive astrocytes in Alzheimer-like pathology. *J. Neuroinflammation* 20:64. doi: 10.1186/s12974-023-02702-3

Sun, H., Luo, C., Chen, X., and Tao, L. (2017). Assessment of cognitive dysfunction in traumatic brain injury patients: a review. *Forensic Sci Res.* 2, 174–179. doi: 10.1080/20961790.2017.1390836

Takahashi, S., Fukushima, H., Yu, Z., Tomita, H., and Kida, S. (2021). Tumor necrosis factor α negatively regulates the retrieval and reconsolidation of hippocampus-dependent memory. *Brain Behav. Immun.* 94, 79–88. doi: 10.1016/j.bbi.2021.02.033

Tartt, A. N., Mariani, M. B., Hen, R., Mann, J. J., and Boldrini, M. (2022). Dysregulation of adult hippocampal neuroplasticity in major depression: pathogenesis and therapeutic implications. *Mol. Psychiatry* 27, 2689–2699. doi: 10.1038/s41380-022-01520-y

Taylor, X., Cisternas, P., You, Y., You, Y., Xiang, S., Marambio, Y., et al. (2020). A1 reactive astrocytes and a loss of TREM2 are associated with an early stage of pathology in a mouse model of cerebral amyloid angiopathy. *J. Neuroinflammation* 17:223. doi: 10.1186/s12974-020-01900-7

Tomaszczyk, J. C., Green, N. L., Frasca, D., Colella, B., Turner, G. R., Christensen, B. K., et al. (2014). Negative neuroplasticity in chronic traumatic brain injury and implications for neurorehabilitation. *Neuropsychol. Rev.* 24, 409–427. doi: 10.1007/s11065-014-9273-6

Toshkezi, G., Kyle, M., Longo, S. L., Chin, L. S., and Zhao, L. R. (2018). Brain repair by hematopoietic growth factors in the subacute phase of traumatic brain injury. *J. Neurosurg.* 129, 1286–1294. doi: 10.3171/2017.7.JNS17878

Tunc-Ozcan, E., Peng, C. Y., Zhu, Y., Dunlop, S. R., Contractor, A., and Kessler, J. A. (2019). Activating newborn neurons suppresses depression and anxiety-like behaviors. *Nat. Commun.* 10:3768. doi: 10.1038/s41467-019-11641-8

Vadlamani, A., and Albrecht, J. S. (2020). Severity of traumatic brain injury in older adults and risk of ischemic stroke and depression. *J. Head Trauma Rehabil.* 35, E436–e440. doi: 10.1097/HTR.0000000000000561

van Vliet, E. A., Ndode-Ekane, X. E., Lehto, L. J., Gorter, J. A., Andrade, P., Aronica, E., et al. (2020). Long-lasting blood-brain barrier dysfunction and neuroinflammation after traumatic brain injury. *Neurobiol. Dis.* 145:105080. doi: 10.1016/j.nbd.2020.105080

VanItallie, T. B. (2019). Traumatic brain injury (TBI) in collision sports: possible mechanisms of transformation into chronic traumatic encephalopathy (CTE). *Metabolism* 100s:153943. doi: 10.1016/j.metabol.2019.07.007

Vázquez-Rosa, E., Shin, M. K., Dhar, M., Chaubey, K., Cintrón-Pérez, C. J., Tang, X., et al. (2020). P7C3-A20 treatment one year after TBI in mice repairs the blood-brain barrier, arrests chronic neurodegeneration, and restores cognition. *Proc. Natl. Acad. Sci. U. S. A.* 117, 27667–27675. doi: 10.1073/pnas.2010430117

Villapol, S., Byrnes, K. R., and Symes, A. J. (2014). Temporal dynamics of cerebral blood flow, cortical damage, apoptosis, astrocyte-vasculature interaction and astrogliosis in the pericontusional region after traumatic brain injury. *Front. Neurol.* 5:82. doi: 10.3389/fneur.2014.00082

Wang, B., Zeldovich, M., Rauen, K., Wu, Y. J., Covic, A., Muller, I., et al. (2021). Longitudinal analyses of the reciprocity of depression and anxiety after traumatic brain injury and its clinical implications. *J. Clin. Med.* 10:5597. doi: 10.3390/jcm10235597

Wang, H., Zhou, X. M., Wu, L. Y., Liu, G. J., Xu, W. D., Zhang, X. S., et al. (2020). Aucubin alleviates oxidative stress and inflammation via Nrf2-mediated signaling activity in experimental traumatic brain injury. *J. Neuroinflammation* 17:188. doi: 10.1186/s12974-020-01863-9

Wu, A. G., Yong, Y. Y., Pan, Y. R., Zhang, L., Wu, J. M., Zhang, Y., et al. (2022). Targeting Nrf2-mediated oxidative stress response in traumatic brain injury: therapeutic perspectives of phytochemicals. *Oxidative Med. Cell. Longev.* 2022:1015791. doi: 10.1155/2022/1015791

Xie, B. S., Wang, Y. Q., Lin, Y., Mao, Q., Feng, J. F., Gao, G. Y., et al. (2019). Inhibition of ferroptosis attenuates tissue damage and improves long-term outcomes after traumatic brain injury in mice. *CNS Neurosci. Ther.* 25, 465–475. doi: 10.1111/cns.13069

Xu, L. B., Yue, J. K., Korley, F., Puccio, A. M., Yuh, E. L., Sun, X., et al. (2021). High-sensitivity C-reactive protein is a prognostic biomarker of six-month disability after traumatic brain injury: results from the TRACK-TBI study. *J. Neurotrauma* 38, 918–927. doi: 10.1089/neu.2020.7177

Yun, S. P., Kam, T. I., Panicker, N., Kim, S., Oh, Y., Park, J. S., et al. (2018). Block of A1 astrocyte conversion by microglia is neuroprotective in models of Parkinson's disease. *Nat. Med.* 24, 931–938. doi: 10.1038/s41591-018-0051-5

Zgorzynska, E., Dziedzic, B., and Walczewska, A. (2021). An overview of the Nrf2/ARE pathway and its role in neurodegenerative diseases. *Int. J. Mol. Sci.* 22:9592. doi: 10.3390/ijms22179592

Zhang, H., Davies, K. J. A., and Forman, H. J. (2015). Oxidative stress response and Nrf2 signaling in aging. *Free Radic. Biol. Med.* 88, 314–336. doi: 10.1016/j.freeradbiomed.2015.05.036

frontiers | Frontiers in Neuroscience

TYPE Systematic Review
PUBLISHED 24 April 2024
DOI 10.3389/fnins.2024.1383355

OPEN ACCESS

EDITED BY
Nicola Simola,
University of Cagliari, Italy

REVIEWED BY
Annibale Antonioni,
University of Ferrara, Italy
Helge Malmgren,
University of Gothenburg, Sweden

*CORRESPONDENCE
Ephrem Tesfaye
ephremtesfaye126@gmail.com

RECEIVED 07 February 2024
ACCEPTED 05 April 2024
PUBLISHED 24 April 2024

CITATION
Tesfaye E, Getnet M, Anmut Bitew D, Adugna DG and Maru L (2024) Brain functional connectivity in hyperthyroid patients: systematic review. *Front. Neurosci.* 18:1383355. doi: 10.3389/fnins.2024.1383355

Brain functional connectivity in hyperthyroid patients: systematic review

Ephrem Tesfaye[1]*, Mihret Getnet[2,3], Desalegn Anmut Bitew[4], Dagnew Getnet Adugna[5] and Lemlemu Maru[2]

[1]Department of Biomedical Sciences, Madda Walabu University Goba Referral Hospital, Bale-Robe, Ethiopia, [2]Department of Human Physiology, School of Medicine, College of Medicine and Health Science, University of Gondar, Gondar, Ethiopia, [3]Department of Epidemiology and Biostatistics, Institute of Public Health, College of Medicine and Health Science, University of Gondar, Gondar, Ethiopia, [4]Department of Reproductive Health, Institute of Public Health, College of Medicine and Health Science, University of Gondar, Gondar, Ethiopia, [5]Department of Anatomy, School of Medicine, College of Medicine and Health Science, University of Gondar, Gondar, Ethiopia

Introduction: Functional connectivity (FC) is the correlation between brain regions' activities, studied through neuroimaging techniques like fMRI. It helps researchers understand brain function, organization, and dysfunction. Hyperthyroidism, characterized by high serum levels of free thyroxin and suppressed thyroid stimulating hormone, can lead to mood disturbance, cognitive impairment, and psychiatric symptoms. Excessive thyroid hormone exposure can enhance neuronal death and decrease brain volume, affecting memory, attention, emotion, vision, and motor planning.

Methods: We conducted thorough searches across Google Scholar, PubMed, Hinari, and Science Direct to locate pertinent articles containing original data investigating FC measures in individuals diagnosed with hyperthyroidism.

Results: The systematic review identified 762 articles, excluding duplicates and non-matching titles and abstracts. Four full-text articles were included in this review. In conclusion, a strong bilateral hippocampal connection in hyperthyroid individuals suggests a possible neurobiological influence on brain networks that may affect cognitive and emotional processing.

Systematic Review Registration: PROSPERO, CRD42024516216.

KEYWORDS

brain, fMRI, functional connectivity, hyperthyroid, resting-state fMRI

Introduction

Functional connectivity (FC) refers to the statistical correlation between the activities of different brain regions, typically observed through neuroimaging techniques such as functional magnetic resonance imaging (fMRI) (Müller, 2013; Cao et al., 2022; Ursino et al., 2022). Studies of it aim to understand how different brain regions communicate and coordinate their activities during various cognitive processes or in different states (Cao et al., 2022). Analyses of it have become increasingly important in neuroscience, offering valuable information about brain function, organization, and dysfunction. Researchers use these analyses to explore normal brain function, investigate neurological and psychiatric disorders, and assess the effects of interventions or treatments on brain connectivity patterns (Wojtalik et al., 2018).

Hyperthyroidism is defined as a high serum level of free thyroxin (FT4) and/or triiodothyronin (T3) and a suppressed thyroid stimulating hormone (TSH) level (Samuels, 2014; Ross et al., 2016). Thyroid hormone (TH) is essential for normal brain development and may also promote recovery and neuronal regeneration after brain injury (Liu and Brent, 2018; Talhada et al., 2019). Thyroid hormones are essential for appropriate growth, reproduction, and regulation of energy metabolism, neuronal development, and cognitive and behavioral development (Stasiolek, 2015; Taylor et al., 2018; Mathew et al., 2020). The mechanisms include the regulation of neuronal plasticity processes, stimulation of angiogenesis and neurogenesis, as we as modulating the dynamics of cytoskeletal elements, and intracellular transport processes (Talhada et al., 2019).

It is clear that without optimal thyroid function, mood disturbance, cognitive impairment, and other psychiatric symptoms can emerge (Lekurwale et al., 2023). In animal studies, changes in the release pattern of acetylcholine and monoamines have been found in the hippocampus and frontal cortex of experimentally induced hyperthyroid rats, along with associated functional changes (Eslami-Amirabadi and Sajjadi, 2021). Particularly in severe cases, thyroid dysfunction can result in a variety of emotional and cognitive disorders, such as executive function deficiencies, depression, anxiety, and irritability (Samuels, 2014; Stasiolek, 2015).

Related to the morphological changes of hyperthyroid individuals in the brain, exposure to excess thyroid hormones has been shown to enhance neuronal death and decrease brain volume (Folkestad et al., 2020), which leads to more severe atrophy of the amygdala (Wu et al., 2016; Eslami-Amirabadi and Sajjadi, 2021) and hippocampus (Wu et al., 2016; Eslami-Amirabadi and Sajjadi, 2021; Quinlan et al., 2022). Hyperthyroid patients exhibited reduced grey matter volume in regions associated with memory, attention, emotion, vision, and motor planning (Zhang et al., 2014).

The exploration of functional connectivity between brain regions is deemed essential to elucidate the neuropsychiatric symptoms associated with hyperthyroidism and the impact of elevated thyroid hormone levels on the adult brain (Cao et al., 2022; Lekurwale et al., 2023). Thyroid hormones play a crucial role in functional connectivity under physiological conditions (Schroeder and Privalsky, 2014). In the brain, T4 is converted to active T3 by type 2 deiodinase produced by glial cells, highlighting the importance of these hormones in brain development and function (Fingeret, 2024). Studies revealed functional connectivity changes in hyperthyroid patients, an increase in functional connectivity in the rostral temporal lobes, which is integrated with the cognitive control network (Göbel et al., 2020), lower amplitude of low-frequency fluctuations (ALFF) was found in the patients in the right posterior cingulate cortex, and increased functional connectivity in the bilateral anterior and posterior insula, and importantly, in the left anterior lobe of the cerebellum (Göbel et al., 2020). Research has shown that thyroid hormone functions may play a crucial role in modulating functional connectivity in early-course schizophrenia, impacting cognition and functional outcomes (George et al., 2023), resting-state brain network functional connectivity, and shedding light on the intricate relationship between thyroid function and brain network dynamics (Li et al., 2022).

Despite the significance of certain brain regions in emotional and cognitive regulation, there is a notable gap in research pertaining to the interactions between and within these regions in hyperthyroid patients. This review highlights hyperthyroidism's potential impact on connectivity between brain regions and improves our understanding of the functional connectivity of targeted regions.

Method

Registration and protocol

This study protocol is registered with the International Prospective Register of Systematic Reviews website (PROSPERO; registration number CRD42024516216).

Eligibility criteria

Hyperthyroid patients: all patients who have elevated serum FT3 or FT4 levels, and decreased TSH levels (Ross et al., 2016; Toyib et al., 2019).

Pre/post studies: one experimental session was performed before and one after the end of administration of medications or procedures to assess the impact of medications like anti-thyroid drugs, radioiodine therapy, beta blockers, and thyroidectomy on patients with hyperthyroidism (Doubleday and Sippel, 2020).

We applied the PICO method as a selection criteria for articles:

Population: hyperthyroid patients.

Interventions: thyroid hormone thyroxin replacement therapies, for example, levothyroxine.

Study type: randomized controlled trials, case–control studies, and quasi-experimental studies.

Cases: hyperthyroid patients.

Control: healthy controls.

Outcomes: primary outcome– brain functional connectivity.

Outcome assessment time: There was no limit to the outcome assessment time.

Publication year and language: English-language literature, with publication year not limited. **List of countries**: all countries in the world.

Search strategy and selection criteria

Four databases– PubMed, Hinari, Science Direct, and Google Scholar– were used to identify studies about brain functional connectivity from the inception date to November 21, 2023. Using title, abstract, and keywords, we searched out the primary studies using the keywords selected: brain, connectivity, network, hyperthyroidism, and their synonyms using AND, OR, and NOT filters as described in Supplementary file 2. This systematic review was prepared according to the instructions of the PRISMA guideline.

Data extraction

We developed a form to extract the suitable data, including the following details: (1) characteristics of the papers (authors, publication year, and country); (2) characteristics of the participants (sample size, age range, and drug use); (3) study design and measurement method; (4) method of analysis; and (5) results. Two authors (ET and LM) independently extracted the data, and disagreements were resolved by discussing with the third author (MG).

Results

Identification of eligible studies

Figure 1 shows the result of our screening process. We identified 762 articles with our searching strategy. Duplicate articles ($n = 85$) were excluded. The articles that according to title and abstract did not match the selection criteria ($n = 667$) were also excluded. Finally, four articles out of 10 available full-text articles were included in this systematic review. The details of the excluded six articles are presented in Supplementary file S1.

Characteristics of included studies

The included studies were either case–control or quasi-experimental studies. The etiology of the disease in the three studies was Graves' disease, and one drug-induced pre-and post-study. They were all small studies, with the largest sample size of 47. General characteristics of the studies, like the first author's name, year of publication, country, sample size (case/control or pre-post), age range of participants, and drug use for the study, are shown in Table 1, and the imaging method, study design, analysis method, and results are presented in Table 2.

Discussion

Reviewing the available evidence, we find significant changes in brain functional connectivity among hyperthyroid patients. These alterations imply that hyperthyroidism may impact brain networks neurobiologically. Studying connectivity patterns in healthy individuals and those with hyperthyroidism can help us understand disruptions in thyroid dysfunction networks, clarify cognitive and emotional symptoms in thyroid disorders, and guide future therapeutic interventions targeting neural circuits. In hyperthyroid patients, alterations in functional connectivity have been observed, particularly in regions associated with emotion regulation, memory, and cognitive processing (Chen et al., 2021). Changes in FC observed in hyperthyroid patients can be attributed to several mechanisms and could explain the manifestations of different disorders.

Recent advancements in neuroimaging techniques have shed light on the intricate neural alterations accompanying this disorder

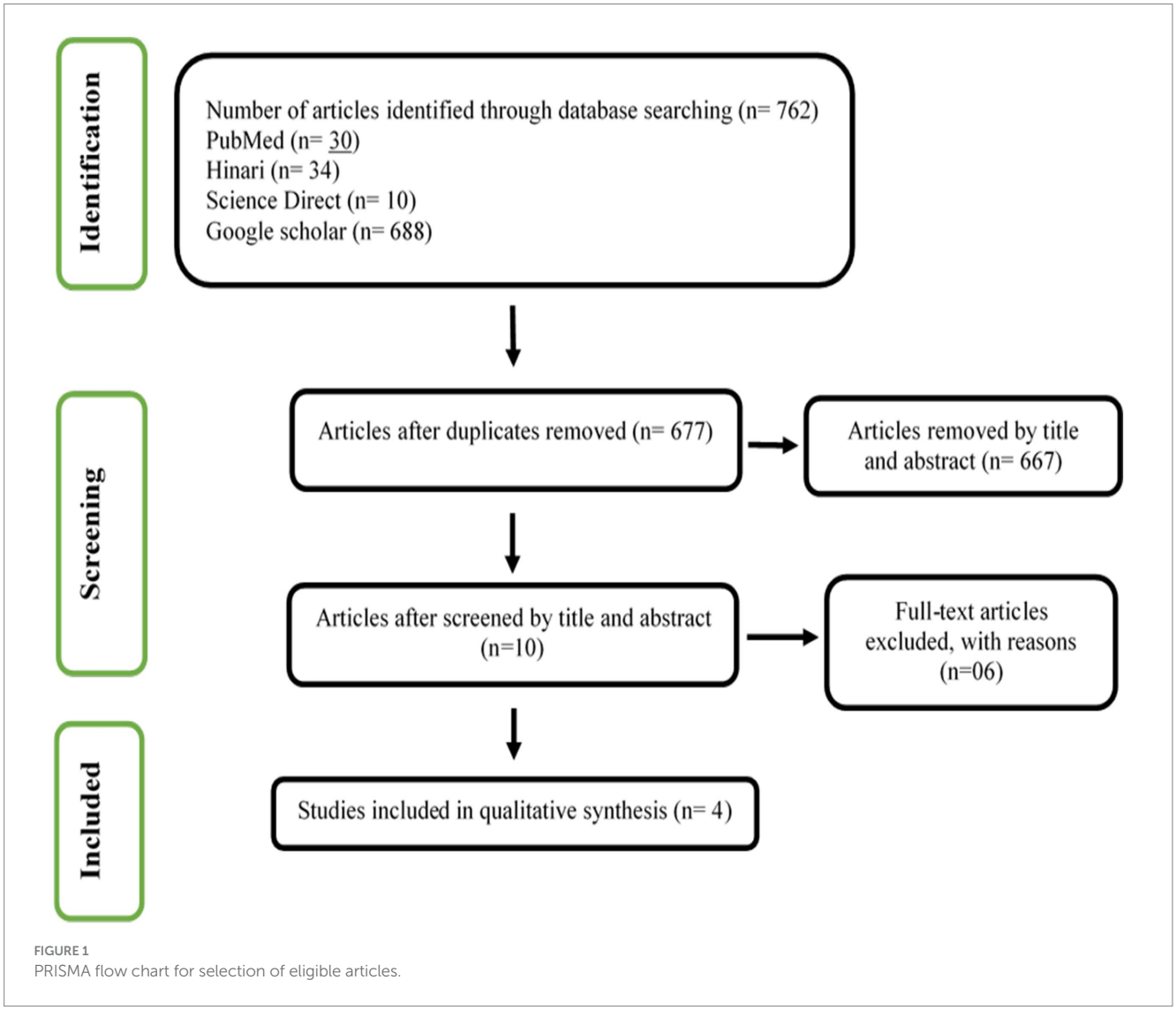

FIGURE 1
PRISMA flow chart for selection of eligible articles.

TABLE 1 General characteristics of the studies included in this systematic review.

Author/year	Country	Patient's characteristics			
		Sample size (n)	Age in years (Mean ± SD)	Duration of disease/ Rx	Etiology of disease
Zhang et al. (2014)	China	-Cases: 46 -Controls: 46	-Case: 29.72 ± 7.93 -Controls: 29.26 ± 6.50	8.74 ± 5.64 months	Graves' disease
Göttlich et al. (2015)	German	$n = 29$	30 (21—49)	Levothyroxine 250 μg per day for 8 weeks	Drug induced
Zhang et al. (2018)	China	-Cases: 13 hyperthyroid pts. -Controls: 13 healthy	-Case: 32.7 ± 10.2 -Controls: 33.2 ± 11.3	–	Graves' disease
Li et al. (2017)	China	-Case: 33 hyperthyroid -Controls: 33 HC	-case: 37.36 ± 12.43 -control: 39.03 ± 13.28	9.94 ± 17.31 months	Graves' disease

(Minnerop et al., 2018; Yen et al., 2023). Among these, changes in FC within the brain have emerged as a critical area of investigation. The observed connectivity between hyperthyroid patients and healthy controls suggests shared neural circuitry, potentially crucial for detecting the hippocampal memory system's operation in humans (Liu et al., 2017; Ma et al., 2022).

One of the central findings of the reviewed papers is the disruption in connectivity patterns involving the hippocampus and cingulate cortex. Zhang et al's. (2014) study found that hyperthyroid individuals show weakened connectivity between the bilateral ACC and PCC and the hippocampi. This suggests that hyperthyroidism affects the limbic system, which is crucial for memory consolidation and emotional regulation. The alterations may indicate cognitive or mental disorders associated with the hippocampus and other brain areas (Li et al., 2017; Yao et al., 2022). Hyper-connectivity patterns may affect the functional connectivity of the default mode network, potentially impacting episodic memory and self-representation (Zanão et al., 2017; Staffaroni et al., 2018; Ursino et al., 2022). The direct effects of thyroid hormones on these brain regions contribute to their functional integrity and connectivity (Biswas and Dey, 2014). Thyroid hormones have receptors in the cingulate cortices and hippocampi. T3 and T4 influence neurotransmitter systems such as glutamate (Ritchie and Yeap, 2015; Zhu et al., 2022), and gamma-aminobutyric acid (GABA) (Yi et al., 2014; Prisciandaro et al., 2021), which are crucial for synaptic transmission and neuronal plasticity in the cingulate cortices (Prisciandaro et al., 2021). Alterations in thyroid hormone levels can disrupt the balance of excitatory and inhibitory neurotransmission, leading to changes in neural connectivity and function within the ACC and PCC and impairing hippocampal function, leading to deficits in memory consolidation, emotional processing, and spatial navigation (Bavarsad et al., 2019).

Moreover, the correlation between FC strength and clinical variables provides valuable insights into the progression of the disease (Zhang et al., 2014). A significant negative correlation was found between disease duration and FC strength between the hippocampi and cingulate cortices (Zhang et al., 2014; Milton et al., 2022). This suggests that as the disease progresses, there is a decline in the integrity of neural circuits linking these regions (Zhi et al., 2018; Johansson et al., 2023), due to adaptive changes or neuronal damage in hyperthyroid patients. In addition, chronic hyperthyroidism could lead to structural (Zhang et al., 2014; Zhe et al., 2021; Duda et al., 2023; Xiong et al., 2023), and functional changes in the hippocampi and cingulate cortices, affecting their connectivity patterns. This is clinically important in identifying neuroimaging markers that can be used to track the progression of hyperthyroidism and assess the effectiveness of treatment interventions (Clerc, 2020).

Beyond hippocampal-cingulate alterations, hyperthyroidism is also associated with changes in FC involving regions crucial for cognitive processing and emotional regulation (Göttlich et al., 2015). Increased degree centrality was observed in temporal regions, including the right inferior temporal gyrus, left middle temporal gyrus, right middle temporal gyrus, and left middle temporal pole. Additionally, there was a significant increase in FC within the bilateral temporal poles and left middle temporal gyrus (Göttlich et al., 2015; Zhang et al., 2018), indicating heightened connectivity within temporal regions. Notably, the left temporal pole exhibited stronger connections with various regions, including the dACC, ITG, and frontal gyrus, underscoring the widespread impact of hyperthyroidism on functional brain networks. Degree centrality refers to the number of connections a node (brain region) has with other nodes in the network (Yoo et al., 2017; Jia et al., 2019). The heightened degree centrality indicates increased functional connectivity and communication within these temporal regions. This indicates increased synchronization and information exchange within these regions (Csató, 2017; Lorenzini et al., 2022). The study suggests that hyperthyroid patients' cognitive deficits may be linked to disrupted functional coordination within the default mode network (DMN), emphasizing the significance of interhemispheric connectivity (Zhi et al., 2018; Berron et al., 2020; Wang et al., 2023).

Conversely, decreased ALFF was noted in regions such as the posterior cingulate gyrus and bilateral inferior parietal gyrus (Zhang et al., 2018), suggesting reduced neural activity. In association with this, Milton et al.'s ROI-based functional connectivity analysis reveals changes in connectivity patterns in the inferior parietal gyrus and posterior cingulate gyrus, indicating complex regional dynamics (Uddin et al., 2009). Additionally, disruptions in FC were observed in cerebellar-frontal circuits, with decreased connectivity between the left PLC and MTG within the attention network (Li et al., 2017). Besides its motor coordination ability, the cerebellum increasingly recognized for its role in cognitive functions, including attention (Li et al., 2017; Liu et al., 2017; Yao et al., 2022). Dysfunction within the cerebellum and frontal regions impairs the coordination and modulation of attention networks (Arif et al., 2020). Damage to the tract and disruptions in neuronal synchronization between the cerebellum and frontal cortex may contribute to decreased functional connectivity (Wang et al., 2023). Cognitive ability is affected by reduced connectivity between cortical regions, particularly the prefrontal cortex, and

TABLE 2 List of studies with their methods and results.

Author/year	Imaging method	Study design	Analysis methods	Result
Zhang et al. (2014)	rs-fMRI	Case–control	Seed voxel correlation approach	Within-group analysis: -The bilateral hippocampus showed strong connectivity to other regions in the bilateral limbic system (hippocampus, parahippocampal gyrus, amygdala, and insula), bilateral temporal lobe (inferior/middle/superior temporal gyrus and temporal pole), thalamus, bilateral basal ganglia (globus pallidus, caudate, and putamen), bilateral frontal lobe (medial/inferior frontal gyrus, orbital frontal cortex, ACC), brainstem, and bilateral cerebellum. Between-group analysis: -The bilateral ACC and PCC showed significantly weaker connectivity to the left hippocampus in the hyperthyroid group. -The hyperthyroid group showed a reduced connection between the bilateral ACC, bilateral PCC, and right medial orbitofrontal cortex (mOFC) with the right hippocampus. Correlation between functional connectivity and clinical variables: -When the seed was located in the left hippocampus, there was a significant negative correlation between disease duration and the strength of FC to both the bilateral ACC and bilateral PCC. -Similarly, when the seed was placed in the right hippocampus, significant negative correlations were found between disease duration and FC strength to both the bilateral ACC and PCC.
Göttlich et al. (2015)	rs-fMRI	Quasi-experimental	-Voxel degree centrality maps -Seed-based functional connectivity	-Increase in degree centrality in the right inferior temporal gyrus, left middle temporal gyrus, right middle temporal gyrus, and left middle temporal pole. -Significantly increase functional connectivity in the bilateral temporal poles and left middle temporal gyrus. -The left temporal pole was significantly stronger and connected to the dorsal anterior cingulate cortex (dACC), inferior temporal gyrus (ITG), inferior frontal gyrus (IFG), middle frontal gyrus (MFG), and supramarginal gyrus (SMG). -The right temporal pole showed significantly stronger connectivity to the MFG, IFG, and SMG.
Zhang et al. (2018)	rs-fMRI	Case–control	-ALFF analysis -region of interest (ROI) -based functional connectivity analysis	-Decreased ALFF values in the patient group included the posterior cingulate gyrus and bilateral inferior parietal gyrus. -Increased ALFF values in the right thalamus and bilateral cuneus -Significant negative correlation between ALFF values of the left inferior parietal gyrus and the left posterior cingulate gyrus -ROI-based FC analysis revealed increased FCs between the left inferior parietal gyrus and left rostral ACC and bilateral frontal lobe; left posterior cingulate gyrus and bilateral left temporal lobe.
Li et al. (2017)	rs-fMRI	Case–control	-Degree centrality -Seed-based connectivity analyses	-Hyperthyroid patients had decreased degree centrality values in the left posterior lobe of the cerebellum and bilateral medial frontal gyrus. -Decreased functional connectivity between seed-1 located in the left posterior lobe of the cerebellum (PLC) and right middle temporal gyrus (MTG) in the attention network. -Lowered functional connectivity from both the left PLC and right cerebellum to the medial frontal gyrus (MeFG).

10.3389/fnins.2024.1383355

sub-cortical regions in schizophrenia (Sheffield and Barch, 2016), bipolar disease (Ursino et al., 2022), depression (Liu et al., 2020), traumatic brain injury (Morelli et al., 2021; Nakuci et al., 2021), stroke (Wang et al., 2023), and functional seizure (Foroughi et al., 2020).

Taken together, these findings highlight the complex nature of the brain changes linked to hyperthyroidism. The dysregulation of thyroid hormones affects multiple pathways and mechanisms within the brain, leading to diverse neurological manifestations. This complexity underscores the need for a comprehensive understanding and management of the neurological aspects of hyperthyroidism. The findings open the door for additional research into the functional implications of these connectivity changes and how they might impact the mental and emotional health of hyperthyroid patients, in addition to expanding our understanding of the brain mechanisms underlying thyroid dysfunction (Ritchie and Yeap, 2015; Eslami-Amirabadi and Sajjadi, 2021). Combining these many viewpoints allows for a more thorough understanding of the complex relationship between thyroid function and brain connections.

Limitations

This systematic review had some limitations.

- The exploration of functional connectivity in neuroscience has encountered limitations, with a paucity of comprehensive studies on the intricate networks that govern brain function. To advance our understanding of the dynamic relationships between distinct brain regions, there is a pressing need for more extensive studies on brain functional connectivity in patients with hyperthyroidism.
- A significant limitation frequently encountered in research is the small sample size. Small sample sizes can magnify individual differences and chance variations, making it challenging to draw robust conclusions or to establish the true effect of an intervention or phenomenon. The studies included in this review had a small sample size, with a minimum of 13 and a maximum of 46.
- All studies used fMRI as the imaging technique. It has limitations compared to other connectivity techniques, including lower temporal resolution (vs. EEG/MEG), sensitivity to motion artifacts, and reliance on blood flow measurement. Techniques like EEG and MEG offer better temporal resolution.

Conclusion and recommendation

In conclusion, research on brain functional connectivity among patients with hyperthyroidism suggests a potential neurobiological impact of hyperthyroidism on intricate brain networks. This study found strong bilateral hippocampal connectivity across various brain regions, suggesting a fundamental neural network. Alterations in connectivity patterns suggest a potential hub role in hyperthyroid states, affecting cognitive and emotional processing. These findings highlight the complex nature of brain changes linked to hyperthyroidism and suggest the need for further investigations into the functional effects of these connectivity alterations on mental and emotional well-being.

We suggest exploring how changes in connectivity affect thinking and emotions in hyperthyroidism patients to help develop better mental health treatments. Furthermore, given the recognized challenge of small sample sizes in research, it is advisable for future studies to strive for larger and more representative samples to enhance the reliability and generalizability of the findings. Additionally, researchers should consider diversifying imaging techniques beyond fMRI to overcome its limitations such as lower temporal resolution and susceptibility to motion artifacts.

Data availability statement

The original contributions presented in the study are included in the article/Supplementary material, further inquiries can be directed to the corresponding author.

Author contributions

ET: Conceptualization, Data curation, Formal analysis, Writing – original draft, Writing – review & editing. MG: Conceptualization, Data curation, Methodology, Supervision, Writing – original draft, Writing – review & editing. DeA: Conceptualization, Data curation, Methodology, Writing – original draft, Writing – review & editing. DaA: Conceptualization, Data curation, Formal analysis, Writing – original draft, Writing – review & editing. LM: Conceptualization, Data curation, Formal analysis, Writing – original draft, Writing – review & editing.

Funding

The author(s) declare that no financial support was received for the research, authorship, and/or publication of this article.

Conflict of interest

The authors declare that the research was conducted in the absence of any commercial or financial relationships that could be construed as a potential conflict of interest.

Publisher's note

All claims expressed in this article are solely those of the authors and do not necessarily represent those of their affiliated organizations, or those of the publisher, the editors and the reviewers. Any product that may be evaluated in this article, or claim that may be made by its manufacturer, is not guaranteed or endorsed by the publisher.

Supplementary material

The Supplementary material for this article can be found online at: https://www.frontiersin.org/articles/10.3389/fnins.2024.1383355/full#supplementary-material

References

Arif, Y., Spooner, R. K., Wiesman, A. I., Embury, C. M., Proskovec, A. L., and Wilson, T. W. (2020). Modulation of attention networks serving reorientation in healthy aging. *Aging (Albany NY)* 12, 12582–12597. doi: 10.18632/aging.103515

Bavarsad, K., Hosseini, M., Hadjzadeh, M. A. R., and Sahebkar, A. (2019). The effects of thyroid hormones on memory impairment and Alzheimer's disease. *J. Cell. Physiol.* 234, 14633–14640. doi: 10.1002/jcp.28198

Berron, D., van Westen, D., Ossenkoppele, R., Strandberg, O., and Hansson, O. (2020). Medial temporal lobe connectivity and its associations with cognition in early Alzheimer's disease. *Brain J. Neurol.* 143, 1233–1248. doi: 10.1093/brain/awaa068

Biswas, T., and Dey, S. K. (2014). Association of Thyroid Dysfunction and Mood Disorders and role of imaging: a review. *Bangladesh J.* 17, 146–152. doi: 10.3329/bjnm.v17i2.28202

Cao, J., Zhao, Y., Shan, X., Wei, H. L., Guo, Y., Chen, L., et al. (2022). Brain functional and effective connectivity based on electroencephalography recordings: a review. *Hum. Brain Mapp.* 43, 860–879. doi: 10.1002/hbm.25683

Chen, W., Wu, Q., Chen, L., Zhou, J., Chen, H.-H., Xu, X.-Q., et al. (2021). Disrupted spontaneous neural activity in patients with thyroid-associated ophthalmopathy: a resting-state fMRI study using amplitude of low-frequency fluctuation. *Front. Hum. Neurosci.* 15:676967. doi: 10.3389/fnhum.2021.676967

Clerc, J. (2020). Quantified 123I-thyroid scan based classification of hyperthyroidism. *Médecine Nucléaire.* 44, 231–249. doi: 10.1016/j.mednuc.2020.07.005

Csató, L. (2017). Measuring centrality by a generalization of degree. *CEJOR* 25, 771–790. doi: 10.1007/s10100-016-0439-6

Doubleday, A. R., and Sippel, R. S. (2020). Hyperthyroidism. *Gland Surg.* 9, 124–135. doi: 10.21037/gs.2019.11.01

Duda, M., Faghiri, A., Belger, A., Bustillo, J. R., Ford, J. M., Mathalon, D. H., et al. (2023). Alterations in grey matter structure linked to frequency-specific cortico-subcortical connectivity in schizophrenia via multimodal data fusion. *bio Rxiv* [Preprint]. doi: 10.1101/2023.07.05.547840

Eslami-Amirabadi, M., and Sajjadi, S. A. (2021). The relation between thyroid dysregulation and impaired cognition/behaviour: an integrative review. *J. Neuroendocrinol.* 33:e12948. doi: 10.1111/jne.12948

Fingeret, MAEAA. *Physiology, thyroid function: Stat pearls*. Treasure Island (FL): StatPearls Publishing, (2024).

Folkestad, L., Brandt, F., Lillevang-Johansen, M., Brix, T. H., and Hegedüs, L. (2020). Graves' disease and toxic nodular goiter, aggravated by duration of hyperthyroidism, are associated with alzheimer's and vascular dementia: a registry-based long-term follow-up of two large cohorts. *Thyroid* 30, 672–680. doi: 10.1089/thy.2019.0672

Foroughi, A. A., Nazeri, M., and Asadi-Pooya, A. A. (2020). Brain connectivity abnormalities in patients with functional (psychogenic nonepileptic) seizures: a systematic review. *Seizure* 81, 269–275. doi: 10.1016/j.seizure.2020.08.024

George, A. B., Beniwal, R. P., Singh, S., Bhatia, T., Khushu, S., and Deshpande, S. N. (2023). Association between thyroid functions, cognition, and functional connectivity of the brain in early-course schizophrenia: a preliminary study. *Ind. Psychiatry J.* 32, S76–s82. doi: 10.4103/ipj.ipj_198_23

Göbel, A., Göttlich, M., Reinwald, J., Rogge, B., Uter, J.-C., Heldmann, M., et al. (2020). The influence of thyroid hormones on brain structure and function in humans. *Exp. Clin. Endocrinol. Diabetes* 128, 432–436. doi: 10.1055/a-1101-9090

Göttlich, M., Heldmann, M., Göbel, A., Dirk, A. L., Brabant, G., and Münte, T. F. (2015). Experimentally induced thyrotoxicosis leads to increased connectivity in temporal lobe structures: a resting state fMRI study. *Psychoneuroendocrinology* 56, 100–109. doi: 10.1016/j.psyneuen.2015.03.009

Jia, P., Liu, J., Huang, C., Liu, L., and Xu, C. (2019). An improvement method for degree and its extending centralities in directed networks. *Physica A* 532:121891. doi: 10.1016/j.physa.2019.121891

Johansson, B., Holmberg, M., Skau, S., Malmgren, H., and Nyström, H. F. (2023). The relationship between mental fatigue, depression, and cognition in graves' disease. *European Thyroid J.* 12. doi: 10.1530/ETJ-23-0040

Lekurwale, V., Acharya, S., Shukla, S., and Kumar, S. (2023). Neuropsychiatric manifestations of thyroid diseases. *Cureus* 15:e33987. doi: 10.7759/cureus.33987

Li, Y., Qin, Y., Luo, Z., and Zhou, J. (2022). The resting-state brain network functional connectivity changes in patients with acute thyrotoxic myopathy based on independent component analysis. *Front. Endocrinol.* 13:829411. doi: 10.3389/fendo.2022.829411

Li, L., Zhi, M., Hou, Z., Zhang, Y., Yue, Y., and Yuan, Y. (2017). Abnormal brain functional connectivity leads to impaired mood and cognition in hyperthyroidism: a resting-state functional MRI study. *Oncotarget* 8, 6283–6294. doi: 10.18632/oncotarget.14060

Liu, Y. Y., and Brent, G. A. (2018). Thyroid hormone and the brain: mechanisms of action in development and role in protection and promotion of recovery after brain injury. *Pharmacol. Ther.* 186, 176–185. doi: 10.1016/j.pharmthera.2018.01.007

Liu, B., Ran, Q., Liu, D., Zhang, S., and Zhang, D. (2017). Changes in resting-state cerebral activity in patients with hyperthyroidism: a short-term follow-up functional MR imaging study. *Sci. Rep.* 7:10627. doi: 10.1038/s41598-017-10747-7

Liu, B., Wen, L., Ran, Q., Zhang, S., Hu, J., Gong, M., et al. (2020). Dysregulation within the salience network and default mode network in hyperthyroid patients: a follow-up resting-state functional MRI study. *Brain Imaging Behav.* 14, 30–41. doi: 10.1007/s11682-018-9961-6

Lorenzini, L., Ingala, S., Collij, L. E., Wottschel, V., Haller, S., Blennow, K., et al. (2022). Functional eigenvector centrality dynamics are related to amyloid deposition in preclinical Alzheimer's disease. *Alzheimers Dement.* 18:e064631. doi: 10.1002/alz.064631

Ma, Q., Rolls, E. T., Huang, C. C., Cheng, W., and Feng, J. (2022). Extensive cortical functional connectivity of the human hippocampal memory system. *Cortex* 147, 83–101. doi: 10.1016/j.cortex.2021.11.014

Mathew, C. J., Jose, M. T., Elshaikh, A. O., Shah, L., Lee, R., and Cancarevic, I. (2020). Is hyperthyroidism a possible etiology of early onset dementia? *Cureus* 12. doi: 10.7759/cureus.10603

Milton, C. K., O'Neal, C. M., and Conner, A. K. (2022). Functional connectivity of hippocampus in temporal lobe epilepsy depends on hippocampal dominance: a systematic review of the literature. *J. Neurol.* 269, 221–232. doi: 10.1007/s00415-020-10391-8

Minnerop, M., Gliem, C., and Kornblum, C. (2018). Current progress in CNS imaging of myotonic dystrophy. *Front. Neurol.* 9:382932. doi: 10.3389/fneur.2018.00646

Morelli, N., Johnson, N. F., Kaiser, K., Andreatta, R. D., Heebner, N. R., and Hoch, M. C. (2021). Resting state functional connectivity responses post-mild traumatic brain injury: a systematic review. *Brain Inj.* 35, 1326–1337. doi: 10.1080/02699052.2021.1972339

Müller, R.-A. (2013). "Functional connectivity" in *Encyclopedia of autism Spectrum disorders*. ed. F. R. Volkmar (Springer New York: New York, NY), 1363–1370.

Nakuci, J., McGuire, M., Schweser, F., Poulsen, D., and Muldoon, S. F. (2021). Differential patterns of change in brain connectivity resulting from traumatic brain injury. *bio Rxiv*. 12, 799–811. doi: 10.1101/2021.10.27.466136

Prisciandaro, J. J., Hoffman, M., Brown, T. R., Voronin, K., Book, S., Bristol, E., et al. (2021). Effects of gabapentin on dorsal anterior cingulate cortex GABA and glutamate levels and their associations with abstinence in alcohol use disorder: a randomized clinical trial. *Am. J. Psychiatry* 178, 829–837. doi: 10.1176/appi.ajp.2021.20121757

Quinlan, P., Horvath, A., Eckerström, C., Wallin, A., and Svensson, J. (2022). Higher thyroid function is associated with accelerated hippocampal volume loss in Alzheimer's disease. *Psychoneuroendocrinology* 139:105710. doi: 10.1016/j.psyneuen.2022.105710

Ritchie, M., and Yeap, B. B. (2015). Thyroid hormone: influences on mood and cognition in adults. *Maturitas* 81, 266–275. doi: 10.1016/j.maturitas.2015.03.016

Ross, D. S., Burch, H. B., Cooper, D. S., Greenlee, M. C., Laurberg, P., Maia, A. L., et al. (2016). 2016 American Thyroid Association guidelines for diagnosis and Management of Hyperthyroidism and Other Causes of thyrotoxicosis. *Thyroid* 26, 1343–1421. doi: 10.1089/thy.2016.0229

Samuels, M. H. (2014). Thyroid disease and cognition. *Endocrinol. Metab. Clin.* 43, 529–543. doi: 10.1016/j.ecl.2014.02.006

Schroeder, A. C., and Privalsky, M. L. (2014). Thyroid hormones, t3 and t4, in the brain. *Front. Endocrinol.* 5:80680. doi: 10.3389/fendo.2014.00040

Sheffield, J. M., and Barch, D. M. (2016). Cognition and resting-state functional connectivity in schizophrenia. *Neurosci. Biobehav. Rev.* 61, 108–120. doi: 10.1016/j.neubiorev.2015.12.007

Staffaroni, A. M., Brown, J. A., Casaletto, K. B., Elahi, F. M., Deng, J., Neuhaus, J., et al. (2018). The longitudinal trajectory of default mode network connectivity in healthy older adults varies as a function of age and is associated with changes in episodic memory and processing speed. *J. Neurosci.* 38, 2809–2817. doi: 10.1523/JNEUROSCI.3067-17.2018

Stasiolek, M. (2015). Neurological symptoms and signs in thyroid disease. *Thyroid. Res.* 8:A25. doi: 10.1186/1756-6614-8-S1-A25

Talhada, D., Santos, C. R. A., Gonçalves, I., and Ruscher, K. (2019). Thyroid hormones in the brain and their impact in recovery mechanisms after stroke. *Front. Neurol.* 10:1103. doi: 10.3389/fneur.2019.01103

Taylor, P. N., Albrecht, D., Scholz, A., Gutierrez-Buey, G., Lazarus, J. H., Dayan, C. M., et al. (2018). Global epidemiology of hyperthyroidism and hypothyroidism. *Nat. Rev. Endocrinol.* 14, 301–316. doi: 10.1038/nrendo.2018.18

Toyib, S., Kabeta, T., Dendir, G., Bariso, M., and Reta, W. (2019). Prevalence, clinical presentation and patterns of thyroid disorders among anterior neck mass patients visiting Jimma medical center, Southwest Ethiopia. *Biomed J Sci Tech Res.* 18, 13431–13435. doi: 10.26717/BJSTR.2019.18.003126

Uddin, L. Q., Kelly, A. M., Biswal, B. B., Castellanos, F. X., and Milham, M. P. (2009). Functional connectivity of default mode network components: correlation, anticorrelation, and causality. *Hum. Brain Mapp.* 30, 625–637. doi: 10.1002/hbm.20531

Ursino, M., Magosso, E., and Petti, M. (2022). Neural networks and connectivity among brain regions. *Brain Sci.* 12:346. doi: 10.3390/brainsci12030346

Wang, X., Xia, J., Wang, W., Lu, J., Liu, Q., Fan, J., et al. (2023). Disrupted functional connectivity of the cerebellum with default mode and frontoparietal networks in young adults with major depressive disorder. *Psychiatry Res.* 324:115192. doi: 10.1016/j.psychres.2023.115192

Wang, Y., Yang, L., and Liu, J. (2023). Causal associations between functional/structural connectivity and stroke: a bidirectional Mendelian randomization study. *Biomedicines* 11:1575. doi: 10.3390/biomedicines11061575

Wang, M., Zhao, G., Jiang, Y., Lu, T., Wang, Y., Zhu, Y., et al. (2023). Disconnection of network hubs underlying the executive function deficit in patients with ischemic Leukoaraiosis. *J. Alzheimers Dis.* 94, 1–10. doi: 10.3233/JAD-230048

Wojtalik, J. A., Eack, S. M., Smith, M. J., and Keshavan, M. S. (2018). Using cognitive neuroscience to improve mental health treatment: a comprehensive review. *J. Soc. Soc. Work Res.* 9, 223–260. doi: 10.1086/697566

Wu, Y., Pei, Y., Wang, F., Xu, D., and Cui, W. (2016). Higher FT4 or TSH below the normal range are associated with increased risk of dementia: a meta-analysis of 11 studies. *Sci. Rep.* 6:31975. doi: 10.1038/srep31975

Xiong, Y., Ye, C., Sun, R., Chen, Y., Zhong, X., Zhang, J., et al. (2023). Disrupted balance of gray matter volume and directed functional connectivity in mild cognitive impairment and Alzheimer's disease. *Curr. Alzheimer Res.* 20, 161–174. doi: 10.2174/1567205020666230602144659

Yao, Y., Lu, C., Chen, J., Sun, J., Zhou, C., Tan, C., et al. (2022). Increased resting-state functional connectivity of the Hippocampus in rats with Sepsis-associated encephalopathy. *Front. Neurosci.* 16. doi: 10.3389/fnins.2022.894720

Yen, C., Lin, C.-L., and Chiang, M.-C. (2023). Exploring the frontiers of neuroimaging: a review of recent advances in understanding brain functioning and disorders. *Life.* 13:1472. doi: 10.3390/life13071472

Yi, J., Zheng, J.-y., Zhang, W., Wang, S., Yang, Z.-f., and Dou, K.-f. (2014). Decreased pain threshold and enhanced synaptic transmission in the anterior cingulate cortex of experimental hypothyroidism mice. *Mol. Pain* 10:1744-8069-10-38. doi: 10.1186/1744-8069-10-38

Yoo, K., Lee, P., Chung, M. K., Sohn, W. S., Chung, S. J., Na, D. L., et al. (2017). Degree-based statistic and center persistency for brain connectivity analysis. *Hum. Brain Mapp.* 38, 165–181. doi: 10.1002/hbm.23352

Zanão, T. A., Martins Lopes, T., Machado de Campos, B., Nogueira, M. H., Yasuda, C. L., and Cendes, F. (2017). Default mode network in temporal lobe epilepsy: interactions with memory performance. *bio Rxiv.*:205476. doi: 10.1101/205476

Zhang, W., Liu, X., Zhang, Y., Song, L., Hou, J., Chen, B., et al. (2014). Disrupted functional connectivity of the hippocampus in patients with hyperthyroidism: evidence from resting-state fMRI. *Eur. J. Radiol.* 83, 1907–1913. doi: 10.1016/j.ejrad.2014.07.003

Zhang, M., Ma, X., Ma, S., and Ling, X. (2018). *Resting-state functional connectivity in untreated overt hyperthyroidism (graves' disease) with mood disorders 2018*. Austria, Vienna: European Congress of Radiology.

Zhang, W., Song, L., Yin, X., Zhang, J., Liu, C., Wang, J., et al. (2014). Grey matter abnormalities in untreated hyperthyroidism: a voxel-based morphometry study using the DARTEL approach. *Eur. J. Radiol.* 83, e43–e48. doi: 10.1016/j.ejrad.2013.09.019

Zhe, X., Zhang, X., and Zhang, D. (2021). Altered gray matter volume and functional connectivity in patients with vestibular migraine. *Front. Neurosci.* 15:683802. doi: 10.3389/fnins.2021.683802

Zhi, M., Hou, Z., Zhang, Y., Yue, Y., Li, L., and Yuan, Y. (2018). Cognitive deficit-related interhemispheric asynchrony within the medial hub of the default mode network aids in classifying the hyperthyroid patients. *Neural Plast.* 2018, 1–7. doi: 10.1155/2018/9023604

Zhu, W., Wu, F., Li, J., Meng, L., Zhang, W., Zhang, H., et al. (2022). Impaired learning and memory generated by hyperthyroidism is rescued by restoration of AMPA and NMDA receptors function. *Neurobiol. Dis.* 171:105807. doi: 10.1016/j.nbd.2022.105807

frontiers | Frontiers in Molecular Neuroscience

TYPE Mini Review
PUBLISHED 02 May 2024
DOI 10.3389/fnmol.2024.1399953

OPEN ACCESS

EDITED BY
Ferdinando Di Cunto,
University of Turin, Italy

REVIEWED BY
Ashwin S. Shetty,
Harvard University, United States

*CORRESPONDENCE
Alessandro Sessa
✉ sessa.alessandro@hsr.it

RECEIVED 12 March 2024
ACCEPTED 22 April 2024
PUBLISHED 02 May 2024

CITATION
Bossini L and Sessa A (2024) Need of orthogonal approaches in neurological disease modeling in mouse.
Front. Mol. Neurosci. 17:1399953.
doi: 10.3389/fnmol.2024.1399953

Need of orthogonal approaches in neurological disease modeling in mouse

Linda Bossini[1,2] and Alessandro Sessa[1]*

[1]Neuroepigenetics Unit, Division of Neuroscience, IRCCS San Raffaele Scientific Institute, Milan, Italy, [2]"Vita e Salute" San Raffaele University, Milan, Italy

Over the years, advancements in modeling neurological diseases have revealed innovative strategies aimed at gaining deeper insights and developing more effective treatments for these complex conditions. However, these progresses have recently been overshadowed by an increasing number of failures in clinical trials, raising doubts about the reliability and translatability of this type of disease modeling. This mini-review does not aim to provide a comprehensive overview of the current state-of-the-art in disease mouse modeling. Instead, it offers a brief excursus over some recent approaches in modeling neurological diseases to pinpoint a few intriguing strategies applied in the field that may serve as sources of inspiration for improving currently available animal models. In particular, we aim to guide the reader toward the potential success of adopting a more orthogonal approach in the study of human diseases.

KEYWORDS

mouse model, genetic engineering, neurodevelopmental disorders, neurodegenerative disorders, reversibility

Introduction

All cells within a complex multicellular organism retain the same genetic information. The regulation of gene expression is the crucial mechanism to interpret and utilize such information and create the overarching diversity of cell types composing those organisms. The interplay of various intrinsic and extrinsic factors influences gene expression. They can induce either expression or silencing at specific time points, ultimately dictating cellular identity, morphology, and function (Savulescu et al., 2020) both during embryonic development and throughout subsequent adult life (Pope and Medzhitov, 2018).

In the central nervous system (CNS), neuronal development unfolds over a series of intricate processes encompassing proliferation, migration, differentiation, synaptogenesis, and pruning, to ensure the formation of functional neuronal connectivity. These biological events are subjected to a tight regulation by specific genetic programs, which operate following precise spatiotemporally-defined fashions (Subramanian et al., 2020). Even subtle alterations to these programs can disrupt the proper assembly and maturation of neuronal circuits, thereby triggering neurological pathology (Griffin et al., 2022).

As a result, decoding the functions of a gene of interest, or its pathological variants, in relevant biological landscapes represents a major challenge. To this endeavor appropriate experimental genetic tools, capable of providing a commensurate level of complexity in terms of controlled gene expression, are fundamental. Employing various scales of investigation, such as cell-type or age-specific approaches, can yield valuable insights into previously unknown gene functions and their roles in disease development or progression.

Understanding the intricacies of these genetic programs and how they are disrupted in disease states is essential for uncovering the underlying mechanisms of neurological disorders and devising effective therapeutic interventions.

Lost in "translation": challenges of animal disease modeling

A spectrum of technologies, spanning from conventional to more advanced *in vitro* and *in vivo* systems, alongside computational modeling, has been explored in the pursuit of elucidating the molecular underpinnings of finely orchestrated processes, all with the overarching goal of reliably recapitulating human diseases (Paşca et al., 2014; Birey et al., 2017; Jönsson et al., 2020; Pomeshchik et al., 2020; Susaimanickam et al., 2022; Li et al., 2023; Meng et al., 2023). In this direction, across many years, mouse models emerged as the cardinal tool for investigating disease mechanisms, progression and potential therapeutic strategies (Lunev et al., 2022).

Nonetheless, despite the advantages and versatility of animal models, their translational utility has faced increasing scrutiny in recent years. One of the main concerns arises from the failure of several clinical trials, despite the promising results obtained from preclinical studies conducted in, mainly, murine models (Bespalov et al., 2016; Seyhan, 2019; Marshall et al., 2023).

Several factors contribute to the translational gap between preclinical animal studies and clinical trials including species differences, model fidelity and disease heterogeneity. For instance, while animal models may recapitulate certain aspects of human diseases, they often fail to fully replicate the complexity of human physiology, and therefore pathology. In addition, heterogeneity should be taken into considerations. In the first place, many human diseases are themselves characterized by significant heterogeneity in terms of etiology, pathophysiology and clinical presentation as exemplified by incomplete penetrance and variable expressivity (Kingdom and Wright, 2022). So it is clear that such heterogeneity can hardly be modeled by a unique disease model. Moreover, genetic (e.g., mouse genetic backgrounds) and environmental factors (e.g., experimental conditions) also may impact on the fidelity of the model (Robinson et al., 2019; Georgiou et al., 2022).

Despite these inherent limitations, animal models have proven to be invaluable tools over the years. Thus, it's crucial to acknowledge and eventually minimize these constraints while exploring approaches to instead maximize the potential of the models. Creating a unique, informative, and robust model for a disease is often hardly feasible. Instead, applying an orthogonal approach, e.g., based on the integration of independent methodologies or model systems to address the same biological topic, may result a more illuminating strategy. The current trend in the animal modeling field is indeed evolving toward a "network" approach, in which multiple types of models are employed, and further experiments are redesigned based on evidence gained from the other models (Pasko et al., 2023). This integrated manner provides complementary insights and validation of findings, enhancing the understanding of complex processes and disease mechanisms, thus facilitating the translation of research findings into clinical applications.

Often the investigation of the pathological consequences of disease-causing gene variants begins with modeling the extreme conditions: either total deletion or overexpression of the gene of interest. Alternatively, since in many complex genetic diseases, there exists a well-established inverse relationship between disease-causing genetic variants and the severity of the corresponding phenotype, researchers often exploit these rarer variants with large effect sizes as a practical starting point for delving into the investigation of the disease's neurobiology to delineate the causal pathways (Amanat et al., 2020; Gordon and Binder, 2023). On this line, constitutive genetically engineered mouse models represent the standard condition to approach the study of the effects of genetic mutations. In fact, they generally provide a broad overview of the disease and its most severe manifestations (Dow, 2015). However, they may fail to represent ideal platform for dissecting relevant phenotypes in depth, especially in the context of neurodevelopmental and neurodegenerative disorders.

These models frequently exhibit such severe manifestations that may obscure the underlying subtle events contributing to pathology. One exemplificative case is the embryonic lethality or reduced survival of genetically modified animals, which make challenging to study the effects of these mutations in mature organs up to adult organisms. Additionally, the intricate and dynamic processes at the basis of neurological disorders may only become evident at specific levels of analysis (e.g., certain developmental stages, cell populations, higher-order brain processes, network connectivity, etc.) (Gordon and Binder, 2023) or may only manifest when different pathological insults or risk factors converge, as suggested by dual-hit hypotheses (Zhu et al., 2007; Rietdijk et al., 2017; Guerrin et al., 2021).

Similarly in the neurodegenerative disorders' scenario, the experimental design of the most commonly used models was indeed to recapitulate the hallmarks of the disease (e.g., cell death, protein aggregation, inflammation etc.), often exacerbating them (e.g., acute induction at extraordinary high levels), to make immediately accessible the study of the desired phenotype. However, these models do not respect the gradual development of the pathology, corresponding symptomatology and, likely, associated underlined biological processes. For this same reason, conventional models, since do not allow for *ad hoc* modulation of gene expression at specific stages, do not represent the ideal platform for studying adult-onset neurodegenerative disorders as well, where precise temporal control over the expression of disease-associated genes should be pursued to align with the natural time course of the disease.

> *To contextualize our premises, let's frame our discussion with a hypothetical neurological condition X arising from the accumulation, and subsequent aggregation, of a mutated protein X. While the exact mechanisms are yet unknown, this buildup is believed to disrupt the function of either excitatory or inhibitory neurons. This results in an altered balance between excitation and inhibition, ultimately leading to cognitive and motor deficits.*
>
> *For an initial investigation, protein accumulation is experimentally mimicked by the generation of constitutive transgenic mouse model overexpressing the gene X (Figure 1A). Unfortunately, the new line is characterized by a high mortality*

rate, making the study of the pathological underpinnings hardly feasible. This outcome opens up the necessity of exploring an alternative strategy to model the condition.

To holistically understand the etiopathogenesis of a disease, both the cellular origin and the precise timing of its pathogenesis are to be carefully considered. In the framework of neurological disorders, this means identifying the critical time window when the CNS becomes vulnerable the most to the pathogenic insult, either protein loss or accumulation, and where this happens. Instead, in a therapeutical perspective, to determine the "point of no return," so when the organ is no longer able to recover from that challenge.

Exploring space and time: novel insights from animal models

While constitutive models are useful for generating experimental conditions with readily observable phenotypes, thus serving as starting point of investigation, conditional genetic engineering may provide higher level of information.

Conditional knock-out or knock-in models, used for an alternative but targeted explorative approach, have revolutionized our ability to ask specific biological questions with greater precision and control. In this framework, the Cre/loxP recombination system represents the cornerstone of conditional genetic manipulation in mice, including gene deletion, insertion, inversion, or translocation. Applied for the first time *in vivo* by Rajewsky and Marth in 1994, this "simple" yet powerful tool soon became indispensable for interrogating the genetic and molecular basis of diseases (Gu et al., 1994; Rajewsky et al., 1996; Heldt and Ressler, 2011).

The system facilitates the controlled insertion of desired genetic modifications by exploiting two key components: the strategical incorporation of loxP sequence recognition sites to flank ("floxed") a DNA sequence (e.g., gene of interest, STOP cassette) and the regulated expression of Cre recombinase under the control of a specific promoter. Therefore, the adaptable nature of the Cre/loxP system provides the sought flexibility in experimental design, making it invaluable for uncovering several information.

To overcome the limitation of the previous constitutive model, a novel conditional allele been generated to modulate ad hoc gene X expression and the consequential protein accumulation. The novel line carries an additional gene X copy preceded by a floxed STOP cassette (Figure 1B). Given the CNS-related phenotype, the disease has been mimicked crossing the new line with the Nestin-Cre, active in neural progenitors (Figure 1C). The resulting mutant recapitulates disease-associated neurological phenotypes, including cognitive (e.g., anxiety, memory) and motor deficits (e.g., balance, coordination).

This approach was nicely exemplified by Li J. et al. (2022) who employed various Cre lines to investigate *AUTS2*'s functions, a gene implicated in autism spectrum disorders (ASDs), within the brain. Since a constitutive knock-out model resulted in embryonic lethality, the authors generated *Auts2* floxed mice subsequently crossed with different Cre lines to conditionally disrupt *Aust2* at distinct developmental stages and in specific forebrain regions. For instance, using Cre lines with region-specific expression patterns enabled them to discern *Auts2*'s role in different phases of dentate gyrus (DG) specification. This temporally-dictated analysis was fundamental to confirm *Auts2* function for DG development only at early postnatal stage, highlighting its critical involvement as transcription repressor in a previously unknown mechanism for neural cell migration. To specifically analyze the gene's function during the postnatal phase, they also took advantage of viral tools for delivering the Cre recombinase. This approach not only offered additional spatial control, through local injections, but also provided temporal control, via the timing of injection. This strategy proved advantageous in avoiding potential compensatory mechanisms triggered by gene knockdown throughout development.

To further deepen the pathological basis of disease X, the Emx1-Cre and the Dlx5/6-Cre have been employed to induce accumulation in either excitatory or inhibitory neurons respectively (Figures 1D, E). Notably, only the excitatory-restricted mutants present few of the neurological phenotypes.

The injection of virally-delivered Cre, using replication-deficient adeno-associated (AAV) or lentiviral (LV) vectors, serves as a potent tool for controlling the expression of the gene of interest (Heldt and Ressler, 2011; Lunev et al., 2022). This approach increases the flexibility of the Cre/loxP system to adapt to various experimental needs, including the exploration of gross structural changes, as well as consequential interrogation of functional aspects, such as neuronal circuit activity, in greater detail (Hui et al., 2022). In a recent study by Yonan and Steward (2023), to examine the deletion of *Pten* in fully mature neurons, a gene implicated in ASDs in humans, an AAV-delivered Cre has been unilaterally injected in the *Pten* floxed model. Specifically, the viral particles have been introduced directly into the DG to induce a focal deletion, while maintaining *Pten* expression in the cells of origin of the input circuits. This strategy is noteworthy because, unlike constitutive models, it allows for investigation of the direct primary effects of the gene, without interferences resulting from gene suppression in other connected regions. This approach revealed how *Pten* suppression at the level of the DG triggers synapse formation, independently of PTEN activity in the presynaptic cells.

Viral delivery is an excellent option for achieving focal expression, or deletion, of a gene of interest, precisely in space and time. In adult animals, viruses can be delivered through various methods, such as tail vein injections for systemic delivery, intrathecal or stereotaxic injections for a more localized delivery. On the other hand, for perinatal expression, intracerebroventricular or retro-orbital injections may be employed. Nevertheless, each of these surgical procedures requires a different level of technical expertise.

Over the years, various advancements of the original recombination system have emerged to achieve even finer spatiotemporal comprehension (Shcholok and Eftekharpour, 2023). These include the tamoxifen-inducible Cre-ER^{T2} system (Belteki et al., 2005; Heldt and Ressler, 2011; Hui et al., 2022; Kellogg et al., 2023), photoactivatable Cre recombinases (Yoshimi

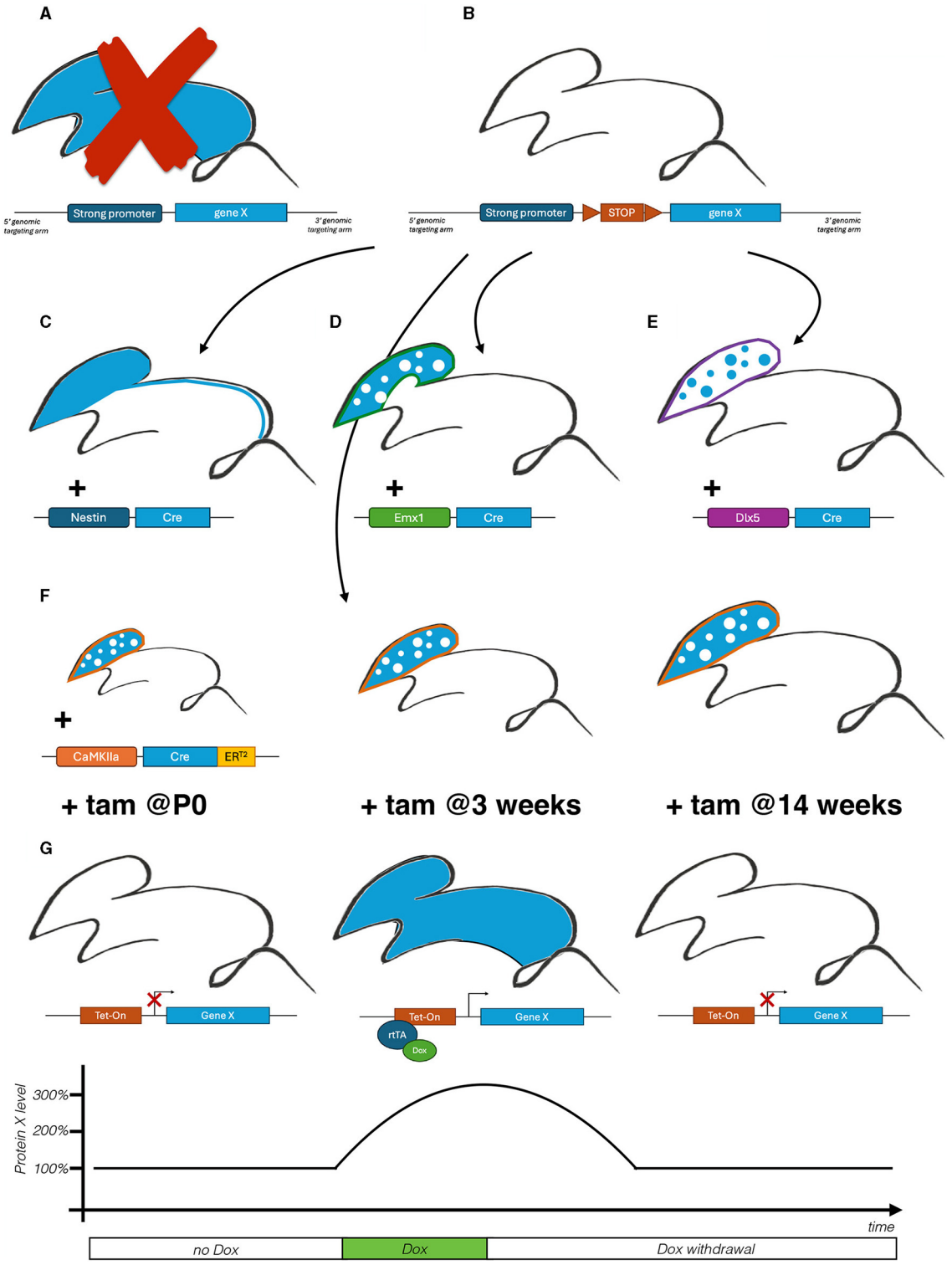

FIGURE 1
Schematic representation of an illustrative orthogonal approach applied on the investigation of a fictitious X disease. **(A)** Generation of a transgenic mouse model to induce constitutive gene X overexpression. **(B)** Generation of a conditional Cre-dependent knock-in mouse line harboring an additional copy of the gene X under the control of a floxed STOP cassette for on demand induction of pathological protein accumulation. **(C)** Generation of a conditional model overexpressing gene X in the entire CNS, including the spinal cord. **(D, E)** Generation of a conditional model overexpressing gene X in excitatory **(D)** and inhibitory neurons **(E)** to explore their contribution to the pathological phenotype. **(F)** Generation a conditional model overexpressing gene X in excitatory neurons upon Tamoxifen (tam) induction, at three postnatal timepoints, to explore their temporal susceptibility to the pathological insult. **(G)** Generation of a tet-inducible reverse transactivator (rtTA)-dependent conditional model. Initial administration of Doxycycline (Dox) induces protein X accumulation, while following Dox withdrawal restores protein levels to mimic various dynamics of therapeutic interventions.

et al., 2021; Li et al., 2022), Cre/Dre dual recombinase systems (Kouvaros et al., 2023) and split Cre systems (Khoo et al., 2020; Kim et al., 2021), among others. Some of these configurations are of extreme help to easily explore the time and the space, inducing the pathological insult within cell types at various embryonic and postnatal timepoints with high specificity.

One effective method involves the tamoxifen-inducible Cre-ER^{T2} system coupled with the plethora of promoters available today to regulate its induction (Hayashi and McMahon, 2002; Shcholok and Eftekharpour, 2023). In this system, the Cre recombinase is fused to a modified estrogen receptor ligand-binding domain (ER^{T2}) that responds to tamoxifen, a synthetic estrogen analog. Once expressed in the cell, this Cre-recombinase variant remains in the cytoplasm without exerting any activity till the administration of the drug, that triggers the translocation of the Cre into the nucleus to perform its activity.

Sonzogni et al. (2019) leveraged the flexibility offered by this inducible system in the context of Angelman syndrome (AS), a severe neurodevelopmental disorder, to investigate the role of UBE3A, a ubiquitin ligase amply implicated in brain development and maturation. Since previous studies predominantly focused on UBE3A critical functions in early brain development, the researchers aimed to understand its role after normal brain development. To address this issue, they generated a conditional mouse model which was crossed with either a constitutive Cre line to induce *Ube3a* embryonic deletion, establishing a baseline for behavioral phenotypes, or the CreER^{T2} to trigger protein loss on demand, e.g., after early brain development and later in adulthood. This system proved crucial in confirming UBE3A's role in normal brain development, specifically its role in shaping neuronal connectivity (e.g., synapse development) and its subsequent involvement in motor coordination and cognitive functions (Greer et al., 2010; Khatri and Man, 2019). This further delineates embryonic and early postnatal stages as the critical window of vulnerability of the brain to UBE3A protein loss. Notably, these findings also suggest that early, transient UBE3A reinstatement is likely to prevent most adverse phenotypes, underscoring the importance of initiating gene reactivation therapies early in life.

> *To define the critical window of vulnerability of excitatory neurons in X disease, a CaMKIIa-ER^{T2}-Cre is employed to induce protein X accumulation at differential timepoints (Figure 1F): at birth (P0), juvenile (3 weeks of age) and adult mice (14 weeks). This longitudinal approach allows to identify early postnatal stage as the most susceptible to damages ensuing protein accumulation.*

This chemically-inducible system can be utilized also to generate improved animal models, e.g., for studying disease stages that were previously inaccessible. A study in the context of Multiple System Atrophy (MSA), an adult-onset synucleinopathy characterized by the presence of cytoplasmic inclusions in oligodendrocytes, represents a nice example. Given the adult-onset nature of the disease, to induce α-synuclein (Syn) expression only in adulthood, Tanji et al. generated a novel floxed Syn knock-in mouse line, which was subsequently crossed with a Cre-ER^{T2} driver line under the control of an oligodendrocyte-restricted promoter (Tanji et al., 2019). This enabled the generation for the first time of a model to investigate the effects of Syn expression on MSA pathophysiology specifically during the initial stages of disease progression, avoiding any latent disturbance or compensatory effect due to sustained promoter activity during the developmental stages. Given the significance of early treatment in slowing MSA progression, this model offers the unique opportunity to enhance understanding of the events driving initial disease progression and to develop novel therapeutics for MSA.

While inducible systems, like virally-delivered or chemically-inducible Cre-dependent ones, offer valuable insights into subtle pathogenic mechanisms, their acute induction represents an artificial deviation from the natural time course of the disease. However, if carefully designed, conditional knockout or knock-in models offer an exclusive platform that can be smartly utilized to systematically address many of the biological questions arising when investigating a pathological condition. This allows researchers to select the desired level of complexity, such as specific cellular populations, brain regions, or temporal stages, in a more controlled and physiologically relevant manner. Therefore, while conditional models may not fully recapitulate the complexity of human diseases, they offer unique advantages for investigating in depth fine pathogenic mechanisms with a level of precision that is often not unattainable with constitutive models.

Unveiling reversibility: flipping the paradigm

By providing precise spatial and temporal control over the disruption or overexpression of a gene, Cre-based systems are invaluable tools for addressing specific biological questions. Nonetheless, a primary constraint lies in the irreversibility of the recombination once Cre activation, whether constitutive or inducible, triggers it. The capability to first induce and subsequently halt the pathological challenge, thus emulating a potential treatment, yields insights into two critical facets: the reversibility of disease symptoms and the temporal necessities for therapeutic intervention.

For such reversible temporal regulation of gene expression, the Tetracycline (Tet)-inducible binary system could be considered. The Tet-On and Tet-Off systems allow to switch gene expression on or off respectively, in response to the presence or absence of tetracycline analogs (e.g., doxycycline). This system requires the combination of two components *in trans*: the tet-inducible transactivator (tTA) or reverse transactivator (rtTA), artificial transcription factors under the control of a tissue-specific promoter, and a modified tet-responsive element, which is activated upon binding of the tTA/rtTA (Dogbevia et al., 2015). Therefore, this system can easily achieve a spatiotemporal regulation similar to the one of the Cre/loxP system, implementing reversibility as an additional layer of control (Belteki et al., 2005).

Although tTA-dependent alleles corresponding to various proteinopathies already exist, one of the significant limitations of current mouse models for neurodegenerative diseases, is their failure to properly mimic the disorder's time course (Koller et al., 2022). For example, in Alzheimer's disease models, clinical signs often manifest earlier than in the corresponding human pathology, implying a need to delay the formation of the pathological

amyloid plaques. Additionally, the limited availability of CNS-targeting tTA driver lines poses a challenge for regional or cell-type-specific studies. To address these limitations, Koller and colleagues proposed using a Cre-to-tTA converter allele to yield Cre-dependent expression of an existing Tet-regulated transgene (Koller et al., 2022). This system allows to draw from the extensive repertoire of Cre driver lines for precise spatial control, including spatiotemporal control when considering Cre-ER^{T2} drivers. This novel model was able to delay amyloid formation adapting it to the natural disease progression, while also restricting this process in specific cell types. This innovative combinatorial approach could be applied to other diseases, neurodegenerative or otherwise, for which tTA-dependent models already exist, maximizing the utility and versatility of these powerful systems.

Combination of both systems, the Cre/loxP with the Tet-O, can be exploited to further enhance control over transgene induction. An example was recently done by Li J. et al. The authors aimed to delineate the temporal requirements for TorsinA in normal motor function in a mouse model of DYT1 dystonia, a neurodevelopmental disease induced by a loss-of-function mutation in the corresponding *TOR1A* gene (Li et al., 2021). Previous studies focused on conditionally deleting TorsinA from various regions of the CNS, thus revealing the existence of a critical period of vulnerability of the brain to TorsinA loss (Tanabe et al., 2012). To describe this existing temporal interval, a mouse line enabling spatiotemporal control over the endogenous *Tor1a* gene was developed by inserting at the 5′ of the *Tor1a* start site a cassette containing a floxed STOP element followed by a tetracycline operator (Tet-O) in a Tet-On-like configuration to confer both Cre and tetracycline responsivity. The Cre system was used to restrict the defect in various brain regions to assess their temporal sensitivity to lack of TorsinA function, while the Tet system was employed to mimic a therapeutic restoration. Using this setting, the authors restored protein levels using three different temporal dynamics to simulate possible schedules of therapeutic intervention. This innovative approach allowed the delineation of a two-stage model for the disease: primary causative events directly related to TorsinA loss and therefore reverted by its restoration (stage 1) and the irreversible downstream molecular or circuit changes independent of TorsinA function (stage 2). Although not strictly physiological, this disease model has provided insights into pathogenic dynamics, with significant implications for the design and timing of effective therapeutic strategies.

The concept of implementing genetic reversibility in disease-mouse models is crucial for determining the possibility and extent of symptom reversion. This concept was pioneered by Guy et al. (2007), in the context of Rett syndrome, an ASD caused by mosaic expression of mutant copies of the X-linked *MECP2* gene in neurons. To understand whether the postnatal restoration of MeCP2 levels could reestablish the neuronal functionality, the scientists inserted a removable floxed STOP cassette in the endogenous mouse gene. The CreER^{T2} transgene was also present to control the reactivation of the gene using tamoxifen injection. This model demonstrated, for the first time, robust reversal of Rett pathology upon *Mecp2* restoration in both immature and mature adult animals, paving the way of the importance of implementing reversibility in the field of animal disease modeling.

As a postsynaptic scaffold protein, SHANK3 regulates synapse formation, function, and plasticity, hence its disruption in disease states results in synaptic defects and autistic-like behaviors. In the perspective of a restorative gene therapy, since increased levels of SHANK3 are connected to other neurological conditions (e.g., bipolar disorder) as well, Mei et al. (2016) proposed a novel conditional knock-in mouse model to investigate the temporal requirement of *Shank3* gene. In their work, they employed a Cre-dependent genetic switch (FLEx) strategy that allows *Shank3* expression upon its Cre-mediated inversion, to conditionally manipulate the endogenous gene (Schnütgen et al., 2003). By utilizing this reversible model, they highlighted an improvement in synaptic function upon impact of *Shank3* re-expression. However, only a few behavioral abnormalities were rescued, thus supporting the developmental origin of the autistic-like impairments due to *SHANK3* haploinsufficiency.

A reversible approach was similarly pursued by Mielnik et al. (2021) to explore the outcomes of counteracting N-methyl-D-aspartate (NMDA) receptor deficiency in the adult brain. Impaired NMDAR signaling has been coupled with various neurodevelopmental disorders over the years, leading to conditions such as intellectual disability, epilepsy, autism or schizophrenia. To assess the beneficial effects of a restorative treatment, they developed a mouse model where the loss-of-function allele of *Grin1*, the gene encoding for an NMDAR subunit, was induced via the insertion of a floxed STOP and thus restored to physiological levels upon Cre recombination. Rescued adult mice displayed robust improvements in cognitive functions, providing insights into the effectiveness of restoring NMDAR activity in adulthood.

Analogously in the context of Dravet syndrome, a severe epileptic encephalopathy primarily caused by haploinsufficiency of the *SCN1A* gene, Valassina et al. recently proposed a conditional knock-in mouse model enabling on-demand *Scn1a* reactivation, via a floxed STOP cassette removal. The authors successfully assessed the reversibility of the epileptic phenotype after disease onset (Valassina et al., 2022). Using this model, the same group recently investigated the effects of reactivating gene expression both perinatally and postnatally to define the critical window of vulnerability of the CNS to *Scn1a* loss, a crucial knowledge for future therapeutic interventions (Di Berardino et al., 2023).

> *To demonstrate the reversibility of X disease, a Tet-On system has been employed to firstly induce and later suppress gene X overexpression to evaluate the effects of the reduction of protein levels (Figure 1G). Interestingly, while protein reduction at a late stage (14 weeks) was not able to revert the reported phenotypes, the recovery in juvenile mice (3 weeks) ameliorated both motor and cognitive impairments. Gathered together this data suggests for an early postnatal disease-modifying therapy.*

These approaches, as demonstrated in an increasingly number of neurological diseases, underscore the feasibility of therapeutically targeting their genetic root causes. However, not all diseases share this fortune, as demonstrated by Silva-Santos et al. in the context of Angelman syndrome (Silva-Santos et al., 2015). A conditional reversible mouse line, via the insertion of a

floxed STOP cassette within *Ube3a* intron 3, has revealed the scarce efficacy of reactivating *Ube3a* in adult organisms, hence confirming the necessity of functional UBE3A at developmental stage.

Discussion

Refining experimental models is essential for obtaining reliable results. Addressing significant biological questions, such as disease pathogenesis, is complex and, in our opinion must require confronting them from multiple perspectives. Tackle smaller aspects at a time, dividing this challenging endeavor, may return more complete answers for the questions the scientific community has. The use of conditional mouse lines harboring the gene of interest, and the different activating tools we have discussed, represent a major avenue to achieve this goal.

The precise spatiotemporal control afforded by these inducible systems enables investigation into the dynamic nature of biological mechanisms or pathological processes (e.g., primary events, compensatory mechanisms etc.) and disease progression over time. Leveraging these advanced genetic engineering tools facilitates the design of refined and physiologically relevant experimental conditions for studying neurodevelopmental and neurodegenerative disorders. This integrative "network" approach allows to uncover novel disease mechanisms and identify potential therapeutic targets that may not be apparent in more "classical" constitutive germline models.

On this line, reversibility is also intriguing and holds promise in addressing some of the limitations and challenges associated with preclinical research. For instance, it provides a framework for evaluating the extent of therapeutic interventions' effectiveness more comprehensively. This resolution is particularly valuable for understanding the trajectory of disease development to optimize treatment. However, it's compulsory to acknowledge that implementing reversibility as a control in animal models may present practical challenges and require careful experimental design. Factors such as the timing and duration of interventions, choice of animal models and selection of appropriate outcome measures must be correctly pondered to ensure the validity and relevance of the findings.

Overall, these advanced technologies have enabled more precise and nuanced investigations, overcoming many limitations associated with traditional animal models and therefore achieving greater fidelity to human biology and pathology. Integrating multiple layers of control in preclinical research holds the potential to enhance the translational significance of experimental findings and accelerate the development of effective therapies for human diseases.

> *The orthogonal approach applied to the fictitious X disease works as scholar example of a successful "network" strategy able to overcome the limitations of the commonly used models and investigatory approaches. The implementation of different systems enables to address the same biological question from three different perspectives: space, time and reversibility. It allows to firstly define the temporal susceptibility of excitatory neurons to protein X accumulation, opening to the prospect of a therapeutic intervention aiming at decreasing protein levels early after birth.*

Continued advancements in technology and interdisciplinary collaborations will be essential in unlocking the full potential of these approaches and addressing the intricate complexities of biological mechanisms at the basis of human diseases.

Author contributions

LB: Conceptualization, Writing – original draft, Writing – review & editing. AS: Conceptualization, Funding acquisition, Supervision, Writing – original draft, Writing – review & editing.

Funding

The author(s) declare that financial support was received for the research, authorship, and/or publication of this article. This work was supported by the Fondazione Regionale per la Ricerca Biomedica (Regione Lombardia), European Joint Program on Rare Disease Project TREAT-SGS (EJPRD20-008).

Acknowledgments

We apologize to those researchers whose work could not be cited owing to space constraints.

Conflict of interest

The authors declare that the research was conducted in the absence of any commercial or financial relationships that could be construed as a potential conflict of interest.

The author(s) declared that they were an editorial board member of Frontiers, at the time of submission. This had no impact on the peer review process and the final decision.

Publisher's note

References

Amanat, S., Requena, T., and Lopez-Escamez, J. A. (2020). A systematic review of extreme phenotype strategies to search for rare variants in genetic studies of complex disorders. *Genes* 11, 1–15. doi: 10.3390/genes11090987

Belteki, G., Haigh, J., Kabacs, N., Haigh, K., Sison, K., Costantini, F., et al. (2005). Conditional and inducible transgene expression in mice through the combinatorial use of Cre-mediated recombination and tetracycline induction. *Nucleic Acids Res.* 33, 1–10. doi: 10.1093/nar/gki559

Bespalov, A., Steckler, T., Altevogt, B., Koustova, E., Skolnick, P., Deaver, D., et al. (2016). Failed trials for central nervous system disorders do not necessarily invalidate preclinical models and drug targets. *Nat. Rev. Drug Discov.* 15:516. doi: 10.1038/nrd.2016.88

Birey, F., Andersen, J., Makinson, C. D., Islam, S., Wei, W., Huber, N., et al. (2017). Assembly of functionally integrated human forebrain spheroids. *Nature* 545, 54–59. doi: 10.1038/nature22330

Di Berardino, C., Mainardi, M., Brusco, S., Benvenuto, G., and Colasante, E. (2023). Temporal manipulation of the Scn1a gene reveals its 1 essential role in adult brain function 2. *Brain* 147, 1216–1230. doi: 10.1093/brain/awad350

Dogbevia, G. K., Marticorena-Alvarez, R., Bausen, M., Sprengel, R., and Hasan, M. T. (2015). Inducible and combinatorial gene manipulation in mouse brain. *Front. Cell Neurosci.* 9:142. doi: 10.3389/fncel.2015.00142

Dow, L. E. (2015). Modeling disease *in vivo* with CRISPR/Cas9. *Trends Mol. Med.* 21, 609–621. doi: 10.1016/j.molmed.2015.07.006

Georgiou, P., Zanos, P., Mou, T. C. M., An, X., Gerhard, D. M., Dryanovski, D. I., et al. (2022). Experimenters' sex modulates mouse behaviors and neural responses to ketamine via corticotropin releasing factor. *Nat. Neurosci.* 25, 1191–1200. doi: 10.1038/s41593-022-01146-x

Gordon, J. A., and Binder, E. (2023). *Exploring and Exploiting Genetic Risk for psychiaTric Disorders*. Cambridge, MA: The MIT Press. doi: 10.7551/mitpress/15380.001.0001

Greer, P. L., Hanayama, R., Bloodgood, B. L., Mardinly, A. R., Lipton, D. M., Flavell, S. W., et al. (2010). The Angelman syndrome protein Ube3A regulates synapse development by ubiquitinating arc. *Cell* 140, 704–716. doi: 10.1016/j.cell.2010.01.026

Griffin, A., Mahesh, A., and Tiwari, V. K. (2022). Disruption of the gene regulatory programme in neurodevelopmental disorders. *Biochim. Biophys. Acta Gene Regul. Mech.* 1865:194860. doi: 10.1016/j.bbagrm.2022.194860

Gu, H., Marth, J. D., Orban, P. C., Mossmann, H., and Rajewsky, K. (1994). Deletion of a DNA polymerase β gene segment in T cells using cell type-specific gene targeting. *Science* 265, 103–106. doi: 10.1126/science.8016642

Guerrin, C. G. J., Doorduin, J., Sommer, I. E., and de Vries, E. F. J. (2021). The dual hit hypothesis of schizophrenia: evidence from animal models. *Neurosci. Biobehav. Rev.* 131, 1150–1168. doi: 10.1016/j.neubiorev.2021.10.025

Guy, J., Gan, J., Selfridge, J., Cobb, S., and Bird, A. (2007). Reversal of neurological defects in a mouse model of rett syndrome. *Science* 315, 1143–1147. doi: 10.1126/science.1138389

Hayashi, S., and McMahon, A. P. (2002). Efficient recombination in diverse tissues by a tamoxifen-inducible form of Cre: a tool for temporally regulated gene activation/inactivation in the mouse. *Dev. Biol.* 244, 305–318. doi: 10.1006/dbio.2002.0597

Heldt, S. A., and Ressler, K. J. (2011). The use of lentiviral vectors and Cre/loxP to investigate the function of genes in complex behaviors. *Front. Mol. Neurosci.* 2:22. doi: 10.3389/neuro.02.022.2009

Hui, Y., Zheng, X., Zhang, H., Li, F., Yu, G., Li, J., et al. (2022). Strategies for targeting neural circuits: how to manipulate neurons using virus vehicles. *Front. Neural. Circuits* 16:882366. doi: 10.3389/fncir.2022.882366

Jönsson, M. E., Garza, R., Johansson, P. A., and Jakobsson, J. (2020). Transposable elements: a common feature of neurodevelopmental and neurodegenerative disorders. *Trends Genet.* 36, 610–623. doi: 10.1016/j.tig.2020.05.004

Kellogg, C. M., Pham, K., Ko, S., Cox, J. E. J., Machalinski, A. H., Stout, M. B., et al. (2023). Specificity and efficiency of tamoxifen-mediated Cre induction is equivalent regardless of age. *IScience* 26:108413. doi: 10.1016/j.isci.2023.108413

Khatri, N., and Man, H. Y. (2019). The autism and Angelman syndrome protein Ube3A/E6AP: the gene, E3 ligase ubiquitination targets and neurobiological functions. *Front. Mol. Neurosci.* 12:109. doi: 10.3389/fnmol.2019.00109

Khoo, A. T. T., Kim, P. J., Kim, H. M., and Je, H. S. (2020). Neural circuit analysis using a novel intersectional split intein-mediated split-Cre recombinase system. *Mol. Brain* 13:101. doi: 10.1186/s13041-020-00640-2

Kim, J. S., Kolesnikov, M., Peled-Hajaj, S., Scheyltjens, I., Xia, Y., Trzebanski, S., et al. (2021). A binary cre transgenic approach dissects microglia and CNS border-associated macrophages. *Immunity* 54, 176–190.e7. doi: 10.1016/j.immuni.2020.11.007

Kingdom, R., and Wright, C. F. (2022). Incomplete penetrance and variable expressivity: from clinical studies to population cohorts. *Front. Genet.* 13:920390. doi: 10.3389/fgene.2022.920390

Koller, E. J., Comstock, M., Bean, J. C., Escobedo, G., Park, K-. W., Jankowsky, J. L., et al. (2022). Temporal and spatially-controlled APP transgene expression using Cre-dependent alleles. *Dis. Model Mech.* 15:dmm049330. doi: 10.1242/dmm.049330

Kouvaros, S., Bizup, B., Solis, O., Kumar, M., Ventriglia, E., Curry, F. P., et al. (2023). A CRE/DRE dual recombinase transgenic mouse reveals synaptic zinc-mediated thalamocortical neuromodulation. *Sci Adv.* 9:eadf3525. doi: 10.1126/sciadv.adf3525

Li, C., Fleck, J. S., Martins-Costa, C., Burkard, T. R., Themann, J., Stuempflen, M., et al. (2023). Single-cell brain organoid screening identifies developmental defects in autism. *Nature* 621, 373–380. doi: 10.1038/s41586-023-06473-y

Li, H., Wu, Y., Qiu, Y., Li, X., Guan, Y., Cao, X., et al. (2022). Stable transgenic mouse strain with enhanced photoactivatable cre recombinase for spatiotemporal genome manipulation. *Adv. Sci.* 9:e2201352. doi: 10.1002/advs.202201352

Li, J., Levin, D. S., Kim, A. J., Pappas, S. S., and Dauer, W. T. (2021). TorsinA restoration in a mouse model identifies a critical therapeutic window for DYT1 dystonia. *J. Clin. Invest.* 131:e139606. doi: 10.1172/JCI139606

Li, J., Sun, X., You, Y., Li, Q., Wei, C., Zhao, L., et al. (2022). Auts2 deletion involves in DG hypoplasia and social recognition deficit: the developmental and neural circuit mechanisms. *Sci. Adv* 8:eabk1238. doi: 10.1126/sciadv.abk1238

Lunev, E., Karan, A., Egorova, T., and Bardina, M. (2022). Adeno-associated viruses for modeling neurological diseases in animals: achievements and prospects. *Biomedicines* 10:1140. doi: 10.3390/biomedicines10051140

Marshall, L. J., Bailey, J., Cassotta, M., Herrmann, K., and Pistollato, F. (2023). Poor translatability of biomedical research using animals — a narrative review. *Altern. Lab. Anim.* 51, 102–135. doi: 10.1177/02611929231157756

Mei, Y., Monteiro, P., Zhou, Y., Kim, J. A., Gao, X., Fu, Z., et al. (2016). Adult restoration of Shank3 expression rescues selective autistic-like phenotypes. *Nature* 530, 481–484. doi: 10.1038/nature16971

Meng, X., Yao, D., Imaizumi, K., Chen, X., Kelley, K. W., Reis, N., et al. (2023). Assembloid CRISPR screens reveal impact of disease genes in human neurodevelopment. *Nature* 622, 359–366. doi: 10.1038/s41586-023-06564-w

Mielnik, C. A., Binko, M. A., Chen, Y., Funk, A. J., Johansson, E. M., Intson, K., et al. (2021). Consequences of NMDA receptor deficiency can be rescued in the adult brain. *Mol. Psychiatry* 26, 2929–2942. doi: 10.1038/s41380-020-00859-4

Paşca, S. P., Panagiotakos, G., and Dolmetsch, R. E. (2014). Generating human neurons *in vitro* and using them to understand neuropsychiatric disease. *Annu. Rev. Neurosci.* 37, 479–501. doi: 10.1146/annurev-neuro-062012-170328

Pasko, V. I., Churkina, A. S., Shakhov, A. S., Kotlobay, A. A., and Alieva, I. B. (2023). Modeling of neurodegenerative diseases: 'step by step' and 'network' organization of the complexes of model systems. *Int. J. Mol. Sci.* 24:604. doi: 10.3390/ijms24010604

Pomeshchik, Y., Klementieva, O., Gil, J., Martinsson, I., Hansen, M. G., de Vries, T., et al. (2020). Human iPSC-derived hippocampal spheroids: an innovative tool for stratifying Alzheimer disease patient-specific cellular phenotypes and developing therapies. *Stem Cell Rep.* 15, 256–273. doi: 10.1016/j.stemcr.2020.06.001

Pope, S. D., and Medzhitov, R. (2018). Emerging principles of gene expression programs and their regulation. *Mol. Cell* 71, 389–397. doi: 10.1016/j.molcel.2018.07.017

Rajewsky, K., Gu, H., Kühn, R., Betz, U. A., Müller, W., Roes, J., et al. (1996). Conditional gene targeting. *J. Clin. Invest.* 98, 600–603. doi: 10.1172/JCI118828

Rietdijk, C. D., Perez-Pardo, P., Garssen, J., van Wezel, R. J. A., and Kraneveld, A. D. (2017). Exploring Braak's hypothesis of Parkinson's disease. *Front. Neurol.* 8:37. doi: 10.3389/fneur.2017.00037

Robinson, N. B., Krieger, K., Khan, F., Huffman, W., Chang, M., Naik, A., et al. (2019). The current state of animal models in research: a review. *Int. J. Surg.* 72, 9–13. doi: 10.1016/j.ijsu.2019.10.015

Savulescu, A. F., Jacobs, C., Negishi, Y., Davignon, L., and Mhlanga, M. M. (2020). Pinpointing cell identity in time and space. *Front. Mol. Biosci.* 7:209. doi: 10.3389/fmolb.2020.00209

Schnütgen, F., Doerflinger, N., Calléja, C., Wendling, O., Chambon, P., Ghyselinck, N. B., et al. (2003). A directional strategy for monitoring Cre-mediated recombination at the cellular level in the mouse. *Nat. Biotechnol.* 21, 562–565. doi: 10.1038/nbt811

Seyhan, A. (2019). "Lost in translation the challenges with the use of animal models in translational research," in *Handbook of Biomarkers and Precision Medicine*, eds C. Carini, M. Fidock, and A. van Gool (Boca Raton, FL: Chapman and Hall/CRC), 36–43. doi: 10.31219/osf.io/kysdu

Shcholok, T., and Eftekharpour, E. (2023). Cre-recombinase systems for induction of neuron-specific knockout models: a guide for biomedical researchers. *Neural Regen. Res.* 18, 273–279. doi: 10.4103/1673-5374.346541

Silva-Santos, S., Van Woerden, G. M., Bruinsma, C. F., Mientjes, E., Jolfaei, M. A., Distel, B., et al. (2015). Ube3a reinstatement identifies distinct developmental windows in a murine Angelman syndrome model. *J. Clin. Invest.* 125, 2069–2076. doi: 10.1172/JCI80554

Sonzogni, M., Hakonen, J., Bernabé Kleijn, M., Silva-Santos, S., Judson, M. C., Philpot, B. D., et al. (2019). Delayed loss of UBE3A reduces the expression of Angelman syndrome-associated phenotypes. *Mol. Autism* 10:23. doi: 10.1186/s13229-019-0277-1

Subramanian, L., Calcagnotto, M. E., and Paredes, M. F. (2020). Cortical malformations: lessons in human brain development. *Front. Cell. Neurosci.* 13. doi: 10.3389/fncel.2019.00576

Susaimanickam, P. J., Kiral, F. R., and Park, I. H. (2022). Region specific brain organoids to study neurodevelopmental disorders. *Int. J. Stem Cells* 15, 26–40. doi: 10.15283/ijsc22006

Tanabe, L. M., Martin, C., and Dauer, W. T. (2012). Genetic background modulates the phenotype of a mouse model of dyt1 dystonia. *PLoS ONE* 7:e0032245. doi: 10.1371/journal.pone.0032245

Tanji, K., Miki, Y., Mori, F., Nikaido, Y., Narita, H., Kakita, A., et al. (2019). A mouse model of adult-onset multiple system atrophy. *Neurobiol. Dis.* 127, 339–349. doi: 10.1016/j.nbd.2019.03.020

Valassina, N., Brusco, S., Salamone, A., Serra, L., Luoni, M., Giannelli, S., et al. (2022). Scn1a gene reactivation after symptom onset rescues pathological phenotypes in a mouse model of Dravet syndrome. *Nat. Commun.* 13:161. doi: 10.1038/s41467-021-27837-w

Yonan, J. M., and Steward, O. (2023). Vector-mediated PTEN deletion in the adult dentate gyrus initiates new growth of granule cell bodies and dendrites and expansion of mossy fiber terminal fields that continues for months. *Neurobiol. Dis.* 184:106190. doi: 10.1016/j.nbd.2023.106190

Yoshimi, K., Yamauchi, Y., Tanaka, T., Shimada, T., Sato, M., Mashimo, T., et al. (2021). Photoactivatable Cre knock-in mice for spatiotemporal control of genetic engineering *in vivo*. *Lab. Invest.* 101, 125–135. doi: 10.1038/s41374-020-00482-5

Zhu, X., Lee, H.-G., Perry, G., and Smith, M. A. (2007). Alzheimer disease, the two-hit hypothesis: an update. *Biochim. Biophys. Acta Mol. Basis Dis.* 1772, 494–502. doi: 10.1016/j.bbadis.2006.10.014

frontiers | Frontiers in Neuroscience

TYPE Review
PUBLISHED 04 June 2024
DOI 10.3389/fnins.2024.1422442

OPEN ACCESS

EDITED BY
Nicola Simola,
University of Cagliari, Italy

REVIEWED BY
Susan L. Perlman,
Ronald Reagan UCLA Medical Center, United States
Bikash Choudhary,
University of California, Riverside, United States

*CORRESPONDENCE
Peng Yu
ypeng@jlu.edu.cn
Ming Dong
dongge@jlu.edu.cn

RECEIVED 24 April 2024
ACCEPTED 08 May 2024
PUBLISHED 04 June 2024

CITATION
Cui Z-T, Mao Z-T, Yang R, Li J-J, Jia S-S, Zhao J-L, Zhong F-T, Yu P and Dong M (2024) Spinocerebellar ataxias: from pathogenesis to recent therapeutic advances. *Front. Neurosci.* 18:1422442. doi: 10.3389/fnins.2024.1422442

Spinocerebellar ataxias: from pathogenesis to recent therapeutic advances

Zi-Ting Cui[1], Zong-Tao Mao[2], Rong Yang[1], Jia-Jia Li[1], Shan-Shan Jia[1], Jian-Li Zhao[1], Fang-Tian Zhong[1], Peng Yu[3]* and Ming Dong[1]*

[1]Department of Neurology and Neuroscience Center, The First Hospital of Jilin University, Changchun, China, [2]Department of Plastic and Reconstructive Surgery, The First Hospital of Jilin University, Changchun, China, [3]Department of Ophthalmology, the Second Hospital of Jilin University, Changchun, China

Spinocerebellar ataxia is a phenotypically and genetically heterogeneous group of autosomal dominant-inherited degenerative disorders. The gene mutation spectrum includes dynamic expansions, point mutations, duplications, insertions, and deletions of varying lengths. Dynamic expansion is the most common form of mutation. Mutations often result in indistinguishable clinical phenotypes, thus requiring validation using multiple genetic testing techniques. Depending on the type of mutation, the pathogenesis may involve proteotoxicity, RNA toxicity, or protein loss-of-function. All of which may disrupt a range of cellular processes, such as impaired protein quality control pathways, ion channel dysfunction, mitochondrial dysfunction, transcriptional dysregulation, DNA damage, loss of nuclear integrity, and ultimately, impairment of neuronal function and integrity which causes diseases. Many disease-modifying therapies, such as gene editing technology, RNA interference, antisense oligonucleotides, stem cell technology, and pharmacological therapies are currently under clinical trials. However, the development of curative approaches for genetic diseases remains a global challenge, beset by technical, ethical, and other challenges. Therefore, the study of the pathogenesis of spinocerebellar ataxia is of great importance for the sustained development of disease-modifying molecular therapies.

KEYWORDS

spinocerebellar ataxias, gene therapy, disease-modifying molecular therapies, neurodegenerative disorders, RNA interference, polyQ diseases

1 Introduction

Hereditary cerebellar ataxia encompasses a highly heterogeneous group of neurodegenerative disorders that are major causes of cerebellar ataxia, with modes of inheritance involving autosomal dominant, autosomal recessive, X-linked, or mitochondrial inheritance. Autosomal dominant cerebellar ataxia, also known as spinocerebellar ataxia (SCA), involves a wide variety of causative genes and mutation types, and in most cases lacks a clear genotype–phenotype correlation, which makes it difficult to reliably differentiate between the SCA subtypes by the clinical phenotype. Therefore, genetic testing is the primary diagnostic tool for this condition. There have been tremendous advances in this field owing to the emergence and application of genetic testing technologies, and the list of genes associated with SCA has been continuously expanding in recent years (Chen et al., 2015). The

clinical features of SCAs overlap with each other, and their core symptoms typically consist of gait instability, ataxia, nystagmus, and dysarthria. Some SCAs present as pure cerebellar syndromes, whereas the majority are frequently accompanied by nonataxic symptoms. The treatment approaches for SCAs are currently limited to symptomatic therapy. Owing to the commonalities in pathogenesis, developmental strategies for disease-modifying therapies applicable to multiple subtypes have been proposed. However, there are different causative proteins of each SCA subtype, and the search for broadly applicable therapeutic approaches should be accompanied by continued research into the pathogenesis and treatment of each disease. The purpose of this review was to broaden our understanding of the status of SCA research by presenting common clinical entities, describing their pathogenesis, and discussing the current and future therapeutic perspectives.

2 Pathogenic mechanisms

Based on the genetic nomenclature, the 50 identified SCAs are numbered in accordance with the order of discovery of their genetic locus. Moreover, SCAs are categorized into two groups according to their underlying mutation type into repeat expansions and point mutations. The former can be further categorized into SCAs induced by polyglutamine (polyQ)-encoding CAG repeat expansions and noncoding repeat expansions, owing to the different pathogeneses of the diseases. Among the SCAs induced by repeat expansion, six were due to the expanded CAG repeats encoding polyQ in their respective genes, which is the most common type. Since other neurodegenerative diseases, such as Huntington's disease (HD) and dentatorubral-pallidoluysian atrophy (DRPLA), share the same mechanism, they are collectively referred to as polyQ diseases (Durr, 2010). Some expanded repeats that cause SCAs are translated into different frames by a mechanism independent of the start codon (AUG) called repeat-associated non-AUG translation (RAN). This mechanism may also act on the antisense transcripts of the opposite strand. For example, in SCA8, noncoding CTG repeat expansion is transcribed from the 3′ untranslated region (3'UTR) of the *ATXN8OS* gene. Another gene, *ATXN8*, on the opposite strand, can generate an antisense transcript, and its CAG repeats can produce polyQ-containing proteins through RAN translation. Expanded CAG repeats in SCA12 occur in the 5′ untranslated region (5'UTR) of the *PPP2R2B* gene. Additionally, SCA10, SCA31, SCA36, and SCA37 are caused by expanded repeats in the intronic region. A heterozygous point mutation in FGF14 is the underlying cause of SCA27A. Recently, heterozygous GAA repeat expansion in intron 1 of FGF14 was reported to contribute to late-onset ataxia, referred to as SCA27B (Figure 1 and Table 1) (Coarelli et al., 2023a). Most SCAs caused by point mutations are results of missense mutations, whereas a small proportion are caused by deletions, translocations, or duplications of small DNA fragments (Table 2) (Ashizawa et al., 2018).

2.1 The polyQ SCAs

The primary pathogenic mechanism of polyQ SCAs are the toxic effects of the proteins encoded by mutant genes containing expanded CAG repeats, and to a lesser extent, the possible toxic effects of RNA transcripts from mutant genes (Coarelli et al., 2018). Mutated genes can also generate antisense transcripts containing complementary RNA repeat expansions from opposite DNA strands, and bidirectional expression of such expanded repeats occurs in SCA2, SCA7, and SCA8 (Ikeda et al., 2008; Sopher et al., 2011; Li et al., 2016). Furthermore, the disruption of natural protein function is correlated with toxic gain-of-function of aberrant polyQ. Altered proteins tend to form abnormal conformations that alter the way they bind to normal molecular chaperones and readily oligomerize and form intraneuronal oligomers and intranuclear inclusions. These aggregates may be directly toxic or produce toxic effects by sequestering proteins or cellular components, such as transcription factors, molecular chaperones, and components of the cellular clearance machinery, thereby triggering aberrant pathological processes leading to neuronal damage, such as impaired protein quality control (PQC) pathways, protein hydrolytic cleavage, transcriptional and post-translational dysregulation, aberrant protein interactions, ion channel dysfunction, impaired DNA repair, and mitochondrial dysfunction (Figure 2) (Paulson et al., 2017).

The PQC pathways include a ubiquitin-proteasome system, molecular chaperones, and autophagy, and the different components are tightly linked and interact with each other to maintain protein homeostasis and degrade misfolded proteins. Autophagy is involved in the degradation of damaged organelles or toxic protein aggregates, and there is growing evidence suggesting that impaired autophagy is associated with many neurodegenerative diseases such as SCA2, SCA3, Parkinson's disease, Alzheimer's disease, and HD (Menzies et al., 2017). The levels of the autophagy marker proteins SQSTM1 and LC3B were altered in SCA2 neuronal cells and lentiviral mouse models, and abnormal accumulation of SQSTM1 and LC3B was observed in the cerebellum and striatum of patients with SCA2, indicating that impaired autophagy may play an important role in the pathogenesis of SCA2 (Marcelo et al., 2021). ATXN3 is directly involved in PQC as a deubiquitinating enzyme, and PQC perturbation in SCA3 may result from a combination of accumulation of mutant ATXN3 aggregates, sequestration of the ubiquitin-proteasome system and autophagy regulators, and destabilization of Beclin1, a key protein of the autophagy pathway (McLoughlin et al., 2020). Almost all polyQ SCAs exhibit extensive mislocalization and aggregation of pathogenic proteins; therefore, the entire type may be associated with disturbed protein homeostasis.

It has been hypothesized that the cleavage of mutant polyQ proteins by proteolytic enzymes may produce more toxic short protein fragments, that are associated with the subsequent induction of aggregate formation. These fragments may translocate to the nucleus and interfere with transcription. Findings from several polyQ disease models, such as SCA3, SCA6, SCA7, and HD, provide evidence for this hypothesis (Buijsen et al., 2019). ATXN3 has multiple proteolytic sites. A study using L-glutamate to excite induced pluripotent stem cell (iPSC)-derived neurons from patients with SCA3 reported that the excitation initiated an inward flow of Ca^{2+}, induced intraneuronal cleavage of ATXN3, and led to the formation of insoluble aggregates. The insoluble substances could completely disappear after treatment with a calpain inhibitor, elucidating the critical role of calpain-mediated ATXN3 cleavage in the formation of aggregates (Koch et al., 2011). Therefore, the reduction of mutant protein aggregation may be achieved by inhibiting proteolytic cleavage, such as proteolytic

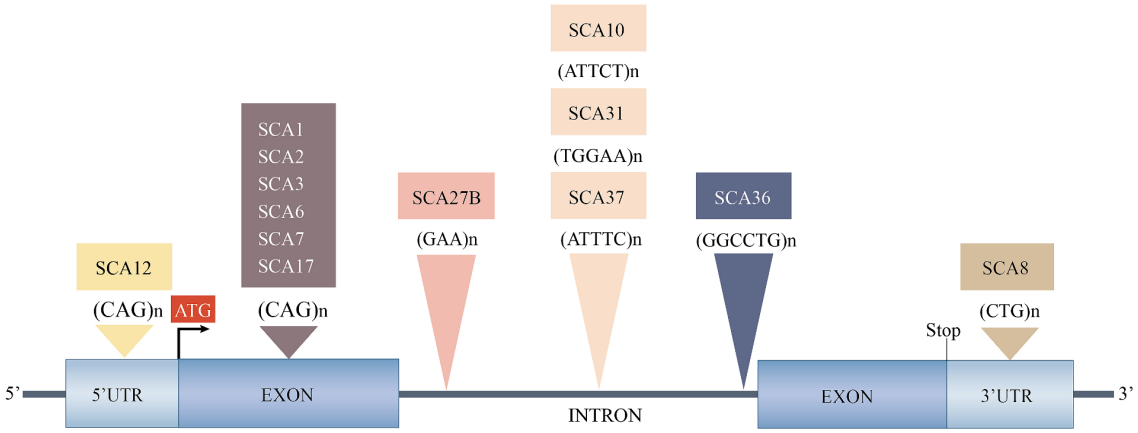

FIGURE 1
Spinocerebellar ataxias caused by expanded repeats. 3'UTR, 3' untranslated region; 5'UTR, 5' untranslated region; SCA, spinocerebellar ataxia. Reproduced from Ashizawa et al. (2018) with permission from Springer Nature.

TABLE 1 Spinocerebellar ataxias caused by repeat expansions.

Disease	Gene and protein (repeat location)	Repeats, principal repeat unit			Notable characteristic clinical signs
		Normal	Intermediate	Disease	
SCAs caused by polyglutamine-coding CAG repeat expansions					
SCA1	*ATXN1*	6–39	40	41–83	Hypermetric saccades, pyramidal signs
SCA2	*ATXN2*	<31	31–33	34–200	Slow saccades, areflexia
SCA3	*ATXN3*	12–44	45–55	56–86	Bulged eyes, motor neuron signs
SCA6	*CACNA1A*	<18	19	20–33	Downbeat nystagmus
SCA7	*ATXN7*	4–19	28–33	34- > 460	Visual loss
SCA17	*TBP*	25–40	-	41–66	Huntington disease-like
SCAs caused by noncoding repeat expansions					
SCA8	*OSATXN8* (3'UTR)	15–34, CTG or CAG	34–89, CTG or CAG	89–250, CTG or CAG	Reduced penetrance
SCA10	*ATXN10* (intron)	8–32 ATTCT	33–799 ATTCT	800–4,500, ATTCT	Some families with epilepsy
SCA12	*PPP2R2B* (5'UTR)	7–28, CAG	29–66, CAG	67–78, CAG	Tremor
SCA27B*	*FGF14* (intron)	Unknown	Unknown	250–300 or > 300, GAA	Late-onset episodic ataxia
SCA31	*BEAN* (intron)	<400, ATTTT	Unknown	500–760, TGGAA	Pure cerebellar ataxia
SCA36	*NOP56* (intron)	3–14, GGCCTG	Unknown	650–2,500	Motor neuron disease
SCA37	*DAB1* (5'UTR; intron)	<400, ATTTT	Unknown	31–75, ATTTC	Pure cerebellar ataxia

SCA, spinocerebellar ataxia.
SCA27B*: Repeats between 250 and 300 were pathogenic but showed incomplete penetrance, while repeats >300 showed complete penetrance.
Data were extracted from OMIM and GeneReviews of corresponding SCAs.
Reproduced from Ashizawa et al. (2018) with permission from Springer Nature.

enzyme inhibitors or gene therapy-based removal of protein regions containing proteolytic cleavage sites associated with toxic fragments.

2.2 SCAs caused by noncoding repeat expansions

In general, SCA10, SCA31, SCA36, and SCA37 are caused by pentanucleotide or hexanucleotide expansions within nonprotein-coding introns, resulting in the accumulation of toxic nonprotein-coding RNAs containing large expanded repeats in the intranuclear RNA foci. These foci sequester key RNA-binding proteins that perturb RNA-dependent RNA homeostasis, which may lead to cytotoxicity (Figure 2) (Zhang and Ashizawa, 2017). For example, RNA foci formed by the accumulation of AUUCU expansion in SCA10 can sequester heterogeneous cytosolic ribonucleoprotein K and impair its function, and its down-regulation can induce translocation and accumulation of protein kinase Cδ in the mitochondria, which subsequently triggers the caspase-3-mediated apoptotic pathway (Kurosaki and Ashizawa, 2022). Repeated ATTTC expansion of the *DAB1* gene leads to overexpression of DAB1 and induces an RNA switch, causing upregulation of the reelin-DAB1 and

TABLE 2 Spinocerebellar ataxias caused by point mutations.

Disease	Gene and protein	Mutation	Notable characteristic clinical signs
SCA5	*SPTBN2*	Missense, in-frame deletion	Downbeat nystagmus and some patients with spasticity, anticipation
SCA11	*TTBK2*	Frameshift	Some patients with pyramidal signs
SCA13	*KCNC3*	Missense	Variable between families
SCA14	*PRKCG*	Missense or exon deletions	Tremor or myoclonus, facial myokymia
SCA15 and SCA16	*ITPR1*	Exon deletions	Pure cerebellar ataxia with tremor
SCA18	*IFRD1*	Missense	Sensorimotor neuropathy
SCA19 and SCA22	*KCND3*	Missense or in-frame deletions	Extracerebellar features variable between families
SCA20	*Multiple*	260 kb duplication	Pure cerebellar ataxia with spasmodic dysphonia, palatal tremor
SCA21	*TMEM240*	Missense	Cognitive impairment, extrapyramidal signs
SCA23	*PDYN*	Missense	Extracerebellar features variable between families
SCA25	*PNPT1*	Splice site	Sensory neuropathy
SCA26	*EEF2*	Missense	Pure cerebellar ataxia
SCA27A	*FGF14*	Missense or frameshift	Mental retardation, tremor
SCA28	*AFG3L2*	Missense or frameshift	Spastic ataxia
SCA29	*ITPR1*	Missense	Pure cerebellar ataxia, congenital nonprogressive
SCA34	*ELOVL4*	Missense	Hyperkeratosis, MSA-C like
SCA35	*TGM6*	Missense or in-frame deletions	Hyperreflexia and variable other extracerebellar features
SCA38	*ELOVL5*	Missense	Pure cerebellar ataxia, some patients have sensory neuropathy
SCA40	*CCDC88C*	Missense	Spastic ataxia
SCA41	*TRPC3*	Missense	Pure cerebellar ataxia
SCA42	*CACNA1G*	Missense	Dementia
SCA43	*MME*	Missense	Peripheral neuropathy
SCA44	*GRM1*	Missense or frameshift	Spasticity
SCA45	*FAT2*	Missense	Pure cerebellar ataxia (single family)
SCA46	*PLD3*	Missense	Sensory neuropathy
SCA47	*PUM1*	Missense	Pure cerebellar ataxia in adults. Juvenile forms have developmental complex phenotype
SCA48	*STUB1*	Missense or frameshift	Cerebellar ataxia or cognitive/affective disorder
SCA49	*SAMD9L*	Missense	Cerebellar ataxia, cytopenia and myeloid malignancies
SCA50	*NPTX1*	Missense	Downbeat nystagmus, myoclonus, cognitive impairment

MSA-C, Multiple system atrophy-cerebellar type; SCA, spinocerebellar ataxia.
Data were extracted from OMIM and GeneReviews of corresponding SCAs.
Reproduced from Ashizawa et al. (2018) with permission from Springer Nature.

PI3K/AKT signaling pathways in the cerebellum of patients with SCA37, leading to cerebellar neuronal degeneration (Corral-Juan et al., 2018).

Bidirectional expression and RAN translation potentially cause the dual pathogenesis of SCA8, with RAN translation products accumulating in cells as toxic aggregates that disrupt the function of nuclear pores and integrity of membrane-free organelles (Figure 2). However, the degree of pathogenicity of RAN translation in relation to the toxic RNA transcripts produced by bidirectional expression remains to be investigated (Lee et al., 2017). In SCA12, expanded CAG repeats in the 5'UTR of *PPP2R2B* have been hypothesized to cause the disease by misregulating the host gene expression through alteration of promoter activity, splicing, and transcript stability. In a recent study, bidirectional expression of repeat sequences, toxic foci of antisense transcripts, and RAN translation were observed in SCA12-iPSCs, iPSC-derived NGN2 neurons, and mouse brains. Therefore, SCA12 may be involved in a pathogenic mechanism similar to that of SCA8 (Cohen and Margolis, 2016; Zhou et al., 2023). SCA27B iPSC-derived motoneurons and cerebellar autopsy specimens of patients with SCA27B showed reduced expression of FGF14 RNA and protein; thus, the causative factor was considered to be a loss of protein function due to transcriptional interference; however, the mechanism leading to FGF14 transcriptional defects still requires further investigation (Rafehi et al., 2023).

2.3 SCAs caused by point mutations

The application of NGS in the diagnosis of genetic ataxia has led to a rapidly increasing number of genetic variations, including

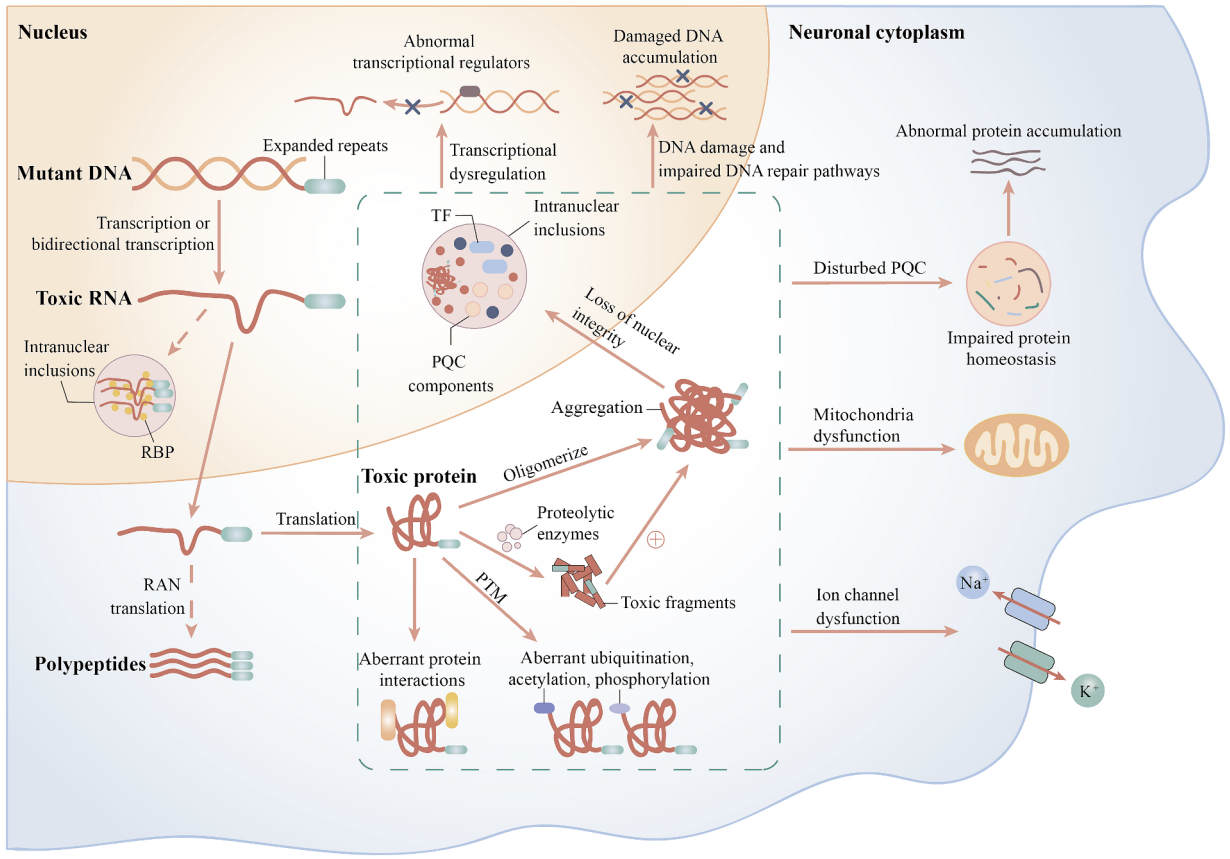

FIGURE 2
Possible pathogenic mechanisms of spinocerebellar ataxias. Solid arrows indicate possible mechanisms for polyQ SCAs and dashed arrows indicate possible mechanisms for SCAs caused by noncoding repeat expansions. RAN, non-AUG translation; RBP, RNA-binding protein; PQC, protein quality control; PTM, post-translational modifier; TF, transcription factor.

disease-causing mutations and variations of unknown significance (VUS). Most known disease-causing mutations are missense mutations, and the pathogenic mechanism may involve a toxic gain-of-function of mutant proteins or a dominant negative effect (Klockgether et al., 2019). For example, SCA35 is caused by mutations in the TGM6 gene encoding TG6, which causes neuronal dysfunction and death, including reduced distribution of mutant proteins in the nucleus compared to the baseline levels, loss of enzyme activity, and abnormal accumulation of mutants in the perinuclear region, with reduced solubility and ease of aggregation, leading to the acquisition of toxicity (Tripathy et al., 2017). In addition, haploinsufficiency caused by loss-of-function mutations in genes may also cause SCAs such as SCA15/16, SCA27, and SCA47 (Iwaki et al., 2008; Misceo et al., 2009; Gennarino et al., 2018).

2.4 Possible downstream mechanisms

2.4.1 Impaired ion channels

Evidence suggests that impaired ion channels in the cerebellar circuitry result in abnormalities in Purkinje cell firing and alterations in the signaling pathways, contributing to neuronal dysfunction. Two pathways can cause ion channel dysfunction; first, mutations in genes encoding the ion channels themselves, such as SCA6, SCA13, SCA19/SCA22, SCA15/SCA16, SCA29, SCA41, SCA42, and SCA44; and second, mutations in genes encoding proteins that regulate the activity of ion channels, which indirectly cause changes in channel function or expression, mainly polyQ SCAs (Bushart and Shakkottai, 2019).

2.4.2 Mitochondrial dysfunction and impaired mitophagy

Any neurodegenerative disease may involve mitochondrial dysfunction in a common pathway, and SCAs disease proteins may directly or indirectly impair mitochondrial function, resulting in increased oxidative stress and impaired bioenergetics. SCA28 is caused by a missense mutation in *AFG3L2*, which encodes a key component of the mitochondrial m-AAA protease, and a study found that fibroblasts from mutant mice exhibited impaired mitochondrial bioenergetics, reduced mitochondrial membrane potential, and altered mitochondrial network connectivity and morphology, proposing that the slow accumulation of toxic mitochondrial proteins is a pathogenic trigger event (Mancini et al., 2019). One study observed increased mitochondrial oxidative stress, altered mitochondrial respiratory chain enzymes, and mitochondrial morphology in fibroblasts from a patient with SCA2 who had not yet demonstrated clinical symptoms, and another study reported that individuals carrying mutant ATXN3 had a significant loss of mitochondrial DNA content in the preclinical phase. These findings

suggest that mitochondrial dysfunction may precede the disease onset (Cornelius et al., 2017; Raposo et al., 2019).

In order to maintain an intact mitochondrial network and thus adequate cellular homeostasis, dysfunctional mitochondria can be selectively removed by the mitophagy process. In neurons, when damaged mitochondria cannot be removed by mitophagy, reactive oxygen species, nitrogen oxides, and other oxidizing substances are produced, which can cause a variety of neurodegenerative diseases, such as Alzheimer's disease, Parkinson's disease, and HD (Okatsu et al., 2013). The pathogenic mechanisms of SCA3 and SCA6 have recently been reported to also involve impaired mitophagy, with fibroblasts from SCA3 patients exhibiting altered mitochondrial morphology, impaired bioenergetics, and dysregulation of Parkin-VDAC1-mediated mitophagy processes, and the accumulation of mitochondrial structural damage in SCA6 Purkinje cells has been proposed to may be partially related to impaired mitophagy during late stages of the disease (Wiatr et al., 2021; Harmuth et al., 2022; Leung et al., 2024). The mechanisms of mitophagy discovered so far are classified into ubiquitin-dependent and ubiquitin-independent pathways, and PINK1 and Parkin are key proteins with interactions in the ubiquitin-dependent pathway. PINK1 is a serine/threonine kinase located in depolarized mitochondria, in depolarized, damaged mitochondria, autophosphorylated PINK1 accumulates in the outer mitochondrial membrane and recruits Parkin located in the cytoplasm (Lu et al., 2023). One known substrate of ataxin-3 is Parkin, which acts as an E3 ubiquitin-protein ligase that ubiquitinates mitochondrial outer membrane proteins, thereby recruiting autophagy proteins to induce mitochondrial degradation. A recent report proposed that in SCA3 disease, mutant ATXN3 is associated with an aberrant loss of Parkin, leading to a reduction in VDAC1 polyubiquitination, which impedes mitophagy and initiates the apoptotic pathway through multiple programs, and ultimately an apoptotic process that leads to cell death and neurodegeneration (Harmuth et al., 2022). Further studies are needed in the future to validate the role of mutant ATXN3 in causing dysregulation of the PINK1/Parkin pathway, to provide a theoretical basis for expanding the understanding of the pathogenesis of SCA3, discovering new therapeutic targets, and designing therapeutic approaches targeting the mitophagy process. Thus, the use of modulators of PINK1/Parkin pathway activity may be able to promote the onset of mitophagy and improve mitochondrial quality control. Previous studies have identified a number of pharmacological molecules with such effects, such as triphosphate kinetin, which has a higher affinity for PINK1 than the natural substrate ATP, and whose application to cells may promote Parkin recruitment levels in depolarized mitochondria by enhancing PINK1 activity. There are also studies focusing on Parkin, the tumor suppressor p53 may inhibit mitophagy by preventing its translocation to mitochondria through direct interaction with Parkin, and p53 inhibitor may improve mitophagy through a feedback loop between Parkin and p53 (Zhang et al., 2011; Osgerby et al., 2017; Zhang et al., 2020).

2.4.3 Transcriptional dysregulation

The pathogenesis of SCAs may involve multiple molecular mechanisms that lead to transcriptional dysregulation, such as protein-DNA interactions, acetylation, phosphorylation, and RNA interference. ATXN1 is a transcriptional cofactor that interacts with transcriptional regulators, RNA splicing factors, and some nuclear receptors during gene expression, and SCA1 pathogenesis is associated with altered interactions between ATXN1 and other proteins (Srinivasan and Shakkottai, 2019). Expanded ATXN1 facilitates the formation of transcriptional repressor complexes by binding to homologs of the transcriptional repressor protein capicua. Studies on mouse models and iPSCs from patients with SCA1 have shown that the ATXN1-capicua complex drives cerebellar toxicity through a gain-of-function mechanism (Rousseaux et al., 2018). The PolyQ expansion in SCA17 occurs within the transcription factor TATA box-binding protein (TBP), and impaired transcriptional activity caused by mutating TBP may be the main form of toxicity that leads to the pathogenesis of SCA17 (Yang et al., 2016). Furthermore, SCA47 is caused by mutations in the *PUM1* gene which belongs to a family of RNA-binding proteins that regulate mRNA stability and inhibit translation. Experiments on patient fibroblasts showed that *PUM1* missense mutations reduced PUM1 protein levels to varying degrees, whereas the levels of PUM1 targets, including ATXN1 and E2F3, were increased. PUM1-deficient mouse models exhibited progressive Purkinje cell degeneration and loss of dendritic arborization, producing a phenotype similar to that of SCA1 mice (Gennarino et al., 2015, 2018). ATXN7 is a component of the SAGA histone acetyltransferase complex and polyQ expansion disrupts its structural integrity, leading to transcriptional dysregulation, abnormal chromatin acetylation, and altered gene expression (McCullough and Grant, 2010).

2.4.4 Other possible mechanisms

DNA damage and impaired DNA repair pathways may also be involved in the pathogenesis of SCAs. Wild-type ATXN3 and its interacting proteins play a role in DNA repair factor recruitment, cell cycle arrest, DNA repair, and accumulation of DNA damage in the SCA3 animal model (Chatterjee et al., 2015; McLoughlin et al., 2020). Mutant PolyQ SCA proteins are frequently concentrated in the nucleus and can form intranuclear inclusions, indicating disruption of transmembrane transport and loss of nuclear integrity. Each SCA subtype may have different downstream consequences owing to differences in the structure, function, and location of normal protein expression.

3 Treatments

Currently, the clinical intervention for patients with SCAs primarily focuses on symptomatic alleviation and functional maintenance because of the absence of effective etiologic treatments, as no medications have been authorized for routine use (Braga Neto et al., 2016). Research on the pathogenesis of SCAs has provided promising therapeutic targets for disease-modifying therapies. This group of diseases may require common therapeutic strategies as well as individualized treatments for the genetic causes of specific SCAs. Since most SCAs are caused by the dominant action of mutant genes, silencing or reducing the expression of the corresponding genes, transcripts, or proteins they encode is a compelling therapeutic strategy. Current therapeutic approaches include gene therapies to reduce toxic gene products, the use of pharmacological molecules to target the affected downstream pathways, and non-pharmacological therapies (Keiser et al., 2016). This review focuses on the latest breakthroughs, challenges, and future directions in gene editing

technologies, RNA interference (RNAi), antisense oligonucleotides (ASOs), stem cell technologies, and pharmacologic treatments (Table 3). Each of these therapies has undergone preclinical studies; however, owing to technological bottlenecks, gene editing technologies and RNAi are still in the preclinical stage, whereas others have successively progressed to clinical trials. Early disease intervention is crucial and studies have revealed that some patients with SCAs have a preataxia phase that lasts for several years before the emergence of noticeable ataxia symptoms. During this time, neurons may still be able to be repaired to some extent. Therefore, it is necessary to conduct early preventive trials and develop sensitive biomarkers for patients with SCAs (Maas et al., 2015).

3.1 Gene editing strategy

Gene editing strategies targeting mutant alleles enable precise and permanent gene correction, which can affect all downstream pathways. The main gene editing platform used in the current study was the clustered regularly interspaced short palindromic repeats (CRISPR)/Cas9 system (Figure 3A) (Nouri Nojadeh et al., 2023). A recent study precisely corrected SCA3-iPSCs using a CRISPR/Cas9-mediated homologous recombination strategy, and the corrected iPSCs differentiated normally into neural stem cells and neuronal cells and maintained normal electrophysiological properties. Another study applied the CRISPR/Cas9 approach to SCA1 fibroblasts and revealed that the expression of disease-related proteins was downregulated. These results support the CRISPR/Cas9 system as an effective gene modification technique (He et al., 2021; Pappadà et al., 2022). However, editing strategies have not yet progressed to animal models and clinical trials, and their implementation faces numerous technological challenges, such as optimizing delivery to target cells and minimizing off-target effects.

3.2 RNA interference

Targeting mutant mRNA transcripts may be the next best therapeutic alternative. Currently, there are two main oligonucleotide-based therapeutic strategies, namely RNAi and ASOs therapies, that can be applied using either non-allele-specific or allele-specific strategies. Non-allele-specific strategies may target both mutant and wild-type transcripts, resulting in unfavorable side effects by suppressing the expression of wild-type proteins. Allele-specific strategies, which typically focus on mutant alleles through single-nucleotide polymorphisms correlated with the disease allele, are technically challenging but more efficient (Vázquez-Mojena et al., 2021). A better understanding of the cellular function and gene regulation of SCAs proteins through studies in patients and disease models and the development of therapeutic approaches that have minimal impact on wild-type proteins or retain wild-type proteins in normal cellular function while specifically inhibiting mutant proteins will be the future direction of clinical research.

In short, RNAi is a sequence-specific post-transcriptional gene silencing technology activated by double-stranded RNA molecules homologous to target genes, which can be mediated by three functionally different molecules: microRNA (miRNA), small interfering RNA (siRNA) and short hairpin RNA (shRNA); the single-stranded RNA formed after processing with Dicer nucleic acid endonuclease can be bound to RNA-induced silencing complexes to achieve the degradation or translational inhibition of target mRNA (Figure 3B) (Santos et al., 2023). Targeting CAG repeat expansion by shRNA was applied to DRPLA, SCA3, SCA7, and HD patient-derived fibroblasts; a reduction in the expression levels of the mutant proteins was reported to varying degrees without significant off-target effects (Kotowska-Zimmer et al., 2020). The primary mechanism of SCA1 is the toxic gain-of-function of mutant expansion-containing ATXN1, accompanied by a partial loss-of-function in the wild-type. A study combining artificial miRNA targeting ATXN1 and ATXN1 homolog ATXN1L into recombinant adeno-associated virus (AAV) vectors demonstrated that mice that administered the two-component AAV vector showed normalization of gene expression and improvement in motor function, with a better therapeutic effect than that in the mice treated with vectors expressing ATXN1L only (Carrell et al., 2022). A study using non-viral, stable nucleic acid-lipid particles as a vehicle, combined with a short peptide derived from the rabies virus glycoprotein and encapsulating siRNA targeting mutant ATXN3, effectively silenced the expression of mutant ATXN3 in SCA3 mouse models by intravenous administration, leading to a reduction in neuropathological and motor behavioral deficits; this is the first preclinical study examining the benefit of non-invasive systemic administration in polyQ diseases (Conceição et al., 2016). Additionally, RNAi-based therapies have been extensively studied preclinically in SCAs models. This provides a theoretical basis for clinical trials. However, their clinical application faces problems such as poor *in vivo* stability, effectiveness of delivery systems, and off-target effects.

3.3 Antisense oligonucleotides

In general, ASOs are single-stranded synthetic antisense oligonucleotides that are complementary to specific mRNA. When combined with the target mRNA, they may cause various mechanisms for blocking gene expression, including RNase H endonuclease-mediated mRNA cleavage, interference with splicing to achieve exon skipping, and interference with translation through steric blockage (Figure 3C) (Vázquez-Mojena et al., 2021). Preclinical studies of ASOs for the treatment of SCAs have yielded promising results, including those on cellular or animal models of SCA1, 2, 3, 7, and 13. A clinical trial of intrathecal injection of non-allele-specific ASOs in patients with SCA3 was initiated in 2022 (NCT05160558) (Coarelli et al., 2023b). Moreover, ASOs are considered the most promising gene therapies for treating SCAs; however, they have shown inconsistent results in clinical studies on patients with other neurodegenerative diseases. Nusersen, a modified ASO, has been approved for intrathecal injection in pediatric and adult patients with spinal muscular atrophy in the United States because of its effectiveness. However, three clinical trials using ASOs to treat patients with HD were interrupted for several reasons, such as worsening of the patients' clinical rating scales, increased frequency of severe adverse events, and failure of reducing the mutant protein levels in cerebrospinal fluid. Therefore, clinical trials involving patients with SCA3 have received considerable attention (Hoy, 2017; Tabrizi et al., 2022). Intravitreal injection of ASOs targeting ATXN7 mRNA in SCA7 mouse models showed better long-term

TABLE 3 Key conclusions of some spinocerebellar ataxia models.

SCAs Models	Therapy	Route of administration	Key conclusion	Ref.
SCA1 patients-derived fibroblasts	*ATXN1*-sgRNAs/Cas9	Nucleofection	ATXN1 expression was significantly down-regulated with no major effects on cell viability and few off-target effects	Pappadà et al. (2022)
SCA3-iPSCs	*ATXN3*-sgRNAs/Cas9	Nucleofection	The corrected SCA3-iPSCs differentiated normally into neural stem cells and neurons, which could maintain electrophysiological properties, and the abnormal phenotype of SCA3 neurons was reversed	He et al. (2021)
DRPLA, SCA3, SCA7, and HD patients-derived fibroblasts	shRNA targeting CAG	Lentiviral vectors transduction	CAG-targeted shRNA reduces mutant protein levels without significant off-target effects and preferentially inhibits mutant Huntington protein expression	Kotowska-Zimmer et al. (2020)
SCA1 mouse models	Human ATXN1L, artificial miRNA targeting *ATXN1*	Direct delivery of recombinant AAV vectors to the deep cerebellar nuclei	Mice treated with vectors expressing ATXN1L alone showed changes in gene expression and improved locomotion. Restoration of dysregulated gene expression was greater when vectors expressing both components were used	Carrell et al. (2022)
SCA3 mouse models	siRNA targeting *ATXN3*	Intravenous administration of stable nucleic acid lipid particles	These nanoparticles successfully crossed the blood–brain barrier and reduced mutant ATXN3 levels in the mouse cerebellum, ameliorated motor deficits, and reduced cerebellar-related neuropathology	Conceição et al. (2016)
SCA7 mouse models	ASO targeting *ATXN7* ASO targeting CAG	Intravitreal injection	Ataxin-7 ASO reduced retinal ATXN7 expression and protein aggregation, improved cone and rod photoreceptor function and gene expression, and rescued retinal degeneration, achieving a significant beneficial therapeutic response in symptomatic mice. CAG ASO transiently improves retinal disease phenotype	Niu et al. (2018)
SCA13 mouse models	ASO targeting *Kcnc3*	Intracerebroventricular injection	Kv3.3 ASO reduced Kv3.3 channel expression in mutant mice, decreased TBK1 activation, reversed the reduction in the level of Hax-1, and restored the ability to maintain balance on the rotating rod to the level of wild-type mice	Zhang et al. (2021)
SCA1 mouse models	Human umbilical MSCs	Transplantation into the cerebella	MSCs did not differentiate into neurons or astrocytes in the cerebellum and had the effect of attenuating Purkinje cell loss and cerebellar atrophy, improving deterioration of motor coordination and limb muscle contraction, and promoting the expression of some growth-promoting factors	Tsai et al. (2019)
SCA3 mouse models	Human bone marrow MSCs, human bone marrow MSCs secretome (CM)	Single transplantation of MSCs or injection of CM in different brain regions (cerebellum, striatum/substantia nigra, and spinal cord)	Single CM administration to the cerebellum or basal ganglia resulted in mild but short-lasting improvements in motor deficits in mice, and no benefit was observed with CM administration to other brain regions or single MSCs transplantation	Correia et al. (2021)
SCA3 mouse models	Calpain inhibitor BDA-410	Oral administration	BDA-410 reduced ATXN3 levels, fragment formation, and aggregation, which served to reduce toxicity to cells, prevent cerebellar cell loss and striatal degeneration, mediate neuroprotection, and alleviate motor deficits	Simões et al. (2014)
SCA3 transgenic zebrafish models	BLD-2736, inhibitor of calpain-1, 2, and 9 and cathepsin K	Submersion in drug dissolved in water	BLD-2736 treatment improved the swimming behavior of SCA3 zebrafish larvae and reduced the presence of insoluble protein aggregates, increased the synthesis of LC3II, a key protein in autophagy, and autophagic activity	Robinson et al. (2021)
SCA3 mouse models	Citalopram	Oral administration	After treatment, mice showed improved motor balance and coordination, reduced brainstem ATXN3 intranuclear inclusions and reactive astrogliosis, and decreased facial neuron loss	Teixeira-Castro et al. (2015)

(Continued)

10.3389/fnins.2024.1422442

TABLE 3 (Continued)

SCAs Models	Therapy	Route of administration	Key conclusion	Ref.
Fibroblast cell lines from patients with SCA2 or ALS-FTD Mouse models of these diseases	siRNA-STAU1, siRNA-mTOR, and rapamycin Stau1 loss-of-function allele mice	Multiple routes	In disease models, STAU1 and mTOR were overabundant, interacted with each other, and inhibited autophagic flux. In cell models, STAU1 was found to bind mTOR mRNA to promote its translation, and when mTOR activity was inhibited, STAU1 levels were reduced. Reducing Staufen1 levels in mice improved autophagy and reduced cell death	Paul et al. (2023)
SCA3 patient iPSC-derived neuron cells models	TFEB nuclear translocation mediated by umbilical cord blood-derived MSCs	Co-culture approach	MSCs with exosomal vesicles induced TFEB nuclear translocation in neuronal cells after co-culture, which may activate autophagy by regulating the AKT/mTOR and AMPK/mTOR signaling pathways, reduce the level and toxic effects of mutant proteins, and the interaction of mutant proteins with Beclin1	Han et al. (2022)
13 patients with SCA3	Trehalose (100 mg daily)	Oral for 6 months	At 6 months, 61% of patients had improved SARA scores, 8-min walk test scores, and quality of life scores. Patients with younger age of onset, shorter disease duration, and lower SARA scores had better responses to trehalose. Oral trehalose was well tolerated, with the main side effects being bloating and diarrhea	Noorasyikin et al. (2020)
38 patients with SCAs and 17 patients with Friedreich's ataxia	Riluzole (50 mg, twice daily) or placebo	Oral for 12 months	The proportion of patients with reduced SARA scores at 12 months was significantly higher in the riluzole group (50%) than in the placebo group (11%), and only sporadic mild adverse events were reported	Romano et al. (2015)
45 patients with SCA2	Riluzole (50 mg, twice daily) or placebo	Oral for 12 months	SARA scores were not significantly different between the two groups, and brain MRI did not show significant differences in volume changes in cerebellar or brainstem regions	Coarelli et al. (2022)
SCA1 mouse models	Chlorzoxazone-baclofen	Oral administration	The agent improves Purkinje neuron firing in a dose-responsive manner and ameliorates motor dysfunction originating in the cerebellum without affecting muscle strength	Bushart et al. (2021)
36 patients with SCA3	Low-dose VPA (400 mg, twice daily), high-dose VPA (600 mg, twice daily) or placebo	Oral for 12 weeks	Motor function was significantly improved in the VPA group compared to the placebo group, with a greater decrease in SARA scores in the high-dose group. Common adverse reactions included dizziness and loss of appetite, which occurred primarily in the high-dose group	Lei et al. (2016)
29 patients with SCA2	NeuroEPO (1.0 mg daily, 3 days per week) or placebo	Nasal administration for 6 months	SCAFI and SARA scores improved in the NeuroEPO group, but a high placebo effect was observed, and only one secondary outcome measure, saccade latency, was significantly lower	Rodriguez-Labrada et al. (2022)
9 patients with SCA38	DHA (600 mg daily)	Oral for 2 years	Clinical symptoms of the patients were stable, SARA or ICARS scores improved, and a significant increase in FDG-PET cerebellar metabolism identified oral DHA as an effective treatment with no observed side effects	Manes et al. (2019)

SgRNA, small guide RNA; iPSCs, induced pluripotent stem cells; DRPLA, dentatorubral-pallidoluysian atrophy; SCA, spinocerebellar ataxia; HD, Huntington's disease; shRNA, short hairpin RNA; miRNA, microRNA; AAV, adeno-associated virus; siRNA, small interfering RNA; ASO, antisense oligonucleotides; MSCs, mesenchymal stem cells; ALS-FTD, amyotrophic lateral sclerosis-frontotemporal dementia; mTOR, mechanistic target of rapamycin; TFEB, transcription factor EB; SARA, Scale for the Assessment and Rating of Ataxia; VPA, valproic acid; SCAFI, spinocerebellar ataxia functional index; DHA, docosahexaenoic acid; FDG-PET, 18-fluorodeoxyglucose-positron emission tomography; ICARS, International Cooperative Ataxia Rating Scale.

10.3389/fnins.2024.1422442

improvements than those observed with the intravitreal injection of ASOs targeting CAG repeat expansion, such as a significant reduction in ATXN7 expression and aggregation, amelioration of vision loss, and alleviation of retinal histopathology (Niu et al., 2018). Lateral ventricular injection of ASOs targeting Kv3.3 channels has little effect on wild-type mice; however, it suppresses the mRNA and protein levels of the Kv3.3 channel in mouse models of SCA13 and restores the behavior of mutant mice to that of age-matched wild-type mice, suggesting that targeting Kv3.3 expression may be a viable therapeutic approach for treating SCA13 (Zhang et al., 2021). The non-permeability of the blood–brain barrier, invasive delivery methods, and the requirement for multiple repeat administrations impede the clinical application of ASO therapies. The development of less invasive brain delivery methods remains challenging, with AAV vectors, nanoparticles, cell-penetrating peptides, or liposome-mediated delivery being promising alternatives (Lee L. K. C. et al., 2021).

3.4 Stem cell therapy

Stem cell technology offers new directions for the treatment of neurodegenerative diseases, possibly via cell replacement or neuronal trophic support. Mesenchymal stem cells (MSCs), with their high availability and paracrine and immunosuppressive effects, are the most widely used cell types for studying SCAs (Figure 3D) (Correia et al., 2023). Transplantation of human umbilical MSCs into the bilateral cerebellar cortex of SCA1 mouse models significantly improve motor behavior, effectively attenuate cerebellar atrophy, and reverse Purkinje cell death (Tsai et al., 2019). A study of single human bone marrow MSCs transplantation or single MSCs secretome administration in relevant brain regions of SCA3 mouse models revealed that MSCs secretome administration was more beneficial, especially when administered to the cerebellum and basal ganglia. However, the therapeutic effect was mild and transient, raising concerns about the replacement of MSCs by MSCs by-products, the efficacy and risk of repeated systemic administration, minimal invasiveness, and effective routes of administration (Correia et al., 2021). There are ongoing clinical studies related to MSCs that involve patients with SCA1, 2, 3, and 6, which have shown varying degrees of improvement in symptoms and ataxia scale scores. However, a systematic evaluation and meta-analysis based on previous clinical trials showed low and statistically indistinguishable evidence supporting functional recovery in patients with SCAs, which could possibly be attributed to some limitations such as the few conducted clinical studies, limited sample sizes, and low-quality study designs (Appelt et al., 2021). Therefore, large-scale, high-quality clinical trials are needed to determine the long-term efficacy, tolerability, and safety of stem cell therapies, and explore the optimal therapeutic doses, frequency, and routes of administration.

3.5 Pharmacological therapy

3.5.1 Reduction of toxic protein levels

Therapies targeting downstream toxic effects should primarily aim at reducing toxic protein levels, including inhibiting the production of toxic protein fragments, reducing mutant protein aggregation, and inducing autophagy to stimulate protein clearance (Buijsen et al., 2019). One approach to inhibit the production of toxic fragments is to inhibit the cleavage of mutant proteins by proteolytic enzymes. One study found that calpain-mediated expression of ataxin-3 cleavage fragments may induce mitochondrial fragmentation and cristae alterations, leading to a significant reduction in mitochondrial respiratory capacity, affecting proper clearance of damaged mitochondria by interfering with mitophagy, and increasing susceptibility to apoptosis (Harmuth et al., 2018). Oral administration of the calpain inhibitor BDA-410 to the SCA3 mouse model reduced the toxic fragments of the mutant ATXN3 protein, decreased the number of its inclusions, and prevented cerebellar cell loss, suggesting that calpain inhibitors may mediate neuroprotection and inhibit proteolysis (Simões et al., 2014). One study tested the efficacy of a novel small-molecule calpain inhibitor compound, BLD-2736, in the SCA3 transgenic zebrafish model and found that the animals showed a dose-dependent improvement in motor behavior, a reduction in insoluble protein aggregates, and an increase in the expression of key proteins for autophagy (Robinson et al., 2021). In the HD mouse model, calpain inhibition had a protective effect, increasing autophagosome levels, improving motor signs, and delaying the onset of tremor, and prolonged calpain inhibition did not lead to any significant deleterious phenotypes (Menzies et al., 2015). Another study found that inhibition of calpains, which is prevalent in the heart after ischemia–reperfusion, improved mitophagy in cardiac cells through processes such as increased translocation of LC3B to mitochondria (Chen et al., 2019). Thus, these studies suggest that calpain inhibitors may have a dual protective effect of reducing cleavage of ATXN3 and stimulating mitophagy or general autophagy. However, for most polyQ diseases, the proteolytic enzymes responsible for the cleavage of their mutant proteins have not been identified, and the inhibition of proteolytic enzymes may affect a wider range of proteins beyond mutant polyQ proteins, leading to side effects. Therefore, the feasibility of this strategy is limited. Citalopram was reported to inhibit ATXN3 aggregation and neurotoxicity; when tested in a mouse model of SCA3, it improved motor and coordination functions, reduced the number of intranuclear inclusions in the brainstem, and rescued motor neuron loss. Moreover, it may affect the folding and stabilization of ATXN3, thereby inhibiting its aggregation, rather than removing the mutant protein. Thus, citalopram may be a viable option to halt the SCA3 progression. Further studies are needed to validate its applicability in other patients or SCA-related diseases (Teixeira-Castro et al., 2015).

Impaired autophagy occurs in a variety of neurodegenerative diseases. Therefore, the activation of autophagy may be a viable approach for treating neurodegeneration, and accordingly, multiple pathways targeting autophagy based on genes, stem cells, and pharmacology have been investigated. The mechanistic target of rapamycin (mTOR) kinase is a key regulator of different steps in the autophagy process, and its activity is regulated by complex interactions between upstream regulators, including AMPK, PI3K/AKT pathway, and ERK1/2 (Lee J. H. et al., 2021). A recent study revealed that the stress granule protein STAU1 is overexpressed in multiple models of neurodegenerative diseases and may interact with mTOR, leading to the overactivation of mTOR and inhibition of autophagic flux. Normalization of mTOR activity and some autophagy marker proteins was shown in an siRNA-STAU1 cell model and a mouse model with a Stau1 loss-of-function allele, suggesting that STAU1 might be a novel

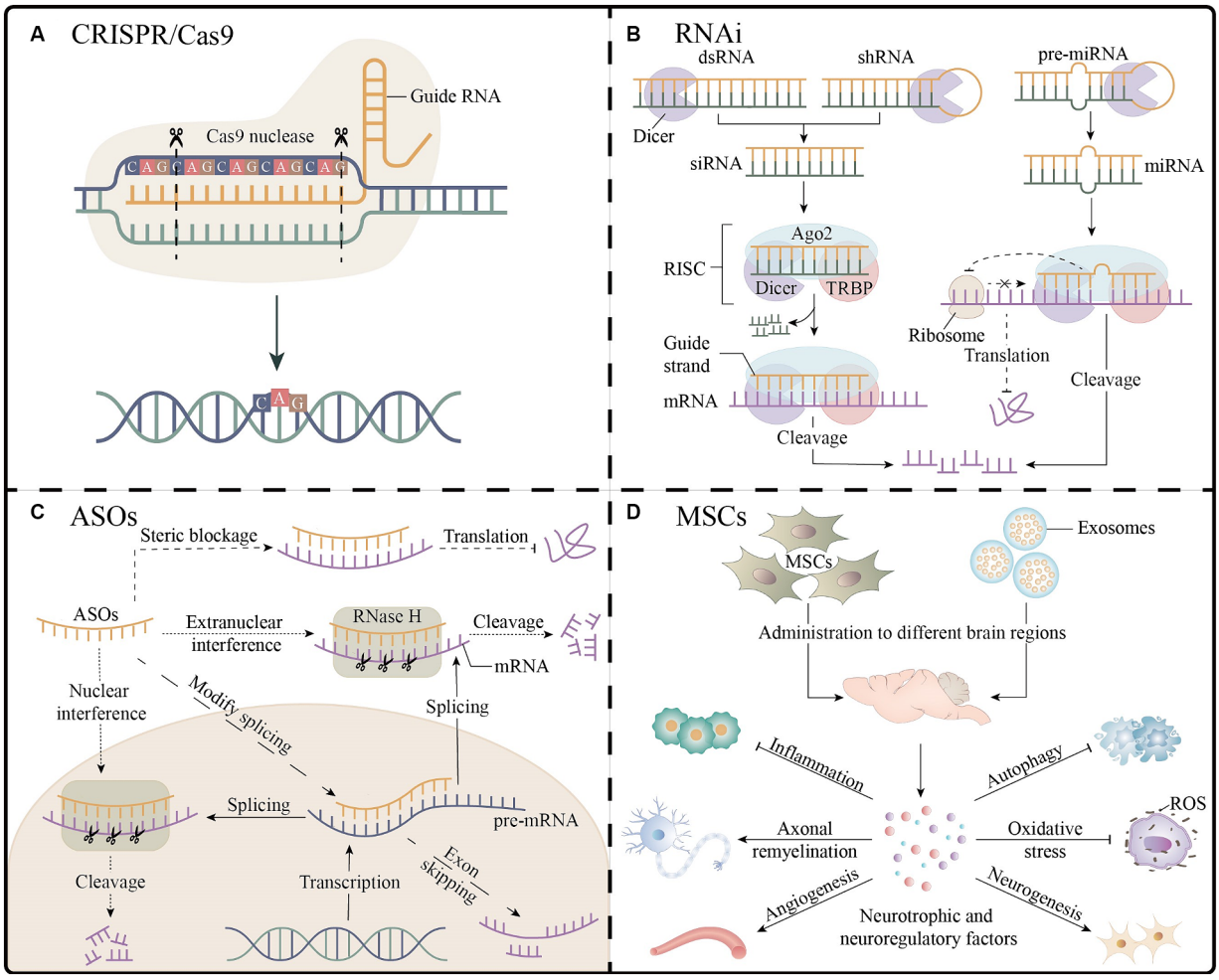

FIGURE 3
Gene therapy and stem cell therapy for spinocerebellar ataxias. **(A)** The CRISPR/Cas9 platform enables gene editing by guiding RNA strands to bind to target DNA, as shown in the figure for the knockdown of the expanded CAG repeats. **(B)** Three RNAi molecules mediate the process of mRNA cleavage and inhibition of translation outside the nucleus. **(C)** The ASOs inhibit gene expression through mRNA cleavage, interference with splicing, and steric blockage. **(D)** After entering different regions of the brain, MSCs or their exosomes secrete a variety of neuroprotective or neuroregulatory factors, which may have the effects of promoting neurogenesis processes (e.g., neuronal proliferation, differentiation, and myelination), improving angiogenesis, antioxidant, reducing inflammation, and inhibiting apoptosis, which is beneficial to neuronal cell survival and neurological function recovery. Ago2, argonaute2; ASOs, antisense oligonucleotides; CRISPR, clustered regularly interspaced short palindromic repeats; dsRNA, double-stranded RNA; miRNA, microRNA; MSCs, mesenchymal stem cells; RISC, RNA-induced silencing complexes; RNAi, RNA interference; ROS, reactive oxygen species; shRNA, short hairpin RNA; siRNA, small interfering RNA; TRBP, TAR RNA binding proteins.

target for regulating autophagy (Paul et al., 2023). The transcription factor EB (TFEB) regulates the expression of key genes for lysosomal biogenesis and autophagy at the transcriptional level. The mTOR can phosphorylate TFEB and anchor it to the cytoplasm; whereas in the mTOR-inactivated state, TFEB translocates to the nucleus, thereby promoting transcription (Menzies et al., 2017). A study that co-cultured umbilical cord blood-derived MSCs with iPSC-derived neurons from patients with SCA3 showed that MSCs induced TFEB nuclear translocation in neuronal cells, activated autophagy, and reduced the intracellular levels of mutant proteins by modulating the AKT/mTOR and AMPK/mTOR signaling pathways (Han et al., 2022). Trehalose is a widely used mTOR-independent autophagy inducer in neurodegenerative models, and clinical trials of oral trehalose have been conducted in patients with SCA3. Clinical symptoms showed improvements or were delayed in most patients; patients with younger age of onset, shorter disease duration, and lower Scale for the Assessment and Rating of Ataxia (SARA) scores displayed better responses to trehalose (Noorasyikin et al., 2020). Other pharmacological inducers, such as lithium, temsirolimus, cordycepin, carbamazepine, and n-butylidenephthalide, were reported to enhance autophagy in preclinical studies related to SCA1, SCA2, and SCA3, with cellular or animal models exhibiting decreased levels of mutant proteins, reduced number of aggregates, and improved neuropathology (Paulino and Nóbrega, 2023). Autophagy is currently one of the most studied targets in neurodegenerative diseases. The continued emergence of novel autophagy-inducing approaches suggests broad prospects for the development of this strategy, which may be a promising treatment alternative for patients with SCAs.

3.5.2 Improvement of ion channel dysfunction

Pharmacological agents potentially target impaired downstream mechanisms by modulating disturbances in cerebellar

electrophysiological circuits, correcting transcriptional dysregulation, improving mitochondrial dysfunction, and reducing other factors that lead to neuronal degeneration and damage. Riluzole is an anti-glutamatergic compound that may exert neuroprotective effects by inhibiting glutamatergic signaling-induced toxicity and opening calcium-activated potassium channels to modulate cerebellar neuronal firing. A randomized double-blind controlled trial included 55 patients diagnosed with SCAs and Friedreich ataxia who were divided into an oral riluzole group and a placebo group. After 12 months, the proportion of patients with decreased SARA scores was significantly higher in the oral riluzole group than in the placebo group. Furthermore, in a systematic review of pharmacological agents for SCAs, riluzole received a grade A recommendation for the treatment of ataxia symptoms (Romano et al., 2015; Yap et al., 2022). However, a homogeneous clinical trial of riluzole for the treatment of patients with SCA2 that was conducted in France reported less favorable outcomes, with no significant improvement in the imaging changes or SARA scores of the patients (Coarelli et al., 2022). Thus, riluzole may have different effects on different clinical forms of ataxia, and its pharmacological effects need to be evaluated in various populations with specific SCAs. Chlorzoxazone and baclofen are potassium channel-activating compounds that may target BK channels, which are large conductance calcium-activated potassium channels, and their reduced expression has been reported in SCA1, SCA2, and SCA7 mouse models. Reduced expression of BK and CaV3.1 ions in the cerebellum of SCA1 mice was also demonstrated in a recent study which combined the application of chlorzoxazone and baclofen with a resulting improvement in the physiology of Purkinje neuron and cerebellar motor dysfunction in mice and identification of the dose level to minimize cerebellar extracerebellar toxicity for potentially applying it to future clinical trials (Bushart et al., 2018, 2021). Given that changes in Purkinje neuronal excitability are present in various SCAs, ion channel modulators, particularly molecules with high target specificity, may be attractive approaches for symptomatic improvement.

3.5.3 Correction of transcription dysregulation

Transcriptional dysregulation is an important pathological process in polyQ diseases, and elevated histone acetylation levels favor transcriptional activation (Xiang et al., 2018). Several cellular and animal models of SCAs have demonstrated that some histone deacetylase inhibitors, such as sodium butyrate, trichostatin A, and valproic acid (VPA), can rescue histone hypoacetylation and transcriptional defects (Buijsen et al., 2019). A previous study determined the maximum tolerated single-dose VPA in patients with SCA3 to be 800 mg twice daily and subsequently tested the efficacy of long-term oral VPA in 36 patients with SCA3. After 12 weeks, patients in the low-dose (400 mg, twice daily) and high-dose (600 mg, twice daily) groups showed significant improvements in their motor function compared with that for the placebo group, with a more significant decrease in the SARA scores in the high-dose group. Based on the observed results, the combination of riluzole and VPA could potentially result in greater therapeutic efficacy (Lei et al., 2016). However, further studies are needed to determine the extent to which transcriptional dysregulation is involved in the pathogenesis of various SCAs and determine whether targeting this pathway will yield the desired outcomes.

3.5.4 Improvement of mitochondrial dysfunction

Many experiments have suggested that erythropoietin (EPO) may have neurotrophic effects, and the non-hematopoietic EPO analog, NeuroEPO, attenuated the glutamate excitotoxicity-induced oxidative stress, neuronal apoptosis, and neuroinflammation by maintaining mitochondrial membrane integrity, upregulating Bcl-2, and inhibiting Bax, cytochrome C, and caspase-3 (Garzón et al., 2018). A randomized, double-blind, placebo-controlled trial using the nasal administration of NeuroEPO in 34 patients with SCA2 was conducted to explore its potential efficacy. It showed a significant improvement in the saccade latency secondary outcome metric only. This, provides evidence of its feasibility for future clinical trials (Rodriguez-Labrada et al., 2022).

3.5.5 Other pharmacological molecules

The ELOVL5 mutation in patients with SCA38 leads to abnormalities and mislocalization of the encoded protein, causing reduced serum levels of the end-product, docosahexaenoic acid (DHA). A study demonstrated that the long-term oral DHA administration to patients with SCA38 slowed the onset and progression of symptoms and significantly improved cerebellar metabolism; accordingly, oral DHA (600 mg/day) administration is an effective treatment for SCA38 and it is essential to develop therapeutic approaches to treat specific SCA subtypes.

Rovatirelin, amantadine, buspirone, and varenicline are other agents that were suggested in previous studies to potentially alleviate symptoms in patients with SCAs. However, clinical trials investigating these drugs have not shown significant effects (Ghanekar et al., 2022). In summary, randomized controlled trials of pharmacological agents for the treatment of SCAs have been extensively conducted worldwide; however, there is no clear evidence of their potential benefits. It is important to note that most of these drugs are pleiotropic, such as the antidepressant effect of citalopram, the central muscle relaxant effect of chlorzoxazone-baclofen, and the anticonvulsant effect of valproic acid. Their possible short-and long-term side effects in patients with SCAs need to be determined in further studies. In addition, the potential applications of these pharmacological agents need to be validated in future clinical trials with adequate sample sizes, rigorous preclinical studies, and more comprehensive data analyses.

4 Discussion

The development of therapeutic approaches for SCAs is inextricably linked to studying their pathogenesis. For toxic gain-of-function mutations, various sites of the pathogenic cascade should be inhibited to reduce the expression of the mutant protein, whereas for loss-of-function mutations, attempts should be made to restore the defective protein to its baseline levels. Gene therapy suggests the possibility of rectifying the underlying factors of SCAs. Many preclinical studies have reported varying degrees of the inhibition of target gene expression *in vivo*, but its clinical application still faces difficulties such as the development of strategies to specifically target the mutated genes, selection of appropriate vectors and delivery modalities, potential toxicity risks, and ethical challenges for patient application. Stem cell therapies primarily focus on replacing degenerated and damaged neural cells; while key issues such as the route of administration, dosage, source, and culture conditions still

need to be addressed. Other therapeutic strategies and pharmacological molecules are being developed rapidly and show promise in improving clinical symptoms and slowing disease progression. Targeting autophagy is a meaningful therapeutic strategy, as its upregulation enhances the clearance of major pathogenic toxicants, may have additional protective effects, and may be beneficial in patients with a wide range of neurodegenerative diseases. Cerebellar circuit perturbations and motor dysfunctions caused by Purkinje cell electrophysiological dysfunction, a common feature of many SCAs, involve changes in a variety of ion channels; thus, approaches to target ion channels with higher specificity and potency should be designed in the future (Bushart et al., 2018). Elevated levels of oxidative stress, mitochondrial dysfunction, and activation of intrinsic apoptotic pathways play crucial roles in cell death in neurodegenerative diseases and provide a theoretical rationale for the use of antioxidants to maintain mitochondrial integrity, modulate redox status, and attenuate neurotoxicity (Garzón et al., 2018). It is worth noting that some SCAs mutant proteins may affect multiple cellular processes, and determining the extent to which each process is involved in the pathogenesis, targeting important pathways, and implementing combination therapies targeting multiple pathways may yield desirable therapeutic outcomes.

The ongoing development and application of genetic testing techniques, such as next-generation sequencing, long-read sequencing, and bioinformatics analyses have identified new mutant genes or new variant forms associated with SCAs. They have helped in improving the diagnostic accuracy of SCAs and discovering novel disease mechanisms. Future studies on the cellular functions of the causative proteins of various SCAs subtypes should be conducted to design novel and specific therapeutic approaches. The development of effective treatments for SCAs poses a significant challenge owing to the heterogeneity of its pathogenesis and pathological changes, the fact that each subtype may require specific treatment, and the insufficient sample size available for clinical trials of SCAs owing to its rare incidence. Previous therapeutic studies have favored common SCAs and provided some promising avenues that suggest the possible success of disease-modifying therapies for common SCAs. Animal and human trials suggest that initiating treatment in the early or pre-onset phase of the disease often results in better therapeutic outcomes, whereas in the most severe cases, it may not be very effective, requiring early diagnosis and intervention. In addition, the selection of appropriate outcome metrics and biomarkers in clinical trials is essential for understanding the underlying mechanisms and targets involved in each treatment, monitoring disease progression in different SCA genotypes, and assessing treatment efficacy. Therefore, the development of relevant and novel biomarkers is necessary to refine clinical trial design; moreover, high-quality clinical trials are needed to assess the efficacy and safety of the various treatments for SCAs.

Author contributions

Z-TC: Writing – original draft. Z-TM: Writing – original draft. RY: Writing – original draft. J-JL: Writing – original draft. S-SJ: Writing – original draft. J-LZ: Writing – original draft. F-TZ: Writing – original draft. PY: Writing – review & editing. MD: Writing – review & editing.

Funding

The author(s) declare financial support was received for the research, authorship, and/or publication of this article. This work was supported by grants from the National Natural Science Foundation of China (grant no. 31872772) and the Natural Science Foundation of Jilin Province of China (grant no. 20200201606JC) to MD.

Acknowledgments

We would like to thank Editage (www.editage.cn) for English language editing.

Conflict of interest

The authors declare that the research was conducted in the absence of any commercial or financial relationships that could be construed as a potential conflict of interest.

Publisher's note

References

Appelt, P. A., Comella, K., de Souza, L., and Luvizutto, G. J. (2021). Effect of stem cell treatment on functional recovery of spinocerebellar ataxia: systematic review and meta-analysis. *Cerebel. Ataxias* 8:8. doi: 10.1186/s40673-021-00130-8

Ashizawa, T., Öz, G., and Paulson, H. L. (2018). Spinocerebellar ataxias: prospects and challenges for therapy development. *Nat. Rev. Neurol.* 14, 590–605. doi: 10.1038/s41582-018-0051-6

Braga Neto, P., Pedroso, J. L., Kuo, S. H., Marcondes Junior, C. F., Teive, H. A., and Barsottini, O. G. (2016). Current concepts in the treatment of hereditary ataxias. *Arq. Neuropsiquiatr.* 74, 244–252. doi: 10.1590/0004-282x20160038

Buijsen, R. A. M., Toonen, L. J. A., Gardiner, S. L., and van Roon-Mom, W. M. C. (2019). Genetics, mechanisms, and therapeutic Progress in Polyglutamine spinocerebellar ataxias. *Neurotherapeutics* 16, 263–286. doi: 10.1007/s13311-018-00696-y

Bushart, D. D., Chopra, R., Singh, V., Murphy, G. G., Wulff, H., and Shakkottai, V. G. (2018). Targeting potassium channels to treat cerebellar ataxia. *Ann. Clin. Transl. Neurol.* 5, 297–314. doi: 10.1002/acn3.527

Bushart, D. D., Huang, H., Man, L. J., Morrison, L. M., and Shakkottai, V. G. (2021). A Chlorzoxazone-baclofen combination improves cerebellar impairment in spinocerebellar Ataxia type 1. *Mov. Disord.* 36, 622–631. doi: 10.1002/mds.28355

Bushart, D. D., and Shakkottai, V. G. (2019). Ion channel dysfunction in cerebellar ataxia. *Neurosci. Lett.* 688, 41–48. doi: 10.1016/j.neulet.2018.02.005

Carrell, E. M., Keiser, M. S., Robbins, A. B., and Davidson, B. L. (2022). Combined overexpression of ATXN1L and mutant ATXN1 knockdown by AAV rescue motor phenotypes and gene signatures in SCA1 mice. *Mol. Ther. Methods Clin. Dev.* 25, 333–343. doi: 10.1016/j.omtm.2022.04.004

Chatterjee, A., Saha, S., Chakraborty, A., Silva-Fernandes, A., Mandal, S. M., Neves-Carvalho, A., et al. (2015). The role of the mammalian DNA end-processing enzyme polynucleotide kinase 3′-phosphatase in spinocerebellar ataxia type 3 pathogenesis. *PLoS Genet.* 11:e1004749. doi: 10.1371/journal.pgen.1004749

Chen, Q., Thompson, J., Hu, Y., Dean, J., and Lesnefsky, E. J. (2019). Inhibition of the ubiquitous calpains protects complex I activity and enables improved mitophagy in the heart following ischemia-reperfusion. *Am. J. Physiol. Cell Physiol.* 317, C910–c921. doi: 10.1152/ajpcell.00190.2019

Chen, J. W., Zhao, L., Zhang, F., Li, L., Gu, Y. H., Zhou, J. Y., et al. (2015). Clinical characteristics, radiological features and gene mutation in 10 Chinese families with spinocerebellar ataxias. *Chin. Med. J.* 128, 1714–1723. doi: 10.4103/0366-6999.159340

Coarelli, G., Brice, A., and Durr, A. (2018). Recent advances in understanding dominant spinocerebellar ataxias from clinical and genetic points of view. *F1000Res* 7:1781. doi: 10.12688/f1000research.15788.1

Coarelli, G., Coutelier, M., and Durr, A. (2023a). Autosomal dominant cerebellar ataxias: new genes and progress towards treatments. *Lancet Neurol.* 22, 735–749. doi: 10.1016/s1474-4422(23)00068-6

Coarelli, G., Heinzmann, A., Ewenczyk, C., Fischer, C., Chupin, M., Monin, M. L., et al. (2022). Safety and efficacy of riluzole in spinocerebellar ataxia type 2 in France (ATRIL): a multicentre, randomised, double-blind, placebo-controlled trial. *Lancet Neurol.* 21, 225–233. doi: 10.1016/s1474-4422(21)00457-9

Coarelli, G., Wirth, T., Tranchant, C., Koenig, M., Durr, A., and Anheim, M. (2023b). The inherited cerebellar ataxias: an update. *J. Neurol.* 270, 208–222. doi: 10.1007/s00415-022-11383-6

Cohen, R. L., and Margolis, R. L. (2016). Spinocerebellar ataxia type 12: clues to pathogenesis. *Curr. Opin. Neurol.* 29, 735–742. doi: 10.1097/wco.0000000000000385

Conceição, M., Mendonça, L., Nóbrega, C., Gomes, C., Costa, P., Hirai, H., et al. (2016). Intravenous administration of brain-targeted stable nucleic acid lipid particles alleviates Machado-Joseph disease neurological phenotype. *Biomaterials* 82, 124–137. doi: 10.1016/j.biomaterials.2015.12.021

Cornelius, N., Wardman, J. H., Hargreaves, I. P., Neergheen, V., Bie, A. S., Tümer, Z., et al. (2017). Evidence of oxidative stress and mitochondrial dysfunction in spinocerebellar ataxia type 2 (SCA2) patient fibroblasts: effect of coenzyme Q10 supplementation on these parameters. *Mitochondrion* 34, 103–114. doi: 10.1016/j.mito.2017.03.001

Corral-Juan, M., Serrano-Munuera, C., Rábano, A., Cota-González, D., Segarra-Roca, A., Ispierto, L., et al. (2018). Clinical, genetic and neuropathological characterization of spinocerebellar ataxia type 37. *Brain* 141, 1981–1997. doi: 10.1093/brain/awy137

Correia, J. S., Duarte-Silva, S., Salgado, A. J., and Maciel, P. (2023). Cell-based therapeutic strategies for treatment of spinocerebellar ataxias: an update. *Neural Regen. Res.* 18, 1203–1212. doi: 10.4103/1673-5374.355981

Correia, J. S., Neves-Carvalho, A., Mendes-Pinheiro, B., Pires, J., Teixeira, F. G., Lima, R., et al. (2021). Preclinical assessment of mesenchymal-stem-cell-based therapies in spinocerebellar Ataxia type 3. *Biomedicines* 9:1754. doi: 10.3390/biomedicines9121754

Durr, A. (2010). Autosomal dominant cerebellar ataxias: polyglutamine expansions and beyond. *Lancet Neurol.* 9, 885–894. doi: 10.1016/s1474-4422(10)70183-6

Garzón, F., Coimbra, D., Parcerisas, A., Rodriguez, Y., García, J. C., Soriano, E., et al. (2018). Neuro EPO preserves neurons from glutamate-induced excitotoxicity. *J. Alzheimers Dis.* 65, 1469–1483. doi: 10.3233/jad-180668

Gennarino, V. A., Palmer, E. E., McDonell, L. M., Wang, L., Adamski, C. J., Koire, A., et al. (2018). A mild PUM1 mutation is associated with adult-onset Ataxia, whereas Haploinsufficiency causes developmental delay and seizures. *Cell* 172, 924–936.e11. doi: 10.1016/j.cell.2018.02.006

Gennarino, V. A., Singh, R. K., White, J. J., De Maio, A., Han, K., Kim, J. Y., et al. (2015). Pumilio1 haploinsufficiency leads to SCA1-like neurodegeneration by increasing wild-type Ataxin1 levels. *Cell* 160, 1087–1098. doi: 10.1016/j.cell.2015.02.012

Ghanekar, S. D., Kuo, S. H., Staffetti, J. S., and Zesiewicz, T. A. (2022). Current and emerging treatment modalities for spinocerebellar ataxias. *Expert. Rev. Neurother.* 22, 101–114. doi: 10.1080/14737175.2022.2029703

Han, X., de Dieu Habimana, J., Li, A. L., Huang, R., Mukama, O., Deng, W., et al. (2022). Transcription factor EB-mediated mesenchymal stem cell therapy induces autophagy and alleviates spinocerebellar ataxia type 3 defects in neuronal cells model. *Cell Death Dis.* 13:622. doi: 10.1038/s41419-022-05085-0

Harmuth, T., Prell-Schicker, C., Weber, J. J., Gellerich, F., Funke, C., Drießen, S., et al. (2018). Mitochondrial morphology, function and homeostasis are impaired by expression of an N-terminal Calpain cleavage fragment of Ataxin-3. *Front. Mol. Neurosci.* 11:368. doi: 10.3389/fnmol.2018.00368

Harmuth, T., Weber, J. J., Zimmer, A. J., Sowa, A. S., Schmidt, J., Fitzgerald, J. C., et al. (2022). Mitochondrial dysfunction in spinocerebellar Ataxia type 3 is linked to VDAC1 Deubiquitination. *Int. J. Mol. Sci.* 23:5933. doi: 10.3390/ijms23115933

He, L., Wang, S., Peng, L., Zhao, H., Li, S., Han, X., et al. (2021). CRISPR/Cas9 mediated gene correction ameliorates abnormal phenotypes in spinocerebellar ataxia type 3 patient-derived induced pluripotent stem cells. *Transl. Psychiatry* 11:479. doi: 10.1038/s41398-021-01605-2

Hoy, S. M. (2017). Nusinersen: first global approval. *Drugs* 77, 473–479. doi: 10.1007/s40265-017-0711-7

Ikeda, Y., Daughters, R. S., and Ranum, L. P. (2008). Bidirectional expression of the SCA8 expansion mutation: one mutation, two genes. *Cerebellum* 7, 150–158. doi: 10.1007/s12311-008-0010-7

Iwaki, A., Kawano, Y., Miura, S., Shibata, H., Matsuse, D., Li, W., et al. (2008). Heterozygous deletion of ITPR1, but not SUMF1, in spinocerebellar ataxia type 16. *J. Med. Genet.* 45, 32–35. doi: 10.1136/jmg.2007.053942

Keiser, M. S., Kordasiewicz, H. B., and McBride, J. L. (2016). Gene suppression strategies for dominantly inherited neurodegenerative diseases: lessons from Huntington's disease and spinocerebellar ataxia. *Hum. Mol. Genet.* 25, R53–R64. doi: 10.1093/hmg/ddv442

Klockgether, T., Mariotti, C., and Paulson, H. L. (2019). Spinocerebellar ataxia. *Nat. Rev. Dis. Primers* 5:24. doi: 10.1038/s41572-019-0074-3

Koch, P., Breuer, P., Peitz, M., Jungverdorben, J., Kesavan, J., Poppe, D., et al. (2011). Excitation-induced ataxin-3 aggregation in neurons from patients with Machado-Joseph disease. *Nature* 480, 543–546. doi: 10.1038/nature10671

Kotowska-Zimmer, A., Ostrovska, Y., and Olejniczak, M. (2020). Universal RNAi triggers for the specific inhibition of mutant huntingtin, Atrophin-1, Ataxin-3, and Ataxin-7 expression. *Mol. Ther. Nucleic Acids* 19, 562–571. doi: 10.1016/j.omtn.2019.12.012

Kurosaki, T., and Ashizawa, T. (2022). The genetic and molecular features of the intronic pentanucleotide repeat expansion in spinocerebellar ataxia type 10. *Front. Genet.* 13:936869. doi: 10.3389/fgene.2022.936869

Lee, Y. B., Baskaran, P., Gomez-Deza, J., Chen, H. J., Nishimura, A. L., Smith, B. N., et al. (2017). C9orf72 poly GA RAN-translated protein plays a key role in amyotrophic lateral sclerosis via aggregation and toxicity. *Hum. Mol. Genet.* 26, 4765–4777. doi: 10.1093/hmg/ddx350

Lee, L. K. C., Leong, L. I., Liu, Y., Luo, M., Chan, H. Y. E., and Choi, C. H. J. (2021). Preclinical nanomedicines for Polyglutamine-based neurodegenerative diseases. *Mol. Pharm.* 18, 610–626. doi: 10.1021/acs.molpharmaceut.0c00506

Lee, J. H., Lin, S. Y., Liu, J. W., Lin, S. Z., Harn, H. J., and Chiou, T. W. (2021). n-Butylidenephthalide modulates autophagy to ameliorate neuropathological Progress of spinocerebellar Ataxia type 3 through mTOR pathway. *Int. J. Mol. Sci.* 22:6339. doi: 10.3390/ijms22126339

Lei, L. F., Yang, G. P., Wang, J. L., Chuang, D. M., Song, W. H., Tang, B. S., et al. (2016). Safety and efficacy of valproic acid treatment in SCA3/MJD patients. *Parkinsonism Relat. Disord.* 26, 55–61. doi: 10.1016/j.parkreldis.2016.03.005

Leung, T. C. S., Fields, E., Rana, N., Shen, R. Y. L., Bernstein, A. E., Cook, A. A., et al. (2024). Mitochondrial damage and impaired mitophagy contribute to disease progression in SCA6. *Acta Neuropathol.* 147:26. doi: 10.1007/s00401-023-02680-z

Li, P. P., Sun, X., Xia, G., Arbez, N., Paul, S., Zhu, S., et al. (2016). ATXN2-AS, a gene antisense to ATXN2, is associated with spinocerebellar ataxia type 2 and amyotrophic lateral sclerosis. *Ann. Neurol.* 80, 600–615. doi: 10.1002/ana.24761

Lu, Y., Li, Z., Zhang, S., Zhang, T., Liu, Y., and Zhang, L. (2023). Cellular mitophagy: mechanism, roles in diseases and small molecule pharmacological regulation. *Theranostics* 13, 736–766. doi: 10.7150/thno.79876

Maas, R. P., van Gaalen, J., Klockgether, T., and van de Warrenburg, B. P. (2015). The preclinical stage of spinocerebellar ataxias. *Neurology* 85, 96–103. doi: 10.1212/wnl.0000000000001711

Mancini, C., Hoxha, E., Iommarini, L., Brussino, A., Richter, U., Montarolo, F., et al. (2019). Mice harbouring a SCA28 patient mutation in AFG3L2 develop late-onset ataxia associated with enhanced mitochondrial proteotoxicity. *Neurobiol. Dis.* 124, 14–28. doi: 10.1016/j.nbd.2018.10.018

Manes, M., Alberici, A., Di Gregorio, E., Boccone, L., Premi, E., Mitro, N., et al. (2019). Long-term efficacy of docosahexaenoic acid (DHA) for spinocerebellar Ataxia 38 (SCA38) treatment: an open label extension study. *Parkinsonism Relat. Disord.* 63, 191–194. doi: 10.1016/j.parkreldis.2019.02.040

Marcelo, A., Afonso, I. T., Afonso-Reis, R., Brito, D. V. C., Costa, R. G., Rosa, A., et al. (2021). Autophagy in spinocerebellar ataxia type 2, a dysregulated pathway, and a target for therapy. *Cell Death Dis.* 12:1117. doi: 10.1038/s41419-021-04404-1

McCullough, S. D., and Grant, P. A. (2010). Histone acetylation, acetyltransferases, and ataxia--alteration of histone acetylation and chromatin dynamics is implicated in the pathogenesis of polyglutamine-expansion disorders. *Adv. Protein Chem. Struct. Biol.* 79, 165–203. doi: 10.1016/s1876-1623(10)79005-2

McLoughlin, H. S., Moore, L. R., and Paulson, H. L. (2020). Pathogenesis of SCA3 and implications for other polyglutamine diseases. *Neurobiol. Dis.* 134:104635. doi: 10.1016/j.nbd.2019.104635

Menzies, F. M., Fleming, A., Caricasole, A., Bento, C. F., Andrews, S. P., Ashkenazi, A., et al. (2017). Autophagy and neurodegeneration: pathogenic mechanisms and therapeutic opportunities. *Neuron* 93, 1015–1034. doi: 10.1016/j.neuron.2017.01.022

Menzies, F. M., Garcia-Arencibia, M., Imarisio, S., O'Sullivan, N. C., Ricketts, T., Kent, B. A., et al. (2015). Calpain inhibition mediates autophagy-dependent protection against polyglutamine toxicity. *Cell Death Differ.* 22, 433–444. doi: 10.1038/cdd.2014.151

Misceo, D., Fannemel, M., Barøy, T., Roberto, R., Tvedt, B., Jaeger, T., et al. (2009). SCA27 caused by a chromosome translocation: further delineation of the phenotype. *Neurogenetics* 10, 371–374. doi: 10.1007/s10048-009-0197-x

Niu, C., Prakash, T. P., Kim, A., Quach, J. L., Huryn, L. A., Yang, Y., et al. (2018). Antisense oligonucleotides targeting mutant Ataxin-7 restore visual function in a mouse model of spinocerebellar ataxia type 7. *Sci. Transl. Med.* 10:eaap8677. doi: 10.1126/scitranslmed.aap8677

Noorasyikin, M. A., Azizan, E. A., Teh, P. C., Farah Waheeda, T., Siti Hajar, M. D., Long, K. C., et al. (2020). Oral trehalose maybe helpful for patients with spinocerebellar ataxia 3 and should be better evaluated. *Parkinsonism Relat. Disord.* 70, 42–44. doi: 10.1016/j.parkreldis.2019.12.007

Nouri Nojadeh, J., Bildiren Eryilmaz, N. S., and Ergüder, B. I. (2023). CRISPR/Cas9 genome editing for neurodegenerative diseases. *EXCLI J.* 22, 567–582. doi: 10.17179/excli2023-6155

Okatsu, K., Uno, M., Koyano, F., Go, E., Kimura, M., Oka, T., et al. (2013). A dimeric PINK1-containing complex on depolarized mitochondria stimulates Parkin recruitment. *J. Biol. Chem.* 288, 36372–36384. doi: 10.1074/jbc.M113.509653

Osgerby, L., Lai, Y. C., Thornton, P. J., Amalfitano, J., Le Duff, C. S., Jabeen, I., et al. (2017). Kinetin riboside and its ProTides activate the Parkinson's disease associated PTEN-induced putative kinase 1 (PINK1) independent of mitochondrial depolarization. *J. Med. Chem.* 60, 3518–3524. doi: 10.1021/acs.jmedchem.6b01897

Pappadà, M., Bonuccelli, O., Buratto, M., Fontana, R., Sicurella, M., Caproni, A., et al. (2022). Suppressing gain-of-function proteins via CRISPR/Cas9 system in SCA1 cells. *Sci. Rep.* 12:20285. doi: 10.1038/s41598-022-24299-y

Paul, S., Dansithong, W., Gandelman, M., Figueroa, K. P., Zu, T., Ranum, L. P. W., et al. (2023). Staufen impairs autophagy in neurodegeneration. *Ann. Neurol.* 93, 398–416. doi: 10.1002/ana.26515

Paulino, R., and Nóbrega, C. (2023). Autophagy in spinocerebellar Ataxia type 3: from pathogenesis to therapeutics. *Int. J. Mol. Sci.* 24:7405. doi: 10.3390/ijms24087405

Paulson, H. L., Shakkottai, V. G., Clark, H. B., and Orr, H. T. (2017). Polyglutamine spinocerebellar ataxias - from genes to potential treatments. *Nat. Rev. Neurosci.* 18, 613–626. doi: 10.1038/nrn.2017.92

Rafehi, H., Read, J., Szmulewicz, D. J., Davies, K. C., Snell, P., Fearnley, L. G., et al. (2023). An intronic GAA repeat expansion in FGF14 causes the autosomal-dominant adult-onset ataxia SCA27B/ATX-FGF14. *Am. J. Hum. Genet.* 110:1018. doi: 10.1016/j.ajhg.2023.05.005

Raposo, M., Ramos, A., Santos, C., Kazachkova, N., Teixeira, B., Bettencourt, C., et al. (2019). Accumulation of mitochondrial DNA common deletion since the Preataxic stage of Machado-Joseph disease. *Mol. Neurobiol.* 56, 119–124. doi: 10.1007/s12035-018-1069-x

Robinson, K. J., Yuan, K., Plenderleith, S. K., Watchon, M., and Laird, A. S. (2021). A novel Calpain inhibitor compound has protective effects on a zebrafish model of fspinocerebellar Ataxia type 3. *Cells* 10:2592. doi: 10.3390/cells10102592

Rodriguez-Labrada, R., Ortega-Sanchez, R., Hernández Casaña, P., Santos Morales, O., Padrón-Estupiñan, M. D. C., Batista-Nuñez, M., et al. (2022). Erythropoietin in spinocerebellar Ataxia type 2: feasibility and proof-of-principle issues from a randomized controlled study. *Mov. Disord.* 37, 1516–1525. doi: 10.1002/mds.29045

Romano, S., Coarelli, G., Marcotulli, C., Leonardi, L., Piccolo, F., Spadaro, M., et al. (2015). Riluzole in patients with hereditary cerebellar ataxia: a randomised, double-blind, placebo-controlled trial. *Lancet Neurol.* 14, 985–991. doi: 10.1016/s1474-4422(15)00201-x

Rousseaux, M. W. C., Tschumperlin, T., Lu, H. C., Lackey, E. P., Bondar, V. V., Wan, Y. W., et al. (2018). ATXN1-CIC complex is the primary driver of cerebellar pathology in spinocerebellar Ataxia type 1 through a gain-of-function mechanism. *Neuron* 97, 1235–1243.e5. doi: 10.1016/j.neuron.2018.02.013

Santos, C., Malheiro, S., Correia, M., and Damásio, J. (2023). Gene suppression therapies in hereditary cerebellar ataxias: a systematic review of animal studies. *Cells* 12:1037. doi: 10.3390/cells12071037

Simões, A. T., Gonçalves, N., Nobre, R. J., Duarte, C. B., and Pereira de Almeida, L. (2014). Calpain inhibition reduces ataxin-3 cleavage alleviating neuropathology and motor impairments in mouse models of Machado-Joseph disease. *Hum. Mol. Genet.* 23, 4932–4944. doi: 10.1093/hmg/ddu209

Sopher, B. L., Ladd, P. D., Pineda, V. V., Libby, R. T., Sunkin, S. M., Hurley, J. B., et al. (2011). CTCF regulates ataxin-7 expression through promotion of a convergently transcribed, antisense noncoding RNA. *Neuron* 70, 1071–1084. doi: 10.1016/j.neuron.2011.05.027

Srinivasan, S. R., and Shakkottai, V. G. (2019). Moving towards therapy in SCA1: insights from molecular mechanisms, identification of novel targets, and planning for human trials. *Neurotherapeutics* 16, 999–1008. doi: 10.1007/s13311-019-00763-y

Tabrizi, S. J., Estevez-Fraga, C., van Roon-Mom, W. M. C., Flower, M. D., Scahill, R. I., Wild, E. J., et al. (2022). Potential disease-modifying therapies for Huntington's disease: lessons learned and future opportunities. *Lancet Neurol.* 21, 645–658. doi: 10.1016/s1474-4422(22)00121-1

Teixeira-Castro, A., Jalles, A., Esteves, S., Kang, S., da Silva Santos, L., Silva-Fernandes, A., et al. (2015). Serotonergic signalling suppresses ataxin 3 aggregation and neurotoxicity in animal models of Machado-Joseph disease. *Brain* 138, 3221–3237. doi: 10.1093/brain/awv262

Tripathy, D., Vignoli, B., Ramesh, N., Polanco, M. J., Coutelier, M., Stephen, C. D., et al. (2017). Mutations in TGM6 induce the unfolded protein response in SCA35. *Hum. Mol. Genet.* 26, 3749–3762. doi: 10.1093/hmg/ddx259

Tsai, P. J., Yeh, C. C., Huang, W. J., Min, M. Y., Huang, T. H., Ko, T. L., et al. (2019). Xenografting of human umbilical mesenchymal stem cells from Wharton's jelly ameliorates mouse spinocerebellar ataxia type 1. *Transl. Neurodegener.* 8:29. doi: 10.1186/s40035-019-0166-8

Vázquez-Mojena, Y., León-Arcia, K., González-Zaldivar, Y., Rodríguez-Labrada, R., and Velázquez-Pérez, L. (2021). Gene therapy for Polyglutamine spinocerebellar ataxias: advances, challenges, and perspectives. *Mov. Disord.* 36, 2731–2744. doi: 10.1002/mds.28819

Wiatr, K., Marczak, Ł., Pérot, J. B., Brouillet, E., Flament, J., and Figiel, M. (2021). Broad influence of mutant Ataxin-3 on the proteome of the adult brain, young neurons, and axons reveals central molecular processes and biomarkers in SCA3/MJD using Knock-in mouse model. *Front. Mol. Neurosci.* 14:658339. doi: 10.3389/fnmol.2021.658339

Xiang, C., Zhang, S., Dong, X., Ma, S., and Cong, S. (2018). Transcriptional dysregulation and post-translational modifications in Polyglutamine diseases: from pathogenesis to potential therapeutic strategies. *Front. Mol. Neurosci.* 11:153. doi: 10.3389/fnmol.2018.00153

Yang, S., Li, X. J., and Li, S. (2016). Molecular mechanisms underlying spinocerebellar Ataxia 17 (SCA17) pathogenesis. *Rare Dis.* 4:e1223580. doi: 10.1080/21675511.2016.1223580

Yap, K. H., Azmin, S., Che Hamzah, J., Ahmad, N., van de Warrenburg, B., and Mohamed Ibrahim, N. (2022). Pharmacological and non-pharmacological management of spinocerebellar ataxia: a systematic review. *J. Neurol.* 269, 2315–2337. doi: 10.1007/s00415-021-10874-2

Zhang, N., and Ashizawa, T. (2017). RNA toxicity and foci formation in microsatellite expansion diseases. *Curr. Opin. Genet. Dev.* 44, 17–29. doi: 10.1016/j.gde.2017.01.005

Zhang, C., Lin, M., Wu, R., Wang, X., Yang, B., Levine, A. J., et al. (2011). Parkin, a p53 target gene, mediates the role of p53 in glucose metabolism and the Warburg effect. *Proc. Natl. Acad. Sci. USA* 108, 16259–16264. doi: 10.1073/pnas.1113884108

Zhang, F., Peng, W., Zhang, J., Dong, W., Wu, J., Wang, T., et al. (2020). P53 and Parkin co-regulate mitophagy in bone marrow mesenchymal stem cells to promote the repair of early steroid-induced osteonecrosis of the femoral head. *Cell Death Dis.* 11:42. doi: 10.1038/s41419-020-2238-1

Zhang, Y., Quraishi, I. H., McClure, H., Williams, L. A., Cheng, Y., Kale, S., et al. (2021). Suppression of Kv3.3 channels by antisense oligonucleotides reverses biochemical effects and motor impairment in spinocerebellar ataxia type 13 mice. *FASEB J.* 35:e22053. doi: 10.1096/fj.202101356R

Zhou, C., Liu, H. B., Jahanbakhsh, F., Deng, L., Wu, B., Ying, M., et al. (2023). Bidirectional transcription at the PPP2R2B gene locus in spinocerebellar Ataxia type 12. *Mov. Disord.* 38, 2230–2240. doi: 10.1002/mds.29605

frontiers | Frontiers in Neuroscience

TYPE Brief Research Report
PUBLISHED 26 July 2024
DOI 10.3389/fnins.2024.1414145

OPEN ACCESS

EDITED BY
Maria Vincenza Catania,
Institute for Biomedical Research and Innovation, National Research Council (CNR), Italy

REVIEWED BY
Janakiraman Udaiyappan,
Southern Methodist University, United States
Wojciech Piotr Paslawski,
Karolinska Institutet (KI), Sweden

*CORRESPONDENCE
Hiroaki Yaguchi
✉ yaguchi-h@pop.med.hokudai.ac.jp
Ichiro Yabe
✉ yabe@med.hokudai.ac.jp

†These authors have contributed equally to this work and share first authorship

RECEIVED 08 April 2024
ACCEPTED 11 July 2024
PUBLISHED 26 July 2024

CITATION
Tanaka D, Yaguchi H, Yoshizaki K, Kudo A, Mori F, Nomura T, Pan J, Miki Y, Takahashi H, Hara T, Wakabayashi K and Yabe I (2024) Behavioral and histological analyses of the mouse *Bassoon* p.P3882A mutation corresponding to the human *BSN* p.P3866A mutation.
Front. Neurosci. 18:1414145.
doi: 10.3389/fnins.2024.1414145

Behavioral and histological analyses of the mouse *Bassoon* p.P3882A mutation corresponding to the human *BSN* p.P3866A mutation

Daiki Tanaka[1†], Hiroaki Yaguchi[1*†], Kaichi Yoshizaki[2,3†], Akihiko Kudo[1†], Fumiaki Mori[4], Taichi Nomura[1], Jing Pan[1], Yasuo Miki[4], Hidehisa Takahashi[5], Taichi Hara[6], Koichi Wakabayashi[4] and Ichiro Yabe[1*]

[1]Department of Neurology, Faculty of Medicine and Graduate School of Medicine, Hokkaido University, Sapporo, Japan, [2]Department of Disease Model, Aichi Developmental Disability Center, Kasugai, Japan, [3]Integrated Analysis of Bioresource and Health Care, Future Medical Sciences, Kobe University Graduate School of Medicine, Kobe, Japan, [4]Department of Neuropathology, Hirosaki University Graduate School of Medicine, Hirosaki, Japan, [5]Department of Molecular Biology, Yokohama City University Graduate School of Medicine, Yokohama, Japan, [6]Laboratory of Food and Life Science, Faculty of Human Sciences, Waseda University, Tokyo, Japan

Tauopathy is known to be a major pathognomonic finding in important neurodegenerative diseases such as progressive supranuclear palsy (PSP) and corticobasal degeneration. However, the mechanism by which tauopathy is triggered remains to be elucidated. We previously identified the point mutation c.11596C > G, p.Pro3866Ala in the *Bassoon* gene (*BSN*) in a Japanese family with PSP-like syndrome. We showed that mutated *BSN* may have been involved in its own insolubilization and tau accumulation. Furthermore, *BSN* mutations have also been related to various neurological diseases. In order to further investigate the pathophysiology of *BSN* mutation in detail, it is essential to study it in mouse models. We generated a mouse model with the mouse *Bassoon* p.P3882A mutation, which corresponds to the human *BSN* p.P3866A mutation, knock-in (KI) and we performed systematic behavioral and histological analyses. Behavioral analyses revealed impaired working memory in a Y-maze test at 3 months of age and decreased locomotor activity in the home cage at 3 and 12 months of age in KI mice compared to those in wild-type mice. Although no obvious structural abnormalities were observed at 3 months of age, immunohistochemical studies showed elevation of Bsn immunoreactivity in the hippocampus and neuronal loss without tau accumulation in the substantia nigra at 12 months of age in KI mice. Although our mice model did not show progressive cognitive dysfunction and locomotor disorder like PSP-like syndrome, dopaminergic neuronal loss was observed in the substantia nigra in 12-month-old KI mice. It is possible that BSN mutation may result in dopaminergic neuronal loss without locomotor symptoms due to the early disease stage. Thus, further clinical course can induce cognitive dysfunction and locomotor symptoms.

KEYWORDS

***Bassoon*, model mouse, behavioral analysis, histological analysis, progressive supranuclear palsy-like syndrome**

Introduction

Progressive supranuclear palsy (PSP) is a clinical syndrome including supranuclear palsy, postural instability, and cognitive decline. Neuropathologically, PSP is defined by neuronal loss in the basal ganglia and brainstem with widespread occurrence of neurofibrillary tangles (NFTs; Williams and Lees, 2009; Yoshida et al., 2022) and accumulation of phosphorylated tau (p-tau) protein in the brain (Williams and Lees, 2009). For patients in whom the diagnosis is unclear, clinicians must continue to accurately describe the clinical situation in each individual instead of labeling them with inaccurate diagnostic categories such as atypical parkinsonism or PSP mimics (Williams and Lees, 2009). We previously identified the point mutation c.11596C > G, p.Pro3866Ala in the *Bassoon* gene (*BSN*) in a Japanese family with PSP-like syndrome (Yabe et al., 2018). We are the first in the world to report the involvement of BSN proteins in neurological diseases (Yabe et al., 2018). We showed that mutated BSN protein may be involved in its own insolubilization and tau accumulation (Yabe et al., 2018).

BSN is an active zone scaffolding protein and it has been suggested that BSN controls presynaptic autophagy (Okerlund et al., 2017; Hoffmann-Conaway and Brockmann, 2020; Montenegro-Venegas et al., 2020). It was also reported that there are associations between BSN and protein quality control systems including autophagy (Okerlund et al., 2017) and ubiquitination (Ivanova et al., 2016). Montenegro-Venegas et al. reported that BSN interacts directly with proteasome and inhibits proteasome activity via interaction with PSMB4 to control its activity at presynapses (Montenegro-Venegas et al., 2021). Moreover, Martinez et al. reported that *BSN* p.P3866A mutation caused tau seeding and showed toxicity in both mouse and Drosophila models for tauopathy and that BSN downregulation decreased tau spreading and overall disease pathology, rescuing synaptic and behavioral impairments and reducing brain atrophy (Martinez et al., 2022). It was shown that the degenerative eye phenotype was intensified in hTau-P301L flies when the BSN p.P3866A mutant was overexpressed (Martinez et al., 2022). Both WT BSN and mutant BSN p.P3866A interacted with tau in a Drosophila model (Martinez et al., 2022). Also, BSN overexpression in hTau-P301L flies led to an increase in tau-seeding activity, which was even higher with mutant *BSN* p.P3866A (Martinez et al., 2022). These studies suggested that BSN protein may play an important role in tauopathy.

The BSN protein and *BSN* gene were reported to be associated with multiple system atrophy (Hashida et al., 1998), Parkinson's disease (PD; Andrews and Kukkle, 2023), Huntington's disease (Huang et al., 2020), schizophrenia, bipolar disorder (Chen and Huang, 2021), multiple sclerosis (Schattling and Engler, 2019) and epilepsy (Ye et al., 2023). Gene burden analyses of rare, predicted deleterious variants provided evidence of *BSN* being linked to PD (Andrews and Kukkle, 2023). These studies have provided a mechanistic explanation for the recently described link between BSN and human diseases associated with pathological protein aggregation. That is why BSN may be one of the key proteins controlling neurological diseases.

To observe physiological changes caused by *BSN* mutations, we generated a mouse model of PSP-like syndrome with the mouse *Bassoon* p.P3882A mutation, which corresponds to the human Bassoon p.P3866A mutation.

Materials and methods

Animals

C57BL6/J male and female mice and ICR female mice were purchased from SLC (Hamamatsu, Japan). We used ICR mice for generating *Bassoon* p.P3882A mice. C57BL6/J male and female mice were used for mating. All experiments and analyses were performed with male C57BL6/J mice. For the generation of model mice with genome editing, 12-week-old males and 4-week-old females were used as sperm and oocyte donors, respectively. ICR female mice were used as recipients for embryo transfer. Male mice at 3 and 12 months of age were used for behavioral analyses. All animals were housed under a 12-h dark–light cycle (light from 7:00 to 19:00) at 23 ± 1°C with *ad libitum* access to food and water. All animal experiments were approved by the Ethics Committee for Animal Experiments of Aichi Institute for Developmental Research (2020-005) and Hokkaido University Graduate School of Medicine (22-0042) and were carried out in accordance with the National Institutes of Health guide for the care and use of laboratory animals.

Generation of *Bassoon* p.P3882A mice

Briefly, pronuclear stage embryos were produced using *in vitro* fertilization. Alt-R™S.p. Cas9 nuclease V3 (Cat#1081058), crRNA, and Alt-R®CRISPR-Cas9 tracrRNA (cat#1072532) were obtained from Integrated DNA Technologies Inc. (Coralville, IA, USA). crRNA was designed to target the *Bassoon* gene of C57BL6/J mice (5′-CCAGAGTACTCAGAGCAATCTCT-3′). Single-stranded oligodeoxyribonucleotides (ssODNs) consisting of 70-bps homology arms flanking the mutation c.11596C > G, p.Pro3866Ala and a modified restricted enzyme site for the *Sca* I site were synthetized by IDT (Coralville, IA, USA). The sequence was as follows: p.Pro3866Ala (Bold)/modified restricted enzyme site for the *Sca* I site (underline), 5′-CAAAGCGCCCCAGCAGGGACGGGCTCCTCAG GCGCAGAC AACTCCAGGAGCTGGACCTGCAGGTGAGCTGTGCCCAGAG ATCTCAGAGCAATCTCTCCCTATACCACTGT-3′. Nucleases were introduced into pronuclear stage embryos using the modified TAKE method (Kaneko and Mashimo, 2015). Two-cell embryos were transferred into the oviducts of pseudo-pregnant ICR females that were mated with vasectomized males the day before embryo transfer.

Behavioral analyses

Systematic behavioral analyses were performed according to previous reports with a total of 44 mice (WT mice at 3 months of age: 11, WT mice at 12 months: 11, KI mice at 3 months: 11, KI mice at 12 months: 11; Yoshizaki et al., 2008; Takagi et al., 2015; Yoshizaki and Asai, 2020; Yoshizaki and Kimura, 2021). Because two of the KI mice at 12 months died due to a water supply problem, we used 42 mice for analysis.

Open-field test

Locomotor activity and anxiety-like behavior were assessed by using a square open-field apparatus (50 × 50 × 50 cm, O'Hara & Co.,

Ltd., Tokyo, Japan) according to our previous report (Yoshizaki and Asai, 2020). Each mouse was placed in the center of the apparatus. The center zone was defined as a square 10 cm area away from the wall. The distance traveled and the time spent in the center zone were recorded for 10 min with a video imaging system (EthoVisionXT; Noldus Information Technology), according to previous papers.

Rotarod test

Motor coordination and learning were assessed by a rotarod test (single-lane apparatus, MK-630B; Muromachi, Tokyo, Japan). Each mouse was placed on a rotarod with a progressive acceleration setting from 4 to 40 rpm over a 10-min period. Five trials were performed for two consecutive days (3 trials on Day 1 and 2 trials on Day 2 at intervals of at least 1 h), and the time until falling was recorded.

Home cage activity test

Home cage activity was measured by the rotational frequency of a running wheel. Each mouse was placed alone in a home cage (180 mm in width × 225 mm in depth × 123 mm in height) with a running wheel (50 mm in width × 143 mm) under a 12-h light–dark cycle (lights on at 07:00 h) and had free access to both food and water. The rotational frequency of the running wheel was automatically recorded with a porcelain sensor (RWC-15; Melquest Ltd., Toyama, Japan) for 5 consecutive days starting at 13:00 on each day (CIF-4; Actmaster, Melquest, Ltd., Toyama, Japan).

Y-maze test

Spatial working memory and exploratory activity were assessed by using a Y-maze apparatus (arm length: 40 cm, arm bottom width: 3 cm, arm upper width: 13 cm, height of wall: 15 cm, BrainSicence Idea, Osaka, Japan). Each mouse was placed in the center area. The number of entries into arms and alterations were recorded for 10 min with a video imaging system (EthoVisionXT; Noldus information Technology). Working memory was calculated as: "number of correct alterations" divided by "number of total arm entries."

Novel object recognition test

Non-spatial working memory was assessed by a novel object recognition test in an open field apparatus (50 × 50 × 50 cm, O'Hara & Co., Ltd., Tokyo, Japan). The objects were made of urethane or metal and had two different shapes and colors: sphere (white) and cylinder (silver). In the first trial on the first day, two identical objects were presented on opposite sides of the apparatus, and the mice were allowed to explore the objects for 10 min. Exploration was considered as directing the nose at a distance of 1 cm from the object. In the second trial on the next day, one of the objects presented in the first trial was replaced with a novel object and the mice were placed in the box for 3 min. The time spent exploring the familiar (F) object and the time spent exploring the novel (N) object were automatically recorded with a video imaging system (EthoVisionXT; Noldus information Technology). A discrimination index was calculated as (N − F)/(N + F). Care was taken to avoid place preference and olfactory stimuli by randomly changing the role (which object is familiar or novel) and positions of the two objects during the second trial and by cleaning them carefully with 70% alcohol.

Histopathological analysis

For immunohistochemical analysis, mice were deeply anesthetized with isoflurane and perfused with 4% paraformaldehyde (PFA) dissolved in phosphate-buffered saline (PBS). Brains were postfixed with the same fixative overnight and then washed with PBS. Histopathological analysis was carried out as reported previously (Tanaka et al., 2022). The cerebrum was anteriorly transected at 1 mm anterior to the anterior edge of the pons and sliced at 2-mm intervals anterior and posterior to this level. The cerebellum and brainstem were sectioned in a midsagittal section. After dehydration through a graded ethanol series, the samples were embedded in paraffin and cut into 4-μm-thick sections. For routine histological examination, sections from each case were stained with hematoxylin and eosin (HE).

Immunohistochemistry

Immunohistochemical analysis was carried out using the above paraffin-embedded sections. The sections were dehydrated and pretreated with heat retrieval using an autoclave for 15 min in 10 mM citrate buffer (pH 6.0) for primary antibodies. The sections were then subjected to immunohistochemical processing using the avidin–biotin-peroxidase complex (ABC) method with a Vectastain ABC kit (Vector, Burlingame, CA) and diaminobenzidine (DAB; Sigma, St. Louis, MO). DAB exposure time was the same for each slide glass. In addition, the sections were counterstained with hematoxylin. We used primary antibodies against BSN (mouse, ab82958, Abcam, Cambridge, UK; 1:100), p-tau (rabbit, ab151559, Abcam; 1:2,000), synaptophysin (mouse, SY38, Dako, Glostrup, Denmark; 1:1,000), alpha-synuclein (mouse, 2A7, Novus Biologicals, Centennial, CO; 1:1,000), tyrosine hydroxylase (TH; mouse, TH-16, Sigma, St. Louis, MO; 1:500), TH (rabbit, CA-101, Protos Biotech Corporation, New York, NY; 1:200), ubiquitin (rabbit, Z0458, Dako; 1:1,000), p62 (mouse, 610,832, BD Biosciences, Franklin Lakes, NJ; 1:100), and vesicular monoamine transporter 2 (VMAT2) antibody (rabbit, 20,873-1-AP, Proteintech, Rosemont, IL, USA; 1:100). All regions of wild-type (WT) and *Bsn* knock-in (KI) mice were examined histopathologically, since BSN immunoreactivity was increased in the hippocampus of KI mice at the age of 12 months.

Semi-quantitative analysis of immunoreactivity for the proteins

Digital images of the caudate-putamen were captured by a digital camera (Provis AX-70, Olympus, Tokyo, Japan) and evaluated semi-quantitatively in terms of gray levels with NIH Image (version 1.61). The data were normalized by subtracting the background. The values were analyzed using Student's *t*-test to examine differences in

immunoreactivity for the proteins (BSN, p-tau, TH, synaptophysin, and alpha-synuclein) in the caudate-putamen between WT and KI mice.

Cell counts of TH-positive neurons

In each mouse, the numbers of TH-positive neurons were counted on both sides of the substantia nigra immunostained with TH-16. This primary antibody works well for both human and mouse samples. The entire substantia nigra was surveyed at a magnification of 200× using an eyepiece graticule and parallel sweeps of the microscope stage. The numbers were analyzed using Student's *t*-test to examine the differences between WT and KI mice.

Statistical analysis

Data are presented as means ± standard error of the mean (SEM). The differences between results of behavioral analyses for wild-type and *Bsn* variant mice were determined by Student's *t*-test and two-way ANOVA. StatPlus was used for statistical analysis and a p value less than 0.05 was considered to be statistically significant. Mann–Whitney's U test was used for statistical comparison of immunostaining intensities.

Results

Generation of the mouse *Bsn* p.P3882A variant that corresponds to the human *BSN* p.P3866A

In order to examine the effect of human *BSN* p.P3866A on the pathogenesis of PSP-like syndrome, we generated a mouse *Bsn* p.P3882A variant (corresponding to human *BSN* p.P3866A, Supplemental Figure 1A) knock-in mouse by using the TAKE (Technique for Animal Knockout system by Electroporation) method as previously described. Briefly, we designed gRNA targeting the coding sequence of *Bsn* and ssODNs with *Bsn* p.P3882A mutation and modified restricted enzyme site for *Sca* I (Supplemental Figure 1B). *Bsn* variant genotyping was conducted using PCR and restriction enzyme with *Sca* I. WT alleles were digested with *Sca* I, while *Bsn* variant alleles were not (Supplemental Figure 1C).

Impaired locomotion and impaired spatial working memory in 3-month-old *Bsn* variant mice

Both the distance traveled and the time spent in the center zone in the OFT were comparable for 3-month-old WT mice and 3-month-old KI mice (Figures 1A,B). Likewise, the mean latency until falling from the rotating rod in the RRT was not different for WT mice and KI mice (Figure 1C). In contrast, daily rotational frequency in the home cage was significantly decreased for KI mice compared with that for WT mice (Figures 1D,E). Intriguingly, the ratio of correct alterations in the YMZ test was significantly decreased for KI mice compared with that for WT mice (Figure 1G), although the total number of entries to the arm in the YMZ test was not different for KI mice (Figure 1F). In contrast, abilities for discrimination of the familiar object and novel object in the NORT were comparable for WT mice and KI mice (Figure 1H). These results suggest decreased locomotor activity in the acclimated home cage and impaired spatial working memory in young KI mice.

Pathological analyses of the *Bsn* p.P3882A mutation in 3-month-old mice

We examined 5 WT and 4 KI mice (Supplemental Table 1). HE staining of the cerebrum, cerebellum, and brainstem showed no structural abnormalities or neuronal loss in WT and KI mice (Figures 2A–D; Supplemental Figures 2A,B). Immunostaining for BSN (Figures 2E–H), p-tau (Figures 2I–L), synaptophysin (Supplemental Figures 2C,D), and alpha-synuclein (Supplemental Figures 2E,F) showed no obvious differences between WT and KI mice. No abnormal structures were found in sections stained with antibodies against p-tau (Figures 2I–L), ubiquitin, or p62. Immunostaining with a TH monoclonal antibody (TH-16) showed that TH immunoreactivity in the striatum of KI mice was stronger than that in the striatum of WT mice (Figures 2M–P), and significant differences were observed by Student's t test ($p < 0.01$; Supplemental Table 1; Supplemental Figure 3C). A similar trend was observed in immunostaining with a TH polyclonal antibody (CA-101; Supplemental Figure 4), but the difference was not statistically significant. There was no significant difference in the number of TH-positive neurons in the substantia nigra between KI and WT mice at 3 months (Supplemental Table 1; Supplemental Figures 3F, 5). The immunoreactivity of VMAT2 in the striatum of KI mice was weaker than that of WT mice at the age of 3 months (Supplemental Figures 9A–D).

Impaired locomotion in 12-month-old *Bsn* variant mice

We also performed systematic behavioral analyses using identical WT mice and KI mice at 12 months of age. WT mice and KI mice showed comparable total distances traveled and times spent in the center zone in the OFT (Figures 3A,B) and comparable mean latencies until falling from the rotating rod in the RRT (Figures 3C). In contrast, daily rotational frequency in the home cage was significantly decreased for KI mice compared with that for WT mice (Figures 3D,E). Working memory and cognitive function in the YMZ test (Figures 3F,G) and the NORT (Figure 3H) were not different in WT mice and KI mice. These results suggest decreased locomotor activity in the acclimated home cage in aged KI mice.

Pathological analyses of the *Bsn* p.P3882A mutation in 12-month-old mice

We examined 8 WT and 6 KI mice (Supplemental Table 2). HE staining of the striatum (Figures 4A,B), hippocampus (Figures 4C,D), cerebellum (Supplemental Figures 6A,B), and

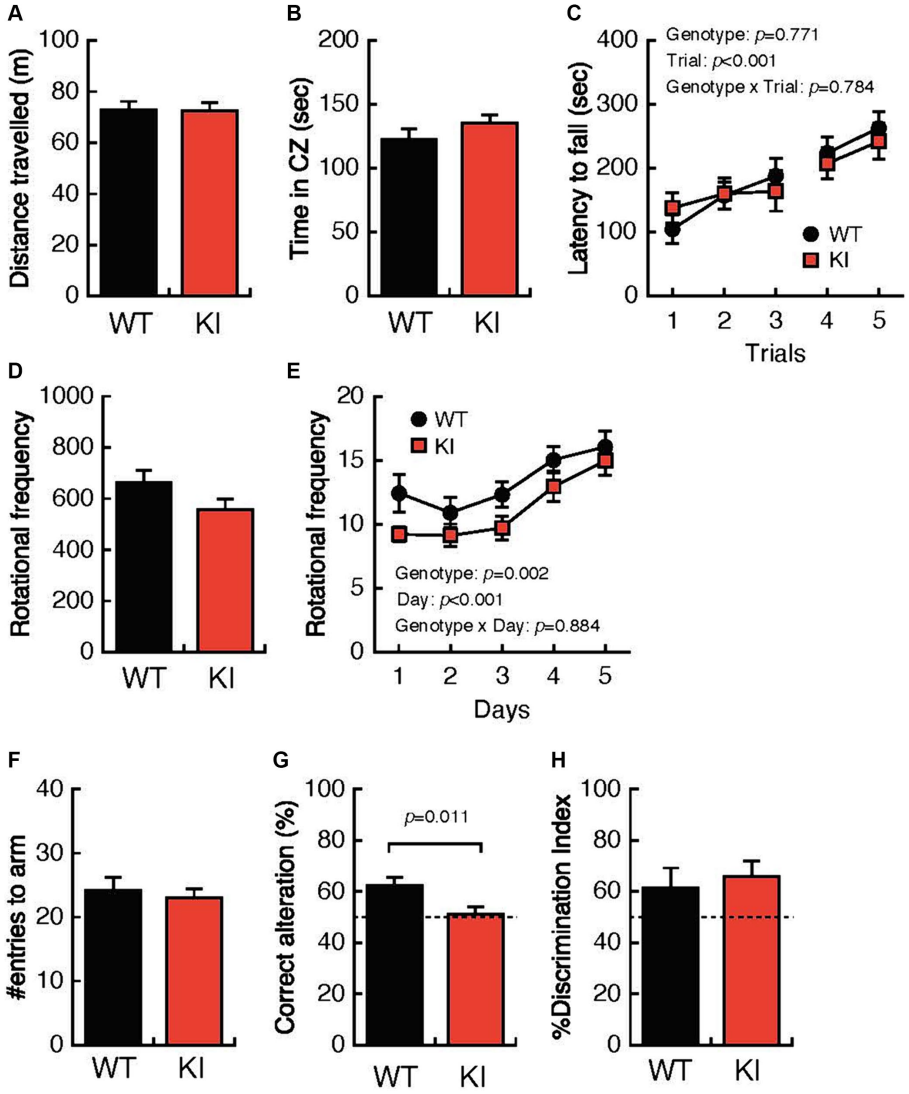

FIGURE 1
Impaired locomotion and spatial working memory in 3-month-old Bsn variant mice. **(A,B)** Both the distance traveled and the time spent in the center zone in the open-field test were comparable in 3-month-old WT mice and 3-month-old KI mice. **(C)** The mean latency until falling from the rotating rod was not different in WT mice and KI mice. **(D,E)** Daily rotational frequency, but not total rotational frequency, in the home cage activity test was significantly decreased in KI mice compared with that in WT mice. **(F)** The total number of entries to the arm in the Y-maze test was not different in KI mice. **(G)** Percentages of correct alterations in the Y-maze test were significantly decreased in KI mice compared with those in WT mice. **(H)** Abilities for discrimination of the familiar object and the novel object were comparable in WT mice and KI mice. WT, wild-type mice; m/m, homozygous KI mice; CZ, center zone.

brainstem (Supplemental Figures 6C,DS1) showed no structural abnormalities in WT and KI mice. Immunostaining for p-tau (Figures 4E–H), synaptophysin, alpha-synuclein (Supplemental Figure 7), and TH (Figures 4I–L), showed no obvious differences between WT and KI mice in the cerebrum, cerebellum and brainstem. No abnormal structures such as neuronal or glial inclusions were observed (Supplemental Figure 8). BSN immunohistochemistry showed stronger staining in the cerebral cortex, striatum (Figures 4M–P), and hippocampus (Figures 4Q–T) in KI mice than in WT mice. Semi-quantitative analysis in the striatum showed significant differences ($p < 0.01$) in Student's *t*-test (Supplemental Table 2; Supplemental Figure 3A). Furthermore, the number of TH-positive neurons in the substantia nigra of KI mice was significantly decreased compared to that in the substantia nigra of WT mice at 12 months of age ($p < 0.01$; Supplemental Table 2; Supplemental Figures 3F, 5). The immunoreactivity of VMAT2 in the striatum of KI mice was weaker than that of WT mice at the age of 12 months (Supplemental Figure 9E–H).

Discussion

There are three important findings in the present study. First, we generated mice with *Bsn* p.P3882A mutation that corresponds to the human *BSN* p.P3866A. Second, at 3 months and 12 months of age, the HCA test showed significant differences between WT mice and KI mice. Third, immunostaining using a BSN monoclonal antibody showed stronger staining in the cerebral cortex, striatum,

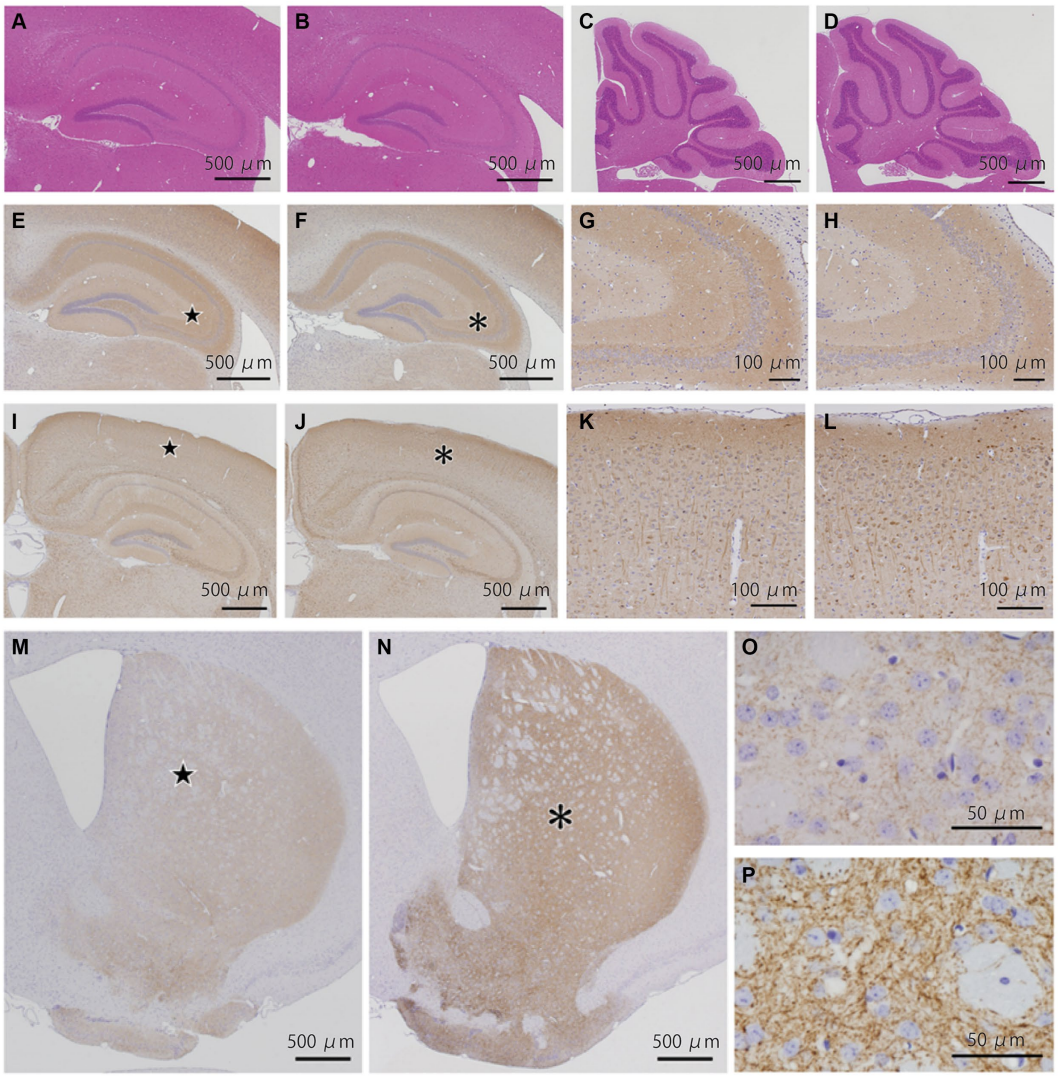

FIGURE 2
Histopathological analyses of the *Bsn* p.P3882A mutation in 3-month-old mice. **(A–D)** HE staining in the hippocampus **(A,B)** and cerebellum **(C,D)** of WT mice **(A,C)** and KI mice **(B,D)**. No apparent abnormality in WT and KI mice. **(E–H)** Immunoreactivity for bassoon in the hippocampus of WT **(E,G)** and KI mice **(F,H)**. Higher-magnification view of the area indicated by the star in **(E)** and asterisk in **(f)** showing similar fine granular staining in the CA2-3 region of WT **(G)** and KI mice **(H)**. **(I–L)** Immunoreactivity for p-tau in the hippocampus of WT **(I,K)** and KI mice **(J,L)**. Higher-magnification view of the area indicated by the star in **(I)** and asterisk in **(J)** showing similar staining patterns in the neocortex of WT **(K)** and KI mice **(L)**. **(M–P)** Immunoreactivity for TH (TH-16) in the striatum of WT **(M,O)** and KI mice **(N,P)**. TH immunoreactivity in the striatum of KI mice was much stronger than that in the striatum of WT mice. Higher-magnification view of the area **(P)** indicated by the asterisk in **(N)** of KI mice showing much stronger immunoreactivity of nerve cell processes than that of the area **(O)** indicated by the star in **(M)** of WT mice. WT, wild-type mice at 3 months of age; KI, *Bsn* knock-in mice at 3 months of age.

hippocampus in KI mice than in WT mice at 12 months of age. TH-positive neuronal loss was observed in the substantia nigra in KI mice at 12 months of age. These findings may suggest changes in dopaminergic innervation and BSN expression.

We previously identified the point mutation c.11596C > G, p.Pro3866Ala in *BSN* in a Japanese family with PSP-like syndrome (Yabe et al., 2018). Domains of the *BSN* p.P3866A mutation were reported to be conserved evolutionarily (Yabe et al., 2018). Mutated BSN (p.Pro3866Ala) may be involved in its own insolubilization and tau accumulation (Yabe et al., 2018). Our report led to a series of reports linking *BSN* and neurological diseases. Using *BSN* knockout mice, it has been shown that *BSN* inhibits proteasome activity (Montenegro-Venegas et al., 2021). It has also been reported that the p.Pro3866Ala mutation exacerbates tau seeding in a Drosophila model (Martinez et al., 2022). These findings strongly indicate a notable link between the presynaptic active zone and neurodegenerative diseases. Alpha-synuclein and tau are important for the maintenance of synaptic vesicle function (Lv et al., 2022). Furthermore, those reports indicate that BSN may be a key molecule in protein accumulation. From the above, it is important to examine what pathological significance the *BSN* mutation, which we have already shown to be pathogenic in our immortalized cell lines, has in actual animal models. Significant differences in the results of behavioral analysis were observed at 3 months and 12 months of age and TH-positive neuronal loss was observed at 12 months of age in our mouse model, suggesting that this mutation plays an important

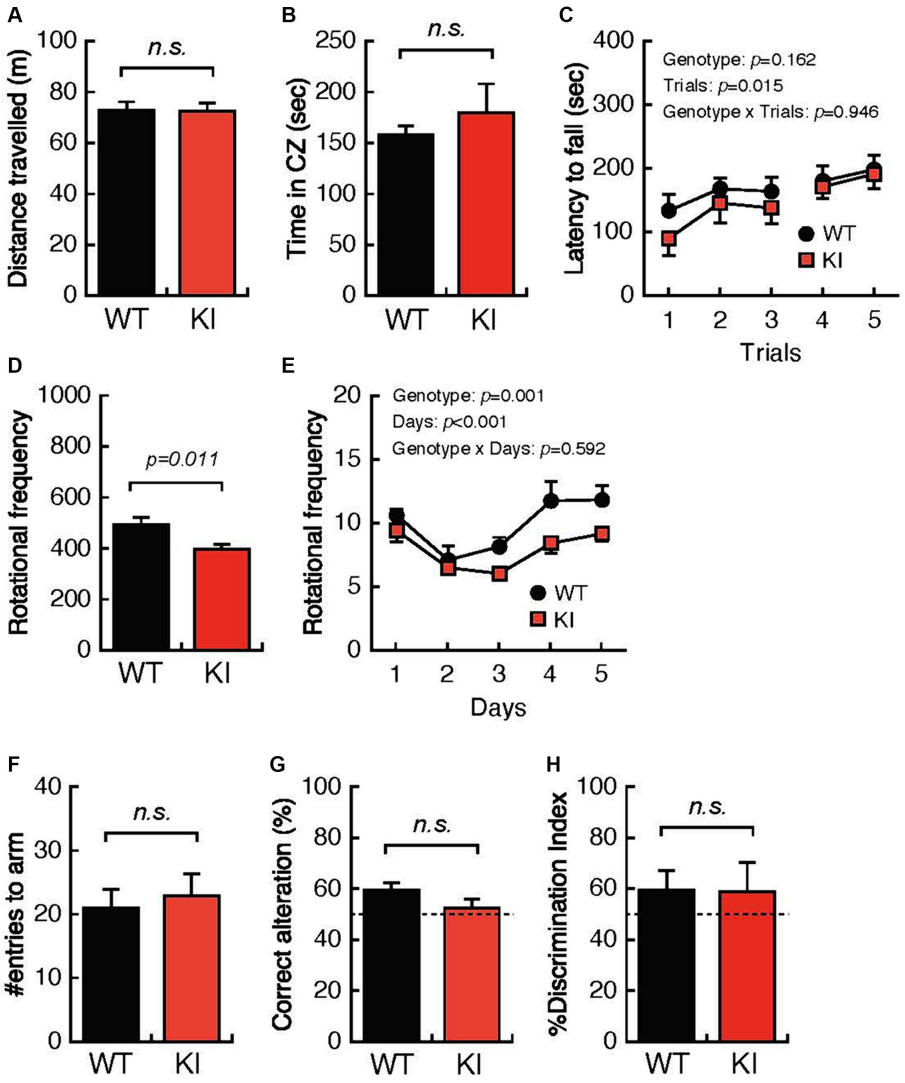

FIGURE 3
Impaired locomotion and spatial working memory in 12-month-old *Bsn* variant mice. **(A,B)** Both the distance traveled and the time spent in the center zone in the open-field test were comparable in 12-month-old WT mice and 12-month-old KI mice. **(C)** The mean latency until falling from the rotating rod was not different in WT mice and KI mice. **(D,E)** Daily rotational frequency, but not total rotational frequency, in the home cage activity test was significantly decreased in KI mice compared with that in WT mice. **(F,G)** Percentages of correct alterations in the Y-maze test were not significantly decreased in KI mice compared with those in WT mice. **(H)** Abilities for discrimination of the familiar object and the novel object were comparable in WT mice and KI mice. WT, wild-type mice; m/m, homozygous *Bsn* KI mice.

role *in vivo*. Working memory was impaired in *Bsn* p.P3882A variant mice at 3 months of age but not at 12 months of age. The impairment of working memory in KI mice at 3 months of age may be due to enhanced immunoreactivity of TH. Some reports have suggested that excessive dopamine impairs spatial working memory (Zahrt et al., 1997; Vijayraghavan et al., 2007). Therefore, appropriate dopamine balance may be essential for maintenance of healthy working memory. In our KI mice, 3-month-old KI mice showed loss of spontaneous activity in the HCA test and early dopaminergic activation. These results indicate the possibility that 3-month-old KI mice showed cognitive impairment due to inappropriate dopamine regulation. Although decrease tendency was also observed in 12-month-old KI mice, the differences did not reach to significance. Since the TH-positive neurons significantly decrease in 12-month-old KI mice, it is possible that cognitive impairment may develop in further aged KI mice. Further study is needed.

Our KI mice showed TH-positive neuronal loss at 12-month-old, while elevation of TH immunoreactivity at 3-month-old. Also, decrease immunoreactivities of VMAT2 were observed in both 3 and 12 months old KI mice. In humans, decrease immunoreactivity of VMAT2 was followed by decrease immunoreactivity of TH (Kang et al., 2021). Moreover, it has been reported that decrease of VMAT2 results in neuronal loss in the substantia nigra in aged mice probably due to oxidative stress from increasing dopamine metabolites in cytosol (Caudle et al., 2007; Guillot and Miller, 2009), and therefore, VMAT2 plays an important role for neuroprotection in dopaminergic neurons. We hypothesized that *BSN* mutation may prevent dopamine packaging and releasing through dysfunction of VMAT2. TH

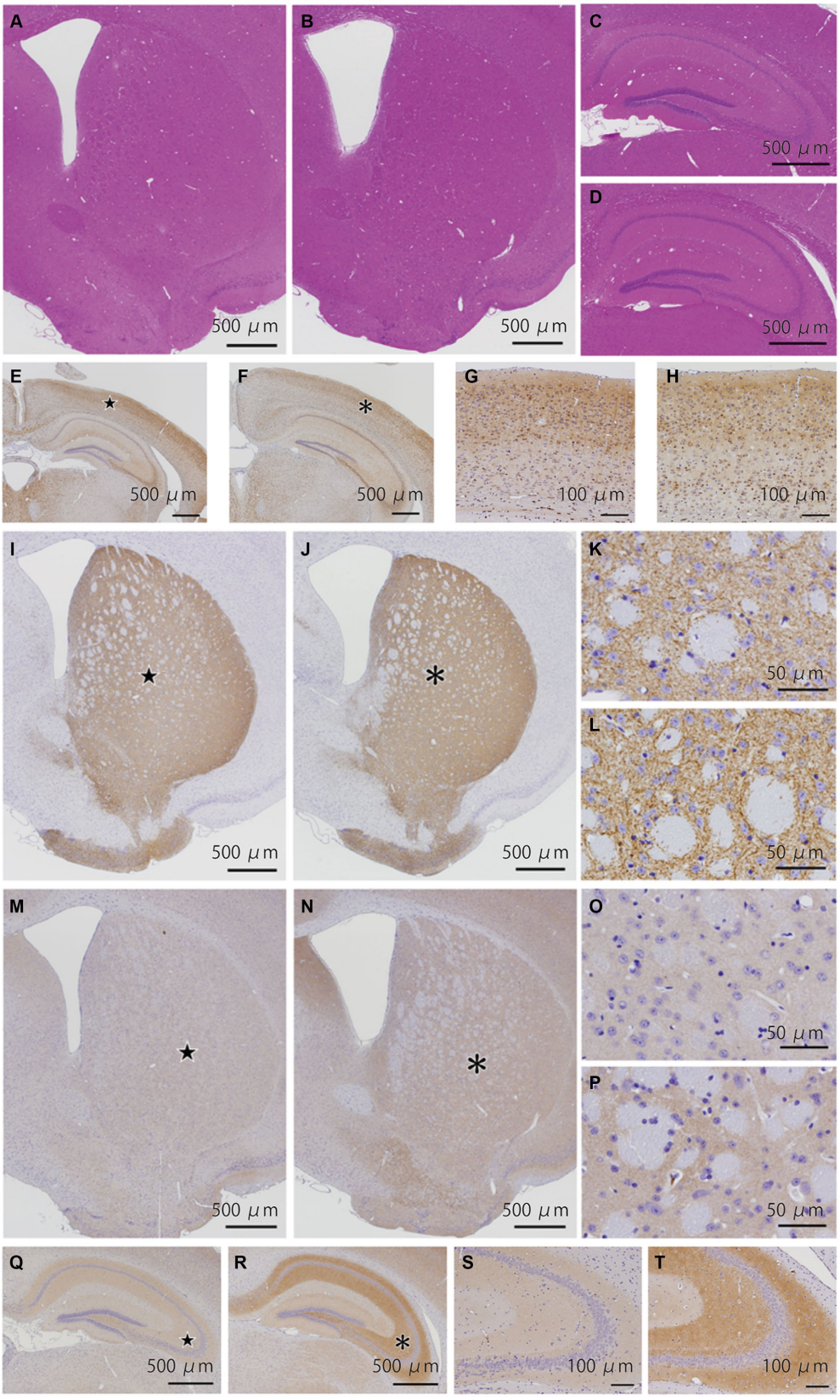

FIGURE 4
Histopathological analyses of the *Bsn* p.P3882A mutation in 12-month-old mice. **(A–D)** HE staining in the striatum **(A,B)** and hippocampus **(C,D)** of WT **(A,C)** and KI mice **(B,D)**. No apparent abnormality in WT and KI mice. **(E–H)** Immunoreactivity for p-tau in the hippocampus of WT **(E,G)** and KI mice **(F,H)**. Higher-magnification view of the area indicated by the star in **(E)** and asterisk in **(F)** showing similar staining patterns in the neocortex of WT

(Continued)

FIGURE 4 (Continued)
(G) and KI mice **(H)**. **(I–L)** Immunoreactivity for TH (TH-16) in the striatum of WT **(I,K)** and KI mice **(J,L)**. Higher-magnification view of the area indicated by the star in **(I)** and asterisk in **(J)** showing similarly strong immunoreactivity of nerve cell processes. **(M–P)** Immunoreactivity for bassoon in the striatum of WT **(M,O)** and KI mice **(N,P)**. **(O,P)** Higher-magnification view of the area indicated by the star in **(O)** and asterisk in **(P)**. Immunoreactivity of the gray matter in KI mice was slightly stronger than that in WT mice. **(Q–T)** Immunoreactivity for bassoon in the hippocampus of WT **(Q,S)** and KI mice **(R,T)**. **(S,T)** Higher-magnification view of the area indicated by the star in **(Q)** and asterisk in **(R)**. Immunoreactivity of the molecular and polymorphic layers in KI mice was stronger than that in WT mice. WT, wild-type mice at 12 months of age; KI, *Bsn* knock-in mice at 12 months of age.

immunoreactivity increased possibly due to inhibition of dopamine releasing in 3-month-old KI mice. Accumulating the stress of dysfunction of packaging and releasing of dopamine may result in increasing neuronal toxicity and neuronal loss in 12-month-old KI mice. Further studies for elucidating the relationship between mutant BSN and VMAT2 are needed.

Elevated BSN at the protein level at 12 months of age may suggest that BSN proteinopathy is associated with cognitive dysfunction. In this study, *Bsn* KI mice showed TH-positive neuronal loss without tauopathy at 12 months of age. Also, no accumulation of alpha-synuclein was observed. The patient with Parkinson disease, one of the most studied neurodegenerative diseases with dopaminergic neuronal loss, shows locomotor symptoms several to two decades of years after onset (Kalia and Lang, 2015). Due to difficulty in diagnosis as Parkinson disease without locomotor symptoms, the pathological changes in the early stage of Parkinson disease have been unknown. This is also the case with other neurodegenerative diseases. Since our previous *in vitro* study showed that mutant Bsn expression induces insolubilized tau accumulation (Yabe et al., 2018), it is possible that older KI mice can represent tauopathy. Other hypothesis is that the mechanism other than protein aggregation, can lead to neuronal loss. In fact, *BSN* mutation was also associated with various neurological diseases without protein aggregation, such as schizophrenia (Chen and Huang, 2021), multiple sclerosis (Schattling and Engler, 2019), and epilepsy (Ye et al., 2023). These reports suggest that *BSN* mutation may be related to the vulnerability of neurons in the central nervous system. Further electrophysiological and biochemical analyses and longer time-course observation are needed to elucidate the mechanism in the future.

In conclusion, the generation of *Bsn* KI mice in this study can be considered a first step toward future important research. Although no structural abnormalities were observed at 3 months and 12 months of age, the HCA test showed slightly significant differences between WT mice and KI mice. Elevated Bsn at the protein level at 12 months of age suggests that BSN proteinopathy may be a gain of function. Unlike our previous report of patients with PSP-like syndrome with *BSN* mutation, our mouse model did not show tauopathy at 12-month-old, but showed dopaminergic neuronal loss. Since *BSN* mutation has been closely related to various neurological diseases, our model can become a useful tool for studying the mechanism for neurodegeneration. Therefore, we will continue to conduct experiments to determine how BSN dysfunction causes neuronal loss. Further elucidation of the molecular and biological mechanisms may lead to the identification of target proteins for treatment of neurological diseases.

Limitations

There are two main limitations of this study. First, protein expression including expression of tyrosine hydroxylase, BSN and p-tau was evaluated only by tissue staining and not by biochemical evaluation. Second, behavioral and histological analyses were carried out only up to the age of 12 months.

Data availability statement

The raw data supporting the conclusions of this article will be made available by the authors, without undue reservation.

Ethics statement

The animal studies were approved by the Ethics Committee for Animal Experiments of Aichi Institute for Developmental Research (2020-005) and Hokkaido University Graduate School of Medicine (22-0042). The studies were conducted in accordance with the local legislation and institutional requirements. Written informed consent was obtained from the owners for the participation of their animals in this study.

Author contributions

DT: Data curation, Investigation, Writing – original draft, Writing – review & editing. HY: Data curation, Investigation, Writing – original draft, Writing – review & editing, Conceptualization, Methodology, Project administration. KY: Investigation, Writing – original draft. AK: Investigation, Methodology, Writing – review & editing. FM: Investigation, Methodology, Writing – review & editing. TN: Investigation, Writing – review & editing. JP: Investigation, Writing – review & editing. YM: Investigation, Writing – review & editing. HT: Supervision, Writing – review & editing. TH: Investigation, Methodology, Writing – review & editing. KW: Supervision, Writing – review & editing, Investigation. IY: Data curation, Formal analysis, Funding acquisition, Project administration, Supervision, Writing – review & editing.

Funding

The author(s) declare that financial support was received for the research, authorship, and/or publication of this article. This work was supported by JSPS KAKENHI Grant Numbers JPK20H03585, JPK23H02820, and JP22K15722 and a grant from the Grants-in Aid from the Research Committee of CNS Degenerative Diseases under Research on Measures for Intractable Diseases from the Ministry of Health, Labour and Welfare, Japan (to IY; 20FC1049).

Conflict of interest

The authors declare that the research was conducted in the absence of any commercial or financial relationships that could be construed as a potential conflict of interest.

Publisher's note

Supplementary material

The Supplementary material for this article can be found online at: https://www.frontiersin.org/articles/10.3389/fnins.2024.1414145/full#supplementary-material

SUPPLEMENTARY FIGURE S1
Generation of the mouse *Bsn* p.P3882A mutation that corresponds to the human BSN p.P3866A. **(a)** Evolutionarily conserved domains of the BSN p.P3866A mutation. **(b)** We generated the mouse *Bsn* p.P3882A mutation that corresponds to the human BSN p.P3866A. **(c)** Genotypes were determined by PCR using primers designed basically on the same site by Sca1. WT, wild-type mice; KI, *Bsn* knock in mice.

SUPPLEMENTARY FIGURE S2
Histopathological analyses of the *Bsn* p.P3882A mutation in 3-month-old mice. **(a,b)** HE staining in the brainstem of WT **(a)** and KI mice **(b)**. No apparent abnormality in WT and KI mice. **(c–f)** Immunoreactivity for alpha-synuclein in the cortex and the hippocampus of WT **(c)** and KI mice **(d)**. Immunoreactivity for synaptophysin in the cortex and the hippocampus of WT **(e)** and KI mice **(f)**. WT, wild-type mice at 3 months of age; KI, *Bsn* knock-in mice at 3 months of age. No abnormal structures were found in sections.

SUPPLEMENTARY FIGURE S3
Semi-quantitative analysis for immunoreactivity and nerve cell counts. Semi-quantitative analysis for immunoreactivity for bassoon (BSN, **a**), phosphorylated tau (p-Tau, **b**), tyrosine hydroxylase (TH-16, **c**), synaptophysin (SYP, **d**) and alpha-synuclein (SYN, **e**) in the caudate-putamen and cell counts of TH-positive neurons in the substantia nigra **(f)**. BSN immunoreactivity in KI mice was more intense than that in WT mice at 12 months of age (p <0.01) **(a)**. TH immunoreactivity in KI mice was more intense than that in WT mice at 3 months of age (p <0.01) **(c)**. The number of TH-positive neurons in the substantia nigra of KI mice was significantly decreased compared to that in the substantia nigra of WT mice at 12 months of age (p <0.05) **(f)**. OD, optical density.

SUPPLEMENTARY FIGURE S4
Immunoreactivity for TH (CA-101) in the striatum of 3-month-old mice. Immunoreactivity for TH (CA-101) in the striatum of WT **(a,c)** and KI mice **(b, d)**. TH immunoreactivity in the striatum of KI mice was slightly stronger than that in the striatum of WT mice. Higher-magnification view of the area **(d)** indicated by the asterisk in **(b)** of KI mice showing slightly stronger immunoreactivity of nerve cell processes than that of the area **(c)** indicated by the star in **(a)** of WT mice. WT, wild-type mice at 3 months of age; KI, *Bsn* knock-in mice at 3 months of age.

SUPPLEMENTARY FIGURE S5
TH immunohistochemistry (TH-16) in the substantia nigra. Immunohistochemistry for TH in the substantia nigra of WT **(a,c)** and KI mice **(b,d)** at 3 and 12 months of age. TH-immunoreactive neurons in the substantia nigra appear to be decreased in KI mice compared to that in WT mice at 12 months of age.

SUPPLEMENTARY FIGURE S6
Histopathological analyses of the *Bsn* p.P3882A mutation in 12-month-old mice. **(a,b)** HE staining in the cerebellum of WT **(a)** and KI mice **(b)**, and that in the brainstem of WT **(c)**, and KI mice **(d)**. No apparent abnormality in WT and KI mice.

SUPPLEMENTARY FIGURE S7
Alpha-synuclein immunoreactivity in the striatum of 3- and 12-month-old mice. There was no significant difference in alpha-synuclein immunoreactivity in the striatum between WT **(a,c)** and KI mice **(b,d)** at 3 months of age as well as between WT **(e,g)** and KI mice **(f,h)** at 12 months of age. Higher-magnification view of the area **(c,d,g,h)** indicated by the star in **(a,e)** and asterisk in **(b,f)**. Because immunostaining treatments of sections from 3- and 12-month-old mice were performed separately, differences between 3- and 12-month-old mice were not examined.

SUPPLEMENTARY FIGURE S8
Immunohistochemistry for BSN, p-Tau, ubiquitin and p62 in the hippocampus of KI mice at 12 months of age. Immunohistochemistry for BSN **(a,b)**, p-Tau **(c,d)**, ubiquitin **(e,f)** and p62 **(g,h)** in the hippocampus of KI mice at 12 months of age. Right panels **(b,d,f,h)** are higher magnification views of the regions indicated by asterisks in left panels **(a,c,e,g)**. No pathological lesions, such as neuronal or glial inclusions, were observed.

SUPPLEMENTARY FIGURE S9
Vesicular monoamine transporter 2 (VMAT2) immunoreactivity in the striatum of 3- and 12-month-old mice. Immunoreactivity for VMAT2 in the striatum of WT **(a,c)** and KI mice **(b,d)** in the 3-month-old. VMAT2 immunoreactivity in the striatum of KI mice was weaker than that in the striatum of WT mice. Higher-magnification view of the area in 3-month-old KI mice **(d)** showing weaker immunoreactivity of nerve cell processes than that of the area in 3-month-old WT mice **(c)**. Immunoreactivity for VMAT2 in the striatum of WT **(e,g)** and KI mice **(f,h)** in the 12-month-old. VMAT2 immunoreactivity in the striatum of KI mice was weaker than that in the striatum of WT mice. Higher-magnification view of the area in 12-month-old KI mice **(h)** showing weaker immunoreactivity of nerve cell processes than that of the area in 12-month-old WT mice **(g)**. WT, wild-type mice at 12 months of age; KI, *Bsn* knock-in mice at 12 months of age.

References

Andrews, S. V., and Kukkle, P. L. (2023). The genetic drivers of juvenile, young, and early-onset Parkinson's disease in India. *Mov. Disord.* 39, 339–349. doi: 10.1002/mds.29676

Caudle, W. M., Richardson, J. R., Wang, M. Z., Taylor, T. N., Guillot, T. S., Mccormack, A. L., et al. (2007). Reduced vesicular storage of dopamine causes progressive nigrostriatal neurodegeneration. *J. Neurosci.* 27, 8138–8148. doi: 10.1523/JNEUROSCI.0319-07.2007

Chen, C. H., and Huang, Y. S. (2021). Identification of rare mutations of two presynaptic Cytomatrix genes Bsn and Pclo in schizophrenia and bipolar disorder. *J. Pers. Med.* 11:1057. doi: 10.3390/jpm11111057

Guillot, T. S., and Miller, G. W. (2009). Protective actions of the vesicular monoamine transporter 2 (Vmat2) in monoaminergic neurons. *Mol. Neurobiol.* 39, 149–170. doi: 10.1007/s12035-009-8059-y

Hashida, H., Goto, J., Zhao, N., Takahashi, N., Hirai, M., Kanazawa, I., et al. (1998). Cloning and mapping of Znf231, a novel brain-specific gene encoding neuronal double zinc finger protein whose expression is enhanced in a neurodegenerative disorder, multiple system atrophy (Msa). *Genomics* 54, 50–58. doi: 10.1006/geno.1998.5516

Hoffmann-Conaway, S., and Brockmann, M. M. (2020). Parkin contributes to synaptic vesicle autophagy in bassoon-deficient mice. *eLife* 9:e56590. doi: 10.7554/eLife.56590

Huang, T. T., Smith, R., Bacos, K., Song, D. Y., Faull, R. M., Waldvogel, H. J., et al. (2020). No symphony without bassoon and piccolo: changes in synaptic active zone proteins in Huntington's disease. *Acta Neuropathol. Commun.* 8:77. doi: 10.1186/s40478-020-00949-y

Ivanova, D., Dirks, A., and Fejtova, A. (2016). Bassoon and piccolo regulate ubiquitination and link presynaptic molecular dynamics with activity-regulated gene expression. *J. Physiol.* 594, 5441–5448. doi: 10.1113/JP271826

Kalia, L. V., and Lang, A. E. (2015). Parkinson's disease. *Lancet* 386, 896–912. doi: 10.1016/S0140-6736(14)61393-3

Kang, S. S., Ahn, E. H., Liu, X., Bryson, M., Miller, G. W., Weinshenker, D., et al. (2021). ApoE4 inhibition of Vmat2 in the locus coeruleus exacerbates tau pathology in Alzheimer's disease. *Acta Neuropathol.* 142, 139–158. doi: 10.1007/s00401-021-02315-1

Kaneko, T., and Mashimo, T. (2015). Creating knockout and knockin rodents using engineered endonucleases via direct embryo injection. *Chromosomal Mutagenesis* 307–315. doi: 10.1007/978-1-4939-1862-1_18

Lv, G., Ko, M. S., Das, T., and Eliezer, D. (2022). Molecular and functional interactions of alpha-synuclein with Rab3a. *J. Biol. Chem.* 298:102239. doi: 10.1016/j.jbc.2022.102239

Martinez, P., Patel, H., You, Y., Jury, N., and Perkins, A. (2022). Bassoon contributes to tau-seed propagation and neurotoxicity. *Nat. Neurosci.* 25, 1597–1607. doi: 10.1038/s41593-022-01191-6

Montenegro-Venegas, C., Annamneedi, A., Hoffmann-Conaway, S., Gundelfinger, E. D., and Garner, C. C. (2020). BSN (bassoon) and PRKN/parkin in concert control presynaptic vesicle autophagy. *Autophagy* 16, 1732–1733. doi: 10.1080/15548627.2020.1801259

Montenegro-Venegas, C., Fienko, S., Anni, D., Pina-Fernández, E., Frischknecht, R., and Fejtova, A. (2021). Bassoon inhibits proteasome activity via interaction with Psmb4. *Cell. Mol. Life Sci.* 78, 1545–1563. doi: 10.1007/s00018-020-03590-z

Okerlund, N. D., Schneider, K., Leal-Ortiz, S., Montenegro-Venegas, C., Kim, S. A., Garner, L. C., et al. (2017). Bassoon controls presynaptic autophagy through Atg5. *Neuron* 93, 897–913.e7. doi: 10.1016/j.neuron.2017.01.026

Schattling, B., and Engler, J. B. (2019). Bassoon proteinopathy drives neurodegeneration in multiple sclerosis. *Nat. Neurosci.* 22, 887–896. doi: 10.1038/s41593-019-0385-4

Takagi, T., Nishizaki, Y., Matsui, F., Wakamatsu, N., and Higashi, Y. (2015). De novo inbred heterozygous Zeb2/Sip1 mutant mice uniquely generated by germ-line conditional knockout exhibit craniofacial, callosal and behavioral defects associated with Mowat-Wilson syndrome. *Hum. Mol. Genet.* 24, 6390–6402. doi: 10.1093/hmg/ddv350

Tanaka, M. T., Tanji, K., Miki, Y., Ozaki, T., Mori, F., Hayashi, H., et al. (2022). Phosphorylation of tau at threonine 231 in patients with multiple system atrophy and in a mouse model. *J. Neuropathol. Exp. Neurol.* 81, 920–930. doi: 10.1093/jnen/nlac082

Vijayraghavan, S., Wang, M., Birnbaum, S. G., Williams, G. V., and Arnsten, A. F. (2007). Inverted-U dopamine D1 receptor actions on prefrontal neurons engaged in working memory. *Nat. Neurosci.* 10, 376–384. doi: 10.1038/nn1846

Williams, D. R., and Lees, A. J. (2009). Progressive supranuclear palsy: clinicopathological concepts and diagnostic challenges. *Lancet Neurol.* 8, 270–279. doi: 10.1016/S1474-4422(09)70042-0

Yabe, I., Yaguchi, H., Kato, Y., Miki, Y., Takahashi, H., Tanikawa, S., et al. (2018). Mutations in bassoon in individuals with familial and sporadic progressive supranuclear palsy-like syndrome. *Sci. Rep.* 8:819. doi: 10.1038/s41598-018-19198-0

Ye, T., Zhang, J., Wang, J., Lan, S., Zeng, T., Wang, H., et al. (2023). Variants in Bsn gene associated with epilepsy with favourable outcome. *J. Med. Genet.* 60, 776–783. doi: 10.1136/jmg-2022-108865

Yoshida, M., Akagi, A., Miyahara, H., Riku, Y., Ando, T., Ikeda, T., et al. (2022). Macroscopic diagnostic clue for parkinsonism. *Neuropathology* 42, 394–419. doi: 10.1111/neup.12853

Yoshizaki, K., Adachi, K., Kataoka, S., Watanabe, A., Tabira, T., Takahashi, K., et al. (2008). Chronic cerebral hypoperfusion induced by right unilateral common carotid artery occlusion causes delayed white matter lesions and cognitive impairment in adult mice. *Exp. Neurol.* 210, 585–591. doi: 10.1016/j.expneurol.2007.12.005

Yoshizaki, K., and Asai, M. (2020). High-fat diet enhances working memory in the Y-maze test in male C57bl/6J mice with less anxiety in the elevated plus maze test. *Neuropathology* 12:2036. doi: 10.3390/nu12072036

Yoshizaki, K., and Kimura, R. (2021). Paternal age affects offspring via an epigenetic mechanism involving Rest/Nrsf. *EMBO Rep.* 22:e51524. doi: 10.15252/embr.202051524

Zahrt, J., Taylor, J. R., Mathew, R. G., and Arnsten, A. F. (1997). Supranormal stimulation of D1 dopamine receptors in the rodent prefrontal cortex impairs spatial working memory performance. *J. Neurosci.* 17, 8528–8535. doi: 10.1523/JNEUROSCI.17-21-08528.1997

frontiers | Frontiers in Molecular Neuroscience

TYPE Review
PUBLISHED 31 July 2024
DOI 10.3389/fnmol.2024.1423132

OPEN ACCESS

EDITED BY
Ferdinando Di Cunto,
University of Turin, Italy

REVIEWED BY
Bharat Prajapati,
University of Gothenburg, Sweden
Sasanka Chakrabarti,
Maharishi Markandeshwar University, India

*CORRESPONDENCE
Wei Zou
1558429536@qq.com

†These authors have contributed equally to this work

RECEIVED 25 April 2024
ACCEPTED 15 July 2024
PUBLISHED 31 July 2024

CITATION
Cong J, Li J-Y and Zou W (2024) Mechanism and treatment of intracerebral hemorrhage focus on mitochondrial permeability transition pore.
Front. Mol. Neurosci. 17:1423132.
doi: 10.3389/fnmol.2024.1423132

Mechanism and treatment of intracerebral hemorrhage focus on mitochondrial permeability transition pore

Jing Cong[1†], Jing-Yi Li[2†] and Wei Zou[3*†]

[1]The First School of Clinical Medicine, Heilongjiang University of Chinese Medicine, Harbin, China, [2]The Second School of Clinical Medicine, Heilongjiang University of Chinese Medicine, Harbin, China, [3]Molecular Biology Laboratory of Clinical Integrated of Traditional Chinese and Western Medicine of Heilong Jiang Province, The First Affiliated Hospital of Heilongjiang University of Chinese Medicine, Harbin, China

Intracerebral hemorrhage (ICH) is the second most common subtype of stroke, characterized by high mortality and a poor prognosis. Despite various treatment methods, there has been limited improvement in the prognosis of ICH over the past decades. Therefore, it is imperative to identify a feasible treatment strategy for ICH. Mitochondria are organelles present in most eukaryotic cells and serve as the primary sites for aerobic respiration and energy production. Under unfavorable cellular conditions, mitochondria can induce changes in permeability through the opening of the mitochondrial permeability transition pore (mPTP), ultimately leading to mitochondrial dysfunction and contributing to various diseases. Recent studies have demonstrated that mPTP plays a role in the pathological processes associated with several neurodegenerative diseases including Parkinson's disease, Alzheimer's disease, Huntington's disease, ischemic stroke and ischemia-reperfusion injury, among others. However, there is limited research on mPTP involvement specifically in ICH. Therefore, this study comprehensively examines the pathological processes associated with mPTP in terms of oxidative stress, apoptosis, necrosis, autophagy, ferroptosis, and other related mechanisms to elucidate the potential mechanism underlying mPTP involvement in ICH. This research aims to provide novel insights for the treatment of secondary injury after ICH.

KEYWORDS

cerebral hemorrhage, mitochondria, mitochondrial permeability transition pore, treatment, mechanism

1 Introduction

Spontaneous intracerebral hemorrhage (ICH), characterized by non-traumatic parenchymal bleeding (de Oliveira Manoel et al., 2016), represents the second most prevalent stroke subtype (Qureshi et al., 2009) and exhibits a substantial mortality rate (Feigin et al., 2009), with 30–55% mortality within 30 days (Balami and Buchan, 2012). Survivors often face an unfavorable prognosis, frequently accompanied by diverse neurological deficits. Despite numerous studies conducted over the past decades to enhance secondary injury management following ICH, significant improvements in patient outcomes have unfortunately not been achieved (Roger et al., 2011). Consequently, it is imperative to explore novel avenues for treating secondary injury subsequent to ICH.

Mitochondria, a double-layered membrane-coated organelle found in the majority of eukaryotic cells, serve as the primary site for aerobic respiration and act as the energy production hub within cells. Mitochondrial dynamics play a crucial role in body development, particularly in the brain (Flippo and Strack, 2017) and heart (Dorn et al., 2015), while also influencing stem cell self-renewal and differentiation (Seo et al., 2018). Under pathological conditions, mitochondria can induce the opening of mPTP, leading to alterations in mitochondrial permeability that result in mitochondrial dysfunction. This dysfunction often initiates a cascade of cellular death processes and contributes to various diseases. Recent studies have demonstrated that mPTP is implicated in the pathological progression of several neurological disorders such as Parkinson's disease (Rasheed et al., 2017), Alzheimer's disease (Jia and Du, 2021), Huntington's disease (Quintanilla et al., 2017), ischemic stroke (Yangxin et al., 2020) and ischemia-reperfusion injury (Norbert et al., 2016), among others. However, there is limited research on mPTP regarding ICH. Therefore, this article aims to review both physiological and pathological processes associated with mPTP, elucidate its relationship with ICH, explore potential mechanisms by which mPTP contributes to secondary injury following ICH, and propose new avenues for research into treating secondary injury after ICH.

2 Composition of the mPTP

Mitochondria, being crucial organelles in the body, participate in a diverse range of cellular processes and are also exposed to various biochemical stimuli, such as oxidative stress. Under these adverse conditions, the permeability of the mitochondrial inner membrane undergoes changes known as mitochondria permeability transition (MPT). Initially believed to be caused by alterations in the phospholipid bilayer of mitochondria, further research has revealed that this permeability transition is triggered by the opening of protein channels on both the inner and outer mitochondrial membranes (Crompton et al., 1987). These protein-based channels are referred to as mPTP. The composition of mPTP has been a subject of controversy since its proposal in 1987. Currently, several models for mPTP have been proposed by scholars (as shown in Table 1). Among them, major candidates for mPTP composition include proteins like cyclophilin D (CypD), adenine nucleotide translocase (ANT), voltage-dependent anion channel (VDAC), mitochondrial phosphate carrier (PiC), ATP synthase, and Paraplegin (SPG7) (as showed in Figures 1, 2).

Cyclophilin is a peptidyl-prolyl cis-trans isomerase that is widely distributed across various species in nature. In the human body, there are 16 cyclophilins, with CypA, CypB, and CypD being the most extensively studied (Fischer et al., 1989; Wang and Heitman, 2005). Unlike other cyclophilins, CypD exhibits unique localization within the mitochondrial matrix. Initially considered as a specific cell membrane binding protein, CypD's activity can be inhibited by the immunosuppressant cyclosporin A (CSA) (Crompton et al., 1988). It has been discovered that CSA can block the opening of mPTP by inhibiting CypD activity. This inhibition prevents the binding of CypD to other mitochondrial membrane proteins and consequently affects mitochondrial pore formation. Recent studies have reported that several mitochondrial membrane proteins including VDAC (Crompton et al., 1998), ANT (Halestrap and Davidson, 1990), PiC (Leung and Halestrap, 2008), and ATP synthase (Bonora et al., 2013) can interact with CypD to form mPTP. Therefore, it is evident that CypD plays a crucial role in regulating mPT. Research has demonstrated that loss of CypD expression can inhibit mPTP opening, reduce cell necrosis, protect cardiomyocytes, and improve cardiac function (Lam et al., 2015). Down-regulation of CypD expression also mitigates neuronal damage caused by amyloid-β and oxidative stress while reducing aging-related conditions (Lin and Beal, 2006) as well as Alzheimer's disease occurrence (Du et al., 2008).

ANT is a member of the mitochondrial carrier family protein, which constitutes 10% of the total mitochondrial protein content (Brand et al., 2005). It is synthesized in the cytoplasm and subsequently inserted into the inner mitochondrial membrane (Ryan et al., 1999). ANT primarily functions as a transporter for metabolites and cofactors on the mitochondrial inner membrane, but its main role is to facilitate ADP/ATP exchange on this membrane (Palmieri, 2004), thereby generating charge difference on it (Duszyński et al., 1981). Although ANT can affect mPTP opening, its exact role in this process remains controversial. Early studies suggested that Ca^{2++} could trigger conformational changes in ANT, promote binding between ANT and CypD, and then cause mPTP opening (Halestrap and Davidson, 1990). It has also been proposed that under certain conditions, VDAC-CypD-ANT forms a multiprotein complex that leads to mPTP opening (Crompton et al., 1998). However, subsequent studies found that Ca^{2+}-induced mPTP opening could still occur even if activity of ANT isoforms was inhibited. Therefore, some scholars believe that rather than participating in composition of mPTP itself, ANT plays a regulatory role in its opening process instead (Leung and Halestrap, 2008).

VDAC, also known as mitochondrial porin, belongs to the eukaryotic mitochondrial porin family. It is situated in the outer membrane of mitochondria and regulates molecular and ion exchange between the cytoplasm and mitochondria, thereby controlling mitochondrial metabolites (Shoshan-Barmatz et al., 2010). VDAC plays a role in cellular energy metabolism by regulating the transport of ATP or ADP across the inner and outer membranes of mitochondria (Maldonado and Lemasters, 2014). Additionally, it modulates mitochondrial calcium uptake (Rosencrans et al., 2021) and is involved in biological processes such as apoptosis (Mazure, 2017), autophagy (Lemasters, 2007), and ferroptosis (Zhao et al., 2020). While VDAC's status as a key component of mPTP remains controversial

Abbreviations: AdipoR1, adiponectin receptor 1; ANT, adenine nucleotide translocase; AMPK, AMP-activated protein kinase; Apaf-1, apoptosis-associated factor 1; A/R, anoxia/reoxygenation; BBB, blood-brain barrier; cGAS, cyclic GMP-AMP synthetase; CSA, cyclosporin A; CypD, proteins like cyclophilin D; DAMPs, damage-associated molecular patterns; ETC, electron transport chain; GPX4, glutathione peroxidase 4; H_2O_2, hydrogen peroxide; ICH, intracerebral hemorrhage; LC3, microtubule-associated protein 1 light chain 3; MT1, melatonin receptor 1; MPT, mitochondria permeability transition; mPTP, mitochondrial permeability transition pore; mtDNA, mitochondrial DNA; NAD+, nicotinamide adenine dinucleotide; NETs, neutrophil extracellular traps; NRF1, nuclear respiratory factor 1; OS, oxidative stress; PGC1α, peroxisome proliferator-activated receptor-gamma coactivator-1 alpha; PiC, phosphate carrier; PP2A, protein phosphatase 2A; RCD, regulated cell death; ROS, reactive oxygen species; SERCA, sarcoplasmic/endoplasmic reticulum Ca^{2+}-ATPase; SPG7, Paraplegin; STING, stimulator of interferon genes; α-SYN, α-synuclein; TCA, tricarboxylic acid; TFAM, mitochondrial transcription factor A; TSN, Tanshinone IIA; VDAC, voltage-dependent anion channel.

TABLE 1 Several current models of mPTP.

Proteins	Condition	Cell culture methods	References
CypD-ANT	The conformational changes of ANT triggered by Ca^{2+} in the matrix	Incubate the isolated rat liver and heart mitochondria in 150 mM-KSCN or sucrose medium	Halestrap and Davidson, 1990
VDAC-CypD-ANT	Ca^{2+} and Pi, binding allow flicker into an open pore form.	The cDNA encoding cyclophilin-D was cloned from a rat liver library and expressed in Escherichia coli XL1 cells.	Crompton et al., 1998
Misfolding and clustering of native membrane proteins-Chaperone-like proteins-CypD	Oxidative damage and other perturbations (e.g., Ca^{2+})	Incubate isolated rat liver mitochondria in sucrose medium	He and Lemasters, 2002
PiC-ANT-CypD	Triggered by calcium, promoted by CypD, regulated by the conformational state of ANT molecules, and caused by conformational changes in PiC	Incubate isolated rat liver and heart mitochondria, as well as bovine heart mitochondria, in sucrose medium	Leung et al., 2008
PiC-CypD	Ca^{2+}	Incubate isolated rat liver and heart mitochondria, as well as bovine heart mitochondria, in sucrose medium	Leung and Halestrap, 2008
FO ATP synthase	The c subunit of the FO ATP synthase plays a critical role in the CsA-dependent opening of the PTPC induced by cytosolic Ca^{2+} overload.	Glycolysis and respiratory cell model of human cervical carcinoma HeLa cells	Bonora et al., 2013
Dimers of mitochondrial ATP synthase	Membrane potential and substrate pH are key regulatory factors for ATP synthase	Glycolysis and respiratory cell models of mitochondria in bovine or mouse heart and human osteosarcoma ahqb17 cells	Giorgio et al., 2013
Dimers of mitochondrial ATP synthase-ANT-PiC	Stress conditions	Hypothesis	Gutiérrez-Aguilar and Baines, 2015
SPG7-CypD-VDAC	ROS, Ca^{2+}	An experimental system using HEK293T and HeLa cells was developed, in which expression of mitochondrial proteins was silenced individually by short hairpin RNA and evaluated for Ca^{2+}- and ROS-induced PTP opening.	Shanmughapriya et al., 2015
FO ATP synthase forms a Ca^{2+}-dependent high-conductance channel	Ca^{2+}	FO ATP synthase was purified from bovine heart mitochondria by a combination of sucrose density gradient centrifugation and ion-exchange chromatography employing the mild.	Mnatsakanyan et al., 2019; Urbani et al., 2019

(Shanmughapriya et al., 2015), its association with mPTP opening is undeniable. Research has demonstrated that the interaction between α-synuclein (α-SYN) and VDAC1 promotes mPTP opening, which can lead to Cytc release and mitochondrial swelling (Shen et al., 2014); this may be one of the pathological mechanisms underlying certain neurodegenerative diseases.

One of the primary functions of mitochondria is to provide energy (ATP) through oxidative phosphorylation, which necessitates the importation of ADP and inorganic phosphate (Pi) across the inner mitochondrial membrane (Ernster and Schatz, 1981). The transport of ADP and Pi requires the involvement of Mitochondrial carrier proteins. Similar to ANT, PiC also belongs to the mitochondrial carrier family protein (Gao et al., 2020), predominantly found in cardiac and skeletal muscle tissues (Seifert et al., 2015). Its main responsibility lies in replenishing consumed Pi within mitochondria either through OH-exchange or proton binding mechanisms (Stappen and Krämer, 1994). It has been reported that PiC plays a crucial role in mPTP formation, with changes in its conformation induced by Ca^{2+} leading to mPTP opening (Seifert et al., 2016). Studies have demonstrated that increased levels of PiC caused by a high Pi environment result in elevated mitochondrial superoxide production and vascular smooth muscle cell death. However, inhibition of PiC reduces mitochondrial Pi uptake while inhibiting mitochondrial oxidative stress and ERK1/2 activation (Thi Nguyen et al., 2023).

The mitochondrial F1FO-ATP synthetase, also known as ATP synthase, is a large multisubunit protein complex (greater than 500 kDa) that consists of an FO domain, a peripheral stalk, and a soluble F1 domain comprising a catalytic head and a central stalk (Pinke et al., 2020; Spikes et al., 2020). It belongs to the rotating ATPase family and is widely distributed in the energy transduction membranes of bacteria, chloroplasts, and mitochondria (Zharova et al., 2023). This enzyme facilitates the synthesis of ATP from ADP and inorganic phosphate through the final step of oxidative phosphorylation (or photophosphorylation), which is a fundamental pathway for energy production in animal, plant, and microbial cells (Trchounian and Trchounian, 2019). While its primary function is ATP synthesis, under certain

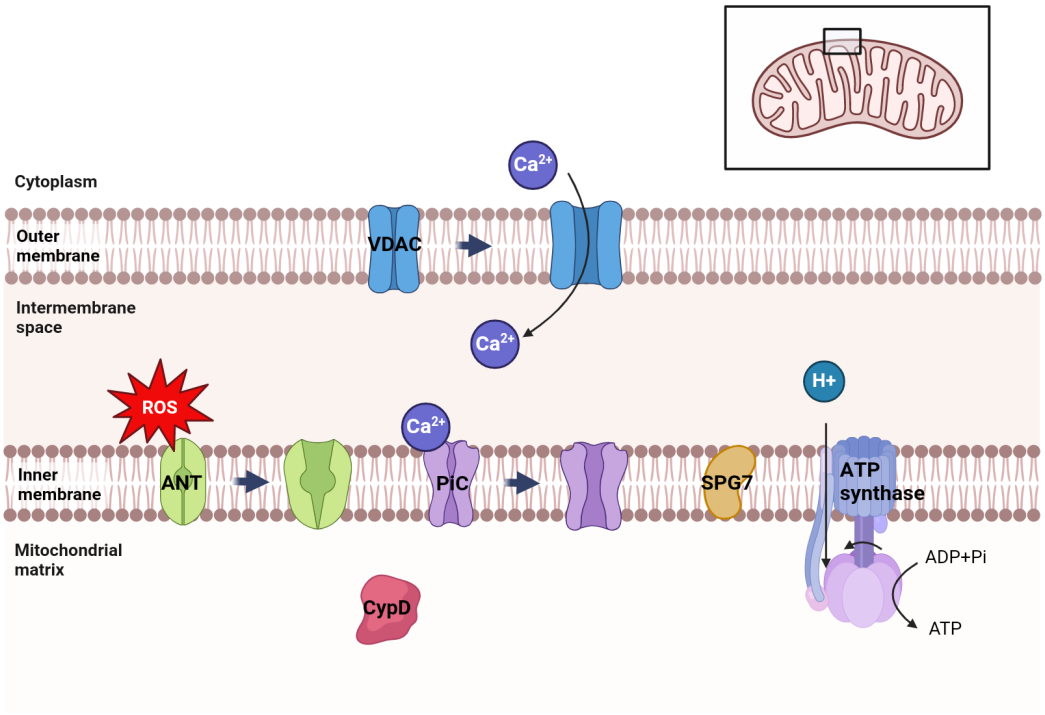

FIGURE 1
Distribution of several major candidate proteins of mPTP. VDAC was distributed in the outer membrane of mitochondria. ANT, PiC, SPG7 and ATP synthase were distributed in the inner membrane of mitochondria. CypD is distributed in the mitochondrial matrix. Among them, VDAC can regulate ATP transport and Ca2+ uptake in mitochondria. Ca2+ can trigger the conformational changes of ANT and PiC, leading to the opening of mPTP. ATP synthase uses the electrochemical membrane gradient of protons to drive the rotation of its own subunits and catalyze ATP synthesis to provide energy to the cell.

pathological and physiological conditions it can also hydrolyze ATP to provide energy to the inner mitochondrial membrane. Additionally, there have been suggestions that ATP synthase contributes to cell death by participating in the opening of mPTP. Under normal circumstances, ATP synthase utilizes the electrochemical transmembrane gradient of protons to drive FO rotation and initiate ATP synthesis at the F1 catalytic center. However, upon mPTP opening leading to depolarization of the mitochondrial inner membrane and loss of proton transmembrane electrochemical gradient necessary for FO rotation initiation occurs resulting in limited ATP synthesis ultimately leading to cell death (Mnatsakanyan et al., 2019).

As a mitochondrial protease, SPG7 is responsible for ribosome assembly and the elimination of misfolded proteins within mitochondria (Koppen et al., 2007). Mutations in SPG7 result in the misformation of the protease complex, leading to defective protein quality control, impaired mitochondrial function, and compromised neuronal signaling. Consequently, this gives rise to a wide range of diseases including spastic paraplegia (Casari et al., 1998), ataxia (Pfeffer et al., 2015), amyotrophic lateral sclerosis (Osmanovic et al., 2020), among others. It has been suggested that SPG7 acts as a core component of mPTP and interacts with VDAC1 and CyPD. Knockout studies have shown that the absence of SPG7 impairs ion efflux from mitochondria to cytoplasm and disrupts calcium retention capacity (Shanmughapriya et al., 2015). However, Bernardi and Forte (2015) propose that SPG7 indirectly regulates rather than serves as a core component for mPTP opening. Recently, genetic research reported that SPG7 neither forms pores in mitochondrial permeability transition nor regulates mPTP opening (Klutho et al., 2020). Therefore, further investigation is required to determine the role of SPG7 in mPTP.

3 Conditions for opening the mPTP

The researchers have made a precise and bold prediction of the mPTP model, postulating that MPTS are induced by two distinct types of pores, each facilitating the passage of two currents: Firstly, a low conductance state with an amplitude ranging from 0.3 to 0.7 nS, allowing for the permeation of ions (such as protons, Ca^{2+}, and K^{+}) and small metabolites (e.g., glutathione) across the inner mitochondrial membrane under physiological conditions. Secondly, a high conductance state with an amplitude of approximately 1.5 nS, enabling the transit of large solutes (like sucrose) (Neginskaya et al., 2019). However, this latter scenario exerts detrimental effects on mitochondrial structure and function leading to irreversible permanent permeability opening and ultimately regulated cell death (RCD).

Under normal physiological conditions, the low conductance state triggers opening due to the accumulation of Ca^{2+}. Upon redistribution of ions between the mitochondria and the cytoplasm, H^{+} ions enter the mitochondria from the cytoplasm, causing rapid closure of mPTP by reducing the pH of the mitochondrial matrix. This spontaneous transition between on and off states of mPTP

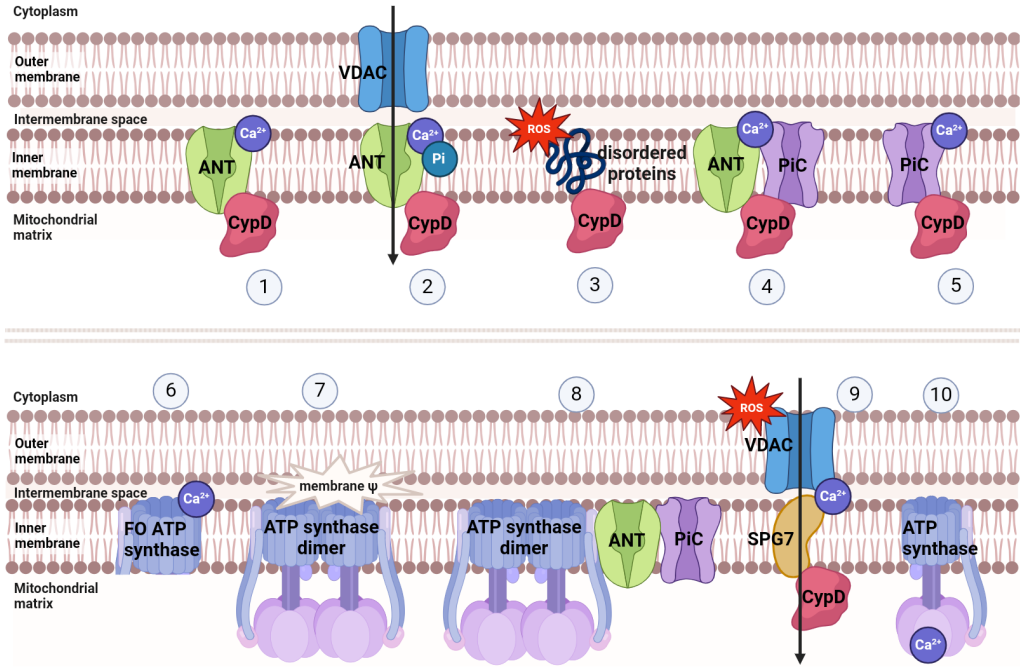

FIGURE 2
Several models of mPTP and factors inducing mPTP opening.

is referred to as "flicker" (Boyman et al., 2019). The flicker of mPTP is a physiological phenomenon that provides an additional mechanism for effluxing Ca^{2+} from the mitochondrial matrix, mitigates persistent overload of Ca^{2+} in the matrix, regulates Ca^{2+} reserves within mitochondria, and further modulates Ca^{2+}-related metabolism (Bernardi and von Stockum, 2012). Moreover, the flicker can facilitate transportation of endogenous ROS and other molecules generated in mitochondria into the cytoplasm; however, this may serve as a self-protective mechanism for mitochondria (Zorov et al., 2000).

Unlike flicker, prolonged opening of mPTP can have detrimental effects on mitochondrial physiology and energy metabolism. When the mPTP is opened to a high conductance, the redistribution of ions and small molecules leads to a reverse redistribution of H_2O. The entry of water into the mitochondrial matrix increases osmotic pressure, resulting in partial expansion of mitochondrial cristae and an increase in matrix volume. This causes mitochondrial swelling accompanied by mechanical rupture of the mitochondrial outer membrane (Bonora et al., 2022). Opening of high-conductance mPTP typically occurs under pathological conditions and often leads to difficult-to-repair damage in mitochondria. Pathological stimuli such as Ca^{2+} overload, oxidative stress, increased phosphate concentration, and decreased adenine nucleotide availability can promote the high permeability of the mitochondrial inner membrane to macromolecular solutes (Halestrap, 2009; Morciano et al., 2015; Boyenle et al., 2022). The substantial non-selective influx of these high molecular solutes and sudden loss of metabolites within mitochondria disrupts mitochondrial homeostasis, ultimately leading to programmed cell death (Izzo et al., 2016).

The opening of mPTP induced by Ca^{2+} overload has been widely acknowledged by scholars. Studies have demonstrated that Ca^{2+}-treated mitochondria can generate reactive oxygen species (ROS) and hydrogen peroxide (H_2O_2), which damage the membrane components in mitochondria and induce mPT (Kowaltowski et al., 2001). Mc Stay et al. discovered that Cys160 and Cys257 sites of ANT were oxidatively modified in Ca^{2+}-treated mitochondria, significantly increasing the affinity of cyclophilin D to ANT and inducing mPTP generation (McStay et al., 2002). Mitochondrial pH also serves as a precise regulator of mPT production. An acidic environment inhibits the opening of mPTP since H^+ ions replace Ca^{2+} and bind to the trigger site of mPTP (Halestrap, 1991). Oxidative stress and Pi concentration are two other known inducers for mPTP opening. Mitochondria are an important source of ROS (Giorgi et al., 2018), and pro-oxidants facilitate Ca^{2+}-induced mPTP opening. Stimulation with Pi can induce mPT and promote ROS generation, leading to enhanced oxidative stress response, further facilitating Pi-induced mPT. This situation reduces the threshold for mPTP opening, making mitochondrial cells prone to spontaneous occurrence of mPT (Kanno et al., 2004). Proapoptotic members Bax, Bak, and Bad from the Bcl-2 family have been reported to regulate mPTP opening. Bax/Bak depletion in mitochondria renders cells resistant to mPTP opening and necrosis; however, recombination of these cells or mitochondria with wild-type Bax can restore susceptibility possibly due to bax-driven cell fusion lowering the threshold form PTP opening (Whelan et al., 2012). Roy et al. proposed that stress factors such as ceramide and huperzine can dephosphorylate Bad by activating protein phosphatase 2A (PP2A), allowing dephosphorylated Bad to firmly bind to the mitochondrial membrane and interact with Bcl. This process shifts VDAC and makes mPTP sensitive to Ca^{2+}, promoting its opening (Roy et al., 2009).

4 Cellular consequences of mPTP opening

Under pathological conditions, the continuous and extensive opening of mPTP disrupts the internal mitochondrial environment and alters mitochondrial osmotic pressure, leading to a cascade of irreversible damage to both mitochondria and the organism as a whole. The persistent mPTP opening triggers the release of ROS, resulting in oxidative stress and subsequent mitochondrial dysfunction (Liu E. et al., 2020; Wacquier et al., 2020). ROS accumulation damages nuclear DNA, activates pro-apoptotic signaling pathways, and induces cellular senescence (Zorov et al., 2014; Liu et al., 2022). Changes in osmotic pressure can cause mitochondria to swell and rupture, ultimately leading to their lysis and demise while regulating cell necrosis (Mnatsakanyan et al., 2017). Furthermore, mPTP opening is also implicated in processes such as mitophagy (Baechler et al., 2019), ferroptosis (Basit et al., 2017), neutrophil extracellular traps (NETs) (Yang et al., 2021), pyroptosis (Zhang et al., 2022b), and inflammatory response (Bonora et al., 2022).

4.1 Oxidative stress

Under physiological conditions, the balance between production and scavenging of ROS is tightly regulated. Depending on the context, controlled oxidative stress can elicit various cellular responses, ranging from activating signaling pathways involved in cytoprotection to initiating coordinated activation of mitochondrial fission and autophagy for efficient clearance of abnormal mitochondria and cells, while preventing damage propagation to neighboring organelles and cells (Bernardi and Di Lisa, 2015; Briston et al., 2017). Conversely, uncontrolled oxidative or reductive stress can result in severe cellular damage and unnecessary cell death, leading to organ failure at both local and systemic levels (Szeto, 2008; Bernardi et al., 2015). In normal physiological conditions, ROS release accounts for approximately 2% of total mitochondrial oxygen consumption (Peuhkurinen et al., 1983). Both low and high ratios of ROS release can have detrimental effects: insufficient ROS release fails to fulfill proper cellular functions; excessive ROS release lacks a regulatory effect. As pivotal organelles governing cellular metabolism and redox homeostasis, mitochondria possess precise mechanisms to regulate ROS levels according to cellular demands (Cadenas, 2018).

However, under certain pathological conditions, the structure and function of mitochondria can become impaired. Mitochondria not only serve as the primary producers of ROS, but also actively contribute to their harmful amplification. Research has demonstrated that electron leakage from mitochondria accounts for approximately 90% of ROS generation (Zheng et al., 2022). The mPTP may play a pivotal role in this cascade of events. mPTP activation promotes ROS production, which in turn leads to further opening of the mPTP; this positive feedback mechanism ultimately results in excessive ROS accumulation and subsequent detrimental effects on mitochondrial function (Gareev et al., 2023).

Changes in cellular redox balance are intricately linked to the respiratory activity of mitochondria (Korshunov et al., 1997). Numerous post-translational modifications have been documented in oxidative phosphorylation complexes, aiding in the regulation of ROS production (Covian and Balaban, 2012). For instance, tyrosine phosphorylation of cytochrome oxidase and cytochrome c serves to inhibit respiration and safeguard mitochondria against hyperpolarization and subsequent elevation of ROS levels (Hüttemann et al., 2012). However, ROS can disrupt the association between cytochrome c and mitochondrial inner membrane cardiolipin, impairing its ability to shuttle electrons from complex III to complex IV. Consequently, electron accumulation occurs within respiratory complexes I and III, further fueling mitochondrial ROS generation. Once mitochondrial ROS reaches a certain threshold level, an influx of Ca^{2+} ensues depleting the robust redox buffering capacity within mitochondria, leading to uncontrolled escalation of mitochondrial ROS (Bernardi et al., 2015). Simultaneously, diffused ROS can affect neighboring mitochondria that have not undergone mPT thereby reducing the threshold for mPTP opening there and initiating a detrimental cycle ultimately resulting in extensive cellular ROS production (Zorov et al., 2014) and deleterious oxidative stress (Bonora et al., 2022).

4.2 Apoptosis

When mitochondrial permeability is impaired, the oxidative stress response becomes interconnected with subsequent damage to both mitochondria and cells, ultimately leading to apoptosis. Recent research has demonstrated that an elevation in reactive ROS production occurs prior to DNA fragmentation-induced apoptosis (Golstein and Kroemer, 2007). Various pathological factors causing cellular hypoxia result in reduced oxygen levels, thereby diminishing mitochondrial ATP production and triggering an increase in intracellular Ca^{2+} concentrations. Concurrently, hypoxia disrupts the functionality of the mitochondrial electron transport chain, leading to heightened ROS generation. Elevated levels of Ca^{2+} and ROS contribute to the opening of the mPTP, further exacerbating Ca^{2+} and ROS accumulation within mitochondria while promoting protein and lipid oxidation within these organelles. The resultant calcium overload and oxidative stress induce mitochondrial dysfunction, subsequently initiating apoptosis (Yao et al., 2022).

Mitochondria serve as the regulatory centers of apoptosis, and multiple lines of evidence suggest that mitochondria-mediated opening of mPTP plays a crucial role in initiating apoptosis (Chakraborti et al., 1999; Lin and Beal, 2006). Upon the opening of mPTP, cytochrome c and its associated proteins are released from mitochondria. However, it is widely acknowledged that the release of cytochrome c from mitochondria represents a pivotal step in apoptosis. Subsequently, cytochrome c released into the cytoplasm binds to apoptosis-associated factor 1 (Apaf-1) in the presence of ATP, leading to polymer formation and subsequent binding with caspase-9 to form apoptotic bodies. Activation of caspase-9 then triggers a cascade effect by activating other caspases such as caspase-3. Consequently, this process promotes cellular apoptosis (Zoratti and Szabò, 1995).

The production of ROS by mitochondria has been demonstrated to oxidize crucial thiol groups of the mPTP-related component ANT, thereby triggering the release of cytochrome

c and initiating a cascade of events leading to apoptosis (Kanno et al., 2004). Furthermore, previous studies have suggested that polythiols, but not monothiols, selectively inhibit the release of cytochrome c (Nishikimi et al., 2001). Subsequent investigations have revealed that adjacent dithiol and/or two proximal thiol residues in ANT and related proteins within the mitochondrial membrane may underlie Ca^{2+}-induced cytochrome c release. This study proposes that Ca^{2+} enhances the cross-linking between two thiol groups, such as Cys160 and Cys257, in ANT, resulting in the liberation of cytochrome c from mPTP (Kanno et al., 2004).

The VDAC protein is located in the outer mitochondrial membrane and was previously believed to be a crucial component of mPTP, although this assertion remains controversial (Shanmughapriya et al., 2015). The activation or deactivation state of VDAC plays a significant role in regulating apoptosis within mitochondria. The N-terminal α-helix domain of VDAC1 is indispensable for stabilizing its original open state; however, it has been reported that the N-terminal region can also form a pore large enough to facilitate the release of cytochrome c from mitochondria, subsequently triggering apoptosis (Abu-Hamad et al., 2009). Interestingly, even when in the closed state, VDAC can induce apoptosis by promoting calcium ion influx into mitochondria and subsequent opening of mPTP (Tan and Colombini, 2007). Moreover, previous studies have demonstrated that overexpression of VDAC1 can initiate apoptosis (Zaid et al., 2005; Weisthal et al., 2014). Under normal circumstances, VDAC exists in various oligomerization states (Shoshan-Barmatz et al., 2013), with overexpression leading to the formation of mPTP and subsequent release of cytochrome c, ultimately resulting in cell apoptosis (Keinan et al., 2010; Khan et al., 2021).

4.3 Necrosis

The process of cell necrosis is distinct from apoptosis, which is a form of programmed cell death. While apoptosis is regulated, cell necrosis is considered to be unregulated; however, some scholars argue that a significant portion of necrosis occurs through highly regulated mechanisms as well. During cell necrosis, the intracellular ATP level decreases to a point where the cell can no longer maintain its physiological activities. This leads to vacuolar appearance in the cytoplasm, damage to the cell membrane, and overflow of cellular contents including broken organelles and chromatin fragments. Consequently, this triggers an inflammatory response in surrounding tissues (Golstein and Kroemer, 2007; Kung et al., 2011).

Although apoptosis and necrosis are mediated by different pathways, there are instances where their production pathways overlap and apoptotic processes can further contribute to the occurrence of necrosis (Golstein and Kroemer, 2007; Chipuk et al., 2010). In mitochondria, caspase activation plays a key role in apoptosis due to the release of cytochrome c and other apoptotic factors. However, primary necrosis does not require involvement of cytochrome c. Nevertheless, if clearance of apoptotic bodies is delayed or absent following apoptosis, secondary necrosis ensues (Kung et al., 2011).

The opening of mPTP triggers mitochondrial membrane depolarization, resulting in the cessation of mitochondrial ATP synthesis and an influx of water into the solute-rich mitochondrial matrix. Consequently, osmotic pressure builds up between the matrix and the protein-dense extramitochondrial environment, leading to matrix swelling and crista folding and stretching, ultimately culminating in mitochondrial swelling, rupture, and initiation of cell death (Lam et al., 2013; Shibata et al., 2019). Furthermore, this swelling-induced dilution hampers enzyme activity and metabolite concentration within mitochondria, impairing tricarboxylic acid (TCA) cycle function as well as respiratory complex activities. As a consequence, ATP synthase ceases ATP synthesis at this stage, causing a rapid blockade of ATP-dependent reactions. Under these circumstances, mitochondria are unable to create conditions necessary for mPTP deactivation; thus, rendering it irreversible while further accelerating cell death onset.

Additionally, extensive opening of the mPTP results in a cellular energy crisis, leading to an uncontrolled escalation in glycolysis rate. This heightened glycolytic activity causes pyruvate accumulation, resulting in acidification of both the cytoplasmic and mitochondrial matrix. Consequently, the plasma membrane ATPase actively extrudes Na^+, Ca^{2+}, and H^+ ions from the cytosol, while the sarcoplasmic/endoplasmic reticulum Ca^{2+}-ATPase (SERCA) pumps Ca^{2+} into the endoplasmic reticulum. Subsequently, there is a disappearance of Na^+ and Ca^{2+} gradients along with a deceleration in H^+ pumping, exacerbating cytoplasmic acidification. The profound loss of ion gradients ultimately culminates in plasma membrane collapse and necrotic cell death (Galluzzi et al., 2018).

4.4 Autophagy

Autophagy is a catabolic process that selectively or non-selectively degrades dysfunctional or unnecessary cellular components in eukaryotic cells, thereby maintaining cellular homeostasis and facilitating stress response under normal conditions (Batoko et al., 2017). Nonselective autophagy serves as a protective mechanism by providing cells with biomolecular fuel to generate energy during periods of starvation (Rabinowitz and White, 2010). However, autophagy also plays a role in regulating cell death when cells are exposed to injury-induced stress or signaling stimulation (Galluzzi et al., 2015; Zhao et al., 2017).

Mitophagy refers to the process through which mitochondria or parts of mitochondria are targeted for degradation within lysosomes (Montava-Garriga and Ganley, 2020; Nguyen and Lazarou, 2021). The occurrence of autophagy leads to internal cristae fragmentation, protein degradation, and even retention of only the outer membrane structure (Minibayeva et al., 2012). Mitophagy occurs conservatively and specifically, serving as an important self-regulatory pathway for maintaining cellular stability.

According to the current study, specific proteins on the surface of mitochondria appear to function as markers for autophagic recruitment in mitochondria, while mPTP plays a crucial role as a component of the mitochondrial membrane. The opening of mPTP can trigger alterations in autophagic activity (Rodriguez-Enriquez et al., 2006). Electron transport chain (ETC), an integral part of mitochondria, generates low levels of ROS to facilitate cell signaling (Maldonado and Lemasters, 2014;

Huang et al., 2016). Through redox reactions that generate ATP in the oxidative phosphorylation system, they establish an electrochemical gradient. Under hypoxic conditions, cellular oxidative metabolism and energy are disrupted, leading to mitochondrial dysfunction and inadequate ATP supply along with excessive ROS production (Zelinová et al., 2019). The generation of ROS induces autophagy while also promoting mPTP opening and continuous ETC impairment (Gomes and Scorrano, 2013), further exacerbating autophagy. Numerous studies have demonstrated that mitochondria undergoing permeability transitions are often targeted by autophagy. Extensive intracellular mPT triggers excessive mitophagy, resulting in programmed cell death (Van Aken et al., 2016). In cases where mammalian hepatocytes experience nutrient starvation, MPT occurrence leads to an accelerated depolarization rate of the mitochondrial membrane and subsequently promotes mitophagy (Reumann et al., 2010).

When mitochondria are damaged, the damaged mitochondria are often transported to lysosomes for degradation, a process frequently observed in the activation of the PINK1-parkin pathway (Palikaras et al., 2018). This mechanism is believed to mediate mPTP-induced mitophagy following deletion of the mitochondrial fission protein DRP1 (Song M. et al., 2015). Fused mitochondria facilitate more efficient diffusion of Ca^{2+} within them, which stimulates mPTP opening (Baumgartner et al., 2009), an event disrupted by Drp1-mediated mitochondrial fission. Inhibition of Drp1-mediated fission results in morphologically elongated mitochondria and increased mPTP opening (Szabadkai et al., 2004). The opening of mPTP can cause depolarization of the mitochondrial membrane, leading to accumulation of PINK1 on the mitochondrial surface and subsequent initiation of mitophagy, ultimately resulting in autophagosome uptake and release (Basit et al., 2017). However, in the absence of DRP1, inhibition of mPTP opening reduces mitochondrial lysosomal phagocytosis while increasing mitochondrial content (Baumgartner et al., 2009).

The involvement of mPTP in autophagy can also occur via the apoptotic pathway. Mitochondrial outer membrane permeability is regulated by BCL2 family proteins, which govern the intrinsic apoptotic pathway. It has been demonstrated that mPTP facilitates the translocation of pro-apoptotic protein Bax to the outer mitochondrial membrane. The anti-apoptotic protein BCL2 forms a heterodimer with BAX to regulate cellular apoptosis. Furthermore, BCL2 interacts with BECN1/Beclin 1 to modulate autophagy. However, phosphorylation of BCL2 enhances its binding affinity for Bax and dissociates it from BECN1, thereby inducing autophagy (Wei et al., 2008). These findings underscore the pivotal role of both BCL2 and mPTP in regulating the delicate balance between apoptosis and autophagy through their regulation of Bax (Liu et al., 2018).

Additionally, mitophagy also impacts mPT, and the accumulation of dysfunctional mitochondria induced by autophagy results in a reduction in mitochondrial membrane potential and an elevation in ROS production. This scenario decreases the threshold for mPTP opening, rendering mitophagy-deficient cells susceptible to spontaneous mPT (Baechler et al., 2019; Sun et al., 2019), thus perpetuating a vicious cycle. In animals, the mitochondrial protease PARL inhibits autophagy through Omi activation, also known as HtrA2, thereby preserving cristae structure and preventing mPTP opening and cytochrome c release (Chao et al., 2008).

4.5 Ferroptosis

Different from apoptosis, necrosis, and autophagy, ferroptosis is a regulated mode of cell death that relies on iron ions. Its primary characteristic is the accumulation of lipid peroxides (Dixon et al., 2012; Xie et al., 2016). The process of lipid peroxidation can be initiated by enzymatic or non-enzymatic reactions catalyzed by lipoxygenase. Once generated, lipid peroxide reacts with Fe^{2+}, oxygen, or surrounding unsaturated fatty acids, leading to continuous generation of free radicals and their diffusion into the surrounding area, ultimately triggering cell death (Tang et al., 2021).

Although unsaturated fatty acids in the cell membrane undergo continuous oxidation, lipid peroxidation and ferroptosis can be inhibited by antioxidant mechanisms under physiological conditions. Glutathione peroxidase 4 (GPX4) plays a crucial role in this process by catalyzing the reaction between glutathione GSH and lipid hydroperoxides, thereby reducing lipid peroxidation to lipid alcohols and preventing the accumulation of lipid peroxides, thus protecting cells (Friedmann Angeli et al., 2014; Conrad et al., 2016). However, the functional activity of GPX4 is regulated by system XC- in the plasma membrane. System xc- encodes heterodimeric amino acid transport through SLC7A11 (xCT) and SLC3A2 (4F2hc), which facilitates cystine-glutamate exchange (Ying and Padanilam, 2016). It transports extracellular cystine into cells where it is converted to cysteine—a necessary substrate for maintaining GPX4 activity. Impaired cystine transport can result in decreased intracellular GSH levels and increased ROS production (Montero et al., 2013), consequently leading to the accumulation of lipid hydroperoxides (Friedmann Angeli et al., 2014).

Currently, an increasing body of research provides crucial evidence implicating mitochondrial damage in the process of iron-induced cell death. Jelinek et al. discovered that exposure to RSL3 induced iron death in neuronal HT 22 cells and mouse embryonic fibroblasts, resulting in a decrease in GPX4 concentration, increased lipid peroxidation and mitochondrial fragmentation, decreased mitochondrial membrane potential and respiration. However, the use of iron death inhibitors reversed these effects. Furthermore, the application of ROS scavengers effectively preserved the integrity of mitochondrial morphology and partially inhibited the occurrence of iron-induced cell death (Jelinek et al., 2018).

An important intersection between mitochondrial dysfunction and iron-induced cell death is the activation of mPTP. It has been observed that Erastin-induced iron-mediated cell death in SH-SY5Y cells is accompanied by a decline in mitochondrial membrane potential, intracellular ATP content, and an accumulation of oxidative stress markers. However, treatment with cyclosporin A can prevent Erastin-induced mitochondrial changes and subsequent cell death by binding to CypD. This suggests that mPTP activation plays a crucial role in iron-induced cell death. Interestingly, it should be noted that ROS production gradually increases over time, while cyclosporin A significantly inhibits this process only during later stages. There is reason to believe that ROS accumulation during these later stages may be triggered by mPTP activation, whereas initial ROS production induced by erastin could potentially result from GSH depletion (Ganguly et al., 2024).

Studies have revealed that mitophagy can trigger uncontrolled degradation of mitochondria, resulting in the release of stored iron and subsequent iron overload-induced ferroptosis (Du et al., 2020). Throughout this process, mitochondria undergo a series of alterations including volume atrophy, outer membrane rupture, crista shrinkage, inner membrane compression, and electron transparent nucleus formation (Xie et al., 2016). Ultimately, these changes culminate in membrane disruption, depolarization of mitochondrial membrane potential, and mPTP opening. However, the activation of mPTP leads to ROS generation which exacerbates mitochondrial energy dysfunction and organelle swelling/rupture while inducing characteristic ferroptotic cell death, thus establishing a vicious cycle (Kwong and Molkentin, 2015; Basit et al., 2017). Additionally demonstrated is that oxidative stress triggers p53 translocation to mitochondria in Bax/Bak double knockout mice's isolated mitochondria. This translocation induces CypD-p53 complex formation which promotes mPTP opening and consequent cell death (Vaseva et al., 2012). Simultaneously activated p53 renders cells more susceptible to ferroptosis by inhibiting SLC7A11 transcription resulting in decreased cystine uptake along with reduced GSH levels leading to an additional increase in ROS production ultimately driving ferroptotic cell demise (Zhang et al., 2018).

As a crucial component of mPTP, VDAC1 plays a pivotal role in the occurrence of ferroptosis, contributing to tissue damage and organ dysfunction associated with various diseases (Niu et al., 2022). Studies have demonstrated that Tanshinone IIA (TSN), an active compound extracted from Danshen, can effectively mitigate myocardial cell injury by suppressing ferroptosis during anoxia/reoxygenation (A/R). Pre-treatment with TSN leads to upregulation of genes involved in ferroptosis inhibition, reduction in total iron content, lipid peroxide levels, and superoxide dismutase expression while inhibiting ferroptotic activation. However, overexpression of VDAC1 can induce mPTP opening and counteract the protective effect exerted by TSN on cells. This suggests that TSN prevents A/R-induced ferroptosis by downregulating VDAC1 expression to prevent mPTP opening (Hu et al., 2023).

4.6 Others

The regulation of inflammation and the opening of mPTP are interconnected (Bonora et al., 2022). Induction of mPTP triggers the activation of inflammatory response through succinate release and the release of damage-associated molecular patterns (DAMPs) associated with mitochondrial damage, thereby leading to tissue damage following cerebral ischemia (Tian H. Y. et al., 2023). The opening of mPTP induces ferroptosis, which in turn leads to secretion of HMGB1, a DAMP that activates pattern recognition receptor (PRR)/NF-κB pathway, resulting in an inflammatory response in peripheral macrophages (Chen et al., 2021). It has been observed that under stress conditions, mitochondrial DNA (mtDNA) is released into the cytoplasm via mPTP, activating cyclic GMP-AMP synthetase (cGAS)-stimulator of interferon genes (STING) pathway and exacerbating downstream inflammatory responses. Genetic deletion or pharmacological inhibition of STING as well as inhibition of mtDNA release reduce inflammatory responses; however, transfection with mtDNA supports cytoplasmic mtDNA-induced inflammatory responses by activating cGAS-STING pathway (Ouyang et al., 2023). Deletion of CypD, a major component of mPTP, attenuates proinflammatory cytokine expression in mouse islets (Liu et al., 2019) and mitigates inflammatory responses induced by exposure to bacterial products such as lipopolysaccharide in macrophages or liver cells (Veres et al., 2021).

The aging process is associated with significant alterations in mitochondrial function. These changes in mitochondrial function are believed to be linked to an increased production of ROS, which contribute to cellular death, senescence, tissue degeneration, and impaired tissue repair over time. The opening of the mPTP may play a crucial role in these processes, as elevated ROS levels activate mPTP opening, further exacerbating ROS production (Zorov et al., 2014). Injury and inflammation are also thought to enhance mPTP opening, and chronic low-grade inflammation is a characteristic feature of aging. Nicotinamide adenine dinucleotide (NAD+) inhibits the frequency and duration of mPTP opening; however, NAD+ levels decline with age, thereby promoting mPTP opening and increasing ROS release. Accumulation of ROS can damage nuclear DNA, trigger pro-apoptotic signaling pathways, and drive cellular senescence (Schaar et al., 2015; Fang et al., 2016). Mitophagy regulates senescent cells by removing fragmented mitochondria with activated mPTP; nevertheless, autophagy is inhibited in senescent cells leading to increased activation of mPTP. However, during aging the heightened activity of mPTP makes autophagy a detrimental process that contributes to cellular senescence and demise (Rottenberg and Hoek, 2021).

NETs are unique structures formed by neutrophils outside the cell, composed of DNA, histones, and granule contents. NETs represent an inflammatory form of cell death in neutrophils. Research has demonstrated that SIRT1 can induce the activation of mPTP channels and release mitochondrial DNA, leading to the formation of mitochondria-dependent NETs which subsequently initiate a cascade of pathological reactions (Yang et al., 2021).

NLRP3 inflammasome-mediated pyroptosis is an inflammatory programmed cell death process that promotes chronic inflammation and tissue degeneration. Human nucleus pulposus cells exposed to oxidative stress conditions exhibit characteristic morphological and functional changes associated with mPTP opening and cytoplasmic release of mtDNA. Inhibiting mPTP opening specifically or preventing mtDNA release into the cytoplasm effectively reduces NLRP3 inflammasome-mediated pyroptosis in nucleus pulposus cells as well as inflammation within the microenvironment in vitro, ultimately mitigating degenerative progression in a rat intervertebral disc acupuncture model (Zhang et al., 2022a).

5 mPTP participating in the pathological process of ICH

The pathological process following ICH can be categorized into two stages: primary brain injury and secondary brain injury. The former refers to the mechanical damage caused by the space-occupying effect of the hematoma, while the latter encompasses a series of pathological processes involving excitatory amino

acid toxicity, reactive oxygen species, vascular inflammatory cell-mediated tissue oxidative stress, apoptosis, necrosis, autophagy, and so forth. Ultimately leading to severe neurological deficits (Wang Z. et al., 2018; Chen et al., 2020; Zheng et al., 2023). Currently, there is substantial evidence linking the opening of mPTP with the pathological process after ICH (as depicted in Figure 3).

5.1 ICH and oxidative stress

Due to its high lipid and iron content and relatively low levels of antioxidants, the brain is susceptible to damage from oxidative stress (OS) (Xu et al., 2018). Numerous studies have demonstrated the association between OS and the pathophysiology of various brain disorders (Salim, 2017), particularly ICH. OS can be triggered by ICH and plays a crucial role in secondary brain injury following such an event (Wang S. et al., 2018). Increasing evidence suggests that ROS levels increase while antioxidant enzyme activity decreases in the brain after ICH (Xie et al., 2017). Experimental models of ICH have shown elevated levels of ROS and malondialdehyde (a marker of oxidative stress) in rats (Liu X. C. et al., 2020). During ICH, an excessive amount of ROS disrupts the delicate balance between the antioxidant system and ROS, resulting in cellular damage including lipid peroxidation, DNA damage, protein oxidation, apoptosis induction, blood-brain barrier (BBB) breakdown and overall brain impairment (Han et al., 2008; Katsu et al., 2010).

Multiple mechanisms can mediate the generation of ROS following ICH, and glutamate is among them. Glutamate serves as a contributing factor to nervous system injury by inducing excitotoxicity in neurons. Following ICH, a substantial release of glutamate occurs from the blood, activating NMDA receptors and resulting in an influx of Ca^{2+}. This excessive increase in cytoplasmic Ca^{2+} subsequently leads to mitochondrial Ca^{2+} overload. Additionally, thrombin production after ICH activates Src kinase, leading to phosphorylation of NMDA receptors and further enhancement of their function (Sharp et al., 2008). However, mitochondrial Ca^{2+} overload causes a decrease in transmembrane potential and opening of mPTP, thereby damaging mitochondria and the respiratory chain, ultimately leading to increased ROS release (Mracsko and Veltkamp, 2014). Furthermore, this destructive damage has the ability to propagate from one mitochondrion to another (Qu et al., 2016), resulting in continuous expansion of the oxidative stress response.

5.2 ICH and apoptosis

The occurrence of apoptosis following ICH is widely observed in the cerebral cortex, subcortical and hippocampal neurons. Additionally, traces of apoptosis can even be detected within the cerebrovascular system alongside brain parenchyma. Studies have demonstrated that vascular endothelial cell apoptosis directly exacerbates vasospasm severity post-intracerebral hemorrhage and further intensifies secondary injury (Zhou et al., 2004). ICH, as an external stress event, can trigger apoptosis through various mechanisms (Hasegawa et al., 2011). The mitochondria-related apoptotic pathway plays a crucial role in secondary injury after ICH (Fujii et al., 2013). Mitochondria are highly dynamic organelles that continuously undergo fusion and division to adapt to changes in energy demand and supply while maintaining cellular function (Zhou et al., 2021). Under normal circumstances, the dynamic balance between mitochondrial fusion and division is a pivotal event regulating mitochondrial morphology for ensuring normal mitochondrial function (Giacomello et al., 2020). However, following ICH, there is abnormal regulation of mitochondrial dynamics with an imbalance between fusion and fission processes leading to a gradual shift towards fission (Wu et al., 2020b). Mounting evidence suggests that excessive mitochondrial division serves as a key factor contributing to ICH development (Wu et al., 2020a; Zhang et al., 2021). Excessive fission disrupts the structural integrity of mitochondria. During this process, a series of morphological changes can be observed, including prominent mitochondrial clustering, spherical shrinkage, loss of integrity, mitochondrial swelling, darkening of the matrix, and irregular cristae formation (Cheng et al., 2021; Zhang et al., 2021). Consequently, mitochondrial oxidative phosphorylation is impaired while ROS production increases. This leads to decreased ATP levels and mitochondrial membrane potential ultimately resulting in mitochondrial dysfunction (Wu et al., 2020a), which also serves as an early indicator of apoptosis. The heightened mitochondrial fission prolongs mPTP opening (Chang et al., 2021), leading to sustained release of apoptotic factors (such as cytochrome C) from mitochondria. Subsequently, activation of the caspase cascade occurs followed by apoptosis (Azarashvili et al., 2016).

The protein p53 has been demonstrated to play a crucial role in coordinating the apoptotic pathway following ICH (Cahill and Zhang, 2009; Lauzier et al., 2023). Upon occurrence of ICH, p53 activates the mitochondrial apoptotic pathway via the Bcl-2 protein family, which subsequently modulates the release of cytochrome C from mPTP based on the prevailing signal (i.e., pro-apoptotic or anti-apoptotic dominance) (Philchenkov, 2004). Moreover, under oxidative stress induced by ROS, p53 accumulates within the mitochondrial matrix and interacts with CypD to trigger mPTP opening, thereby initiating a detrimental cycle of enhanced ROS release and apoptosis induction (Vaseva et al., 2012; Munro and Treberg, 2017).

5.3 ICH and necrosis

As previously discussed, apoptosis is a delayed form of cell death that occurs as a result of less severe injury and is associated with the activation of a "genetic program." In contrast, necrosis is a rapid response to severe injury such as hypoxia and cell trauma. Despite their morphological differences, there is increasing evidence suggesting the existence of similar mechanisms for apoptosis and bad cell color, both of which are linked to the opening of mPTP. Following ICH, the opening of mPTP can directly lead to mitochondrial dysfunction and neuronal damage (Banasiak et al., 2000).

Under normal circumstances, mitochondria primarily play a crucial role in supplying cellular energy. However, when mitochondrial dysfunction occurs, it can lead to various

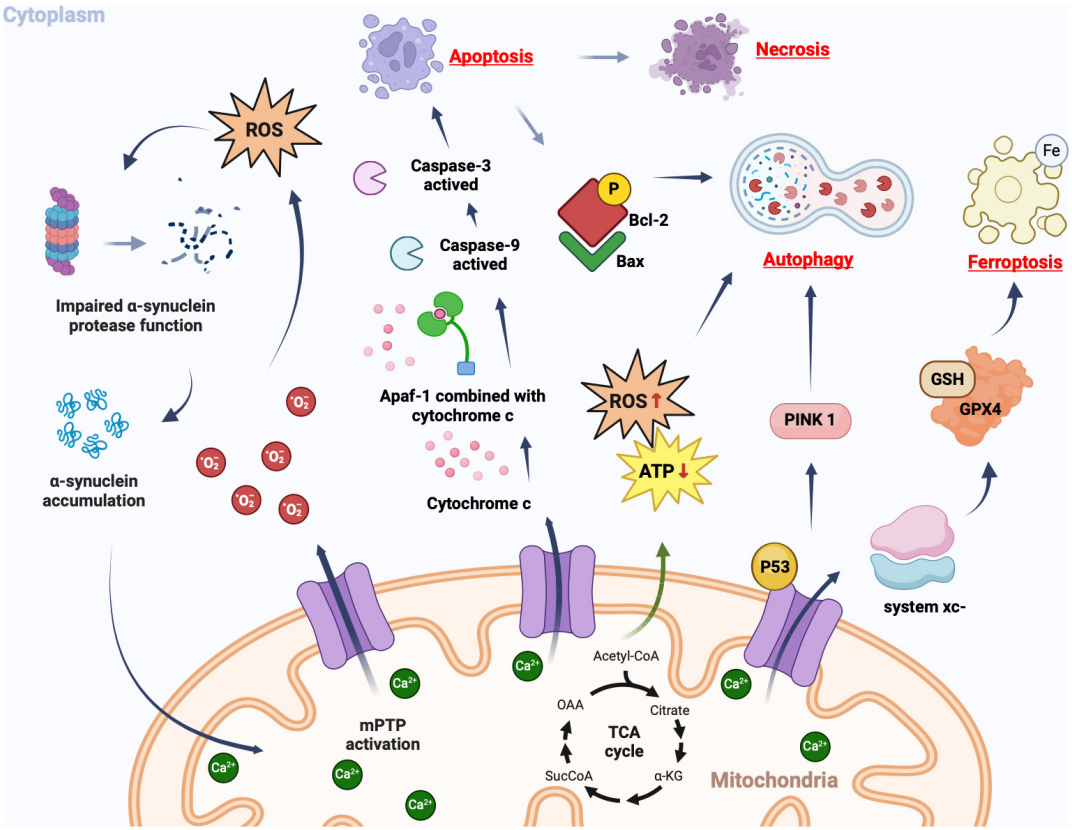

FIGURE 3
Cellular consequences of mPTP opening. In pathological conditions, mPT promotes the production of ROS, which in turn leads to further opening of the mPTP. Simultaneously, ROS can impair proteomic clearance of α-synuclein, resulting in its accumulation and interaction with mitochondria, thereby further activating mPTP opening. This creates a vicious cycle that triggers oxidative stress reactions. Upon mPTP opening, cytochrome c is released from mitochondria and binds to apoptosis-related factor 1 (Apaf-1), facilitating caspase-9 binding and subsequent activation of caspase-3, ultimately triggering apoptosis. If apoptotic bodies are not promptly cleared, secondary cell necrosis occurs immediately after apoptosis. The opening of mPTP can cause ATP supply insufficiency and excessive ROS production, inducing autophagy. Mitochondrial damage-induced accumulation of PINK1 further promotes autophagy. Phosphorylated Bcl-2 following mPTP opening can induce autophagy by binding to Bax protein. The opening of mPTP results in decreased GPX4 concentration and affects the regulation system xc-, as well as GSH expression catalyzed by it; this reduction impairs cystine transport leading to lipid hydroperoxide accumulation and subsequently iron death.

consequences in neuronal damage, ranging from temporary metabolic inhibition to cell necrosis depending on the severity of mitochondrial impairment (Yu et al., 2019). Following ICH, the release of glutamate triggers neuronal necrosis, and this specific mechanism is associated with mitochondrial dysfunction (Nicotera and Lipton, 1999). A subset of cerebellar granule cells was observed to undergo necrotic death during and shortly after exposure to glutamate. These neurons experienced a collapse in mitochondrial membrane potential, swelling of the nucleus, and dispersion of intracellular debris into the culture medium. Glutamate stimulation resulted in decreased mitochondrial membrane potential and ATP levels in numerous neurons. In cases where there was irreversible dissipation of the mitochondrial membrane potential, rapid necrosis occurred (Nicotera and Lipton, 1999). Insufficient ATP production leading to reduced intracellular energy can further contribute to cytotoxic edema development and cell necrosis. Neurons have higher energy demands compared to other cells; therefore, inadequate energy supply causes more significant damage to neurons (Prentice et al., 2015). Additionally, mitochondria can induce ROS production. The accumulation of ROS disrupts the pro-oxidation-antioxidant balance within cells and contributes to oxidative stress occurrence—ROS being a key factor in neuronal cell necrosis (Prentice et al., 2015). Henceforth, maintaining the integrity of both mitochondrial morphology and function plays a vital role in protecting nerve cells following ICH; mPTP serves as a critical determinant influencing this process.

5.4 ICH and autophagy

Autophagy is a vital lysosomal degradation and recycling process in eukaryotic cells, responsible for maintaining cellular function, homeostasis, and the delicate balance between cell survival and death (Tian Z. et al., 2023). Studies have demonstrated the sensitivity of vascular smooth muscle cells (VSMCs) to alterations in autophagic regulation (Salabei and Hill, 2015). Autophagy is indispensable for VSMC survival, as knockdown of autophagy-related genes increases their susceptibility to cell death (Grootaert et al., 2018). Furthermore, autophagy plays a significant role in various cardiovascular and cerebrovascular diseases such as atherosclerosis (Shao et al., 2016) and ischemic stroke (Mo et al., 2020). Recent evidence has also implicated autophagy in

secondary injury following ICH (Zhang and Liu, 2020). Miro1, a mitochondrial transport protein highly expressed after ICH, exhibits superior maintenance of mitochondrial membrane potential and promotes mitochondrial health. Consequently, researchers speculate that Miro1 may safeguard neurons by regulating intercellular mitochondrial transport to mitigate secondary injury post-cerebral hemorrhage (Li B. et al., 2021). Additionally, Miro1 serves as a substrate for the E3 ubiquitin ligase Parkin. The PINK1-Parkin pathway induces mitophagy by triggering mPTP opening (Song M. et al., 2015), which is crucial for eliminating damaged mitochondria subsequent to ICH occurrence (Kazlauskaite et al., 2014).

The microtubule-associated protein 1 light chain 3 (LC3) serves as a specific autophagy marker, appearing exclusively during the initiation of phagocytosis and exhibiting correlation with ROS expression (Tooze and Yoshimori, 2010). Studies have demonstrated that VDAC1, a crucial component of mPTP, co-localizes with LC3 following ICH. Positive staining for TUNEL and propidium iodide PI indicates that VDAC1 (mPTP) plays a pivotal role in inducing mitophagy, apoptosis, and necrosis. Inhibition of VDAC by VDAC 1 siRNA attenuates LC3 expression while upregulating ROS protein accumulation, histological manifestations of apoptosis and necrosis, as well as caspase-3 protein levels. Conversely, activation of autophagy through rapamycin significantly enhances LC3 expression while reducing ROS protein expression and abolishing histological manifestations of apoptosis and necrosis (Li et al., 2014). This finding offers a novel direction for future treatment strategies targeting secondary injury in ICH.

5.5 ICH and ferroptosis

As a form of iron-dependent programmed cell death, ferroptosis can be triggered by lipid peroxidation (Stockwell et al., 2017; Guo et al., 2020). However, both the iron and lipid pathways are implicated in the pathological process following ICH. Early studies have demonstrated that iron, a major component of hemoglobin, is highly neurotoxic and can be released during hematoma formation after ICH to initiate the Fenton reaction. The lipid pathway can induce the generation of various hydroxyl radicals, thereby promoting tissue oxidation, damaging cell membranes, DNA and proteins, ultimately leading to ferroptotic death of nerve cells (Djulbegovic and Uversky, 2019; He et al., 2020). Studies have revealed that ICH can result in diverse forms of neuronal cell death with ferroptosis accounting for over 80% of total neuronal deaths in ICH models; thus, highlighting its indispensable role in ICH pathology (Li Y. et al., 2021). During the acute phase of ICH, microglia and infiltrating macrophages phagocytose and decompose hemoglobin (Hu et al., 2016; Wan et al., 2019), resulting in substantial production of extracellular iron biliverdin and carbon monoxide (Zhou et al., 2020), which further facilitates intracerebral hematoma development (Chen et al., 2019). This process leads to mitochondrial damage causing excessive reactive oxygen species production (Lemasters, 2017) while disrupting glutamine metabolism leading to impaired antioxidant pathways and hydroxyl radical synthesis ultimately culminating in ferroptotic demise of nerve cells (Magtanong and Dixon, 2018; DeGregorio-Rocasolano et al., 2019).

Cheng et al. proposed a close association between mitochondria and ferroptosis following ICH. Their study revealed impaired mitochondrial function in both human and murine models of ICH, with specific inhibitors targeting mitochondria triggering and exacerbating neuronal ferroptosis, thereby worsening neurological deficits post-ICH (Cheng et al., 2023). Furthermore, this study identified the most prominent morphological characteristic of ferroptotic cells as alterations in mitochondrial morphology observed under electron microscopy (Dixon et al., 2012). Post-ferroptosis, there was a reduction in mitochondrial volume, increased concentration of mitochondrial membrane density, thinning or disappearance of mitochondrial cristae, and rupture of the outer mitochondrial membrane. These distinct changes make monitoring mitochondrial morphological alterations an effective method for assessing ferroptosis both in vitro and in vivo alongside measuring cellular levels of ROS and iron (Xie et al., 2016).

5.6 Neuronal axons and mPTP

A substantial body of evidence supports the essential role of mitochondrial functional integrity in neuronal survival following ICH (Diao et al., 2020). Mitochondrial dysfunction contributes to a cascade of secondary injuries after ICH, primarily due to their involvement in eliminating damaged mitochondria and repairing injured neurons (Zhou et al., 2017). Several studies have indicated that axonal injury after ICH is predominantly caused by mitochondrial dysfunction resulting from mPTP opening, which offers a novel avenue for investigating axonal degeneration post-ICH (Yang et al., 2022). Axonal injury mainly occurs in the extra-hematoma parenchyma following ICH and generally exhibits an increasing trend during the initial three days post-ICH (Wasserman and Schlichter, 2008). As the primary energy generators within neuronal cells, mitochondria play a crucial role in regulating nutrient transport and physiological functions of neuronal axons (Chang et al., 2006; Nikić et al., 2011). The survival of axonal and dendritic neuronal fibers is heavily reliant on mitochondrial transport, as mitochondria provide sufficient energy to distal synapses for normal ion channel, transporter, and synaptic transmission activities (Chang et al., 2006). Mitochondria are now considered fundamental components of axon elongation/regeneration and branching (Smith and Gallo, 2018). Mitochondrial damage not only reduces ATP release but also increases axonal degeneration (Smith and Gallo, 2018). The interaction between microtubules and actin filaments mediates axonal extension and guidance. Studies have found that microtubule replacement and mitochondrial dysfunction are the initial events of axonal injury after ICH. ATP deficiency caused by mitochondrial dysfunction and mPTP opening is a crucial initial link in axonal injury that directly leads to microtubule disassembly (Li et al., 2022).

6 Explore the treatment of ICH from the perspective of mPTP

The latest research has revealed that mitochondrial dysfunction and the subsequent opening of mPTP play a pivotal role in

the occurrence of secondary injury following ICH. Consequently, targeting mPTP as a means to enhance EBI represents a promising therapeutic avenue.

mPTP is implicated in various cellular death processes associated with ICH, and targeting specific components of mPTP may serve as an effective approach to enhance EBI. VDAC functions as a channel-forming protein situated in the outer mitochondrial membrane, facilitating the passage of metabolites and iron across the outer membrane (Hodge and Colombini, 1997; Colombini, 2012). Partial inhibition of VDAC hampers mitochondrial metabolism and diminishes mitochondrial membrane potential (Maldonado and Lemasters, 2012; Yao et al., 2018). The ferroptosis activator erastin can induce VDAC opening, facilitate mitochondrial iron uptake, elevate mitochondrial membrane potential, leading to depolarization of the mitochondria and subsequent induction of neuronal death through mitochondrial dysfunction. However, targeted application of VDAC inhibitors can reverse the occurrence of EBI (Ismael et al., 2020). Therefore, stable expression of VADC can be employed as an effective target for EBI treatment. mPTP is implicated in various cellular death processes associated with ICH, and targeting specific components of mPTP may serve as an effective approach to enhance EBI. VDAC functions as a channel-forming protein situated in the outer mitochondrial membrane, facilitating the passage of metabolites and iron across the outer membrane (Hodge and Colombini, 1997; Colombini, 2012). Partial inhibition of VDAC hampers mitochondrial metabolism and diminishes mitochondrial membrane potential (Hodge and Colombini, 1997; Colombini, 2012). The ferroptosis activator erastin can induce VDAC opening, facilitate mitochondrial iron uptake, elevate mitochondrial membrane potential, leading to depolarization of the mitochondria and subsequent induction of neuronal death through mitochondrial dysfunction. However, targeted application of VDAC inhibitors can reverse the occurrence of EBI (Hodge and Colombini, 1997; Colombini, 2012). Therefore, stable expression of VADC can be employed as an effective target for EBI treatment. Additionally, targeted modulation of CypD can confer a significant protective effect on the organism. It has been observed that endogenous SO2 can sulfonate the Cys104 residue of CypD, thereby impeding the opening mechanism of mPTP and effectively inhibiting apoptosis (Boyang et al., 2022).

The neuroprotective effect of cyclosporine A, which effectively attenuates the excessive generation of reactive oxygen species and enhances the activation of mitogen-activated protein kinase and protein kinase C, is unequivocal in both in vitro and preclinical models (Pignataro et al., 2008; Xuwen et al., 2008). Additionally, cyclosporin A also hinders the activation of mPTP (Norbert et al., 2016). It has been observed that its inhibition on mPTP opening is achieved by binding to CypD (Davis et al., 2010). The compound has the ability to bind to CyPD, effectively inhibit its isomerase activity, and displace it from mPTP (Shohei et al., 2018). Cyclosporine A exhibits potent activity in inhibiting mPTP opening at low concentrations (0.2–1.2 μM). Inhibited mPTP can reduce tissue expression levels of cytochrome c and AIF while improving secondary damage factors such as brain edema, cortical apoptosis, and neurobehavioral defects in a rat model with ICH (Xie et al., 2012). The neuroprotective drug Edaravone, similar to cyclosporin A, is believed by some scholars to exert its protective mechanism through modulation of mPTP. This modulation inhibits upstream ROS events and subsequently prevents mPTP opening, ultimately leading to neuronal survival (Shohei et al., 2018).

Studies have revealed that mitochondria accumulate high concentrations of melatonin (Leon et al., 2004), and the substantial synthesis of melatonin in mitochondria plays a crucial role in maintaining cellular energy metabolism and mitochondrial function (He et al., 2016). Apart from its antioxidant effects, melatonin exerts neuroprotective actions by modulating mPTP activity and cell death processes (Petrosillo et al., 2009; Espino et al., 2010), which has emerged as a novel approach for intervening in mPTP-related secondary damage following ICH. Initial observations in rat brain astrocytes demonstrated that melatonin appeared to inhibit mitochondrial ROS formation and prevent cell death by targeting Ca^{2+}-mediated mPT (Jou et al., 2010). Subsequent research found that when Ca^{2+} homeostasis was disrupted, melatonin effectively prevented mitochondrial depolarization and attenuated mPTP-induced neurotoxicity (Jou, 2011). Furthermore, the addition of melatonin to isolated brain mitochondria inhibited the opening of mPTP, suggesting its potential to impede mPTP-mediated mitochondrial dysfunction (Waseem et al., 2016). In animal models of ICH, melatonin mitigates mitochondrial dysfunction by upregulating antioxidants, thereby inhibiting the opening of mPTP to attenuate secondary damage following ICH and safeguard brain tissue (Wang Z. et al., 2018). Additionally, it has been observed that melatonin significantly diminishes mitochondrial swelling and membrane potential while enhancing mitochondrial respiration (Morciano et al., 2021). A recent mechanistic study demonstrated that antagonists of melatonin receptor 1 (MT1) nullify the inhibition of mPTP opening induced by melatonin, whereas MT1 agonists exert an opposite effect (Fang et al., 2020). However, the precise mechanism through which melatonin regulates mPTP remains unclear, with one possible molecular mechanism being the interaction between melatonin and CypD (Zhou et al., 2018).

The opening of mPTP will result in various forms of cell death, thereby inducing further mPTP opening and leading to more severe cellular damage. Abnormal mPTP opening can cause disruption in mitochondrial structure and function. Therefore, preserving the integrity of mitochondrial structure and function is crucial for preventing the progression of secondary damage following ICH. Adiponectin receptor 1 (AdipoR1) is widely expressed in neurons and its activation has a beneficial impact on damaged neurons (Song J. et al., 2015; Duan et al., 2016). Activation of AdipoR1 enhances AMP-activated protein kinase (AMPK) phosphorylation. As a downstream signaling molecule of AMPK, peroxisome proliferator-activated receptor-gamma coactivator-1 alpha (PGC1α) plays a pivotal role in regulating mitochondrial biosynthesis. In cases of ICH, PGC1α activation can stimulate the NRF1/TFAM axis (nuclear respiratory factor 1, NRF1; Mitochondrial transcription factor A, TFAM), thus improving mitochondrial DNA and ATP production (You et al., 2016). Furthermore, PGC1α activation also mitigates the collapse of mitochondrial membrane potential ($\Delta\psi m$) and reduces mitochondrial ROS production through a SIRT3-dependent mechanism (Zhang et al., 2016; Yu et al., 2017; Zheng et al., 2018). In conclusion, the Adipor1-AMPK-PGC1α axis may play a role in the progression of mitochondrial damage following ICH. Activation of AdipoR1 expression can mitigate secondary damage after ICH by preserving mitochondrial structure and function.

SS31, an antioxidant peptide that targets mitochondria, has demonstrated beneficial effects in various diseases due to its potent antioxidant and neuroprotective properties. Studies have shown that SS31 ameliorates oxidative damage induced by ICH by reducing reactive oxygen species generation, alleviating lipid peroxidation, and enhancing antioxidant enzyme activity. Additionally, SS31 significantly attenuates neurological deficits, brain edema, neuronal apoptosis, and blood-brain barrier disruption after ICH. The specific mechanism involves activating the Nrf2 signaling pathway, increasing mtDNA copy number, and reversing mitochondrial dysfunction (Zhou et al., 2023). Previous studies have indicated that astaxanthin improves mitochondrial function in SH-SY5Y neuronal cells exposed to 1-methyl-4-phenylpyridine and suggests its potential as a therapeutic agent for neurodegenerative diseases (Lee et al., 2011). In an ICH rat model treated with astaxanthin in the cortex region, it was observed that Cyt C release from mitochondria was reduced along with down-regulation of Bax/Bcl-2 ratio and inhibition of caspase-3 activity. These changes in apoptosis-related indicators support the role of astaxanthin in improving mitochondrial function after ICH (Wang et al., 2019).

7 Summary

Mitochondria, being a crucial organelle in the body, actively participate in various cellular processes and are also exposed to diverse biochemical stimuli. Detrimental biochemical stimuli alter the cellular environment where mitochondria reside and induce a permeability transition in these organelles. With further research advancements, scholars have discovered that the transition of mitochondrial permeability is triggered by the opening of mPTP. The specific composition of mPTP remains controversial; however, several conformational models have been proposed by scholars including CypD, ANT, VDAC, PiC, ATP synthase, and SPG7 as potential candidates for mPTP composition. Studies have revealed that the opening of mPTP disrupts mitochondrial morphology and function while exacerbating cell damage. This mechanism may be associated with pathological processes such as oxidative stress, apoptosis, cell necrosis, autophagy, ferroptosis among others – all commonly observed after ICH. Therefore, targeting mPTP represents a promising treatment approach for improving secondary injury following ICH. However, current research primarily exists in animal experiments with limited clinical investigations conducted thus far. In future studies on both the composition of mPTP and its precise involvement in secondary injury after ICH are required to provide clearer directions for ICH treatment.

Author contributions

JC: Writing—original draft. J-YL: Writing—review and editing. WZ: Investigation, Writing—review and editing.

Funding

The author(s) declare financial support was received for the research, authorship, and/or publication of the article. This study was supported by the National Natural Science Foundation of China: Study on the mechanism of nerve remodeling in acute cerebral hemorrhage treated with acupuncture (30772840).

Acknowledgments

We express gratitude for the help of graphs by BioRender.com and the editors who diligently review this manuscript.

Conflict of interest

The authors declare that the research was conducted in the absence of any commercial or financial relationships that could be construed as a potential conflict of interest.

Publisher's note

Supplementary material

The Supplementary Material for this article can be found online at: https://www.frontiersin.org/articles/10.3389/fnmol.2024.1423132/full#supplementary-material

References

Abu-Hamad, S., Arbel, N., Calo, D., Arzoine, L., Israelson, A., Keinan, N., et al. (2009). The VDAC1 N-terminus is essential both for apoptosis and the protective effect of anti-apoptotic proteins. *J. Cell Sci.* 122, 1906–1916. doi: 10.1242/jcs.040188

Azarashvili, T., Krestinina, O., Baburina, Y., Odinokova, I., Akatov, V., Beletsky, I., et al. (2016). Effect of the CRAC peptide, VLNYYVW, on mPTP opening in rat brain and liver mitochondria. *Int. J. Mol. Sci.* 17:2096. doi: 10.3390/ijms17122096

Baechler, B. L., Bloemberg, D., and Quadrilatero, J. (2019). Mitophagy regulates mitochondrial network signaling, oxidative stress, and apoptosis during myoblast differentiation. *Autophagy* 15, 1606–1619. doi: 10.1080/15548627.2019.1591672

Balami, J. S., and Buchan, A. M. (2012). Complications of intracerebral haemorrhage. *Lancet Neurol.* 11, 101–118. doi: 10.1016/s1474-4422(11)70264-2

Banasiak, K. J., Xia, Y., and Haddad, G. G. (2000). Mechanisms underlying hypoxia-induced neuronal apoptosis. *Prog. Neurobiol.* 62, 215–249. doi: 10.1016/s0301-0082(00)00011-3

Basit, F., van Oppen, L. M., Schöckel, L., Bossenbroek, H. M., van Emst-de Vries, S. E., Hermeling, J. C., et al. (2017). Mitochondrial complex I inhibition triggers a mitophagy-dependent ROS increase leading to necroptosis and ferroptosis in melanoma cells. *Cell Death Dis.* 8:e2716. doi: 10.1038/cddis.2017.133

Batoko, H., Dagdas, Y., Baluska, F., and Sirko, A. (2017). Understanding and exploiting autophagy signaling in plants. *Essays Biochem.* 61, 675–685. doi: 10.1042/ebc20170034

Baumgartner, H. K., Gerasimenko, J. V., Thorne, C., Ferdek, P., Pozzan, T., Tepikin, A. V., et al. (2009). Calcium elevation in mitochondria is the main Ca2+ requirement for mitochondrial permeability transition pore (mPTP) opening. *J. Biol. Chem.* 284, 20796–20803. doi: 10.1074/jbc.M109.025353

Bernardi, P., and Di Lisa, F. (2015). The mitochondrial permeability transition pore: Molecular nature and role as a target in cardioprotection. *J. Mol. Cell Cardiol.* 78, 100–106. doi: 10.1016/j.yjmcc.2014.09.023

Bernardi, P., and Forte, M. (2015). Commentary: SPG7 is an essential and conserved component of the mitochondrial permeability transition pore. *Front. Physiol.* 6:320. doi: 10.3389/fphys.2015.00320

Bernardi, P., and von Stockum, S. (2012). The permeability transition pore as a Ca(2+) release channel: New answers to an old question. *Cell Calcium* 52, 22–27. doi: 10.1016/j.ceca.2012.03.004

Bernardi, P., Rasola, A., Forte, M., and Lippe, G. (2015). The mitochondrial permeability transition pore: Channel formation by F-ATP synthase, integration in signal transduction, and role in pathophysiology. *Physiol. Rev.* 95, 1111–1155. doi: 10.1152/physrev.00001.2015

Bonora, M., Bononi, A., De Marchi, E., Giorgi, C., Lebiedzinska, M., Marchi, S., et al. (2013). Role of the c subunit of the FO ATP synthase in mitochondrial permeability transition. *Cell Cycle* 12, 674–683. doi: 10.4161/cc.23599

Bonora, M., Giorgi, C., and Pinton, P. (2022). Molecular mechanisms and consequences of mitochondrial permeability transition. *Nat. Rev. Mol. Cell Biol.* 23, 266–285. doi: 10.1038/s41580-021-00433-y

Boyang, L., Hanlin, P., Bingquan, Q., Lulu, Z., Mei, G., Dingfang, B., et al. (2022). Sulphenylation of CypD at cysteine 104: A novel mechanism by which SO2 inhibits cardiomyocyte apoptosis. *Front. Cell Dev. Biol.* 9:784799.

Boyenle, I. D., Oyedele, A. K., Ogunlana, A. T., Adeyemo, A. F., Oyelere, F. S., Akinola, O. B., et al. (2022). Targeting the mitochondrial permeability transition pore for drug discovery: Challenges and opportunities. *Mitochondrion* 63, 57–71. doi: 10.1016/j.mito.2022.01.006

Boyman, L., Coleman, A. K., Zhao, G., Wescott, A. P., Joca, H. C., Greiser, B. M., et al. (2019). Dynamics of the mitochondrial permeability transition pore: Transient and permanent opening events. *Arch. Biochem. Biophys.* 666, 31–39. doi: 10.1016/j.abb.2019.03.016

Brand, M. D., Pakay, J. L., Ocloo, A., Kokoszka, J., Wallace, D. C., Brookes, P. S., et al. (2005). The basal proton conductance of mitochondria depends on adenine nucleotide translocase content. *Biochem. J.* 392, 353–362. doi: 10.1042/bj20050890

Briston, T., Roberts, M., Lewis, S., Powney, B., Szabadkai, G., and Duchen, M. R. (2017). Mitochondrial permeability transition pore: Sensitivity to opening and mechanistic dependence on substrate availability. *Sci. Rep.* 7:10492. doi: 10.1038/s41598-017-10673-8

Cadenas, S. (2018). ROS and redox signaling in myocardial ischemia-reperfusion injury and cardioprotection. *Free Radic. Biol. Med.* 117, 76–89. doi: 10.1016/j.freeradbiomed.2018.01.024

Cahill, J., and Zhang, J. H. (2009). Subarachnoid hemorrhage: Is it time for a new direction? *Stroke* 40, S86–S87. doi: 10.1161/strokeaha.108.533315

Casari, G., De Fusco, M., Ciarmatori, S., Zeviani, M., Mora, M., Fernandez, P., et al. (1998). Spastic paraplegia and OXPHOS impairment caused by mutations in paraplegin, a nuclear-encoded mitochondrial metalloprotease. *Cell* 93, 973–983. doi: 10.1016/s0092-8674(00)81203-9

Chakraborti, T., Das, S., Mondal, M., Roychoudhury, S., and Chakraborti, S. (1999). Oxidant, mitochondria and calcium: An overview. *Cell Signal.* 11, 77–85. doi: 10.1016/s0898-6568(98)00025-4

Chang, D. T., Honick, A. S., and Reynolds, I. J. (2006). Mitochondrial trafficking to synapses in cultured primary cortical neurons. *J. Neurosci.* 26, 7035–7045. doi: 10.1523/jneurosci.1012-06.2006

Chang, X., Lochner, A., Wang, H. H., Wang, S., Zhu, H., Ren, J., et al. (2021). Coronary microvascular injury in myocardial infarction: Perception and knowledge for mitochondrial quality control. *Theranostics* 11, 6766–6785. doi: 10.7150/thno.60143

Chao, J. R., Parganas, E., Boyd, K., Hong, C. Y., Opferman, J. T., and Ihle, J. N. (2008). Hax1-mediated processing of HtrA2 by Parl allows survival of lymphocytes and neurons. *Nature* 452, 98–102. doi: 10.1038/nature06604

Chen, B., Chen, Z., Liu, M., Gao, X., Cheng, Y., Wei, Y., et al. (2019). Inhibition of neuronal ferroptosis in the acute phase of intracerebral hemorrhage shows long-term cerebroprotective effects. *Brain Res. Bull.* 153, 122–132. doi: 10.1016/j.brainresbull.2019.08.013

Chen, S., Peng, J., Sherchan, P., Ma, Y., Xiang, S., Yan, F., et al. (2020). TREM2 activation attenuates neuroinflammation and neuronal apoptosis via PI3K/Akt pathway after intracerebral hemorrhage in mice. *J. Neuroinflamm.* 17:168. doi: 10.1186/s12974-020-01853-x

Chen, X., Comish, P. B., Tang, D., and Kang, R. (2021). Characteristics and biomarkers of ferroptosis. *Front. Cell. Dev. Biol.* 9:637162. doi: 10.3389/fcell.2021.637162

Cheng, Y., Liu, M., Tang, H., Chen, B., Yang, G., Zhao, W., et al. (2021). iTRAQ-Based Quantitative Proteomics Indicated Nrf2/OPTN-Mediated Mitophagy Inhibits NLRP3 Inflammasome Activation after Intracerebral Hemorrhage. *Oxid. Med. Cell. Longev.* 2021:6630281. doi: 10.1155/2021/6630281

Cheng, Y., Zhang, Z., Tang, H., Chen, B., Cai, Y., Wei, Y., et al. (2023). Mitochondrial inhibitor rotenone triggers and enhances neuronal ferroptosis following intracerebral hemorrhage. *ACS Chem. Neurosci.* 14, 1071–1079. doi: 10.1021/acschemneuro.2c00308

Chipuk, J. E., Moldoveanu, T., Llambi, F., Parsons, M. J., and Green, D. R. (2010). The BCL-2 family reunion. *Mol. Cell* 37, 299–310. doi: 10.1016/j.molcel.2010.01.025

Colombini, M. (2012). VDAC structure, selectivity, and dynamics. *Biochim. Biophys. Acta* 1818, 1457–1465. doi: 10.1016/j.bbamem.2011.12.026

Conrad, M., Angeli, J. P., Vandenabeele, P., and Stockwell, B. R. (2016). Regulated necrosis: Disease relevance and therapeutic opportunities. *Nat. Rev. Drug Discov.* 15, 348–366. doi: 10.1038/nrd.2015.6

Covian, R., and Balaban, R. S. (2012). Cardiac mitochondrial matrix and respiratory complex protein phosphorylation. *Am J Physiol. Heart Circ. Physiol.* 303, H940–H966. doi: 10.1152/ajpheart.00077.2012

Crompton, M., Costi, A., and Hayat, L. (1987). Evidence for the presence of a reversible Ca2+-dependent pore activated by oxidative stress in heart mitochondria. *Biochem. J.* 245, 915–918. doi: 10.1042/bj2450915

Crompton, M., Ellinger, H., and Costi, A. (1988). Inhibition by cyclosporin A of a Ca2+-dependent pore in heart mitochondria activated by inorganic phosphate and oxidative stress. *Biochem. J.* 255, 357–360.

Crompton, M., Virji, S., and Ward, J. M. (1998). Cyclophilin-D binds strongly to complexes of the voltage-dependent anion channel and the adenine nucleotide translocase to form the permeability transition pore. *Eur. J. Biochem.* 258, 729–735. doi: 10.1046/j.1432-1327.1998.2580729.x

Davis, T. L., Walker, J. R., Campagna-Slater, V., Finerty, P. J., Paramanathan, R., Bernstein, G., et al. (2010). Structural and biochemical characterization of the human cyclophilin family of peptidyl-prolyl isomerases. *PLoS Biol.* 8:e1000439. doi: 10.1371/journal.pbio.1000439

de Oliveira Manoel, A. L., Goffi, A., Zampieri, F. G., Turkel-Parrella, D., Duggal, A., Marotta, T. R., et al. (2016). The critical care management of spontaneous intracranial hemorrhage: A contemporary review. *Crit. Care* 20:272. doi: 10.1186/s13054-016-1432-0

DeGregorio-Rocasolano, N., Martí-Sistac, O., and Gasull, T. (2019). Deciphering the iron side of stroke: Neurodegeneration at the crossroads between iron dyshomeostasis, excitotoxicity, and ferroptosis. *Front. Neurosci.* 13:85. doi: 10.3389/fnins.2019.00085

Diao, X., Zhou, Z., Xiang, W., Jiang, Y., Tian, N., Tang, X., et al. (2020). Glutathione alleviates acute intracerebral hemorrhage injury via reversing mitochondrial dysfunction. *Brain Res.* 1727:146514. doi: 10.1016/j.brainres.2019.146514

Dixon, S. J., Lemberg, K. M., Lamprecht, M. R., Skouta, R., Zaitsev, E. M., Gleason, C. E., et al. (2012). Ferroptosis: An iron-dependent form of nonapoptotic cell death. *Cell* 149, 1060–1072. doi: 10.1016/j.cell.2012.03.042

Djulbegovic, M. B., and Uversky, V. N. (2019). Ferroptosis - An iron- and disorder-dependent programmed cell death. *Int. J. Biol. Macromol.* 135, 1052–1069. doi: 10.1016/j.ijbiomac.2019.05.221

Dorn, G. W. II, Vega, R. B., and Kelly, D. P. (2015). Mitochondrial biogenesis and dynamics in the developing and diseased heart. *Genes Dev.* 29, 1981–1991. doi: 10.1101/gad.269894.115

Du, H., Guo, L., Fang, F., Chen, D., Sosunov, A. A., McKhann, G. M., et al. (2008). Cyclophilin D deficiency attenuates mitochondrial and neuronal perturbation and ameliorates learning and memory in Alzheimer's disease. *Nat. Med.* 14, 1097–1105. doi: 10.1038/nm.1868

Du, J., Zhou, Y., Li, Y., Xia, J., Chen, Y., Chen, S., et al. (2020). Identification of Frataxin as a regulator of ferroptosis. *Redox Biol.* 32:101483. doi: 10.1016/j.redox.2020.101483

Duan, J., Yin, Y., Cui, J., Yan, J., Zhu, Y., Guan, Y., et al. (2016). Chikusetsu Saponin IVa ameliorates cerebral ischemia reperfusion injury in diabetic mice via adiponectin-mediated AMPK/GSK-3β pathway in vivo and in vitro. *Mol. Neurobiol.* 53, 728–743. doi: 10.1007/s12035-014-9033-x

Duszyński, J., Bogucka, K., Letko, G., Küster, U., Kunz, W., and Wojtczak, L. (1981). Relationship between the energy cost of ATP transport and ATP synthesis

in mitochondria. *Biochim. Biophys. Acta* 637, 217–223. doi: 10.1016/0005-2728(81)90160-2

Ernster, L., and Schatz, G. (1981). Mitochondria: A historical review. *J. Cell Biol.* 91, 227s–255s. doi: 10.1083/jcb.91.3.227s

Espino, J., Bejarano, I., Redondo, P. C., Rosado, J. A., Barriga, C., Reiter, R. J., et al. (2010). Melatonin reduces apoptosis induced by calcium signaling in human leukocytes: Evidence for the involvement of mitochondria and Bax activation. *J. Membr. Biol.* 233, 105–118. doi: 10.1007/s00232-010-9230-0

Fang, E. F., Scheibye-Knudsen, M., Chua, K. F., Mattson, M. P., Croteau, D. L., and Bohr, V. A. (2016). Nuclear DNA damage signalling to mitochondria in ageing. *Nat. Rev. Mol. Cell Biol.* 17, 308–321. doi: 10.1038/nrm.2016.14

Fang, Y., Zhao, C., Xiang, H., Jia, G., and Zhong, R. (2020). Melatonin improves cryopreservation of ram sperm by inhibiting mitochondrial permeability transition pore opening. *Reprod. Domest Anim.* 55, 1240–1249. doi: 10.1111/rda.13771

Feigin, V. L., Lawes, C. M., Bennett, D. A., Barker-Collo, S. L., and Parag, V. (2009). Worldwide stroke incidence and early case fatality reported in 56 population-based studies: A systematic review. *Lancet Neurol.* 8, 355–369. doi: 10.1016/s1474-4422(09)70025-0

Fischer, G., Wittmann-Liebold, B., Lang, K., Kiefhaber, T., and Schmid, F. X. (1989). Cyclophilin and peptidyl-prolyl cis-trans isomerase are probably identical proteins. *Nature* 337, 476–478. doi: 10.1038/337476a0

Flippo, K. H., and Strack, S. (2017). Mitochondrial dynamics in neuronal injury, development and plasticity. *J. Cell Sci.* 130, 671–681. doi: 10.1242/jcs.171017

Friedmann Angeli, J. P., Schneider, M., Proneth, B., Tyurina, Y. Y., Tyurin, V. A., Hammond, V. J., et al. (2014). Inactivation of the ferroptosis regulator Gpx4 triggers acute renal failure in mice. *Nat. Cell Biol.* 16, 1180–1191. doi: 10.1038/ncb3064

Fujii, M., Yan, J., Rolland, W. B., Soejima, Y., Caner, B., and Zhang, J. H. (2013). Early brain injury, an evolving frontier in subarachnoid hemorrhage research. *Transl. Stroke Res.* 4, 432–446. doi: 10.1007/s12975-013-0257-2

Galluzzi, L., Pietrocola, F., Bravo-San Pedro, J. M., Amaravadi, R. K., Baehrecke, E. H., Cecconi, F., et al. (2015). Autophagy in malignant transformation and cancer progression. *Embo J.* 34, 856–880. doi: 10.15252/embj.201490784

Galluzzi, L., Vitale, I., Aaronson, S. A., Abrams, J. M., Adam, D., Agostinis, P., et al. (2018). Molecular mechanisms of cell death: Recommendations of the nomenclature committee on cell death 2018. *Cell Death Differ.* 25, 486–541. doi: 10.1038/s41418-017-0012-4

Ganguly, U., Singh, S., Bir, A., Ghosh, A., Chakrabarti, S. S., Saini, R. V., et al. (2024). Alpha-synuclein interaction with mitochondria is the final mechanism of ferroptotic death induced by erastin in SH-SY5Y cells. *Free Rad. Res.* 58, 11–12.

Gao, F., Voncken, F., and Colasante, C. (2020). The mitochondrial phosphate carrier TbMCP11 is essential for mitochondrial function in the procyclic form of *Trypanosoma brucei*. *Mol. Biochem. Parasitol.* 237:111275. doi: 10.1016/j.molbiopara.2020.111275

Gareev, I., Beylerli, O., Liang, Y., Lu, E., Ilyasova, T., Sufianov, A., et al. (2023). The role of mitochondria-targeting miRNAs in intracerebral hemorrhage. *Curr. Neuropharmacol.* 21, 1065–1080. doi: 10.2174/1570159x20666220507021445

Giacomello, M., Pyakurel, A., Glytsou, C., and Scorrano, L. (2020). The cell biology of mitochondrial membrane dynamics. *Nat. Rev. Mol. Cell. Biol.* 21, 204–224. doi: 10.1038/s41580-020-0210-7

Giorgi, C., Marchi, S., Simoes, I. C. M., Ren, Z., Morciano, G., Perrone, M., et al. (2018). Mitochondria and reactive oxygen species in aging and age-related diseases. *Int. Rev. Cell Mol. Biol.* 340, 209–344. doi: 10.1016/bs.ircmb.2018.05.006

Giorgio, V., von Stockum, S., Antoniel, M., Fabbro, A., Fogolari, F., Forte, M., et al. (2013). Dimers of mitochondrial ATP synthase form the permeability transition pore. *Proc. Natl. Acad. Sci. U.S.A.* 110, 5887–5892. doi: 10.1073/pnas.1217823110

Golstein, P., and Kroemer, G. (2007). Cell death by necrosis: Towards a molecular definition. *Trends Biochem. Sci.* 32, 37–43. doi: 10.1016/j.tibs.2006.11.001

Gomes, L. C., and Scorrano, L. (2013). Mitochondrial morphology in mitophagy and macroautophagy. *Biochim. Biophys. Acta* 1833, 205–212. doi: 10.1016/j.bbamcr.2012.02.012

Grootaert, M. O. J., Moulis, M., Roth, L., Martinet, W., Vindis, C., Bennett, M. R., et al. (2018). Vascular smooth muscle cell death, autophagy and senescence in atherosclerosis. *Cardiovasc. Res.* 114, 622–634. doi: 10.1093/cvr/cvy007

Guo, X., Ma, L., Li, H., Qi, X., Wei, Y., Duan, Z., et al. (2020). Brainstem iron overload and injury in a rat model of brainstem hemorrhage. *J. Stroke Cerebrovasc. Dis.* 29:104956. doi: 10.1016/j.jstrokecerebrovasdis.2020.104956

Gutiérrez-Aguilar, M., and Baines, C. P. (2015). Structural mechanisms of cyclophilin D-dependent control of the mitochondrial permeability transition pore. *Biochim. Biophys. Acta* 1850, 2041–2047. doi: 10.1016/j.bbagen.2014.11.009

Halestrap, A. P. (1991). Calcium-dependent opening of a non-specific pore in the mitochondrial inner membrane is inhibited at pH values below 7. Implications for the protective effect of low pH against chemical and hypoxic cell damage. *Biochem. J.* 278, 715–719. doi: 10.1042/bj2780715

Halestrap, A. P. (2009). What is the mitochondrial permeability transition pore? *J. Mol. Cell Cardiol.* 46, 821–831. doi: 10.1016/j.yjmcc.2009.02.021

Halestrap, A. P., and Davidson, A. M. (1990). Inhibition of Ca2(+)-induced large-amplitude swelling of liver and heart mitochondria by cyclosporin is probably caused by the inhibitor binding to mitochondrial-matrix peptidyl-prolyl cis-trans isomerase and preventing it interacting with the adenine nucleotide translocase. *Biochem. J.* 268, 153–160. doi: 10.1042/bj2680153

Han, N., Ding, S. J., Wu, T., and Zhu, Y. L. (2008). Correlation of free radical level and apoptosis after intracerebral hemorrhage in rats. *Neurosci. Bull.* 24, 351–358. doi: 10.1007/s12264-008-0711-4

Hasegawa, Y., Suzuki, H., Sozen, T., Altay, O., and Zhang, J. H. (2011). Apoptotic mechanisms for neuronal cells in early brain injury after subarachnoid hemorrhage. *Acta Neurochir. Suppl.* 110, 43–48. doi: 10.1007/978-3-7091-0353-1_8

He, L., and Lemasters, J. J. (2002). Regulated and unregulated mitochondrial permeability transition pores: a new paradigm of pore structure and function? *FEBS Lett.* 512, 1–7. doi: 10.1016/s0014-5793(01)03314-2

He, C., Wang, J., Zhang, Z., Yang, M., Li, Y., Tian, X., et al. (2016). Mitochondria synthesize melatonin to ameliorate its function and improve mice oocyte's quality under in vitro conditions. *Int. J. Mol. Sci.* 17:939. doi: 10.3390/ijms17060939

He, P., Hua, H., Tian, W., Zhu, H., Liu, Y., and Xu, X. (2020). Holly (*Ilex latifolia* Thunb.) polyphenols extracts alleviate hepatic damage by regulating ferroptosis following diquat challenge in a piglet model. *Front. Nutr.* 7:604328. doi: 10.3389/fnut.2020.604328

Hodge, T., and Colombini, M. (1997). Regulation of metabolite flux through voltage-gating of VDAC channels. *J. Membr. Biol.* 157, 271–279. doi: 10.1007/s002329900235

Hu, T., Zou, H. X., Le, S. Y., Wang, Y. R., Qiao, Y. M., Yuan, Y., et al. (2023). Tanshinone IIA confers protection against myocardial ischemia/reperfusion injury by inhibiting ferroptosis and apoptosis via VDAC1. *Int. J. Mol. Med.* 52:109. doi: 10.3892/ijmm.2023.5312

Hu, X., Tao, C., Gan, Q., Zheng, J., Li, H., and You, C. (2016). Oxidative stress in intracerebral hemorrhage: Sources, mechanisms, and therapeutic targets. *Oxid. Med. Cell Longev.* 2016:3215391. doi: 10.1155/2016/3215391

Huang, S., Van Aken, O., Schwarzländer, M., Belt, K., and Millar, A. H. (2016). The roles of mitochondrial reactive oxygen species in cellular signaling and stress response in plants. *Plant Physiol.* 171, 1551–1559. doi: 10.1104/pp.16.00166

Hüttemann, M., Helling, S., Sanderson, T. H., Sinkler, C., Samavati, L., Mahapatra, G., et al. (2012). Regulation of mitochondrial respiration and apoptosis through cell signaling: Cytochrome c oxidase and cytochrome c in ischemia/reperfusion injury and inflammation. *Biochim. Biophys. Acta* 1817, 598–609. doi: 10.1016/j.bbabio.2011.07.001

Ismael, S., Nasoohi, S., Yoo, A., Ahmed, H. A., and Ishrat, T. (2020). Tissue plasminogen activator promotes TXNIP-NLRP3 inflammasome activation after hyperglycemic stroke in mice. *Mol. Neurobiol.* 57, 2495–2508. doi: 10.1007/s12035-020-01893-7

Izzo, V., Bravo-San Pedro, J. M., Sica, V., Kroemer, G., and Galluzzi, L. (2016). Mitochondrial permeability transition: New findings and persisting uncertainties. *Trends Cell Biol.* 26, 655–667. doi: 10.1016/j.tcb.2016.04.006

Jelinek, A., Heyder, L., Daude, M., Plessner, M., Krippner, S., Grosse, R., et al. (2018). Mitochondrial rescue prevents glutathione peroxidase-dependent ferroptosis. *Free Radic. Biol. Med.* 117, 45–57. doi: 10.1016/j.freeradbiomed.2018.01.019

Jia, K., and Du, H. (2021). Mitochondrial permeability transition: A pore intertwines brain aging and Alzheimer's disease. *Cells* 10:649. doi: 10.3390/cells10030649

Jou, M. J. (2011). Melatonin preserves the transient mitochondrial permeability transition for protection during mitochondrial Ca(2+) stress in astrocyte. *J. Pineal Res.* 50, 427–435. doi: 10.1111/j.1600-079X.2011.00861.x

Jou, M. J., Peng, T. I., Hsu, L. F., Jou, S. B., Reiter, R. J., Yang, C. M., et al. (2010). Visualization of melatonin's multiple mitochondrial levels of protection against mitochondrial Ca(2+)-mediated permeability transition and beyond in rat brain astrocytes. *J. Pineal Res.* 48, 20–38. doi: 10.1111/j.1600-079X.2009.00721.x

Kanno, T., Sato, E. E., Muranaka, S., Fujita, H., Fujiwara, T., Utsumi, T., et al. (2004). Oxidative stress underlies the mechanism for Ca(2+)-induced permeability transition of mitochondria. *Free Radic. Res.* 38, 27–35. doi: 10.1080/10715760310001626266

Katsu, M., Niizuma, K., Yoshioka, H., Okami, N., Sakata, H., and Chan, P. H. (2010). Hemoglobin-induced oxidative stress contributes to matrix metalloproteinase activation and blood-brain barrier dysfunction in vivo. *J. Cereb. Blood Flow Metab.* 30, 1939–1950. doi: 10.1038/jcbfm.2010.45

Kazlauskaite, A., Kelly, V., Johnson, C., Baillie, C., Hastie, C. J., Peggie, M., et al. (2014). Phosphorylation of Parkin at Serine65 is essential for activation: Elaboration of a Miro1 substrate-based assay of Parkin E3 ligase activity. *Open Biol.* 4:130213. doi: 10.1098/rsob.130213

Keinan, N., Tyomkin, D., and Shoshan-Barmatz, V. (2010). Oligomerization of the mitochondrial protein voltage-dependent anion channel is coupled to the induction of apoptosis. *Mol. Cell Biol.* 30, 5698–5709. doi: 10.1128/mcb.00165-10

Khan, A., Kuriachan, G., and Mahalakshmi, R. (2021). Cellular interactome of mitochondrial voltage-dependent anion channels: Oligomerization and channel

(Mis)Regulation. *ACS Chem. Neurosci.* 12, 3497–3515. doi: 10.1021/acschemneuro.1c00429

Klutho, P. J., Dashek, R. J., Song, L., and Baines, C. P. (2020). Genetic manipulation of SPG7 or NipSnap2 does not affect mitochondrial permeability transition. *Cell Death Discov.* 6:5. doi: 10.1038/s41420-020-0239-6

Koppen, M., Metodiev, M. D., Casari, G., Rugarli, E. I., and Langer, T. (2007). Variable and tissue-specific subunit composition of mitochondrial m-AAA protease complexes linked to hereditary spastic paraplegia. *Mol. Cell Biol.* 27, 758–767. doi: 10.1128/mcb.01470-06

Korshunov, S. S., Skulachev, V. P., and Starkov, A. A. (1997). High protonic potential actuates a mechanism of production of reactive oxygen species in mitochondria. *FEBS Lett.* 416, 15–18. doi: 10.1016/s0014-5793(97)01159-9

Kowaltowski, A. J., Castilho, R. F., and Vercesi, A. E. (2001). Mitochondrial permeability transition and oxidative stress. *FEBS Lett.* 495, 12–15. doi: 10.1016/s0014-5793(01)02316-x

Kung, G., Konstantinidis, K., and Kitsis, R. N. (2011). Programmed necrosis, not apoptosis, in the heart. *Circ. Res.* 108, 1017–1036. doi: 10.1161/circresaha.110.225730

Kwong, J. Q., and Molkentin, J. D. (2015). Physiological and pathological roles of the mitochondrial permeability transition pore in the heart. *Cell Metab.* 21, 206–214. doi: 10.1016/j.cmet.2014.12.001

Lam, C. K., Zhao, W., Liu, G. S., Cai, W. F., Gardner, G., Adly, G., et al. (2015). HAX-1 regulates cyclophilin-D levels and mitochondria permeability transition pore in the heart. *Proc. Natl. Acad. Sci. U.S.A.* 112, E6466–E6475. doi: 10.1073/pnas.1508760112

Lam, M. P., Lau, E., Liem, D. A., and Ping, P. (2013). Cyclophilin D and acetylation: A new link in cardiac signaling. *Circ. Res.* 113, 1268–1269. doi: 10.1161/circresaha.113.302687

Lauzier, D. C., Jayaraman, K., Yuan, J. Y., Diwan, D., Vellimana, A. K., Osbun, J. W., et al. (2023). Early brain injury after subarachnoid hemorrhage: Incidence and mechanisms. *Stroke* 54, 1426–1440. doi: 10.1161/strokeaha.122.040072

Lee, D. H., Kim, C. S., and Lee, Y. J. (2011). Astaxanthin protects against MPTP/MPP+-induced mitochondrial dysfunction and ROS production in vivo and in vitro. *Food Chem. Toxicol.* 49, 271–280. doi: 10.1016/j.fct.2010.10.029

Lemasters, J. J. (2007). Modulation of mitochondrial membrane permeability in pathogenesis, autophagy and control of metabolism. *J. Gastroenterol. Hepatol.* 22, S31–S37. doi: 10.1111/j.1440-1746.2006.04643.x

Lemasters, J. J. (2017). Evolution of Voltage-dependent anion channel function: From molecular sieve to governator to actuator of ferroptosis. *Front. Oncol.* 7:303. doi: 10.3389/fonc.2017.00303

Leon, J., Acuña-Castroviejo, D., Sainz, R. M., Mayo, J. C., Tan, D. X., and Reiter, R. J. (2004). Melatonin and mitochondrial function. *Life Sci.* 75, 765–790. doi: 10.1016/j.lfs.2004.03.003

Leung, A. W., and Halestrap, A. P. (2008). Recent progress in elucidating the molecular mechanism of the mitochondrial permeability transition pore. *Biochim. Biophys. Acta* 1777, 946–952. doi: 10.1016/j.bbabio.2008.03.009

Leung, A. W., Varanyuwatana, P., and Halestrap, A. P. (2008). The mitochondrial phosphate carrier interacts with cyclophilin D and may play a key role in the permeability transition. *J. Biol. Chem.* 283, 26312–26323. doi: 10.1074/jbc.M805235200

Li, B., Zhang, Y., Li, H., Shen, H., Wang, Y., Li, X., et al. (2021). Miro1 regulates neuronal mitochondrial transport and distribution to alleviate neuronal damage in secondary brain injury after intracerebral hemorrhage in rats. *Cell Mol. Neurobiol.* 41, 795–812. doi: 10.1007/s10571-020-00887-2

Li, Y., Liu, Y., Wu, P., Tian, Y., Liu, B., Wang, J., et al. (2021). Inhibition of ferroptosis alleviates early brain injury after subarachnoid hemorrhage in vitro and in vivo via reduction of lipid peroxidation. *Cell Mol. Neurobiol.* 41, 263–278. doi: 10.1007/s10571-020-00850-1

Li, J., Lu, J., Mi, Y., Shi, Z., Chen, C., Riley, J., et al. (2014). Voltage-dependent anion channels (VDACs) promote mitophagy to protect neuron from death in an early brain injury following a subarachnoid hemorrhage in rats. *Brain Res.* 1573, 74–83. doi: 10.1016/j.brainres.2014.05.021

Li, Y., Liu, H., Tian, C., An, N., Song, K., Wei, Y., et al. (2022). Targeting the multifaceted roles of mitochondria in intracerebral hemorrhage and therapeutic prospects. *Biomed. Pharmacother.* 148:112749. doi: 10.1016/j.biopha.2022.112749

Lin, M. T., and Beal, M. F. (2006). Mitochondrial dysfunction and oxidative stress in neurodegenerative diseases. *Nature* 443, 787–795. doi: 10.1038/nature05292

Liu, E., Sun, H., Wu, J., and Kuang, Y. (2020). MiR-92b-3p regulates oxygen and glucose deprivation-reperfusion-mediated apoptosis and inflammation by targeting TRAF3 in PC12 cells. *Exp. Physiol.* 105, 1792–1801. doi: 10.1113/ep088708

Liu, X. C., Wu, C. Z., Hu, X. F., Wang, T. L., Jin, X. P., Ke, S. F., et al. (2020). Gastrodin attenuates neuronal apoptosis and neurological deficits after experimental intracerebral hemorrhage. *J. Stroke Cerebrovasc. Dis.* 29:104483. doi: 10.1016/j.jstrokecerebrovasdis.2019.104483

Liu, J., Liu, W., Lu, Y., Tian, H., Duan, C., Lu, L., et al. (2018). Piperlongumine restores the balance of autophagy and apoptosis by increasing BCL2 phosphorylation in rotenone-induced Parkinson disease models. *Autophagy* 14, 845–861. doi: 10.1080/15548627.2017.1390636

Liu, X., Du, H., Chen, D., Yuan, H., Chen, W., Jia, W., et al. (2019). Cyclophilin D deficiency protects against the development of mitochondrial ROS and cellular inflammation in aorta. *Biochem. Biophys. Res. Commun.* 508, 1202–1208. doi: 10.1016/j.bbrc.2018.12.064

Liu, X., Yang, Y., Song, J., Li, D., Liu, X., Li, C., et al. (2022). Knockdown of forkhead box protein P1 alleviates hypoxia reoxygenation injury in H9c2 cells through regulating Pik3ip1/Akt/eNOS and ROS/mPTP pathway. *Bioengineered* 13, 1320–1334. doi: 10.1080/21655979.2021.2016046

Magtanong, L., and Dixon, S. J. (2018). Ferroptosis and brain injury. *Dev. Neurosci.* 40, 382–395. doi: 10.1159/000496922

Maldonado, E. N., and Lemasters, J. J. (2012). Warburg revisited: Regulation of mitochondrial metabolism by voltage-dependent anion channels in cancer cells. *J. Pharmacol. Exp. Ther.* 342, 637–641. doi: 10.1124/jpet.112.192153

Maldonado, E. N., and Lemasters, J. J. (2014). ATP/ADP ratio, the missed connection between mitochondria and the Warburg effect. *Mitochondrion* 19, 78–84. doi: 10.1016/j.mito.2014.09.002

Mazure, N. M. (2017). VDAC in cancer. *Biochim. Biophys. Acta Bioenerg.* 1858, 665–673. doi: 10.1016/j.bbabio.2017.03.002

McStay, G. P., Clarke, S. J., and Halestrap, A. P. (2002). Role of critical thiol groups on the matrix surface of the adenine nucleotide translocase in the mechanism of the mitochondrial permeability transition pore. *Biochem. J.* 367, 541–548. doi: 10.1042/bj20011672

Minibayeva, F., Dmitrieva, S., Ponomareva, A., and Ryabovol, V. (2012). Oxidative stress-induced autophagy in plants: The role of mitochondria. *Plant Physiol. Biochem.* 59, 11–19. doi: 10.1016/j.plaphy.2012.02.013

Mnatsakanyan, N., Beutner, G., Porter, G. A., Alavian, K. N., and Jonas, E. A. (2017). Physiological roles of the mitochondrial permeability transition pore. *J. Bioenerg. Biomembr.* 49, 13–25. doi: 10.1007/s10863-016-9652-1

Mnatsakanyan, N., Llaguno, M. C., Yang, Y., Yan, Y., Weber, J., Sigworth, F. J., et al. (2019). A mitochondrial megachannel resides in monomeric F(1)F(O) ATP synthase. *Nat. Commun.* 10:5823. doi: 10.1038/s41467-019-13766-2

Mo, Y., Sun, Y. Y., and Liu, K. Y. (2020). Autophagy and inflammation in ischemic stroke. *Neural Regen. Res.* 15, 1388–1396. doi: 10.4103/1673-5374.274331

Montava-Garriga, L., and Ganley, I. G. (2020). Outstanding questions in mitophagy: What we do and do not know. *J. Mol. Biol.* 432, 206–230. doi: 10.1016/j.jmb.2019.06.032

Montero, J., Dutta, C., van Bodegom, D., Weinstock, D., and Letai, A. (2013). p53 regulates a non-apoptotic death induced by ROS. *Cell Death Differ.* 20, 1465–1474. doi: 10.1038/cdd.2013.52

Morciano, G., Giorgi, C., Bonora, M., Punzetti, S., Pavasini, R., Wieckowski, M. R., et al. (2015). Molecular identity of the mitochondrial permeability transition pore and its role in ischemia-reperfusion injury. *J. Mol. Cell Cardiol.* 78, 142–153. doi: 10.1016/j.yjmcc.2014.08.015

Morciano, G., Naumova, N., Koprowski, P., Valente, S., Sardão, V. A., Potes, Y., et al. (2021). The mitochondrial permeability transition pore: An evolving concept critical for cell life and death. *Biol. Rev. Camb. Philos. Soc.* 96, 2489–2521. doi: 10.1111/brv.12764

Mracsko, E., and Veltkamp, R. (2014). Neuroinflammation after intracerebral hemorrhage. *Front. Cell. Neurosci.* 8:388. doi: 10.3389/fncel.2014.00388

Munro, D., and Treberg, J. R. (2017). A radical shift in perspective: Mitochondria as regulators of reactive oxygen species. *J. Exp. Biol.* 220, 1170–1180. doi: 10.1242/jeb.132142

Neginskaya, M. A., Solesio, M. E., Berezhnaya, E. V., Amodeo, G. F., Mnatsakanyan, N., Jonas, E. A., et al. (2019). ATP synthase C-subunit-deficient mitochondria have a small cyclosporine A-sensitive channel, but lack the permeability transition pore. *Cell Rep.* 26:11–17.e12. doi: 10.1016/j.celrep.2018.12.033

Nguyen, T. N., and Lazarou, M. (2021). Plant mitophagy: Beware of friendly or you might get eaten. *Curr. Biol.* 31, R457–R458. doi: 10.1016/j.cub.2021.02.059

Nicotera, P., and Lipton, S. A. (1999). Excitotoxins in neuronal apoptosis and necrosis. *J. Cereb. Blood Flow Metab.* 19, 583–591. doi: 10.1097/00004647-199906000-00001

Nikić, I., Merkler, D., Sorbara, C., Brinkoetter, M., Kreutzfeldt, M., Bareyre, F. M., et al. (2011). A reversible form of axon damage in experimental autoimmune encephalomyelitis and multiple sclerosis. *Nat. Med.* 17, 495–499. doi: 10.1038/nm.2324

Nishikimi, A., Kira, Y., Kasahara, E., Sato, E. F., Kanno, T., Utsumi, K., et al. (2001). Tributyltin interacts with mitochondria and induces cytochrome c release. *Biochem. J.* 356, 621–626. doi: 10.1042/0264-6021:3560621

Niu, B., Lei, X., Xu, Q., Ju, Y., Xu, D., Mao, L., et al. (2022). Protecting mitochondria via inhibiting VDAC1 oligomerization alleviates ferroptosis in acetaminophen-induced acute liver injury. *Cell Biol. Toxicol.* 38, 505–530. doi: 10.1007/s10565-021-09624-x

Norbert, N., Michel, O., Nathan, M., Elodie, O., and Tae-Hee, C. (2016). Cyclosporine A, a potential therapy of ischemic reperfusion injury. A common history for heart and brain. *Cerebrovasc. Dis.* 42, 309–318.

Osmanovic, A., Widjaja, M., Förster, A., Weder, J., Wattjes, M. P., Lange, I., et al. (2020). SPG7 mutations in amyotrophic lateral sclerosis: A genetic link to hereditary spastic paraplegia. *J. Neurol.* 267, 2732–2743. doi: 10.1007/s00415-020-09861-w

Ouyang, W., Wang, S., Yan, D., Wu, J., Zhang, Y., Li, W., et al. (2023). The cGAS-STING pathway-dependent sensing of mitochondrial DNA mediates ocular surface inflammation. *Signal. Transduct. Target. Ther.* 8:371. doi: 10.1038/s41392-023-01624-z

Palikaras, K., Lionaki, E., and Tavernarakis, N. (2018). Mechanisms of mitophagy in cellular homeostasis, physiology and pathology. *Nat. Cell Biol.* 20, 1013–1022. doi: 10.1038/s41556-018-0176-2

Palmieri, F. (2004). The mitochondrial transporter family (SLC25): Physiological and pathological implications. *Pflugers Arch.* 447, 689–709. doi: 10.1007/s00424-003-1099-7

Petrosillo, G., Colantuono, G., Moro, N., Ruggiero, F. M., Tiravanti, E., Di Venosa, N., et al. (2009). Melatonin protects against heart ischemia-reperfusion injury by inhibiting mitochondrial permeability transition pore opening. *Am. J. Physiol. Heart Circ. Physiol.* 297, H1487–H1493. doi: 10.1152/ajpheart.00163.2009

Peuhkurinen, K. J., Takala, T. E., Nuutinen, E. M., and Hassinen, I. E. (1983). Tricarboxylic acid cycle metabolites during ischemia in isolated perfused rat heart. *Am. J. Physiol.* 244, H281–H288. doi: 10.1152/ajpheart.1983.244.2.H281

Pfeffer, G., Pyle, A., Griffin, H., Miller, J., Wilson, V., Turnbull, L., et al. (2015). SPG7 mutations are a common cause of undiagnosed ataxia. *Neurology* 84, 1174–1176. doi: 10.1212/wnl.0000000000001369

Philchenkov, A. (2004). Caspases: Potential targets for regulating cell death. *J. Cell Mol. Med.* 8, 432–444. doi: 10.1111/j.1582-4934.2004.tb00468.x

Pignataro, G., Meller, R., Inoue, K., Ordonez, A. N., Ashley, M. D., Zhigang, X., et al. (2008). In Vivo and in vitro characterization of a novel neuroprotective strategy for stroke: Ischemic postconditioning. *J. Cereb. Blood Flow Metab.* 28, 232–241.

Pinke, G., Zhou, L., and Sazanov, L. A. (2020). Cryo-EM structure of the entire mammalian F-type ATP synthase. *Nat. Struct. Mol. Biol.* 27, 1077–1085. doi: 10.1038/s41594-020-0503-8

Prentice, H., Modi, J. P., and Wu, J. Y. (2015). Mechanisms of neuronal protection against excitotoxicity, endoplasmic reticulum stress, and mitochondrial dysfunction in stroke and neurodegenerative diseases. *Oxid. Med. Cell Longev.* 2015:964518. doi: 10.1155/2015/964518

Qu, J., Chen, W., Hu, R., and Feng, H. (2016). The injury and therapy of reactive oxygen species in intracerebral hemorrhage looking at mitochondria. *Oxid. Med. Cell Longev.* 2016:2592935. doi: 10.1155/2016/2592935

Quintanilla, R. A., Tapia, C., and Pérez, M. J. (2017). Possible role of mitochondrial permeability transition pore in the pathogenesis of Huntington disease. *Biochem. Biophys. Res. Commun.* 483, 1078–1083. doi: 10.1016/j.bbrc.2016.09.054

Qureshi, A. I., Mendelow, A. D., and Hanley, D. F. (2009). Intracerebral haemorrhage. *Lancet* 373, 1632–1644. doi: 10.1016/s0140-6736(09)60371-8

Rabinowitz, J. D., and White, E. (2010). Autophagy and metabolism. *Science* 330, 1344–1348. doi: 10.1126/science.1193497

Rasheed, M. Z., Tabassum, H., and Parvez, S. (2017). Mitochondrial permeability transition pore: A promising target for the treatment of Parkinson's disease. *Protoplasma* 254, 33–42. doi: 10.1007/s00709-015-0930-2

Reumann, S., Voitsekhovskaja, O., and Lillo, C. (2010). From signal transduction to autophagy of plant cell organelles: Lessons from yeast and mammals and plant-specific features. *Protoplasma* 247, 233–256. doi: 10.1007/s00709-010-0190-0

Rodriguez-Enriquez, S., Kim, I., Currin, R. T., and Lemasters, J. J. (2006). Tracker dyes to probe mitochondrial autophagy (mitophagy) in rat hepatocytes. *Autophagy* 2, 39–46. doi: 10.4161/auto.2229

Roger, V. L., Go, A. S., Lloyd-Jones, D. M., Adams, R. J., Berry, J. D., Brown, T. M., et al. (2011). Heart disease and stroke statistics–2011 update: A report from the American heart association. *Circulation* 123, e18–e209. doi: 10.1161/CIR.0b013e3182009701

Rosencrans, W. M., Rajendran, M., Bezrukov, S. M., and Rostovtseva, T. K. (2021). VDAC regulation of mitochondrial calcium flux: From channel biophysics to disease. *Cell Calcium* 94:102356. doi: 10.1016/j.ceca.2021.102356

Rottenberg, H., and Hoek, J. B. (2021). The mitochondrial permeability transition: Nexus of aging, disease and longevity. *Cells* 10:79. doi: 10.3390/cells10010079

Roy, S. S., Madesh, M., Davies, E., Antonsson, B., Danial, N., and Hajnóczky, G. (2009). Bad targets the permeability transition pore independent of Bax or Bak to switch between Ca2+-dependent cell survival and death. *Mol. Cell* 33, 377–388. doi: 10.1016/j.molcel.2009.01.018

Ryan, M. T., Müller, H., and Pfanner, N. (1999). Functional staging of ADP/ATP carrier translocation across the outer mitochondrial membrane. *J. Biol. Chem.* 274, 20619–20627. doi: 10.1074/jbc.274.29.20619

Salabei, J. K., and Hill, B. G. (2015). Autophagic regulation of smooth muscle cell biology. *Redox. Biol.* 4, 97–103. doi: 10.1016/j.redox.2014.12.007

Salim, S. (2017). Oxidative stress and the central nervous system. *J. Pharmacol. Exp. Ther.* 360, 201–205. doi: 10.1124/jpet.116.237503

Schaar, C. E., Dues, D. J., Spielbauer, K. K., Machiela, E., Cooper, J. F., Senchuk, M., et al. (2015). Mitochondrial and cytoplasmic ROS have opposing effects on lifespan. *PLoS Genet.* 11:e1004972. doi: 10.1371/journal.pgen.1004972

Seifert, E. L., Gál, A., Acoba, M. G., Li, Q., Anderson-Pullinger, L., Golenár, T., et al. (2016). Natural and induced mitochondrial phosphate carrier loss: DIFFERENTIAL DEPENDENCE OF MITOCHONDRIAL METABOLISM AND DYNAMICS AND CELL SURVIVAL ON THE EXTENT OF DEPLETION. *J. Biol. Chem.* 291, 26126–26137. doi: 10.1074/jbc.M116.744714

Seifert, E. L., Ligeti, E., Mayr, J. A., Sondheimer, N., and Hajnóczky, G. (2015). The mitochondrial phosphate carrier: Role in oxidative metabolism, calcium handling and mitochondrial disease. *Biochem. Biophys. Res. Commun.* 464, 369–375. doi: 10.1016/j.bbrc.2015.06.031

Seo, B. J., Yoon, S. H., and Do, J. T. (2018). Mitochondrial dynamics in stem cells and differentiation. *Int. J. Mol. Sci.* 19:3893. doi: 10.3390/ijms19123893

Shanmughapriya, S., Rajan, S., Hoffman, N. E., Higgins, A. M., Tomar, D., Nemani, N., et al. (2015). SPG7 is an essential and conserved component of the mitochondrial permeability transition pore. *Mol. Cell* 60, 47–62. doi: 10.1016/j.molcel.2015.08.009

Shao, B. Z., Han, B. Z., Zeng, Y. X., Su, D. F., and Liu, C. (2016). The roles of macrophage autophagy in atherosclerosis. *Acta Pharmacol. Sin.* 37, 150–156. doi: 10.1038/aps.2015.87

Sharp, F., Liu, D. Z., Zhan, X., and Ander, B. P. (2008). Intracerebral hemorrhage injury mechanisms: Glutamate neurotoxicity, thrombin, and Src. *Acta Neurochir. Suppl.* 105, 43–46. doi: 10.1007/978-3-211-09469-3_9

Shen, J., Du, T., Wang, X., Duan, C., Gao, G., Zhang, J., et al. (2014). α-Synuclein amino terminus regulates mitochondrial membrane permeability. *Brain Res.* 1591, 14–26. doi: 10.1016/j.brainres.2014.09.046

Shibata, T., Yoneda, M., Morikawa, D., and Ohta, Y. (2019). Time-lapse imaging of Ca(2+)-induced swelling and permeability transition: Single mitochondrion study. *Arch Biochem. Biophys.* 663, 288–296. doi: 10.1016/j.abb.2019.01.016

Shohei, M., Michihiro, M., Masahiro, K., Takeshi, N., Takuro, O., and Yasuo, W. (2018). Edaravone and cyclosporine A as neuroprotective agents for acute ischemic stroke. *Acute Med. Surg.* 5, 213–221.

Shoshan-Barmatz, V., De Pinto, V., Zweckstetter, M., Raviv, Z., Keinan, N., and Arbel, N. (2010). VDAC, a multi-functional mitochondrial protein regulating cell life and death. *Mol. Aspects Med.* 31, 227–285. doi: 10.1016/j.mam.2010.03.002

Shoshan-Barmatz, V., Mizrachi, D., and Keinan, N. (2013). Oligomerization of the mitochondrial protein VDAC1: From structure to function and cancer therapy. *Prog. Mol. Biol. Transl. Sci.* 117, 303–334. doi: 10.1016/b978-0-12-386931-9.00011-8

Smith, G. M., and Gallo, G. (2018). The role of mitochondria in axon development and regeneration. *Dev. Neurobiol.* 78, 221–237. doi: 10.1002/dneu.22546

Song, M., Mihara, K., Chen, Y., Scorrano, L., and Dorn, G. W. II (2015). Mitochondrial fission and fusion factors reciprocally orchestrate mitophagic culling in mouse hearts and cultured fibroblasts. *Cell Metab.* 21, 273–286. doi: 10.1016/j.cmet.2014.12.011

Song, J., Kang, S. M., Kim, E., Kim, C. H., Song, H. T., and Lee, J. E. (2015). Adiponectin receptor-mediated signaling ameliorates cerebral cell damage and regulates the neurogenesis of neural stem cells at high glucose concentrations: An in vivo and in vitro study. *Cell Death Dis.* 6:e1844. doi: 10.1038/cddis.2015.220

Spikes, T. E., Montgomery, M. G., and Walker, J. E. (2020). Structure of the dimeric ATP synthase from bovine mitochondria. *Proc. Natl. Acad. Sci. U.S.A.* 117, 23519–23526. doi: 10.1073/pnas.2013998117

Stappen, R., and Krämer, R. (1994). Kinetic mechanism of phosphate/phosphate and phosphate/OH- antiports catalyzed by reconstituted phosphate carrier from beef heart mitochondria. *J. Biol. Chem.* 269, 11240–11246.

Stockwell, B. R., Friedmann Angeli, J. P., Bayir, H., Bush, A. I., Conrad, M., Dixon, S. J., et al. (2017). Ferroptosis: A regulated cell death nexus linking metabolism, redox biology, and disease. *Cell* 171, 273–285. doi: 10.1016/j.cell.2017.09.021

Sun, T., Ding, W., Xu, T., Ao, X., Yu, T., Li, M., et al. (2019). Parkin regulates programmed necrosis and myocardial ischemia/reperfusion injury by targeting cyclophilin-D. *Antioxid. Redox Signal.* 31, 1177–1193. doi: 10.1089/ars.2019.7734

Szabadkai, G., Simoni, A. M., Chami, M., Wieckowski, M. R., Youle, R. J., and Rizzuto, R. (2004). Drp-1-dependent division of the mitochondrial network blocks intraorganellar Ca2+ waves and protects against Ca2+-mediated apoptosis. *Mol. Cell* 16, 59–68. doi: 10.1016/j.molcel.2004.09.026

Szeto, H. H. (2008). Mitochondria-targeted cytoprotective peptides for ischemia-reperfusion injury. *Antioxid. Redox Signal.* 10, 601–619. doi: 10.1089/ars.2007.1892

Tan, W., and Colombini, M. (2007). VDAC closure increases calcium ion flux. *Biochim. Biophys. Acta* 1768, 2510–2515. doi: 10.1016/j.bbamem.2007.06.002

Tang, D., Chen, X., Kang, R., and Kroemer, G. (2021). Ferroptosis: Molecular mechanisms and health implications. *Cell Res.* 31, 107–125. doi: 10.1038/s41422-020-00441-1

Thi Nguyen, N., Thi Nguyen, T., Nguyen, H. T., Lee, J. M., Kim, M. J., Qi, X. F., et al. (2023). Inhibition of mitochondrial phosphate carrier prevents high phosphate-induced superoxide generation and vascular calcification. *Exp. Mol. Med.* 55, 532–540. doi: 10.1038/s12276-023-00950-0

Tian, H. Y., Huang, B. Y., Nie, H. F., Chen, X. Y., Zhou, Y., Yang, T., et al. (2023). The interplay between mitochondrial dysfunction and ferroptosis during ischemia-associated central nervous system diseases. *Brain Sci.* 13:1367. doi: 10.3390/brainsci13101367

Tian, Z., Liu, M., Zhang, Z., Yan, T., Guo, S., Miao, Y., et al. (2023). Association between intracerebral hemorrhage and cholesterol levels, and molecular mechanism underlying low cholesterol inhibiting autophagy in cerebral arterial smooth muscle cells leading to cell necrosis. *Int. J. Cardiol.* 387:131134. doi: 10.1016/j.ijcard.2023.131134

Tooze, S. A., and Yoshimori, T. (2010). The origin of the autophagosomal membrane. *Nat. Cell Biol.* 12, 831–835. doi: 10.1038/ncb0910-831

Trchounian, A., and Trchounian, K. (2019). Fermentation revisited: How do microorganisms survive under energy-limited conditions? *Trends Biochem. Sci.* 44, 391–400. doi: 10.1016/j.tibs.2018.12.009

Urbani, A., Giorgio, V., Carrer, A., Franchin, C., Arrigoni, G., Jiko, C., et al. (2019). Purified F-ATP synthase forms a Ca2+-dependent high-conductance channel matching the mitochondrial permeability transition pore. *Nat. Commun.* 10:4341. doi: 10.1038/s41467-019-12331-1

Van Aken, O., Ford, E., Lister, R., Huang, S., and Millar, A. H. (2016). Retrograde signalling caused by heritable mitochondrial dysfunction is partially mediated by ANAC017 and improves plant performance. *Plant J.* 88, 542–558. doi: 10.1111/tpj.13276

Vaseva, A. V., Marchenko, N. D., Ji, K., Tsirka, S. E., Holzmann, S., and Moll, U. M. (2012). p53 opens the mitochondrial permeability transition pore to trigger necrosis. *Cell* 149, 1536–1548. doi: 10.1016/j.cell.2012.05.014

Veres, B., Eros, K., Antus, C., Kalman, N., Fonai, F., Jakus, P. B., et al. (2021). Cyclophilin D-dependent mitochondrial permeability transition amplifies inflammatory reprogramming in endotoxemia. *FEBS Open Bio* 11, 684–704. doi: 10.1002/2211-5463.13091

Wacquier, B., Combettes, L., and Dupont, G. (2020). Dual dynamics of mitochondrial permeability transition pore opening. *Sci. Rep.* 10:3924. doi: 10.1038/s41598-020-60177-1

Wan, J., Ren, H., and Wang, J. (2019). Iron toxicity, lipid peroxidation and ferroptosis after intracerebral haemorrhage. *Stroke Vasc. Neurol.* 4, 93–95. doi: 10.1136/svn-2018-000205

Wang, P., and Heitman, J. (2005). The cyclophilins. *Genome Biol.* 6:226. doi: 10.1186/gb-2005-6-7-226

Wang, Z., Zhou, F., Dou, Y., Tian, X., Liu, C., Li, H., et al. (2018). Melatonin alleviates intracerebral hemorrhage-induced secondary brain injury in rats via suppressing apoptosis, inflammation, oxidative stress, DNA damage, and mitochondria injury. *Transl. Stroke Res.* 9, 74–91. doi: 10.1007/s12975-017-0559-x

Wang, S., Li, D., Huang, C., Wan, Y., Wang, J., Zan, X., et al. (2018). Overexpression of adiponectin alleviates intracerebral hemorrhage-induced brain injury in rats via suppression of oxidative stress. *Neurosci. Lett.* 681, 110–116. doi: 10.1016/j.neulet.2018.05.050

Wang, Y., Liu, Y., Li, Y., Liu, B., Wu, P., Xu, S., et al. (2019). Protective effects of astaxanthin on subarachnoid hemorrhage-induced early brain injury: Reduction of cerebral vasospasm and improvement of neuron survival and mitochondrial function. *Acta Histochem.* 121, 56–63. doi: 10.1016/j.acthis.2018.10.014

Waseem, M., Tabassum, H., and Parvez, S. (2016). Melatonin modulates permeability transition pore and 5-hydroxydecanoate induced K(ATP) channel inhibition in isolated brain mitochondria. *Mitochondrion* 31, 1–8. doi: 10.1016/j.mito.2016.08.005

Wasserman, J. K., and Schlichter, L. C. (2008). White matter injury in young and aged rats after intracerebral hemorrhage. *Exp. Neurol.* 214, 266–275. doi: 10.1016/j.expneurol.2008.08.010

Wei, Y., Pattingre, S., Sinha, S., Bassik, M., and Levine, B. (2008). JNK1-mediated phosphorylation of Bcl-2 regulates starvation-induced autophagy. *Mol. Cell* 30, 678–688. doi: 10.1016/j.molcel.2008.06.001

Weisthal, S., Keinan, N., Ben-Hail, D., Arif, T., and Shoshan-Barmatz, V. (2014). Ca(2+)-mediated regulation of VDAC1 expression levels is associated with cell death induction. *Biochim. Biophys. Acta* 1843, 2270–2281. doi: 10.1016/j.bbamcr.2014.03.021

Whelan, R. S., Konstantinidis, K., Wei, A. C., Chen, Y., Reyna, D. E., Jha, S., et al. (2012). Bax regulates primary necrosis through mitochondrial dynamics. *Proc. Natl. Acad. Sci. U.S.A.* 109, 6566–6571. doi: 10.1073/pnas.1201608109

Wu, X., Luo, J., Liu, H., Cui, W., Guo, K., Zhao, L., et al. (2020b). Recombinant adiponectin peptide ameliorates brain injury following intracerebral hemorrhage by suppressing astrocyte-derived inflammation via the inhibition of Drp1-mediated mitochondrial fission. *Transl. Stroke Res.* 11, 924–939. doi: 10.1007/s12975-019-00768-x

Wu, X., Cui, W., Guo, W., Liu, H., Luo, J., Zhao, L., et al. (2020a). Acrolein aggravates secondary brain injury after intracerebral hemorrhage through Drp1-mediated mitochondrial oxidative damage in mice. *Neurosci. Bull.* 36, 1158–1170. doi: 10.1007/s12264-020-00505-7

Xie, R. X., Li, D. W., Liu, X. C., Yang, M. F., Fang, J., Sun, B. L., et al. (2017). Carnosine attenuates brain oxidative stress and apoptosis after intracerebral hemorrhage in rats. *Neurochem. Res.* 42, 541–551. doi: 10.1007/s11064-016-2104-9

Xie, Y., Hou, W., Song, X., Yu, Y., Huang, J., Sun, X., et al. (2016). Ferroptosis: Process and function. *Cell Death Differ.* 23, 369–379. doi: 10.1038/cdd.2015.158

Xie, Z., Lei, B., Huang, Q., Deng, J., Wu, M., Shen, W., et al. (2012). Neuroprotective effect of cyclosporin A on the development of early brain injury in a subarachnoid hemorrhage model: A pilot study. *Brain Res.* 1472, 113–123. doi: 10.1016/j.brainres.2012.06.053

Xu, W., Gao, L., Zheng, J., Li, T., Shao, A., Reis, C., et al. (2018). The roles of MicroRNAs in stroke: Possible therapeutic targets. *Cell Transplant.* 27, 1778–1788. doi: 10.1177/0963689718773361

Xuwen, G., Chuancheng, R., and Heng, Z. (2008). Protective effects of ischemic postconditioning compared with gradual reperfusion or preconditioning. *J. Neurosci. Res.* 86, 2505–2511.

Yang, C., Wang, Z., Li, L., Zhang, Z., Jin, X., Wu, P., et al. (2021). Aged neutrophils form mitochondria-dependent vital NETs to promote breast cancer lung metastasis. *J. Immunother. Cancer* 9:2875. doi: 10.1136/jitc-2021-002875

Yang, Y., Chen, X., Feng, Z., Cai, X., Zhu, X., Cao, M., et al. (2022). MEC17-induced α-tubulin acetylation restores mitochondrial transport function and alleviates axonal injury after intracerebral hemorrhage in mice. *J. Neurochem.* 160, 51–63. doi: 10.1111/jnc.15493

Yangxin, L., Jiayi, S., Ruixia, W., Jinrong, B., Ya, H., Yong, Z., et al. (2020). Mitochondrial MPTP: A novel target of ethnomedicine for stroke treatment by apoptosis inhibition. *Front. Pharmacol.* 11:352.

Yao, G. Y., Zhu, Q., Xia, J., Chen, F. J., Huang, M., Liu, J., et al. (2018). Ischemic postconditioning confers cerebroprotection by stabilizing VDACs after brain ischemia. *Cell Death Dis.* 9:1033. doi: 10.1038/s41419-018-1089-5

Yao, H., Xie, Q., He, Q., Zeng, L., Long, J., Gong, Y., et al. (2022). Pretreatment with panaxatriol saponin attenuates mitochondrial apoptosis and oxidative stress to facilitate treatment of myocardial ischemia-reperfusion injury via the regulation of Keap1/Nrf2 activity. *Oxid. Med. Cell Longev.* 2022:9626703. doi: 10.1155/2022/9626703

Ying, Y., and Padanilam, B. J. (2016). Regulation of necrotic cell death: p53, PARP1 and cyclophilin D-overlapping pathways of regulated necrosis? *Cell Mol. Life Sci.* 73, 2309–2324. doi: 10.1007/s00018-016-2202-5

You, Y., Hou, Y., Zhai, X., Li, Z., Li, L., Zhao, Y., et al. (2016). Protective effects of PGC-1α via the mitochondrial pathway in rat brains after intracerebral hemorrhage. *Brain Res.* 1646, 34–43. doi: 10.1016/j.brainres.2016.04.076

Yu, J., Zheng, J., Lu, J., Sun, Z., Wang, Z., and Zhang, J. (2019). AdipoRon protects against secondary brain injury after intracerebral hemorrhage via alleviating mitochondrial dysfunction: Possible involvement of AdipoR1-AMPK-PGC1α pathway. *Neurochem. Res.* 44, 1678–1689. doi: 10.1007/s11064-019-02794-5

Yu, L., Gong, B., Duan, W., Fan, C., Zhang, J., Li, Z., et al. (2017). Melatonin ameliorates myocardial ischemia/reperfusion injury in type 1 diabetic rats by preserving mitochondrial function: Role of AMPK-PGC-1α-SIRT3 signaling. *Sci. Rep.* 7:41337. doi: 10.1038/srep41337

Zaid, H., Abu-Hamad, S., Israelson, A., Nathan, I., and Shoshan-Barmatz, V. (2005). The voltage-dependent anion channel-1 modulates apoptotic cell death. *Cell Death Differ.* 12, 751–760. doi: 10.1038/sj.cdd.4401599

Zelinová, V., Demecsová, L., and Tamás, L. (2019). Impact of antimycin A and myxothiazol on cadmium-induced superoxide, hydrogen peroxide, and nitric oxide generation in barley root tip. *Protoplasma* 256, 1375–1383. doi: 10.1007/s00709-019-01389-9

Zhang, W., Gai, C., Ding, D., Wang, F., and Li, W. (2018). Targeted p53 on small-molecules-induced ferroptosis in cancers. *Front. Oncol.* 8:507. doi: 10.3389/fonc.2018.00507

Zhang, W., Wang, L., Wang, R., Duan, Z., and Wang, H. (2022b). A blockade of microRNA-155 signal pathway has a beneficial effect on neural injury after intracerebral haemorrhage via reduction in neuroinflammation and oxidative stress. *Arch. Physiol. Biochem.* 128, 1235–1241. doi: 10.1080/13813455.2020.1764047

Zhang, W., Li, G., Luo, R., Lei, J., Song, Y., Wang, B., et al. (2022a). Cytosolic escape of mitochondrial DNA triggers cGAS-STING-NLRP3 axis-dependent nucleus pulposus cell pyroptosis. *Exp. Mol. Med.* 54, 129–142. doi: 10.1038/s12276-022-00729-9

Zhang, X., Ren, X., Zhang, Q., Li, Z., Ma, S., Bao, J., et al. (2016). PGC-1α/ERRα-Sirt3 pathway regulates daergic neuronal death by directly deacetylating SOD2 and ATP synthase β. *Antioxid. Redox Signal.* 24, 312–328. doi: 10.1089/ars.2015.6403

Zhang, Y., and Liu, C. (2020). Autophagy and hemorrhagic stroke. *Adv. Exp. Med. Biol.* 1207, 135–147. doi: 10.1007/978-981-15-4272-5_8

Zhang, Y., Rui, T., Luo, C., and Li, Q. (2021). Mdivi-1 alleviates brain damage and synaptic dysfunction after intracerebral hemorrhage in mice. *Exp. Brain Res.* 239, 1581–1593. doi: 10.1007/s00221-021-06089-6

Zhao, C., Chen, Z., Qi, J., Duan, S., Huang, Z., Zhang, C., et al. (2017). Drp1-dependent mitophagy protects against cisplatin-induced apoptosis of renal tubular epithelial cells by improving mitochondrial function. *Oncotarget* 8, 20988–21000. doi: 10.18632/oncotarget.15470

Zhao, Y., Li, Y., Zhang, R., Wang, F., Wang, T., and Jiao, Y. (2020). The Role of Erastin in Ferroptosis and Its Prospects in Cancer Therapy. *Onco Targets Ther.* 13, 5429–5441. doi: 10.2147/ott.S254995

Zharova, T. V., Grivennikova, V. G., and Borisov, V. B. (2023). F(1)·F(o) ATP Synthase/ATPase: Contemporary View on Unidirectional Catalysis. *Int. J. Mol. Sci.* 24:5417. doi: 10.3390/ijms24065417

Zheng, H., Huang, S., Wei, G., Sun, Y., Li, C., Si, X., et al. (2022). CircRNA Samd4 induces cardiac repair after myocardial infarction by blocking mitochondria-derived ROS output. *Mol. Ther.* 30, 3477–3498. doi: 10.1016/j.ymthe.2022.06.016

Zheng, J., Shi, L., Liang, F., Xu, W., Li, T., Gao, L., et al. (2018). Sirt3 ameliorates oxidative stress and mitochondrial dysfunction after intracerebral hemorrhage in diabetic rats. *Front. Neurosci.* 12:414. doi: 10.3389/fnins.2018.00414

Zheng, X., Gao, J., Zhao, M., Han, L., Zhang, D., Wang, K., et al. (2023). Honokiol attenuates mitochondrial fission and cell apoptosis by activating Sirt3 in intracerebral hemorrhage. *Chin. Med. J.* 136, 719–731. doi: 10.1097/cm9.0000000000002178

Zhou, C., Yamaguchi, M., Kusaka, G., Schonholz, C., Nanda, A., and Zhang, J. H. (2004). Caspase inhibitors prevent endothelial apoptosis and cerebral vasospasm in dog model of experimental subarachnoid hemorrhage. *J. Cereb. Blood Flow Metab.* 24, 419–431. doi: 10.1097/00004647-200404000-00007

Zhou, H., Li, D., Zhu, P., Ma, Q., Toan, S., Wang, J., et al. (2018). Inhibitory effect of melatonin on necroptosis via repressing the Ripk3-PGAM5-CypD-mPTP pathway attenuates cardiac microvascular ischemia-reperfusion injury. *J. Pineal Res.* 65:e12503. doi: 10.1111/jpi.12503

Zhou, H., Ren, J., Toan, S., and Mui, D. (2021). Role of mitochondrial quality surveillance in myocardial infarction: From bench to bedside. *Ageing Res. Rev.* 66:101250. doi: 10.1016/j.arr.2020.101250

Zhou, J., Shen, R., Makale, E. C., Zhong, W., Chen, Z., and Huang, Q. (2023). SS31 confers cerebral protection by reversing mitochondrial dysfunction in early brain injury following subarachnoid hemorrhage, via the Nrf2- and PGC-1α-dependent pathways. *Neurochem. Res.* 48, 1580–1595. doi: 10.1007/s11064-022-03850-3

Zhou, S. Y., Cui, G. Z., Yan, X. L., Wang, X., Qu, Y., Guo, Z. N., et al. (2020). Mechanism of ferroptosis and its relationships with other types of programmed cell death: Insights for potential interventions after intracerebral hemorrhage. *Front. Neurosci.* 14:589042. doi: 10.3389/fnins.2020.589042

Zhou, Y., Wang, S., Li, Y., Yu, S., and Zhao, Y. (2017). SIRT1/PGC-1α signaling promotes mitochondrial functional recovery and reduces apoptosis after intracerebral hemorrhage in rats. *Front. Mol. Neurosci.* 10:443. doi: 10.3389/fnmol.2017.00443

Zoratti, M., and Szabò, I. (1995). The mitochondrial permeability transition. *Biochim. Biophys. Acta* 1241, 139–176. doi: 10.1016/0304-4157(95)00003-a

Zorov, D. B., Filburn, C. R., Klotz, L. O., Zweier, J. L., and Sollott, S. J. (2000). Reactive oxygen species (ROS)-induced ROS release: A new phenomenon accompanying induction of the mitochondrial permeability transition in cardiac myocytes. *J. Exp. Med.* 192, 1001–1014. doi: 10.1084/jem.192.7.1001

Zorov, D. B., Juhaszova, M., and Sollott, S. J. (2014). Mitochondrial reactive oxygen species (ROS) and ROS-induced ROS release. *Physiol. Rev.* 94, 909–950. doi: 10.1152/physrev.00026.2013

frontiers | Frontiers in Neuroscience

TYPE Mini Review
PUBLISHED 07 August 2024
DOI 10.3389/fnins.2024.1451845

OPEN ACCESS

EDITED BY
Nicola Simola,
University of Cagliari, Italy

REVIEWED BY
Brent Roy Bill,
University of Texas at Tyler, United States
T. Tamilanban,
SRM Institute of Science and Technology, India

*CORRESPONDENCE
Jessica Larsen
✉ larsenj@clemson.edu

RECEIVED 19 June 2024
ACCEPTED 29 July 2024
PUBLISHED 07 August 2024

CITATION
Bagwell E and Larsen J (2024) A review of MPTP-induced parkinsonism in adult zebrafish to explore pharmacological interventions for human Parkinson's disease. *Front. Neurosci.* 18:1451845.
doi: 10.3389/fnins.2024.1451845

A review of MPTP-induced parkinsonism in adult zebrafish to explore pharmacological interventions for human Parkinson's disease

Emmeline Bagwell[1] and Jessica Larsen[1,2]*

[1]Department of Bioengineering, Clemson University, Clemson, SC, United States, [2]Department of Chemical and Biomolecular Engineering, Clemson University, Clemson, SC, United States

Novel work in adult zebrafish, *Danio rerio,* to recapitulate human neurodegenerative disease has proven useful in both pharmaceutical development and research on genetic disease. Due to high genetic homology to humans, affordable husbandry, relatively quick life cycle breeding times, and robust embryo production, zebrafish offer a promising model to test pharmaceutical performance in a high throughput, *in vivo* setting. Currently, most research in zebrafish models of Parkinson's disease induces the disease in larval or embryonic stage organisms due to ease of administration, with advancement through developmental stages taking only a matter of days. The use of early-stage organisms limits the usability of zebrafish as models for adult disease and specifically age-related neurodegenerative conditions. Recently, researchers have sought to extend the usability of zebrafish into models for Parkinson's disease. Specifically, 1-Methyl-4-phenyl-1,2,3,6-tetrahydropyridine (MPTP) has emerged as a prodrug that upon injection well-encompasses the biochemical mechanisms and symptomology associated with Parkinson's disease. By utilizing MPTP in an adult zebrafish model, advancements in Parkinson's disease research may be achieved. This paper highlights the recent research on this model, comparing it to the human form of Parkinson's disease.

KEYWORDS

zebrafish, parkinsonism, animal models, neurodegeneration, MPTP

Introduction

Parkinson's Disease (PD) is a neurodegenerative disorder that affects nearly 10 million patients worldwide. Several symptoms of the disorder include neurological-based dysfunction, such as tremor, muscle stiffness, impaired balance, confusion, insomnia, difficulty speaking, and smooth muscle spasms (Armstrong and Okun, 2020; Parkinson's Foundation, 2024). Several mechanisms are involved in the disease, stemming from both environmental and genetic components. Specifically looking at the pathophysiology of the disease, PD damages the dopaminergic (DA) neurons located in the substantia nigra and the diencephalon, the portion of the midbrain responsible for sensory and autonomic control and processing (Tabrez et al., 2012). Alpha-synuclein, a protein responsible for neurotransmitter and synaptic vesicle trafficking, is overproduced due to the upregulation of the SCNA (synuclein alpha) gene in PD patients. This upregulation causes the accumulation of alpha-synuclein, creating plaques

that are responsible for several synucleinopathic neurodegenerative diseases, including PD (Stefanis, 2012). The aggregation of alpha-synuclein plaques at the synaptic cleft eventually prevents neurotransmitter signaling, causing dopamine production to lower. As these plaques continue to accumulate, dopamine transmission occurs at lower levels until the neurons are eventually tagged for apoptosis, or programmed cell death. These plaques can accumulate so rapidly that lysosome cannot control the overload of alpha-synuclein, leading to necrosis (Stefanis, 2012). The pathophysiology and etiology of PD has been extensively reviewed elsewhere (Poewe et al., 2017; Bloem et al., 2021; Zaman et al., 2021).

Due to the several genes and pathophysiological mechanisms at play, PD has no known cure. Current research interests in PD have shifted toward understanding disease mechanisms and identifying pharmaceuticals that could alleviate the excruciating symptoms instead of aiming to treat the cause (Lee et al., 2017). The current gold-standard pharmaceutical treatments for PD are Levodopa (L-dopa) compounds. These compounds mimic the natural pathway intermediate involved in the production of dopamine. Levodopa is often prescribed to patients in intermediate to late-stage PD (Abbott, 2010).

Beyond making treatment difficult, isolation of a common etiology for PD and its complex pathophysiology has made it difficult to model. Research has focused on the use of zebrafish as models for PD research in recent years since the first published zebrafish paper in 2003 (Figure 1). Its exponential growth in use as a PD model is likely due to affordability, accessibility, and replicability (Lam et al., 2005) of zebrafish. In this review article we discuss the relevance of zebrafish as a model organism for human PD, including the reasoning behind its use and its homology to human disease. We specifically highlight the use of neurotoxin MPTP for PD model induction, with a focus on comparing the very few (< 20) studies using this adult-aged model and a call for more uniform protocols. Finally, we end with a discussion on the relevance of testing of explored neurotherapeutics for PD in MPTP zebrafish.

Zebrafish as a model organism

Danio rerio, the zebrafish, is a species that has become popular in research of neurological diseases due to high genetic homology to humans (Mrinalini et al., 2023). Zebrafish belong to the class Actinopterygii, which accounts for over half of all vertebrates (Lawrence and Mason, 2012). Specifically, zebrafish are teleost, meaning that they have complete bone formation in homology with most vertebrates. This homology makes zebrafish excellent in studying neurological diseases, bone diseases, genome editing, and embryonic development. In addition to high genetic homology and conserved biological function, zebrafish reproduce quickly. Development of the embryonic features occurs quickly, within 24 h of fertilization, and the larvae hatch around 2.5 days post fertilization. Specifically, zebrafish can produce 100–600 embryos at a time. This ease of breeding and rapid growth cycle provides researchers with a quick and easily renewable animal model (Chia et al., 2022), unlike traditional mammalian rodent models.

Many researchers utilize the embryonic model of zebrafish in research, as development is modeled well in this early stage (Lee et al., 2017). Specifically, zebrafish can be easily genetically modified during embryonic development. At the embryonic stage, zebrafish can be made fully transparent, leading to an optical advantage, allowing

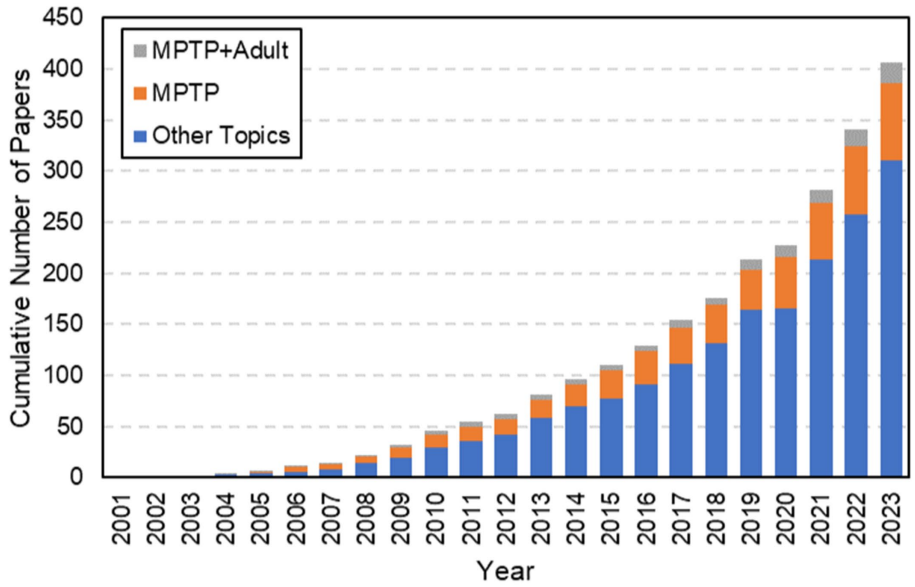

FIGURE 1
Results from a web of science search using the terms "Zebrafish" + "Parkinson's Disease." Highlighted here is the exponential growth in the use of Zebrafish as models for Parkinson's disease from its first published paper in 2003. Note that although there has been a significant amount of growth over the last twenty years, the cumulative number of papers focused on this model is still quite small. MPTP has been used to induce PD since 2005 and has grown in popularity. However, despite the age-related behavior of PD, a very limited number of papers have focused on using MPTP to create PD in adult zebrafish, as highlighted by the gray contribution to the bars each year. When this search was performed, there were only 20 total papers that focused on MPTP in adult zebrafish.

researchers to observe drug effects in real-time as opposed to relying solely on post-sacrificial analysis. However, debate has now turned many researchers of neurodegenerative disease toward sexually mature adult zebrafish (≥ 6 months post fertilization). Due to the nature of neurodegenerative diseases, like PD, occurring primarily in adults over the age of 55, many researchers feel that adult zebrafish maintain developmental homology, including age-related pathology, to humans and should therefore be utilized as a model for these diseases (Chia et al., 2022). Furthermore, it is easy to dose zebrafish with drugs through aquatic environment at all stages, which can provide ease of drug administration and decrease the need for invasive procedures to establish small molecule drug induced disease models (Lam et al., 2005).

Beyond rapid maturation, large clutch sizes, and affordability of husbandry, zebrafish have proven to become a beneficial research animal model of many neurological diseases. The human brain and zebrafish brain may have different configurations, but many homologous and highly conserved structures can be observed in both (Figure 2; Diotel et al., 2020). The same areas implicated by PD in humans are often also implicated in PD models that are created experimentally in zebrafish. These areas include the olfactory bulb, and telencephalon. The olfactory bulb is a dopaminergic-neuron dense region of the brain that is responsible for sense of smell and has a strong relationship with memory and learning (Kozol et al., 2016; Diotel et al., 2020). The telencephalon, or the cerebrum in humans, is one of the largest portions of the brain responsible for all voluntary motor control and most sensory processing. The diencephalon in fish, or equivalent to substantia nigra in humans, is a neuron-dense region of the brain that is responsible for nearly all coordinated movements.

Unlike commonly used invertebrate models, such as *Drosophila melanogaster* and *Caenorhabditis elegans*, *D. rerio* are vertebrate teleosts with orthologs of over 78% of genes found in humans (Ellis and Soanes, 2012). In addition to this high genetic homology, the catecholamine production cascade in this model is highly conserved, making the process nearly identical to humans. In this cascade, dopamine is transported by vesicular monoamine transporter 2 (VMAT2) to signal to other neurons. The dopamine transporter (DAT) at the synaptic cleft on the terminal end of signaling neurons then releases dopamine into the synapse. On the dendritic end of a receiving neuron, the dopamine receptor (D1 Receptor) takes up dopamine, leading to the activation of cyclic adenosine monophosphate (cAMP). cAMP serves as a secondary messenger that allows for signal transduction across neurons in the central nervous system (Lebowitz and Khoshbouei, 2020). Specifically in zebrafish, the neurotransmitter pathways for noradrenergic, serotonergic, histaminergic, and dopaminergic systems are highly conserved and relevant in the discussion of PD (Anichtchik et al., 2003; Tay et al., 2011). Due to the importance of dopamine when studying PD, the production of this neurotransmitter cannot go overlooked. Dopamine is produced from the key amino acid tyrosine. L-tyrosine is hydroxylated by the rate-limiting enzyme tyrosine hydroxylase (TH) to form the precursor to dopamine, L-DOPA (Albarran et al., 2014). L-DOPA can then be converted into dopamine by aromatic amino acid decarboxylase in microglia and in TH-positive neurons (Figure 3).

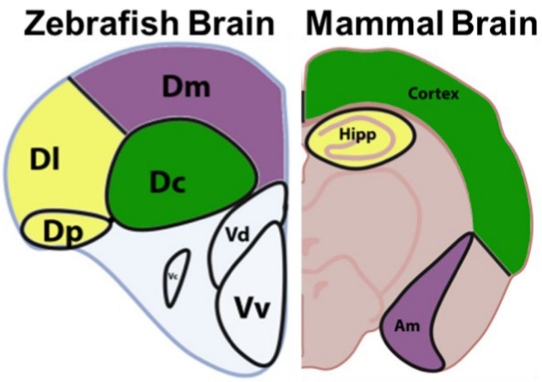

FIGURE 2
Anatomy of the zebrafish brain *vs* a mammalian brain, highlighting proposed homologs. The zebrafish central zone of the dorsal telencephalon (Dc) is proposed to be homologous to the mammalian cortex. The lateral zone of the dorsal telencephalon (Dl) and the posterior zone of the dorsal telencephalon (Dp) are proposed to be homologous to the mammalian Hippocampus (Hipp). While the dorsomedial zone of the dorsal telencephalon (Dm) is proposed to be homologous to the amygdala (Am). Adapted from Source (Lawrence and Mason, 2012). Image copyrighted under CC-BY Version 4.0.

Zebrafish models are ideal for high-throughput small molecule screens. This approach can identify new drug candidates and potential therapeutic targets through systematic testing of various compounds for their impact on disease-related phenotypes (Lam and Peterson, 2019). Due to the homology of the catecholamine production cascade, zebrafish models have been developed and used to study compounds and interventions that protect dopaminergic neurons from degeneration. Zebrafish models allow for the study of compounds that modulate dopamine levels and neurotransmitter function (Wang et al., 2021). Potential therapies to explore include drugs that enhance dopamine release, dopamine receptor agonists, or alternative neurotransmitter-based treatments like discovery of medications currently on-market (Martel and Gatti McArthur, 2020). One of the biggest benefits of the zebrafish model is that they are amenable to genetic manipulations. Researchers have explored gene therapy approaches, which have been extensively reviewed elsewhere (Chen et al., 2023; Dumbhare and Gaurkar, 2023; Muleiro Alvarez et al., 2024), to deliver neuroprotective genes to dopaminergic neurons, potentially slowing down their degeneration.

Beyond dopamine production, targeting molecules that improve mitochondrial function and energy production in dopaminergic neurons is a potential therapeutic strategy for PD (Prasuhn et al., 2021) for which zebrafish models have provided invaluable insight (Razali et al., 2021). The process of mitochondrial fusion in dopaminergic and TH-positive neurons is disrupted by PD, leading to higher ROS levels. This eventually results in disrupted cell energy pathways and can therefore cause apoptosis.

Furthermore, targeting the immune response in the brain may help mitigate neurodegeneration in PD (Cai et al., 2022). Neuroinflammation is an important aspect of PD pathology, and zebrafish as a model may aid in identifying anti-inflammatory agents that modulate the immune response within the central nervous system and reduce neuronal damage (Araújo et al., 2022). Neuroinflammation associated with PD includes activated glial cells and increased levels of tumor necrosis factors (TNFs), IFNγ, IL-1, IL-6, IL-2, CXC-chemokine ligand 8 (CXCL8), and monocyte chemoattractant

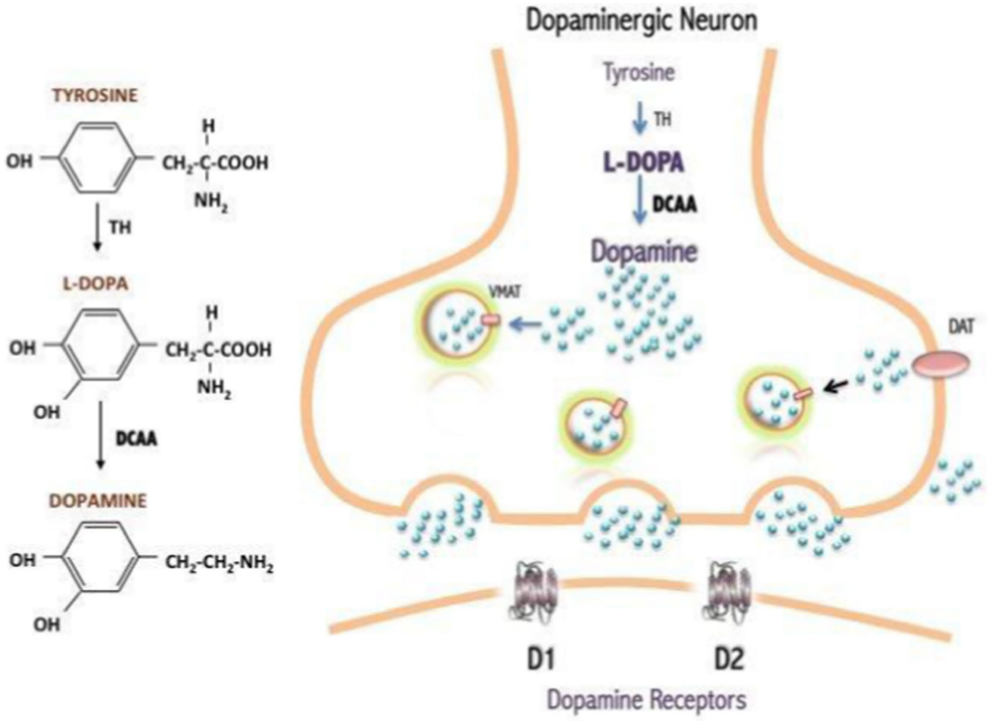

FIGURE 3
Dopamine production from the amino acid, tyrosine (Albarran et al., 2014). Originally published in A Synopsis of Parkinson's Disease, 2014 under Creative Commons Attribution 3.0 Unported (CC By 3.0) license. Available from: https://doi.org/10.5772/57102.

protein-2 (CCL2). Zebrafish have several homologs that are similar to these human cytokines, though very few are identical in function or form. Minimal research looks at these pro-inflammatory cytokines in zebrafish, nor their activation by the prodrug MPTP.

A mechanism that still remains unclear is the mechanism of autophagy involved in the clearance of misfolded proteins, including alpha-synuclein (Fellner et al., 2021). Targeting pathways that enhance autophagy may alleviate the accumulation of toxic protein aggregates in zebrafish and, potentially, in humans. Alpha-synuclein aggregation is a hallmark of PD. However, this pathophysiological aspect of PD is difficult to recapitulate in zebrafish due to the genetic differences in alpha-synuclein (SCNA) in humans, while fish only produce homologs that behave differently (SNCB and SNCG1) (Toni and Cioni, 2015). Alpha-synuclein and beta-synuclein are two related proteins found in the human brain, each with distinct roles and behaviors. Alpha-synuclein is well-known for its involvement in PD, as it forms aggregate structures within neurons in humans, which is a hallmark of the disease (Stefanis, 2012). Zebrafish do not naturally develop alpha-synuclein aggregates, as they lack the SNCA gene (Lopez et al., 2022). However, both humans and zebrafish have the protein-coding gene for beta-synuclein (SNCB). Beta-synuclein is a closely related protein to alpha-synuclein but has different properties (Toni and Cioni, 2015). Unlike alpha-synuclein, beta-synuclein is not commonly associated with PD pathology or Lewy body formation, but it appears to have a protective role against alpha-synuclein aggregation and toxicity (Calabresi et al., 2023). Zebrafish lack alpha-synuclein but have been shown to express the analog proteins beta-synuclein and gamma synuclein (Doyle and Croll, 2022). In knockdown models of zebrafish, beta-synuclein has proven to be directly affiliated with PD-like motor and behavioral issues, making it a relevant marker in modeling of PD (Ninkina et al., 2021). Researchers have studied beta-synuclein in zebrafish models to investigate its functions and its potential protective effects against alpha-synuclein-induced toxicity (Lopez et al., 2022). This research may contribute to a better understanding of the interplay between these two synuclein proteins in the context of neurodegenerative diseases.

Zebrafish models can recapitulate some aspects of parkinsonism due to the anatomical, biochemical, and cellular pathologic similarities to human systems involved, but likely do not fully capture the diversity seen in human PD etiology (Gialluisi et al., 2021). In addition to physiological differences, the mechanism of disease induction in these fish fails to account for the gradual and progressive nature of human PD. Human PD is characterized by progressive loss of dopaminergic neurons and the accumulation of alpha-synuclein over many years (DeMaagd and Philip, 2015). In contrast, zebrafish models often develop symptoms more rapidly after toxin exposure, making it challenging to study the long-term, age-related aspects of PD (Cassar et al., 2020). The pharmacokinetics of drug metabolism, blood–brain barrier characteristics, and drug responses can differ between zebrafish and humans. Therefore, drug testing results may not be directly translatable and must be confirmed in mammalian models before proceeding with development (Cassar et al., 2020; Knap et al., 2023). Despite these differences, zebrafish models offer significant advantages, including rapid development, optical transparency, and genetic manipulability. They are particularly useful for investigating fundamental mechanisms of neurodegeneration and for drug screening (Kim and Jin, 2012). Combining insights from zebrafish with other animal models and human studies will be crucial for a

comprehensive understanding of PD. However, due to the homology of catecholamine cascade, there are benefits to the use of neurotoxin models in zebrafish to develop appropriate therapeutics for PD. Specifically, we focus our discussion on the use of a neurotoxin 1-Methyl-4-phenyl-1,2,3,6-tetrahydropyridine (MPTP) as a highly promising model of PD with relatively facile administration in zebrafish.

MPTP for modeling PD

It can be difficult to recapitulate the full complexity of any human disease in an animal model, but research has identified the use of different types of small molecule drugs that can mimic Parkinsonian symptoms in zebrafish. These different types of drugs to induce Parkinson's in zebrafish have been explained elsewhere (Makhija and Jagtap, 2014). In this review, we focus on MPTP as a highly promising model of PD with relatively facile administration in zebrafish. The specific MPTP induction of PD has been used since 2004 and has grown in popularity, though its limitations are still up for debate. When a general search was performed from 2001 to 2023, there were only 20 total papers that focused on MPTP in adult zebrafish (Figure 1).

MPTP is a highly lipophilic prodrug analgesic discovered when a batch of desmethylprodine was produced incorrectly (Sallinen et al., 2009). MPTP is metabolized into 1-methyl-4-phenylpyridinium (MPP+) once taken up by astrocytes containing monoamine oxidase-B (MAO-B). The MPP+ metabolite is then taken up by the dopamine transporter (DAT) located on DA neurons. Once this toxin enters the DA neuron, it inhibits oxidative-level phosphorylation in the mitochondria, causing necrosis (Tabrez et al., 2012). This oxidative stress induced by MPTP, which causes neurotoxicity, is similar to a well-known induction of PD in humans (Dias et al., 2013). Mitochondrial dysfunction is a hallmark of PD as well. The process of mitochondrial fusion in dopaminergic and TH-positive neurons is disrupted by Parkinson's disease, leading to higher ROS levels. This eventually results in disrupted cell energy pathways and can therefore cause apoptosis. The use of zebrafish to study mitochondrial dysfunction also emerging, though MPTP has not been associated with significant changes in mitochondrial function. This mechanism mimics PD by causing necrosis of DA neurons specifically located in the substantia nigra and diencephalon. Dopaminergic neurons are particularly vulnerable to these effects due to their high energy demands and the oxidative environment they operate in Dias et al. (2013). The necrosis of these cells causes the tremor and muscle rigidity characteristic of PD, as well as lowering free dopamine levels and DA neuron numbers in these regions (Anichtchik et al., 2003). The loss of dopaminergic neurons in the substantia nigra and other regions of the brain result in motor symptoms that resemble those seen in PD, such as bradykinesia, tremors, rigidity, and postural instability. The toxic mechanism of MPTP and its conversion to MPP+ serves as a valuable tool for creating animal models of PD in research, as it recapitulates some of the key pathological features of the condition (Mat Taib and Mustapha, 2020). However, it is important to note that the progression of MPTP-induced parkinsonism is often more rapid and severe than that of idiopathic Parkinson's disease in humans, and MPTP is not considered a causative agent of idiopathic Parkinson's disease in human patients.

Despite its downfalls, MPTP has emerged as a highly beneficial drug product in research of PD due to its pharmacodynamic behavior in neural tissues (Vaz et al., 2018). MPTP is beneficial due to its ability to recapitulate both effects on catecholaminergic production as well as behavioral and motor deficits. However, despite this fact most MPTP zebrafish models still involve the use of fish in early stages of development. One of the leading reasons for the use of the zebrafish embryonic model of PD is ease of induction, as MPTP can simply be dissolved to appropriate dilutions in tank water. The embryonic stage zebrafish are able to absorb the neurotoxic MPTP through their gill capillaries, causing permanent neurological deficits within hours. Several researchers have utilized this method and allowed the fish to reach sexual maturity after incubation in MPTP during the larval stage of development (Vaz et al., 2018; Razali et al., 2021). Figure 1 highlights the growing interest in establishing an adult model of disease over the last 20 years; these adult zebrafish may more adequately recapitulate human aging processes and enable a more in depth understanding of human PD.

MPTP, combined with the use of adult zebrafish, have led to animal models that encompass some quantifiable and observable changes associated with human PD (Anichtchik et al., 2003). However, despite the growth of this field, the use of MPTP in adult zebrafish still lacks universally accepted and uniform protocols, as delivery routes and doses for MPTP, tissue analysis methods, and movement analysis methods vary widely (Vaz et al., 2018). Below, we highlight the use of MPTP in adult zebrafish as a model for PD by comparing the presentation of PD in these animals versus what is observed in human patients (Vaz et al., 2018). We aim to identify best practices associated with model development and provide guidance for the field. Although not a perfect recapitulation of disease, this model has the potential to expand upon our knowledge of PD and identify new treatment modalities for human clinical trials.

Adult MPTP- treated zebrafish as models for PD

Table 1 highlights the current experimental papers focused on the use of MPTP in adult zebrafish to induce models of PD. It becomes quite clear with the lack of experimentation being done on adult zebrafish that there is a lack of consistency in the procedural set up and the fish characteristics, which may be contributing to a lack of consistency in both the behavioral and neurochemical observations. As MPTP with zebrafish becomes an increasingly popular research topic for animal models of PD, several research groups have produced foundational knowledge that could be used in the development of a more uniform model. There is a lack of consistency in the age, genders, and strain of zebrafish being used in experimentation. In the context of zebrafish, "adult" typically means reaching sexual maturity which happens around 3 months (Singleman and Holtzman, 2014). The aging of zebrafish is being explored and is linked to functional changes (Kishi, 2004), which could impact study outcomes and make comparison of findings irresponsible.

The method and concentration for dosing MPTP became a point of debate due to the bioavailability and safe dose that could be of therapeutic importance. Clearly, from Table 1, the great majority of MPTP injections performed in adult zebrafish are intraperitoneal (IP) (Sallinen et al., 2009; Tabrez et al., 2012; Dias et al., 2013; Makhija and

TABLE 1 A summary of current literature on adult-induced parkinsonism in zebrafish using MPTP.

Fish line	Procedural set up		Fish characteristics		Behavioral analysis		Neurochemical analysis			References
	Injection route	MPTP concentration	Age	Gender	Locomotor activity	Cognitive function	Dopamine	Tyrosine Hydroxylase (TH)	Synuclein	
Transgenic zebrafish Tg(dat:eGFP); Tg(dat:tom20 MLS:mCherry)	Cerebroventricular microinjection (CVMI)	10, 25, 35, 100 mM	10 months	-	- 47% decrease in avg. velocity and distance - 51% increase in freezing	marked motor and olfactory function decline	65% of dopaminergic neuron mitochondria fragmented	- 47% loss in occipital lobe - 25% loss in periventricular pretectal nucleus - 41% low in telencephalon	-	Kalyn and Ekker (2021)
AB zebrafish	Intraperitoneal (IP)	Single dose or double dose of 50 µg	6 months	50:50 M:F	decreased distance by 25% in single dose and 68% in double dose	-	-	TH reduced, but not significantly	Decreased SCNA and increased α-synuclein after 2 doses	Sarath Babu et al. (2016)
Outbred and AB Zebrafish	Intramuscular (AM)	20, 40, 60 or 80 mg/kg	Adult	M:F	20% decrease in distance and 80% decrease in velocity 9 days after injection	Decreased tank exploration	Sustained decrease of 30%	TH decrease shown via western blot	-	Anichtchik et al. (2003)
Wild Type (WT) outbred long-fin strain	IP	0, 50, 100, 200 and 400 µg in 1 %DMSO/ PBS	~ 1 year old	50:50 M:F	No locomotor deficits observed	Y-maze showed that spontaneous alternation behavior decreased	Linked social behavior to dopamine D3 receptor agonism in zebrafish	-	-	Bashirzade et al. (2022)
AB Zebrafish	IP	200 µg/g body weight	3 to 4 months	-	Statistically decreased velocity and distance at 24 h post injection	Increase in freezing bouts that remained high for 96 h	-	Fewer expressed TH+ neurons in substantia nigra	-	Razali et al. (2022)
Zebrafish from a local aquarium	IP	100 µg/g	5 months	-	Significant decrease in length and distance traveled 24 h post injection	Significant increase in freezing + significant decrease in rapid movement	Fold change in dopamine expression of 0.5	-	-	Selvaraj et al. (2019)
WT zebrafish	IP	225 mg/kg	< 8 months	-	3x decrease in distance traveled and mean speed	50% decrease in number of line crossings	3-fold decrease in dopamine content from 900 to 300 ng/g	-	-	Nellore et al. (2013)

10.3389/fnins.2024.1451845

Jagtap, 2014), with one using a direct-to-brain approach via cerebroventricular (CV) administration (Kalyn and Ekker, 2021) and one exploring an intramuscular (IM) route (Anichtchik et al., 2003). These routes all lead to different pharmacokinetic profiles for MPTP, with bioavailability expected to vary significantly, but in all cases MPTP is able to affect neurologic tissue. It does appear that the direct-to-brain, CV injection led to the greatest decrease in TH, which may mean that this injection route leads to the most MPTP activity in the brain. With regards to dosing, MPTP concentrations also varied, even within IP-injected studies. Omar et al. (2023) determined toxic IP-injected MPTP doses, which had them settle on injections of 100 µg/g, but other groups have still explored up to double this dose (Razali et al., 2021).

Due to the broad spectrum of symptoms associated with human PD, MPTP zebrafish studies have focused on assessing the fish for both their behavioral and neurochemical changes. One of the most consistent findings in the adult zebrafish MPTP model confirms that locomotor changes mimic human PD. Decreases in both average velocity and average distance traveled during study periods were consistently observed regardless of MPTP injection route, MPTP concentration, or precise fish age. When assessments were performed, cognitive function declines were also consistently observed. Specifically, cognitive tests have been performed to identify freezing periods (Selvaraj et al., 2019; Kalyn and Ekker, 2021), similar to human bradykinesia, behavioral alterations, like changing swimming patterns (Anichtchik et al., 2003; Nellore et al., 2013) and decreasing in exploration of new spaces (Bashirzade et al., 2022). Overall, these studies all conclude that adult zebrafish experience similarities in movement related symptoms, specifically bradykinesia-like, regardless of method of administration of MPTP.

Though much of the groundwork establishing locomotor activity change and behavioral change has been replicated by several groups, assessing for neurotransmitter and gene expression is still being discovered. Dopamine expression, either the neurotransmitter form or dopamine transporter expression, have become an increasingly popular hallmark to assess for when discovering the underlying mechanisms of PD. After imaging of neurological tissue, counting the number of dopaminergic (DA) neurons has become a quantifiable way to determine a decrease in MPTP-treated zebrafish (Matsui and Sugie, 2017). Some studies did quantify DA neuron losses, while others quantified changes in dopamine expression, with three papers seeing between 30 and 50% decreases in detectable dopamine after MPTP injection. Similar observations with TH are observed, with reductions in both number of TH+ neurons and in TH levels. However, around half of currently published assessments do not look at any quantification of dopamine or TH, despite their marked importance in human PD. A second major component associated with the pathophysiology of PD is the aggregation of the neural protein alpha-synuclein. These aggregates, though a known mechanism of PD, have minimal *in vivo* research with zebrafish models. Though zebrafish do not have genetic markers capable of producing alpha-synuclein, they are able to produce sister proteins beta-synuclein and gamma1-synuclein. Though research on the function of these other synuclein proteins is still emerging in zebrafish research, many studies have concluded that these functions are similar to alpha-synuclein in human adults, as highlighted above.

Although clearly an emerging model, MPTP-induction of PD in adult zebrafish demonstrates a lot of promise. Because zebrafish experience aging related phenomena, it may be significant to develop a consensus of best practices regarding age at MPTP injection. Because the ultimate cognitive and functional decline, as well as dopaminergic and TH level decline is consistent regardless of MPTP dose or injection method, these factors do not currently appear to be significant when developing a PD model. However, as this model matures it may be significant to delineate biochemical changes associated with specific MPTP doses in order to study the various stages of neurodegenerative progression which could lead credence toward therapeutic discovery and development for PD.

Conclusion

Though the affordability, mass sample size, and high genetic homology makes the zebrafish model promising, much work still is required to bridge the gaps in knowledge. PD is a widespread neurodegenerative disorder affecting millions of individuals worldwide, manifesting with a range of debilitating symptoms, including tremors, muscle stiffness, impaired balance, cognitive impairment, and more. The disease's complex pathophysiology involves genetic and environmental factors, ultimately resulting in the degeneration of dopaminergic neurons in critical brain regions. Although zebrafish offer a promising model for PD research due to genetic homology, the study of pro-inflammatory cytokines, reactive oxygen species, and mitochondrial dysfunction, all hallmarks of human PD, remains underexplored in this model.

As MPTP with zebrafish becomes an increasingly popular research topic for animal models of PD, several research groups have produced foundational knowledge pertaining to creating a uniform model. The method for dosing MPTP became a point of debate due to the bioavailability and safe dose that could be of therapeutic importance. Two injection routes, IP and CVMI, provided physiological changes that mirrored some of those seen in human PD patients. Research in this model has focused on assessing cognitive function, locomotor activity, dopamine expression, and TH expression. One of the most well-established findings in the adult zebrafish MPTP model confirms that cognitive function declines after a working dose of MPTP. Behavioral tests assess for freezing periods, velocity, and behavioral alterations and have established that zebrafish dosed with MPTP exhibited behavioral deficits and cognitive decline. There has, thus far, been less consistency in other observed neurochemical PD-related changes, as summarized in Table 1.

The pursuit of PD treatments has shifted toward alleviating symptoms, as a cure remains elusive. However, the emergence of zebrafish as a valuable model organism offers hope for advancing our understanding of PD mechanisms and potentially identifying new treatment modalities. Overall, zebrafish hold great promise as a versatile and cost-effective model organism for studying neurological disorders, including PD. The continued exploration of zebrafish models, coupled with a better understanding of PD pathophysiology, may ultimately lead to new insights and potential therapies for this challenging disease.

Author contributions

EB: Writing – original draft, Writing – review & editing. JL: Funding acquisition, Supervision, Writing – original draft, Writing – review & editing.

Funding

The author(s) declare that financial support was received for the research, authorship, and/or publication of this article. This work was partially supported by Clemson's Core Incentivized Access and Creative Inquiry programs. Publication funding has been provided through Clemson Libraries' OA Publishing Fund.

Conflict of interest

The authors declare that the research was conducted in the absence of any commercial or financial relationships that could be construed as a potential conflict of interest.

Publisher's note

References

Abbott, A. (2010). Levodopa: the story so far. *Nature* 466, S6–S7. doi: 10.1038/466S6a

Albarran, S., Rangel-Barajas, C., and Garduo, B. F. (2014). "Pathophysiology of L-Dopa induced dyskinesia — changes in D1/D3 receptors and their signaling pathway" in A synopsis of Parkinson's disease. ed. A. Q. Rana (London: IntechOpen Limited).

Anichtchik, O. V., Kaslin, J., Peitsaro, N., Scheinin, M., and Panula, P. (2003). Neurochemical and behavioural changes in zebrafish *Danio rerio* after systemic administration of 6-hydroxydopamine and 1-methyl-4-phenyl-1,2,3,6-tetrahydropyridine. *J. Neurochem.* 88, 443–453. doi: 10.1111/j.1471-4159.2004.02190.x

Armstrong, M. J., and Okun, M. S. (2020). Diagnosis and treatment of Parkinson disease. *JAMA* 323:548. doi: 10.1001/jama.2019.22360

Araújo, Bruna, Caridade-Silva, R., Soares-Guedes, C., Martins-Macedo, J., Gomes, E. D., et al. (2022). "Neuroinflammation and Parkinson's Disease—From Neurodegeneration to Therapeutic Opportunities". *Cells 11* 18:2908. doi: 10.3390/cells11182908

Bashirzade, A. A. O., Cheresiz, S. V., Belova, A. S., Drobkov, A. V., Korotaeva, A. D., Azizi-Arani, S., et al. (2022). MPTP-treated zebrafish recapitulate 'late-stage' Parkinson's-like cognitive decline. *Toxics* 10:69. doi: 10.3390/toxics10020069

Bloem, B. R., Okun, M. S., and Klein, C. (2021). Parkinson's disease. *Lancet* 397, 2284–2303. doi: 10.1016/S0140-6736(21)00218-X

Cai, Y., Liu, J., Wang, B., Sun, M., and Yang, H. (2022). Microglia in the Neuroinflammatory pathogenesis of Alzheimer's disease and related therapeutic targets. *Front. Immunol.* 13:856376. doi: 10.3389/fimmu.2022.856376

Calabresi, P., Mechelli, A., Natale, G., Volpicelli-Daley, L., Di Lazzaro, G., and Ghiglieri, V. (2023). Alpha-synuclein in Parkinson's disease and other synucleinopathies: from overt neurodegeneration back to early synaptic dysfunction. *Cell Death Dis.* 14:176. doi: 10.1038/s41419-023-05672-9

Cassar, S., Adatto, I., Freeman, J. L., Gamse, J. T., Iturria, I., Lawrence, C., et al. (2020). Use of zebrafish in drug discovery toxicology. *Chem. Res. Toxicol.* 33, 95–118. doi: 10.1021/acs.chemrestox.9b00335

Chen, Y., Hong, Z., Wang, J., Liu, K., Liu, J., Lin, J., et al. (2023). Circuit-specific gene therapy reverses core symptoms in a primate Parkinson's disease model. *Cell* 186, 5394–5410.e18. doi: 10.1016/j.cell.2023.10.004

Chia, K., Klingseisen, A., Sieger, D., and Priller, J. (2022). Zebrafish as a model organism for neurodegenerative disease. *Front. Mol. Neurosci.* 15:940484. doi: 10.3389/fnmol.2022.940484

DeMaagd, G., and Philip, A. (2015). Parkinson's disease and its management: part 1: disease entity, risk factors, pathophysiology, clinical presentation, and diagnosis. *P T* 40, 504–532

Dias, V., Junn, E., and Mouradian, M. M. (2013). The role of oxidative stress in Parkinson's disease. *J. Parkinsons Dis.* 3, 461–491. doi: 10.3233/JPD-130230

Diotel, N., Lübke, L., Strähle, U., and Rastegar, S. (2020). Common and distinct features of adult neurogenesis and regeneration in the telencephalon of zebrafish and mammals. *Front. Neurosci.* 14:568930. doi: 10.3389/fnins.2020.568930

Doyle, J. M., and Croll, R. P. (2022). A critical review of zebrafish models of Parkinson's disease. *Front. Pharmacol.* 13:835827. doi: 10.3389/fphar.2022.835827

Dumbhare, O., and Gaurkar, S. S. (2023). A review of genetic and gene therapy for Parkinson's disease. *Cureus* 15:e34657. doi: 10.7759/cureus.34657

Ellis, L. D., and Soanes, K. H. (2012). A larval zebrafish model of bipolar disorder as a screening platform for neuro-therapeutics. *Behav. Brain Res.* 233, 450–457. doi: 10.1016/j.bbr.2012.05.043

Fellner, L., Gabassi, E., Haybaeck, J., and Edenhofer, F. (2021). Autophagy in α-Synucleinopathies—an overstrained system. *Cells* 10:3143. doi: 10.3390/cells10113143

Gialluisi, A., Reccia, M. G., Modugno, N., Nutile, T., Lombardi, A., Di Giovannantonio, L. G., et al. (2021). Identification of sixteen novel candidate genes for late onset Parkinson's disease. *Mol. Neurodegener.* 16:35. doi: 10.1186/s13024-021-00455-2

Kalyn, M., and Ekker, M. (2021). Cerebroventricular microinjections of MPTP on adult zebrafish induces dopaminergic neuronal death, mitochondrial fragmentation, and sensorimotor impairments. *Front. Neurosci.* 15:718244. doi: 10.3389/fnins.2021.718244

Kim, H.-J., and Jin, C. Y. (2012). Stem cells in drug screening for neurodegenerative disease. *Korean J. Physiol. Pharmacol.* 16, 1–9. doi: 10.4196/kjpp.2012.16.1.1

Kishi, S. (2004). "Functional aging and gradual senescence in zebrafish" in Annals of the new York Academy of Sciences, vol. *1019* (New York: New York Academy of Sciences), 521–526.

Knap, B., Nieoczym, D., Kundap, U., Kusio-Targonska, K., Kukula-Koch, W., Turski, W. A., et al. (2023). Zebrafish as a robust preclinical platform for screening plant-derived drugs with anticonvulsant properties—a review. *Front. Mol. Neurosci.* 16:1221665. doi: 10.3389/fnmol.2023.1221665

Kozol, R. A., Abrams, A. J., James, D. M., Buglo, E., Yan, Q., and Dallman, J. E. (2016). Function over form: modeling groups of inherited neurological conditions in zebrafish. *Front. Mol. Neurosci.* 9:55. doi: 10.3389/fnmol.2016.00055

Lam, C. S., Korzh, V., and Strahle, U. (2005). Zebrafish embryos are susceptible to the dopaminergic neurotoxin MPTP. *Eur. J. Neurosci.* 21, 1758–1762. doi: 10.1111/j.1460-9568.2005.03988.x

Lam, P.-Y., and Peterson, R. T. (2019). Developing zebrafish disease models for *in vivo* small molecule screens. *Curr. Opin. Chem. Biol.* 50, 37–44. doi: 10.1016/j.cbpa.2019.02.005

Lawrence, C., and Mason, T. (2012). Zebrafish housing systems: A review of basic operating principles and considerations for design and functionality. *ILAR J.* 53, 179–191. doi: 10.1093/ilar.53.2.179

Lebowitz, J. J., and Khoshbouei, H. (2020). Heterogeneity of dopamine release sites in health and degeneration. *Neurobiol. Dis.* 134:104633. doi: 10.1016/j.nbd.2019.104633

Lee, K. Y., Jang, G. H., Byun, C. H., Jeun, M., Searson, P. C., and Lee, K. H. (2017). Zebrafish models for functional and toxicological screening of nanoscale drug delivery systems: promoting preclinical applications. *Biosci. Rep.* 37:199. doi: 10.1042/BSR20170199

Lopez, A., Gorb, A., Palha, N., Fleming, A., and Rubinsztein, D. C. (2022). A new zebrafish model to measure neuronal α-Synuclein clearance in vivo. *Genes (Basel)* 13:868. doi: 10.3390/genes13050868

Makhija, D. T., and Jagtap, A. G. (2014). Studies on sensitivity of zebrafish as a model organism for Parkinson's disease: comparison with rat model. *J. Pharmacol. Pharmacother.* 5, 39–46. doi: 10.4103/0976-500X.124422

Martel, J. C., and Gatti McArthur, S. (2020). Dopamine receptor subtypes, physiology and pharmacology: new ligands and concepts in schizophrenia. *Front. Pharmacol.* 11:1003. doi: 10.3389/fphar.2020.01003

Mat Taib, C. N., and Mustapha, M. (2020). MPTP-induced mouse model of Parkinson's disease: A promising direction of therapeutic strategies. *Bosn. J. Basic Med. Sci.* 21, 422–433. doi: 10.17305/bjbms.2020.5181

Matsui, H., and Sugie, A. (2017). An optimized method for counting dopaminergic neurons in zebrafish. *PLoS One* 12:e0184363. doi: 10.1371/journal.pone.0184363

Mrinalini, R., Tamilanban, T., Naveen Kumar, V., and Manasa, K. (2023). Zebrafish – the Neurobehavioural model in trend. *Neuroscience* 520, 95–118. doi: 10.1016/j.neuroscience.2022.12.016

Muleiro Alvarez, M., Cano-Herrera, G., Osorio Martínez, M. F., Vega Gonzales-Portillo, J., Monroy, G. R., Murguiondo Pérez, R., et al. (2024). A comprehensive approach to Parkinson's disease: addressing its molecular, clinical, and therapeutic aspects. *Int. J. Mol. Sci.* 25:7183. doi: 10.3390/ijms25137183

Nellore, J., Pauline, C., and Amarnath, K. (2013). *Bacopa monnieri* phytochemicals mediated synthesis of platinum nanoparticles and its Neurorescue effect on 1-methyl 4-phenyl 1,2,3,6 Tetrahydropyridine-induced experimental parkinsonism in zebrafish. *J. Neurodegener. Dis.* 2013, 1–8. doi: 10.1155/2013/972391

Ninkina, N., Millership, S. J., Peters, O. M., Connor-Robson, N., Chaprov, K., Kopylov, A. T., et al. (2021). β-Synuclein potentiates synaptic vesicle dopamine uptake and rescues dopaminergic neurons from MPTP-induced death in the absence of other synucleins. *J. Biol. Chem.* 297:101375. doi: 10.1016/j.jbc.2021.101375

Omar, N. A., Kumar, J., and Teoh, S. L. (2023). Neuroprotective effects of Neurotrophin-3 in MPTP-induced zebrafish Parkinson's disease model. *Front. Pharmacol.* 14:1307447. doi: 10.3389/fphar.2023.1307447

Parkinson's Foundation. (2024). Prevalence & Incidence. Available at: https://www.parkinson.org/understanding-parkinsons/statistics/prevalence-incidence

Poewe, W., Seppi, K., Tanner, C. M., Halliday, G. M., Brundin, P., Volkmann, J., et al. (2017). Parkinson disease. *Nat Rev Dis Primers* 3, 1–21. doi: 10.1038/nrdp.2017.13

Prasuhn, J., Davis, R. L., and Kumar, K. R. (2021). Targeting mitochondrial impairment in Parkinson's disease: challenges and opportunities. *Front. Cell Dev. Biol.* 8:615461. doi: 10.3389/fcell.2020.615461

Razali, K., Mohd Nasir, M. H., Othman, N., Doolaanea, A. A., Kumar, J., Nabeel Ibrahim, W., et al. (2022). Characterization of neurobehavioral pattern in a zebrafish 1-methyl-4-phenyl-1,2,3,6-tetrahydropyridine (MPTP)-induced model: A 96-hour behavioral study. *PLoS One* 17:e0274844. doi: 10.1371/journal.pone.0274844

Razali, K., Othman, N., Mohd Nasir, M. H., Doolaanea, A. A., Kumar, J., Ibrahim, W. N., et al. (2021). The promise of the zebrafish model for Parkinson's disease: Today's science and Tomorrow's treatment. *Front. Genet.* 12:655550. doi: 10.3389/fgene.2021.655550

Sallinen, V., Torkko, V., Sundvik, M., Reenilä, I., Khrustalyov, D., Kaslin, J., et al. (2009). MPTP and MPP+ target specific aminergic cell populations in larval zebrafish. *J. Neurochem.* 108, 719–731. doi: 10.1111/j.1471-4159.2008.05793.x

Sarath Babu, N., Murthy, C. L. N., Kakara, S., Sharma, R., Brahmendra Swamy, C. V., and Idris, M. M. (2016). 1-Methyl-4-phenyl-1,2,3,6-tetrahydropyridine induced Parkinson's disease in zebrafish. *Proteomics* 16, 1407–1420. doi: 10.1002/pmic.201500291

Selvaraj, V., Venkatasubramanian, H., Ilango, K., and Santhakumar, K. (2019). A simple method to study motor and non-motor behaviors in adult zebrafish. *J. Neurosci. Methods* 320, 16–25. doi: 10.1016/j.jneumeth.2019.03.008

Singleman, C., and Holtzman, N. G. (2014). Growth and maturation in the zebrafish, *Danio Rerio*: A staging tool for teaching and research. *Zebrafish* 11, 396–406. doi: 10.1089/zeb.2014.0976

Stefanis, L. (2012). Synuclein in Parkinson's disease. *Cold Spring Harb. Perspect. Med.* 2, –a009399. doi: 10.1101/cshperspect.a009399

Tabrez, S., Jabir, N. R., Shakil, S., Greig, N. H., Alam, Q., Abuzenadah, A. M., et al. (2012). A synopsis on the role of tyrosine hydroxylase in Parkinson's disease. *CNS Neurol. Disord. Drug Targets* 11, 395–409. doi: 10.2174/187152712800792785

Tay, T. L., Ronneberger, O., Ryu, S., Nitschke, R., and Driever, W. (2011). Comprehensive catecholaminergic projectome analysis reveals single-neuron integration of zebrafish ascending and descending dopaminergic systems. *Nat. Commun.* 2:1171. doi: 10.1038/ncomms1171

Toni, M., and Cioni, C. (2015). Fish Synucleins: an update. *Mar. Drugs* 13, 6665–6686. doi: 10.3390/md13116665

Vaz, R. L., Outeiro, T. F., and Ferreira, J. J. (2018). Zebrafish as an animal model for drug discovery in Parkinson's disease and other movement disorders: A systematic review. *Front. Neurol.* 9:347. doi: 10.3389/fneur.2018.00347

Wang, X., Zhang, J.-B., He, K.-J., Wang, F., and Liu, C.-F. (2021). Advances of zebrafish in neurodegenerative disease: from models to drug discovery. *Front. Pharmacol.* 12:713963. doi: 10.3389/fphar.2021.713963

Zaman, V., Shields, D. C., Shams, R., Drasites, K. P., Matzelle, D., Haque, A., et al. (2021). Cellular and molecular pathophysiology in the progression of Parkinson's disease. *Metab. Brain Dis.* 36, 815–827. doi: 10.1007/s11011-021-00689-5

frontiers | Frontiers in Neuroscience

TYPE Original Research
PUBLISHED 30 August 2024
DOI 10.3389/fnins.2024.1461178

OPEN ACCESS

EDITED BY
Maria Vincenza Catania,
National Research Council (CNR), Italy

REVIEWED BY
Edith González Guevara,
Instituto Nacional de Neurología y Neurocirugía MVS, Mexico
Shuai Wang,
University of South Florida, United States

*CORRESPONDENCE
Atsu Aiba
✉ aiba@m.u-tokyo.ac.jp

RECEIVED 08 July 2024
ACCEPTED 19 August 2024
PUBLISHED 30 August 2024

CITATION
Chen L, Saito R, Noda-Narita S, Kassai H and Aiba A (2024) Hyperactive mTORC1 in striatum dysregulates dopamine receptor expression and odor preference behavior. *Front. Neurosci.* 18:1461178. doi: 10.3389/fnins.2024.1461178

Hyperactive mTORC1 in striatum dysregulates dopamine receptor expression and odor preference behavior

Lin Chen[1,2], Ryo Saito[1], Shoko Noda-Narita[1], Hidetoshi Kassai[1,3] and Atsu Aiba[1,2]*

[1]Laboratory of Animal Resources, Center for Disease Biology and Integrated Medicine, Graduate School of Medicine, The University of Tokyo, Tokyo, Japan, [2]Department of Biological Sciences, Graduate School of Science, The University of Tokyo, Tokyo, Japan, [3]Central Animal Division, National Cancer Center Research Institute, Tokyo, Japan

Mechanistic target of rapamycin (mTOR) plays an important role in brain development and synaptic plasticity. Dysregulation of the mTOR pathway is observed in various human central nervous system diseases, including tuberous sclerosis complex, autism spectrum disorder (ASD), and neurodegenerative diseases, including Parkinson's disease and Huntington's disease. Numerous studies focused on the effects of hyperactivation of mTOR on cortical excitatory neurons, while only a few studies focused on inhibitory neurons. Here we generated transgenic mice in which mTORC1 signaling is hyperactivated in inhibitory neurons in the striatum, while cortical neurons left unaffected. The hyperactivation of mTORC1 signaling increased GABAergic inhibitory neurons in the striatum. The transgenic mice exhibited the upregulation of dopamine receptor D1 and the downregulation of dopamine receptor D2 in medium spiny neurons in the ventral striatum. Finally, the transgenic mice demonstrated impaired motor learning and dysregulated olfactory preference behavior, though the basic function of olfaction was preserved. These findings reveal that the mTORC1 signaling pathway plays an essential role in the development and function of the striatal inhibitory neurons and suggest the critical involvement of the mTORC1 pathway in the locomotor abnormalities in neurodegenerative diseases and the sensory defects in ASD.

KEYWORDS

mTOR, inhibitory neuron, dopamine receptor, medium spiny neuron, olfactory tubercle, olfactory behavior

1 Introduction

mTOR is an evolutionarily conserved Ser/Thr protein kinase. It interacts with multiple proteins and forms two distinct protein complexes, termed mTORC1 and mTORC2 (Albert and Hall, 2015). mTORC1 is a master growth regulator involved in various cellular processes, including cell growth, proliferation, and survival. Several environmental cues can stimulate the mTORC1 pathway, including energy, stress, amino acids and growth factors (Foster and Fingar, 2010). mTORC1 promotes protein synthesis by phosphorylation of p70 S6 kinase (S6K1 and S6K2) and eukaryotic initiation factor 4-binding protein (4EBP1 and 4EBP2). As mTORC1 is an important regulator of many cellular processes, dysregulation of mTORC1

signaling contributes to a variety of human diseases, including cancer and metabolic diseases (Laplante and Sabatini, 2012). mTORC1 also plays an important role in development and synaptic plasticity in the central nervous systems (CNS) (Jaworski and Sheng, 2006). Dysregulation of mTORC1 signaling is observed in several human CNS disorders, such as tuberous sclerosis complex (TSC), fragile X syndrome, and neurodegenerative diseases (Orlova and Crino, 2010; Busquets-Garcia et al., 2013; Sato et al., 2012; Bové et al., 2011). Animal models of these mTORC1-related diseases are conventionally established by loss of *Tsc1, Tsc2* or *Pten*, but our group previously generated transgenic (Tg) mice expressing a gain-of-function mutant of mTOR (Kassai et al., 2014), which directly and constitutively activates the mTORC1 signaling. Excitatory neuron-specific activation of mTORC1 signaling in the forebrain leads to lethal seizure and recapitulates TSC and neurodegeneration. However, little is known about the mTORC1 dysregulation in inhibitory neurons.

Medium spiny neurons (MSNs) are a specific type of GABAergic inhibitory neurons which represents 90% of the neurons in human dorsal striatum (neostriatum, caudate putamen). The dorsal striatum controls the motor and reward systems. MSNs have two characteristic subtypes, called dopamine receptor D1-expressing (D1-type) and dopamine receptor D2-expressing (D2-type) MSNs (Yager et al., 2015). D1- and D2-type MSNs are mainly involved in striatal direct and indirect pathways, respectively. The dyscoordination of D1-type and D2-type MSNs is observed in neurodegenerative diseases, including Parkinson's disease and Huntington's disease. In recent studies, dysregulation of mTORC1 signaling is shown to contribute to the dysfunction of MSNs in these neurodegenerative diseases (Santini et al., 2009; Pryor et al., 2014). Further, the involvement of the dorsal striatal activation of mTORC1 signaling in the repetitive behaviors in ASD was recently shown using *Tsc1*-KO mouse model (Benthall et al., 2021). However, it is unclear how activation of the mTORC1 pathway directly affects D1- or D2-type MSN population of the striatum and how the discoordination of MSNs affects the downstream neuronal circuits. Moreover, the ventral striatum, which includes nucleus accumbens and olfactory tubercle (OT), also processes the motivation, reward, and fear (Ikemoto, 2007). Though the ventral striatum contains D1- and D2-type MSNs and is dysregulated in psychiatric disorders, almost no studies have analyzed the relationship between mTORC1 signaling and neuronal dysfunction in the ventral striatum.

There are a few animal models of mTOR-related diseases focusing on the inhibitory neurons. GABAergic interneuron-specific *Tsc1*-KO mice using *Dlx5/6*-Cre mice showed impaired growth and decreased survival with seizure susceptibility (Fu et al., 2012). The conditional *Tsc1*-KO mice had enlarged soma size and impaired migration of the cortical interneurons. Somatostatin (SST)-specific and parvalbumin (PV)-specific conditional KO of *Tsc1* also demonstrated the disrupted morphological and functional development of cortical interneurons and deficits in social behavior (Malik et al., 2019; Amegandjin et al., 2021). These studies suggest that hyperactive mTORC1 signaling in cortical interneurons may be responsible for human *TSC* patient-like spontaneous seizures and ASD-related social abnormalities. ASD-related behavioral phenotypes are also observed in an animal model generated by deleting *Pten* gene in SST-specific and PV-specific interneurons (Shin et al., 2021). The conditional *Pten*-KO mice exhibited impaired motor learning and social deficits. However, most of those animal models with hyperactivation of mTORC1 pathway in inhibitory neurons showed abnormalities according to the dysfunction of cortical interneurons. Only a few studies have focused on the mTORC1 function in the striatum and almost no animal models were generated to figure out the mTORC1 contribution to the development and function in striatal MSNs.

In the present study, to address mTORC1-specific contribution in the function of dorsal and ventral striatum, we generated Tg mice in which mTORC1 signaling is constitutively activated in the dorsal and ventral striatal MSNs. Hyperactivation of mTORC1 increased the cell number and the cell size of GABAergic inhibitory neurons in the striatum, and the Tg mice exhibited impaired motor learning. Furthermore, the hyperactivation of mTORC1 increased D1-type MSNs, while decreasing D2-type MSNs in the OT, and olfactory preference behavior was disrupted in the Tg mice. Taken together, the mTORC1 signaling plays a critical role in the proliferation and function of the striatal MSNs.

2 Materials and methods

2.1 Mice

All animal experiments were approved by the Institutional Animal Care and Use Committee of the University of Tokyo (Permit No. P21-038 and A2023M004) and were conducted in accordance with the guidelines of the University of Tokyo. All mice were housed under specific pathogen-free conditions with a temperature of 23 ± 1°C, humidity of 50 ± 10%, a 12-h light/12-h dark cycle (light: 8:00–20:00/dark: 20:00–8:00), in cages with food and water available *ad libitum*.

Dlx1-CreER^{T2} mice (JAX stock #014551) (Taniguchi et al., 2011) and ROSA26R-lacZ mice (JAX stock # 003474) (Soriano, 1999) were provided by Dr. Hiroki Kurihara. CAG-mTOR Tg mice were generated as described previously (Kassai et al., 2014). In CAG-mTOR Tg mice, active mTOR^{SL1+IT} can be conditionally expressed upon excision of the *loxP*-flanked *neo* gene in response to Cre-*loxP* recombination. CAG-mTOR Tg mice were crossed with Dlx1-CreER^{T2} mice to obtain Dlx1-mTOR Tg mice (*Dlx1-CreER^{T2}/+; CAG-mTOR^{SL1+IT}/+*) and the control mice (*CAG-mTOR^{SL1+IT}/+*). Genetic background of the Tg mice used in this study was a hybrid of C57BL/6 and ICR. For induction of Cre recombinase activity, tamoxifen (T5648, SIGMA) was dissolved in sesame oil and administered to the pregnant mice by oral gavage at a dose of 0.1 mg/g body weight at 12.5 day postcoitum (dpc), and the pups were used for the histological and behavioral experiments. For behavioral tests, 8- to 14-week-old mice were used, and mice were placed in the testing room for at least 1 h to acclimate to the experimental environments. In open field test, Y-maze test, elevated plus maze test and rota-rod test, male and female mice were analyzed separately. In olfactory habituation and dishabituation test, buried food-seeking test and three-chamber odor preference test, both male and female mice were included in the same analyses. For histological analysis, 14-week-old mice were used.

2.2 β- galactosidase staining

Mice were deeply anesthetized and perfused with 4% paraformaldehyde (PFA) in 0.1 M phosphate buffer (pH 7.4, PB). The fixed brains were immersed in 4% PFA for 2 h and transferred to 30% sucrose in 0.1 M PB. The brains were embedded in the OTC compound

(Sakura Finetek Japan). Sections of 30-μm-thickness were prepared by using a cryostat (CM1850, Leica Microsystems) and mounted on MAS-coated glass slides. The sections were incubated in *β*-galactosidase staining solution containing 5 mM potassium hexacyanoferrate (III), 5 mM potassium hexacyanoferrate (II), 2 mM $MgCl_2$, and 4% X-gal in PB saline (PBS) at 37°C overnight. The slides were dehydrated in ethanol, and cleared in xylene, and coverslipped with Entellan solution (Merck). The brain sections were viewed by the all-in-one fluorescence microscope (BZ-X800, KEYENCE).

2.3 *In situ* hybridization combined with immunohistochemistry

In situ hybridization for *Gad67, Drd1, Drd2*, and *c-Fos* mRNAs was performed as described previously (Yamasaki et al., 2010) with minor modification. Plasmids templated for *in vitro* transcription for *Gad67, Drd1 and Drd2* mRNAs were kindly provided by Dr. Masahiko Watanabe, and that for *c-Fos* mRNA was kindly provided by Dr. Haruhiko Bito, and Digoxigenin (DIG)- or fluorescein isothiocyanate (FITC)-labeled cRNA proves were prepared. Fresh-frozen mouse brains were sectioned into 30-μm-thickness slices using a cryostat (CM1850, Leica Microsystems) and mounted on MAS-coated glass slides. Sections were acetylated with 0.25% acetic anhydride in 0.1 M triethanolamine-HCl and hybridization was performed at 63.5°C for 12 h in hybridization buffer supplemented with cRNA probes at a dilution of 1:1000. Post-hybridization washing was at 61°C with standard sodium citrate and formamide. After stringent washing, sections were blocked with DIG blocking solution for 30 min and 0.5% TSA blocking reagent (PerkinElmer) for 30 min. The detection was performed with a peroxidase-conjugated anti-fluorescein antibody (1:1000, 1 h, Invitrogen) followed by incubation with the FITC-TSA plus amplification kit (PerkinElmer) for FITC-labeled cRNA probe or with cyanin 3 (Cy3)-TSA plus amplification kit (PerkinElmer) for DIG-labeled cRNA probe. After inactivation of residual peroxidase activities by dipping sections in 1% H_2O_2 for 30 min, sections were subjected to immunostaining.

Immunostaining for phosphorylated S6 (p-S6) was carried out after *in situ* hybridization. Sections were incubated in a blocking solution containing 10% donkey serum and 0.2% Triton X-100 in PBS for 30 min. Sections were immunostained with primary antibody against p-S6 ribosomal protein (Ser235/236) (1:500; #2211, Cell Signaling Technology) overnight at 4°C. The bound antibody was visualized with Cy3 conjugated secondary antibody (1:400; 711-166-152, Jackson ImmunoResearch) or Alexa-488 conjugated secondary antibody (1:400; A11008, Invitrogen) and Hoechst 33258 (SIGMA) was used for staining of cell nuclei. Slides were coverslipped with Vectashield Mounting Medium (H-1000, Vector Laboratories). The brain sections were viewed by the all-in-one fluorescence microscope (BZ-X800, KEYENCE). To analyze horizontal limb of the diagonal band of Broca (HDB) and magnocellular preoptic area (MCPO), we used the right and left sides of a single coronal section at the coordinates of 0.14 mm from bregma. To analyze the other brain regions, we used 2 to 3 coronal sections at the coordinates of 0.5 to 1.18 mm from bregma. Each brain region was identified by aligning the sagittal axis and comparing the sections to the brain atlas (Paxinos and Franklin, 2001). Cell number, fluorescence intensity, and soma size were automatically measured using a hybrid cell count application (BZ-H4C and BZ-H4CM) in the BZ-X analyzer software (BZ-H4A, KEYENCE).

2.4 Open field test

The open field test was used to assess anxiety and locomotor activity as described previously with minor modifications (Saito et al., 2020, 2021). A circular arena (diameter: 75 cm) was used with a wall to prevent mice from escaping (height: 35 cm). The area 50 cm from the center of the circle is defined as the inner zone, and the area outside the inner zone is defined as the outer zone. During the test, mice were placed in the center of the circular arena and allowed to explore freely for 10 min under the moderate light condition (30 lux), and the total distance traveled was recorded and scored by Smart V3.0 tracking software (Panlab).

2.5 Y-maze test

The Y-maze test was used for the assessment of spatial working memory in mice as described previously (Saito et al., 2020). The Y-maze consists of 3 arms that are the same length and have the same distance from each other (50 cm long, 12 cm high, and 4 cm wide). The light conditions on each arm were adjusted to 35 ± 2 lux. The mouse was placed in the center of the maze and allowed to explore freely for 10 min. The number of arm entries and the number of triads were recorded to calculate the percentage of spontaneous alternation. Spontaneous alternation behavior was defined as the entry into all three arms (i.e., arm A, arm B, and arm C) on consecutive choices in triplet set (i.e., ABC, ACB, BAC, BCA, CAB, and CBA). The percentage of spontaneous alternation behavior was calculated as the percentage of actual alterations to possible alternations, defined as (the total number of arm entries – 2).

2.6 Elevated plus maze test

An elevated plus maze test was used to assess anxiety-related behavior in mice as described previously (Saito et al., 2020). The elevated plus maze apparatus consists of two opposing open (25 cm × 8 cm) and two closed arms (25 cm × 8 cm × 20 cm), linked by a neutral area (8 cm × 8 cm) in the center of the apparatus. The entire apparatus was elevated to a height of 5 cm above floor level. The light intensity was adjusted to 20 and 15 lux for open and closed arms, respectively. The mouse was placed in the center of the maze facing the open arm. The mouse was allowed to freely explore the maze for 10 min, and the number of arm entries and the amount of time spent in each arm were recorded.

2.7 Rota-rod test

In order to assess motor coordination and motor learning, we performed the rota-rod test, using Rota-Rod Treadmill (MK660C, Muromachi Kikai), as described previously (Sakai et al., 2019). The mouse was placed on a rotating rod with a 30 mm diameter that accelerated from 4 to 40 rpm over 300 s. The

maximum observation time was 300 s with constant acceleration, and the latency to fall was recorded. The rod was cleaned by ethanol between the trials. The test was performed on 5 consecutive days under bright-light conditions (approximately 800 lux).

2.8 Olfactory habituation and dishabituation test

Olfactory habituation and dishabituation test was performed to assess basic olfactory function and olfactory discrimination (Yang and Crawley, 2009). In this test, acclimation to the test cage was conducted in the separate room from the test room to prevent the mice from exposing the odors before the test. For acclimation to the novel test cage, the mouse was placed in an empty cage and allowed to explore freely for 45 min under the room light conditions (approximately 800 lux). Three odors were presented to the mouse: water (control), vanilla (McCormick), and almond extract (McCormick) (1:100 dilution). Fifty µl of the odors were pipetted onto the tip of the cotton swab. The cotton swab was placed on the wire top of the cage. Each odorant was presented to the mouse 3 times consecutively for 2 min each. Sniffing time was recorded. Active sniffing was defined as the mouse directing its nose 2 cm or closer to the tip of the swab. To analyze the olfactory habituation, the sniffing time of the first and third time of the same odor was compared. To analyze the olfactory dishabituation, the sniffing time was compared between the familiar and novel odors.

2.9 Buried food-seeking test

The buried food-seeking test is used to assess olfactory function and odor-induced food-seeking motivation in mice (Machado et al., 2018). Prior to the test, mice were deprived of food for 22 h. Fresh wood bedding was laid in the test cage and 3 g of food pellets were buried 2 cm or 8 cm beneath the surface. The mouse was placed in the cage under room light conditions (approximately 800 lux) and the latency to reach the food was recorded.

2.10 Three-chamber odor preference test

Three-chamber odor preference behavior test was conducted as previously described with minor modification (Fitzgerald et al., 2014). Rectangular, three-chambered opaque Plexiglas box (BS-402260, BrainScience Idea) was used. The apparatus is separated into three chambers (each chamber is 20 cm long, 40.5 cm wide, 22 cm high) by transparent plates with the door (50 mm width × 80 mm height). Two plastic cups covered with aluminum foil were placed on either side of the chamber (right and left chamber) to contain the odorants. The light condition was 15 lux. This test consists of 2 sessions: a familiarization session and a test session. During the familiarization session, the mouse was placed in the three-chamber arena and allowed to explore freely for 10 min. During the testing period, 3 g of crushed peanuts were placed in one of two plastic cups. In the other plastic cup, cotton soaked in 300 µL of 10% 2,4,5-trimethylthiazole (TMT) (T1068, TCI Chemical) was placed, and the mouse was allowed to explore freely for 10 min. TMT is a component of fox urine, and it is used to induce unconditioned fear and avoidance in mice (Buron et al., 2007). The amount of time spent in each chamber was recorded.

2.11 The *c-Fos* mapping analysis

The *c-Fos* mapping analysis by *in situ* hybridization was performed to detect *c-Fos* expression after the three-chamber odor preference test. The mice that had never performed the behavior tests were divided into two groups, the control group and the experimental group. Three-chamber odor preference tests were performed on the mice in the experimental group as described above. The mice in the control group were placed in the three-chamber with the plastic cups only containing cotton moistened with 300 µL milli-Q water instead of peanuts or 10% TMT. One hour after the experiment, the mice were dissected, and the brain sections were used for the *in situ* hybridization for *c-Fos* mRNA.

2.12 Statistical analysis

The significance of differences ($p < 0.05$) was assessed by Welch's *t*-test for comparison of two groups. In multiple comparison, the significance of differences was evaluated using the analysis of variance (ANOVA) with two-way repeated measure, followed by multiple comparison *post hoc* test; Sidak's for rota-rod tests and *c-Fos* mapping, and Fisher's LSD test for olfactory habituation and dishabituation tests and odor preference tests. All data are expressed as the mean ± standard error of the mean (SEM). The detailed statistical methods and values are described in Supplementary Table S1.

3 Results

3.1 Activation of mTORC1 in striatal MSNs

To examine how activation of mTORC1 pathway affects MSNs in the striatum, we used CAG-mTOR Tg mice in which hyperactive mutant *mTOR*$^{SL1+IT}$ can be conditionally expressed upon excision of the *loxP*-flanked *neo* gene in response to Cre-*loxP* recombination (Kassai et al., 2014; Sakai et al., 2019). The mutant mTOR^{SL1+IT} can retain its kinase activity toward the mTORC1 pathway but not the mTORC2 pathway under the starvation condition in the cultured cells (Ohne et al., 2008) and brains (Kassai et al., 2014). CAG-mTOR Tg mice were crossed with Dlx1-CreER^{T2} mice to obtain Dlx1-mTOR Tg mice (*Dlx1-CreER*^{T2}*/+; CAG-mTOR*$^{SL1+IT}$*/+*) (Figure 1A). Cre recombinase activity was induced by administering tamoxifen to the pregnant mice at 12.5 dpc, when the Dlx1 promoter is highly active in the ventral neural precursors of the ganglionic eminences. The ganglionic eminences contain three subregions; lateral, caudal, and medial ganglionic eminences (LGE, CGE, and MGE). Inhibitory neurons derived from MGE and CGE are distributed in the cerebral cortex, while inhibitory neurons of the striatum and olfactory bulb are derived from LGE. With the single administration of tamoxifen at 12.5 dpc, Cre-*loxP* recombination was expected to induce activation of mTORC1 pathway within the LGE, leaving MGE and CGE unaffected. To visualize tamoxifen-induced Cre-*loxP* recombination in the brain, Dlx1-CreER^{T2} and Dlx1-mTOR Tg mice were crossed with *lacZ*

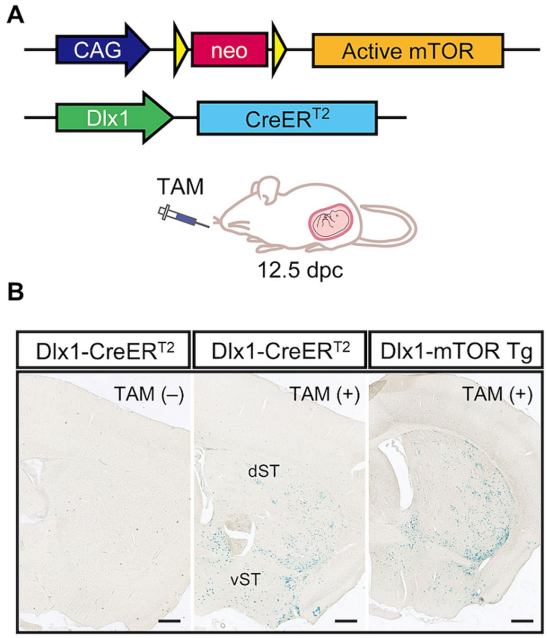

FIGURE 1
Hyperactivation of the mTORC1 pathway in dorsal and ventral striatum. **(A)** Transgenic strategy for conditional expression of active mTOR kinase by the Cre-*loxP* system. Excision of the floxed *neo* gene by Cre recombinase induces the expression of active mTOR driven by CAG promoter. The *Dlx1* promoter drives CreER^{T2} expression, followed by Cre activation induced by tamoxifen administration at 12.5 dpc. **(B)** Expression pattern of Cre recombinase in Dlx1-CreER^{T2} and Dlx1-mTOR Tg mice. Dlx1-CreER^{T2} and Dlx1-mTOR Tg mice were crossed with Cre-activatable *lacZ* reporter mice (ROSA26R-lacZ), and administered tamoxifen at 12.5 dpc. The brain sections were stained with X-gal. Dlx1-CreER^{T2} mice without tamoxifen administration showed no leaky expression of Cre recombinase. Cre expression was restricted in the dorsal and ventral striatum in both Dlx1-CreER^{T2} and Dlx1-mTOR Tg mice. TAM: tamoxifen. Scale bars, 500 μm.

reporter mice (ROSA26R-lacZ mice). Dlx1-CreER^{T2} mice did not show leaky expression of Cre recombinase without tamoxifen administration. Upon tamoxifen administration, both Dlx1-CreER^{T2} and Dlx1-mTOR Tg mice expressed Cre recombinase prominently in the dorsal and ventral striatum leaving the cortical cortex scarcely affected (Figure 1B).

3.2 GABAergic neurons are increased in the ventral striatum upon induction of active mTOR

Dlx1-mTOR Tg mice are viable with no overt abnormality in their appearances. We first observed the brain morphology and the distribution of Cre-activated cells of Dlx1-mTOR Tg mice using *lacZ* reporter mice. Though active mTOR in excitatory neurons leads to impaired neuronal migration (Kassai et al., 2014), the cell distributions of *lacZ*-positive cells in Dlx1-mTOR Tg mice were not different from those in Dlx1-CreER^{T2} mice (Figure 1B). To perform a detailed analysis on the differences caused by the induction of active mTOR in the striatum, we made histological and behavioral analysis on Dlx1-mTOR Tg mice (*Dlx1-CreER^{T2}/+; CAG-mTOR^{SL1+IT}/+*). *CAG-mTOR^{SL1+IT}/+* mice were used as the experimental control mice in the following experiments. We examined the activation of the mTORC1 pathway in the striatum by immunohistochemical analysis for phosphorylation of ribosomal S6 protein, which is used as a readout of mTORC1 activity. The density of p-S6-positive cells was increased in the striatum of Dlx1-mTOR Tg mice (Figures 2E, 3E), while that in the cerebral cortex was not significantly different between Dlx1-mTOR Tg and the control mice (Supplementary Figures S1A,E). To confirm the activation of mTORC1 pathway in the inhibitory neurons, we carried out *in situ* hybridization for *Gad67* mRNA and immunohistochemistry for p-S6 simultaneously in HDB/MCPO, where *Gad67*-positive neurons most densely exist among the ventral striatum (McKenna et al., 2013, Figure 2A). Dlx1-mTOR Tg mice showed increased *Gad67*-positive GABAergic inhibitory neurons compared to the control mice (Figures 2A,B). The soma size of *Gad67*-positive GABAergic inhibitory neurons was also increased in Dlx1-mTOR Tg mice (Figure 2C), while the intensity of *Gad67* mRNA was not significantly changed (Figure 2D). The double staining confirmed that 99% of p-S6-positive mTORC1-hyperactivated neurons were *Gad67*-positive. While *Gad67*-positive GABAergic inhibitory neurons increased in the ventral striatum, the cell density and soma size of *Gad67*-positive GABAergic inhibitory neurons in the cerebral cortex were not significantly different between Dlx1-mTOR Tg and the control mice (Supplementary Figures S1A–C).

3.3 Active mTOR dysregulates the expression pattern of the dopamine receptors in MSNs

MSNs expressing *Drd1*and *Drd2* in the striatum are derived from the subventricular zone progenitors of LGE, and Dlx1 serves a regulatory role in the development of the MSNs (Anderson et al., 1997). To investigate the physiological roles of active mTOR in the differentiation of the MSNs, we carried out *in situ* hybridization for *Drd1* and *Drd2* mRNA in the OT (Figure 3). D1- and D2-type MSNs are densely clustered in the OT, and make up 90% of all the OT neurons (Cansler et al., 2020). The number and soma size of *Drd1*-positive MSNs were increased in the OT of Dlx1-mTOR Tg mice (Figures 3A,C,D). p-S6-positive cells were increased in the OT of Dlx1-mTOR Tg mice (Figure 3E) and signals for *Drd1* mRNA and for p-S6 were overlapped (Figure 3A), suggesting that hyperactivation of mTORC1 pathway increases the *Drd1*-positive MSNs. While *Drd1*-positive MSNs were increased, *Drd2*-positive MSNs were decreased in the OT of Dlx1-mTOR Tg mice, compared to the control mice (Figures 3B,F). The *Drd2* signals and p-S6 signals were mutually exclusive (Figure 3B), and the soma size of *Drd2*-positive MSNs was not significantly changed in the OT of Dlx1-mTOR Tg mice (Figure 3G). These results demonstrate that hyperactivation of mTORC1 pathway in MSNs of the OT dysregulates the dopamine receptor expression pattern, leading to the increase of D1-type MSNs and the decrease of D2-type MSNs.

We also analyzed the expression pattern of dopamine receptors in the dorsal striatum of Dlx1-mTOR Tg mice (Figure 4). Though p-S6-positive cells tended to increase in the dorsal striatum of Dlx1-mTOR Tg mice (Figures 4A,B,G, $p = 0.057$), which suggests a potential elevation in mTORC1 activity in this region, no significant differences were observed in cell number or soma size of *Drd1*- and *Drd2*-positive

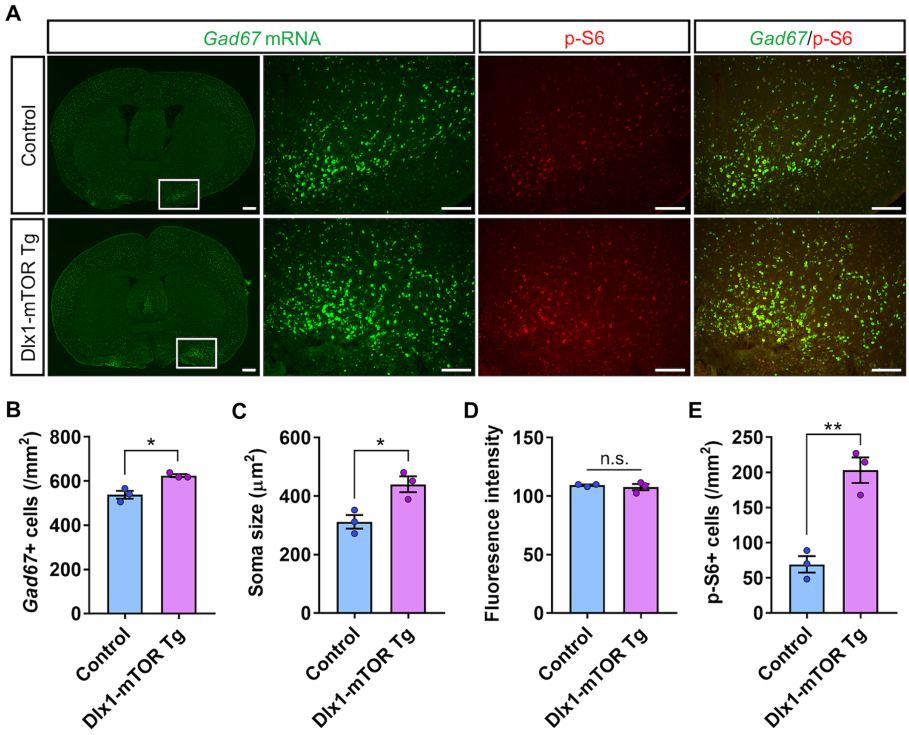

FIGURE 2
Increase of the cell density of GABAergic neurons by hyperactivation of mTORC1 pathway. **(A)** *In situ* hybridization for *Gad67* (green) and immunohistochemistry of p-S6 (red) in the ventral striatum of control and Dlx1-mTOR Tg mice. The cell density **(B)** and the soma size **(C)** of GABAergic neurons were increased in Dlx1-mTOR Tg mice. **(D)** *Gad67* fluorescence intensity. The cell density of p-S6-positive cells **(E)** was increased in Dlx1-mTOR Tg mice. All data are expressed as mean ± SEM. * $p < 0.05$, ** $p < 0.01$, n.s.: not significant. *p*-value was measured by Welch's *t*-test. For each analysis, the right and left sides of a brain slice of each mouse were analyzed ($n = 3$). Scale bars, 500 μm (wide angle images); 200 μm (narrow angle images).

cells between Dlx1-mTOR Tg and the control mice (Figures 4C–F). Taken together, these results demonstrate that hyperactivation of mTORC1 pathway in MSNs dysregulates the dopamine receptor expression pattern in the ventral striatum, while leaving MSNs in the dorsal striatum apparently unaffected. Since we aimed to restrict the Cre-*loxP* recombination to the inhibitory neurons in the striatum, we apply the single administration schedule of tamoxifen at 12.5 dpc. The hyperactivation of mTORC1 pathway in MSNs in dorsal striatum was possibly insufficient to alter the expression of dopamine receptors or make morphological changes, while it might affect the functional differences of MSNs between Dlx1-mTOR Tg and the control mice.

3.4 Hyperlocomotion and dysfunction of motor learning in Dlx1-mTOR Tg mice

We found that activation of mTORC1 signaling in the MSNs of the striatum resulted in increased cell number and size of GABAergic neurons in the ventral striatum. To investigate how these changes in GABAergic neurons affect mouse behaviors, we performed several behavioral experiments. First, to assess the general locomotor activity and anxiety-like behavior, we conducted the open field test. The total distance traveled and mean speed of locomotion in male Dlx1-mTOR Tg mice were increased compared to the control mice (Figures 5A,B), though only the total distance traveled in Dlx1-mTOR Tg mice was increased in the female cohort (Supplementary Figures S2A,B). These results indicate that the hyperactivation of mTORC1 pathway in the MSNs led to the increased general locomotor activity. The transition number between outer and inter zones was not different between two groups (Figure 5C; Supplementary Figure S2C). The time spent in the outer zone was not changed (Figure 5D; Supplementary Figure S2D), suggesting that Dlx1-mTOR Tg mice did not exhibit anxiety-like behavior. Second, to assess the spatial working memory, we performed Y-maze test. The percentage of spontaneous alternation and the number of total entries were not significantly different in Dlx1-mTOR Tg mice compared to the control mice (Figures 5E,F; Supplementary Figures S2E,F). Next, we conducted an elevated plus maze test to assess anxiety-related behavior in Dlx1-mTOR Tg mice. There were no significant differences in the number of total arm entries or time spent in open arm between Dlx1-mTOR Tg mice and the control mice (Figures 5G,H; Supplementary Figures S2G,H).

Dysregulation of the MSNs in the striatum is associated with the motor dysfunction seen in Parkinson's and Huntington's diseases (Chu, 2020; Ehrlich, 2012). Actually, animals with the dysfunction of D1- and D2-type MSNs cause the impairment of the motor behaviors (Bateup et al., 2010; Liang et al., 2022). Therefore, to confirm whether hyperactivation of mTORC1 signaling in the MSNs affects motor coordination and learning, we performed the rota-rod test. Dlx1-mTOR Tg mice showed a significant deficit in the ability to maintain balance on a rotating rod compared to the control mice on day 4, and relatively on day 5 ($p = 0.07$) (Figure 5I), while there was no significant difference in body weight between Dlx1-mTOR Tg and the control

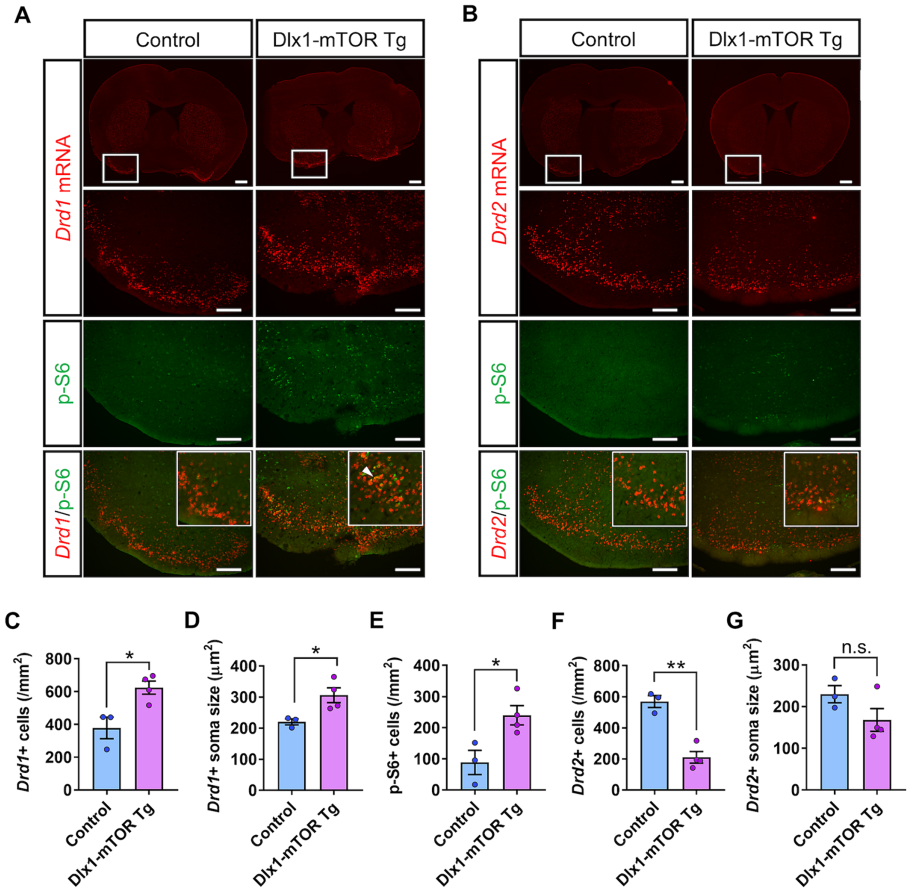

FIGURE 3
Dysregulation of D1- and D2-expressing MSNs in olfactory tubercle by hyperactivation of mTORC1 pathway. **(A)** *In situ* hybridization of *Drd1* (red) and immunohistochemistry of p-S6 (green) in the olfactory tubercle of control and Dlx1-mTOR Tg mice. A white arrowhead shows *Drd1*/p-S6 double positive cells. **(B)** *In situ* hybridization of *Drd2* (red) and immunohistochemistry of p-S6 (green) in the olfactory tubercle of control and Dlx1-mTOR Tg mice. The cell density **(C)** and the soma size **(D)** of *Drd1*-positive cells were increased in Dlx1-mTOR Tg mice. The cell density of p-S6-positive cells **(E)** was increased in Dlx1-mTOR Tg mice. The cell density of *Drd2*-positive cells **(F)** was decreased in Dlx1-mTOR Tg mice. The soma size of *Drd2*-positive cells **(G)** was not significantly different between both groups. All data are expressed as mean ± SEM. * $p < 0.05$, ** $p < 0.01$, n.s.: not significant. p-value was measured by Welch's t-test. For each analysis, 3 brain slices of each mouse were analyzed ($n = 3$ for control, $n = 4$ for Dlx1-mTOR Tg mice). Scale bars, 500 μm (wide angle images); 200 μm (narrow angle images).

mice (Figure 5J). The female cohort also showed significantly shorter time to fall on day 4 and 5 in Dlx1-mTOR Tg mice (Supplementary Figure S2I), though it is difficult to compare Dlx1-mTOR Tg mice to the control mice because of the increased body weight in Dlx1-mTOR Tg mice (Supplementary Figure S2J).

3.5 Impaired odor preference behavior in Dlx1-mTOR Tg mice

Hyperactivation of mTORC1 signaling in the MSNs resulted in increased cell density of inhibitory neurons and p-S6-positive cells in the ventral striatum. The ventral striatum receives direct input from olfactory bulb, and includes many brain areas involved in olfactory behaviors, such as nucleus accumbens, OT and HDB/MCPO. To assess whether the active mTOR in MSNs affects the olfactory function, we carried out several olfactory behavior tests. First, we performed the olfactory habituation and dishabituation test to measure the basic olfaction and olfactory discrimination behavior in Dlx1-mTOR Tg mice. When we repeatedly presented the same odor to Dlx1-mTOR Tg mice, the sniffing time was gradually decreased within each trial (Figure 6A, $p < 0.05$). On the other hand, when a novel odor was presented, the sniffing time was increased compared to familiar odors (Figure 6A, $p < 0.05$). These results indicated that the basic olfactory function and olfactory discrimination behavior were not impaired in Dlx-mTORC1 Tg mice.

The OT interconnects with amygdala, thalamus, hypothalamus, hippocampus, and brain stem, and is considered as an important area for multi-sensory processing (Wesson and Wilson, 2011). For instance, the OT is involved in the food-seeking-related motivation, odor preference and reward cognition (Murata et al., 2015; Fitzgerald et al., 2014). Therefore, we carried out the buried food-seeking test to assess the odor-induced food-seeking motivation of Dlx1-mTOR Tg mice. There was no significant difference in the latency to reach the reward food between Dlx1-mTORC1 Tg and the control mice (Figures 6B,C). Our results suggest that the odor-induced food-seeking motivation of Dlx1-mTOR Tg mice was not affected by active mTOR. Next, to examine the influence of mTOR activation in MSNs

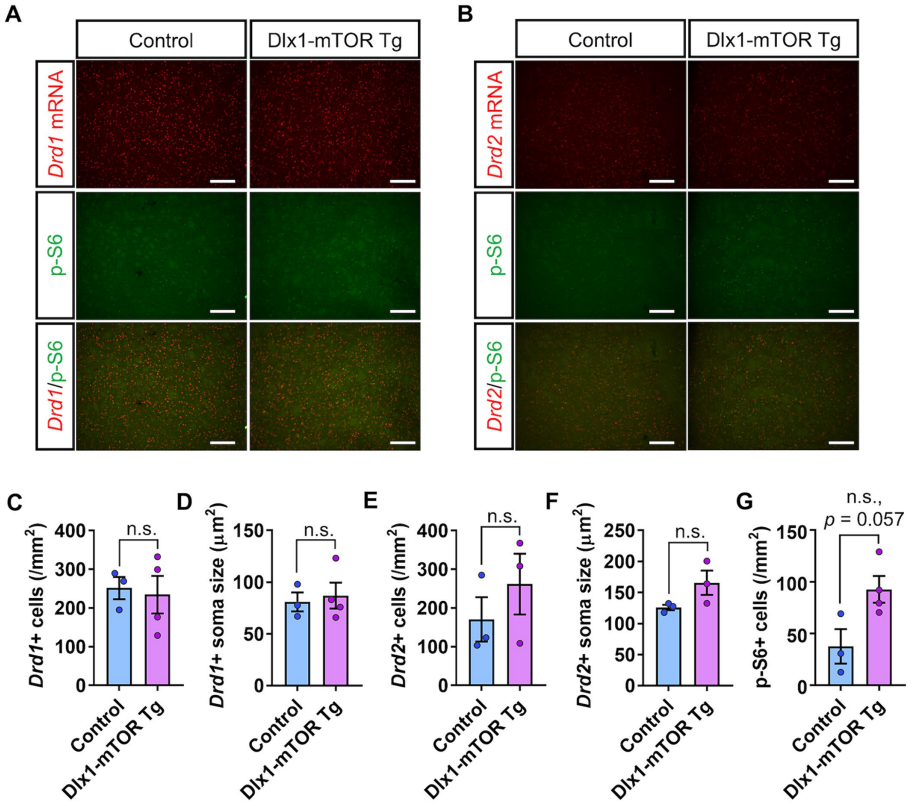

FIGURE 4
D1- and D2-expressing MSNs in dorsal striatum of Dlx1-mTOR Tg mice. **(A)** *In situ* hybridization of *Drd1* (red) and immunohistochemistry of p-S6 (green) in the dorsal striatum of control and Dlx1-mTOR Tg mice. **(B)** *In situ* hybridization of *Drd2* (red) and immunohistochemistry of p-S6 (green) in the dorsal striatum of control and Dlx1-mTOR Tg mice. The cell density **(C)** and the soma size **(D)** of *Drd1*-positive cells. The cell density **(E)** and the soma size **(F)** of *Drd2*- positive cells. The cell density of p-S6-positive cells **(G)**. All data are expressed as mean ± SEM; n.s.: not significant. *p*-value was measured by Welch's *t*-test. For each analysis, 3 brain slices of each mouse were analyzed ($n = 3$ for control, $n = 4$ for Dlx1-mTOR Tg mice). Scale bars, 200 μm.

on odor preference behavior, we performed three-chamber odor preference test (Figure 6D). In general, mice prefer peanuts odor and avoid the TMT odor, a component of fox urine, and therefore, mice tend to spend more time in the chamber with peanuts. In the control mice, time spent in the peanut chamber was significantly longer than that in the TMT chamber (Figure 6E). However, in Dlx1-mTOR Tg mice, there was no significant difference between the time spent in the peanut and TMT chambers. These results suggest that the preference for the peanut chamber was abolished in Dlx1-mTOR Tg mice.

3.6 Olfactory circuit in piriform cortex was altered in Dlx1-mTOR Tg mice

To assess the alteration of neural circuit in odor preference behavior, *in situ* hybridization of *c-Fos* in the olfactory cortex was performed after three-chamber odor preference test. Dlx1-mTOR Tg and the control mice were divided into two groups, the odor-guided experimental group and the odor-free control group. The three-chamber odor preference tests were performed using peanut and 10% TMT for the odor-guided group and using only water for the odor-free group. The control mice in odor-guided experimental group showed increased *c-Fos* signals in piriform cortex but not in other olfactory cortex areas including the OT. No significant difference was detected between the odor-guided and odor-free groups of Dlx1-mTOR Tg mice (Figures 7A,B). These results indicate that hyperactivation of mTORC1 pathway in MSNs altered the neuronal activation in the piriform cortex during the odor preference behavior.

4 Discussion

In this study, we demonstrated that hyperactivation of mTORC1 signaling has a significant impact on cell size regulation and dopamine receptor expression patterns in striatal MSNs. We also showed the impaired motor learning and disrupted odor preference behavior in Dlx1-mTOR Tg mice. Previous animal models for mTOR activation in inhibitory neurons have shown enlarged soma size and disrupted functional development of the cortical interneurons (Fu et al., 2012; Malik et al., 2019; Amegandjin et al., 2021). Morphological and functional impairment of inhibitory neurons of the striatum of Dlx1-mTOR Tg mice were consistent with these results. Mice with SST-specific and PV-specific conditional deletion of *Pten* gene demonstrated impaired motor learning and social deficits (Shin et al., 2021). Impaired motor learning in Dlx1-mTOR Tg mice was consistent with this result. However, our animal model of striatal specific hyperactivation of mTOR showed several different

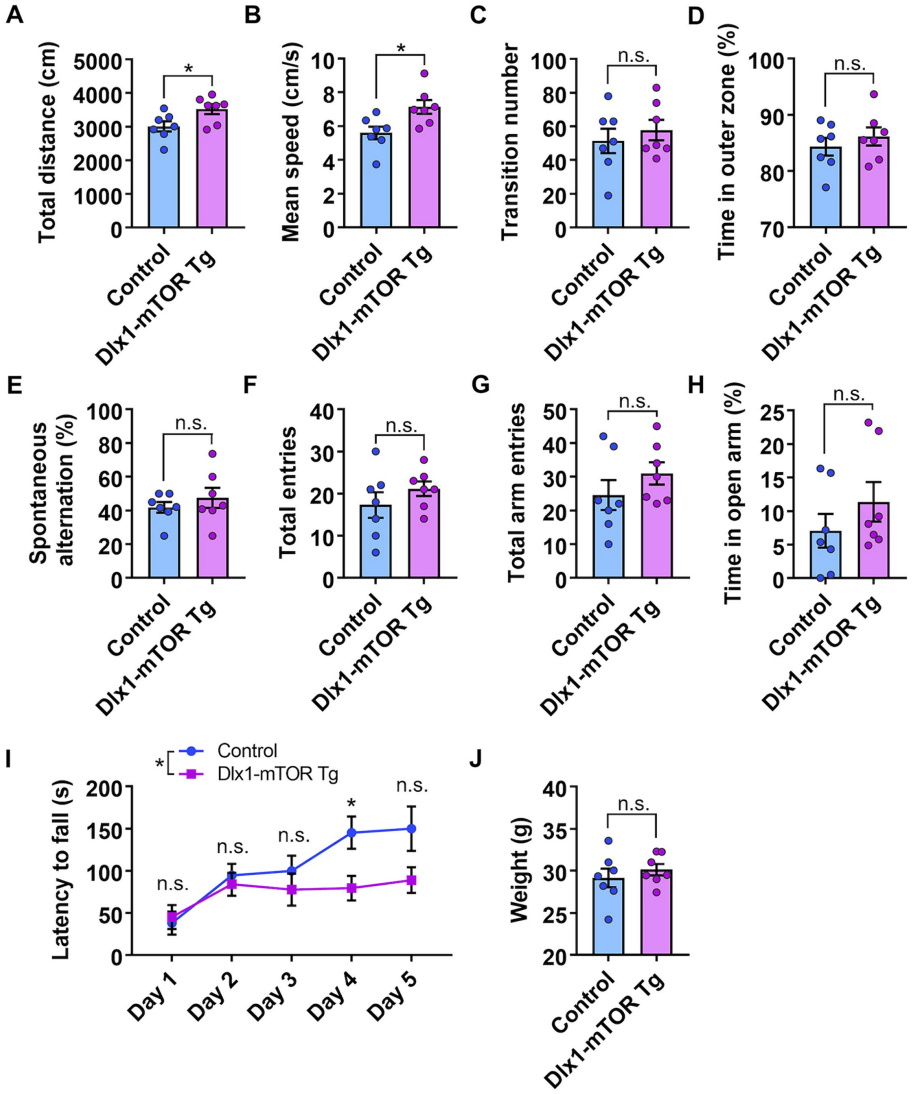

FIGURE 5
Hyperlocomotion and dysfunction of motor learning in Dlx1-mTOR Tg mice. **(A–D)** Open field test. The total distance traveled **(A)** and the mean speed **(B)** in the open field test were increased in Dlx1-mTOR Tg mice. **(C)** The transition times between outer and inner zones. **(D)** The percentage of time spent in the outer zone. **(E,F)** Y-mase test. The percentage of spontaneous alternation **(E)** and total arm entries **(F)**. **(G,H)** Elevated plus maze test. Total arm entries **(G)** and spent time in the open arm **(H)**. **(I,J)** Rota-rod test. The latency to fall off the rotating rod **(I)** and the body weight at day 1 **(J)**. All data are expressed as mean ± SEM. * $p < 0.05$, n.s.: not significant. p-value was measured by Welch's t-test, except for the rota-rod test. For rota-rod test, two-way ANOVA was performed to compare 2 groups, and the p-value in each day was analyzed by Sidak's multiple comparisons test. Each point represents data from an individual male mouse ($n = 7$).

phenotypes including olfactory preference behavior from the other models.

With our tamoxifen administration schedule, Dlx1-mTOR Tg mice showed maximum induction of Cre-*loxP* recombination and resulted in highly abnormal MSNs in the ventral striatum. Ventral striatum not only functions as the center of reward-guided behaviors but also has the pivotal role in olfactory-related behaviors. We found that sustained activation of mTORC1 pathway impaired odor preference behavior, leaving the fundamental sensing of olfaction preserved. As D1- and D2-type MSNs in OT regulate odor-attractive and odor-aversive behaviors, respectively (Murata, 2020), dysregulated expression of dopamine receptors seems to have caused loss of preference for peanuts odor against TMT. Moreover, *in situ* hybridization analysis for *c-Fos* showed that the neuronal activation of the piriform cortex during the odor preference behavior was inhibited in Dlx1-mTOR Tg mice. Though the neural circuits underlying the olfactory preference behavior are still unrevealed, the results provide fascinating insights into the possible projection of the striatal MSNs to the piriform cortex regulating the odor preference behavior. The piriform cortex is the largest component of the olfactory cortex and OT has the massive input proportion from piriform cortex (Bekkers and Suzuki, 2013). Though the reciprocal connections between piriform cortex and the other olfactory cortex, including OT, have been revealed (Zhang et al., 2017; Wang et al., 2020), the function of the neuronal circuits between piriform cortex and the other olfactory cortex are still unclear. Further investigation is needed to

10.3389/fnins.2024.1461178

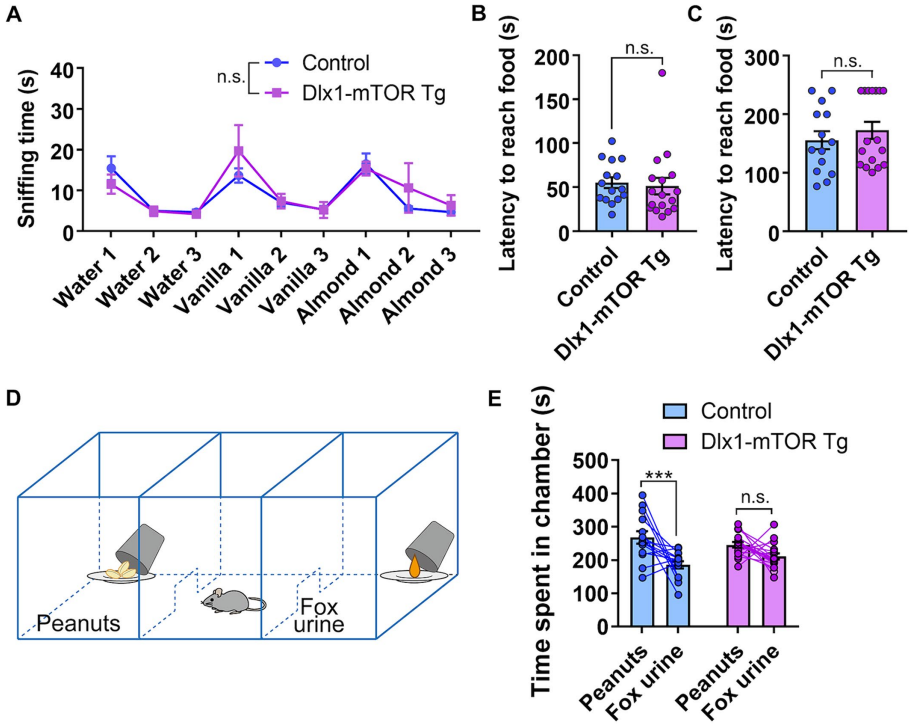

FIGURE 6
Disruption of odor preference behavior in Dlx1-mTOR Tg mice. **(A)** The sniffing time for each odor in olfactory habituation and dishabituation test. **(B,C)** Buried food-seeking test. The latency to reach the food with 2 cm **(B)** and 8 cm bedding **(C)**. **(D)** Schema of three-chamber odor preference test. **(E)** Time spent in each chamber during three-chamber odor preference test. All data are expressed as mean ± SEM. *** $p < 0.001$, n.s.: not significant. p-value was measured by Welch's t-test, except for the olfactory habituation and dishabituation test and the odor preference behavior test. For the olfactory habituation and dishabituation test and the odor preference behavior test, two-way ANOVA followed by Fisher's LSD multiple comparisons test was used to calculate the p-value. Each point represents data from an individual mouse [$n = 15$ for control, $n = 17$ for Dlx1-mTOR Tg mice in **(A–C)**, n = 14 for control, n = 17 for Dlx1-mTOR Tg mice in **(E)**].

elucidate the neuronal mechanism underlying the olfactory preference behavior.

Hyperactivation of mTOR in Dlx1-mTOR Tg mice increases D1-type MSNs and decreases D2-type MSNs in the ventral striatum. Further, MSNs in the dorsal striatum might have been affected in Dlx1-mTOR Tg mice, since p-S6 positive cells were relatively increased in the dorsal striatum. Dysregulation of D1- and D2-type MSNs in dorsal striatum is reported in patients harboring neurodegenerative diseases including Parkinson's disease and Huntington's disease (Stephens et al., 2005; Cicchetti et al., 2000). To examine the function of D1- and D2-type MSNs, several animal models were generated. Conditional KO of dopamine- and cAMP-regulated phosphoprotein Mr. 32 kDa (DARPP-32), which regulates dopamine signaling, in D1- and D2-type MSNs both altered motor behaviors (Bateup et al., 2010). While D1-expressing cell-specific DARPP-32 KO mice showed decreased basal locomotor activity, D2-expressing cell-specific DARPP-32 KO mice showed increased basal locomotor activity, which was consistent with our results showing the increased total distance traveled and mean speed of locomotion in Dlx1-mTOR Tg mice in open field test. D1- and D2-type MSNs are also important in motor learning, which was indicated by the impaired locomotor activity and motor learning in whole-body D1 and D2 KO mice (Nakamura et al., 2014). Further, conditional KO of D2 in indirect pathway projecting MSNs showed dysfunction of motor and other learning skills (Augustin et al., 2020), which was consistent with our results showing the impaired performance of Dlx1-mTOR Tg mice on the rota-rod test. Though the further investigation is indispensable for understanding the mechanism, impaired motor learning of Dlx1-mTOR Tg mice might have been caused by the impaired function of MSNs in dorsal striatam.

The striatum-specific hyperactivation of mTOR revealed that mTORC1 signaling plays an important role in morphological and functional development of MSNs and the dysregulated MSNs caused the impaired motor learning and odor preference. Though the dysregulated MSNs in dorsal striatum and the motor abnormalities have been already reported in patients with Parkinson's disease and Huntington's disease, our study showed the pivotal insight into the contribution of mTORC1 pathway to the motor abnormalities in neurodegenerative diseases. Further, our animal model showed impaired odor preference. The hyperactivation of mTORC1 pathway occurs in the inhibitory neurons of TSC patients exhibiting neuropsychiatric symptoms such as ASD. Our results imply the relationships between the sensory defects in mTOR-related neuropsychiatric disease and activation of mTORC1 pathway in the inhibitory neurons of the striatum. Further investigation is needed to elucidate the underlying mechanism.

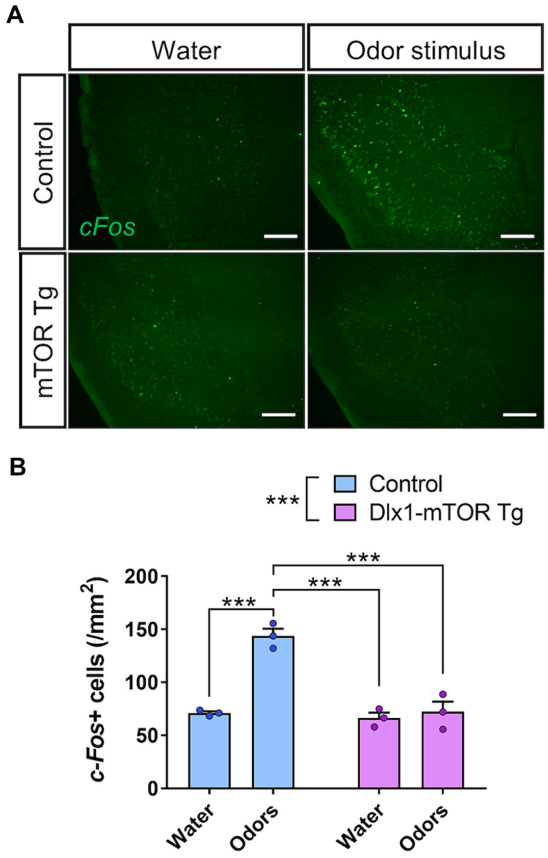

FIGURE 7
Impairment of olfactory circuit in piriform cortex of Dlx1-mTOR Tg mice. **(A)** *In situ* hybridization of *c-Fos* in the piriform cortex of the control and Dlx1-mTOR Tg mice. Neuronal activity was increased by odors in control but not in Dlx1-mTOR Tg mice. **(B)** The cell density of *c-Fos*-positive cells in the piriform cortex. All data are expressed as mean ± SEM. *** $p < 0.001$, n.s.: not significant. Two-way ANOVA followed by Sidak's multiple comparisons test was used to calculate the *p*-value. For the analysis, 2 brain slices of each mouse were analyzed ($n = 3$). Scale bars, 200 μm.

Data availability statement

The raw data supporting the conclusions of this article will be made available by the authors, without undue reservation.

Ethics statement

The animal study was approved by the Institutional Animal Care and Use Committee of the University of Tokyo. The study was conducted in accordance with the local legislation and institutional requirements.

Author contributions

LC: Conceptualization, Formal analysis, Investigation, Methodology, Resources, Writing – original draft. RS: Visualization, Writing – review & editing. SN-N: Validation, Writing – review & editing. HK: Resources, Writing – review & editing. AA: Project administration, Supervision, Writing – review & editing, Funding acquisition.

Funding

The author(s) declare that financial support was received for the research, authorship, and/or publication of this article. This research was supported by Japan Agency for Medical Research and Development (AMED) under grant number JP19dm0207071 (AA).

Acknowledgments

We thank Dr. Hiroki Kurihara for providing Dlx1-CreER^{T2} and Rosa26R-lacZ mice, Dr. Masahiko Watanabe for plasmids carrying *Gad67*, *Drd1*, and *Drd2*, and Dr. Haruhiko Bito for a plasmid carrying *c-Fos*, Dr. Yusuke Sakai for providing advice for behavioral analysis, Mr. Motoki Goto, Dr. Ryoko Kudo, and Ms. Moe Tamano for generation of the Tg mice, Dr. Toshikuni Sasaoka, Dr. Yuichi Hiraoka and Dr. Harumi Nakao for their useful advice to improve our manuscript.

Conflict of interest

The authors declare that the research was conducted in the absence of any commercial or financial relationships that could be construed as a potential conflict of interest.

Publisher's note

All claims expressed in this article are solely those of the authors and do not necessarily represent those of their affiliated organizations, or those of the publisher, the editors and the reviewers. Any product that may be evaluated in this article, or claim that may be made by its manufacturer, is not guaranteed or endorsed by the publisher.

Supplementary material

The Supplementary material for this article can be found online at: https://www.frontiersin.org/articles/10.3389/fnins.2024.1461178/full#supplementary-material

References

Albert, V., and Hall, M. N. (2015). mTOR signaling in cellular and organismal energetics. *Curr. Opin. Cell Biol.* 33, 55–66. doi: 10.1016/j.ceb.2014.12.001

Amegandjin, C. A., Choudhury, M., Jadhav, V., Carriço, J. N., Quintal, A., Berryer, M., et al. (2021). Sensitive period for rescuing parvalbumin interneurons connectivity and social behavior deficits caused by TSC1 loss. *Nat. Commun.* 12:3653. doi: 10.1038/s41467-021-23939-7

Anderson, S. A., Qiu, M., Bulfone, A., Eisenstat, D. D., Meneses, J., Pederson, R., et al. (1997). Mutations of the homeobox genes Dlx-1 and Dlx-2 disrupt the striatal

subventricular zone and differentiation of late born striatal neurons. *Neuron* 19, 27–37. doi: 10.1016/s0896-6273(00)80345-1

Augustin, S. M., Loewinger, G. C., O'Neal, T. J., Kravitz, A. V., and Lovinger, D. M. (2020). Dopamine D2 receptor signaling on iMSNs is required for initiation and vigor of learned actions. *Neuropsychopharmacology* 45, 2087–2097. doi: 10.1038/s41386-020-00799-1

Bateup, H. S., Santini, E., Shen, W., Birnbaum, S., Valjent, E., Surmeier, D. J., et al. (2010). Distinct subclasses of medium spiny neurons differentially regulate striatal motor behaviors. *Proc. Natl. Acad. Sci. USA* 107, 14845–14850. doi: 10.1073/pnas.1009874107

Benthall, K. N., Cording, K. R., Agopyan-Miu, A. H. C. W., Wong, C. D., Chen, E. Y., and Bateup, H. S. (2021). Loss of Tsc1 from striatal direct pathway neurons impairs endocannabinoid-LTD and enhances motor routine learning. *Cell Rep.* 36:109511. doi: 10.1016/j.celrep.2021.109511

Bekkers, J. M., and Suzuki, N. (2013). Neurons and circuits for odor processing in the piriform cortex. *Trends Neurosci.* 36, 429–438. doi: 10.1016/j.tins.2013.04.005

Bové, J., Martínez-Vicente, M., and Vila, M. (2011). Fighting neurodegeneration with rapamycin: mechanistic insights. *Nat. Rev. Neurosci.* 12, 437–452. doi: 10.1038/nrn3068

Buron, G., Hacquemand, R., Pourie, G., Lucarz, A., Jacquot, L., and Brand, G. (2007). Comparative behavioral effects between synthetic 2,4,5-trimethylthiazoline (TMT) and the odor of natural fox (*Vulpes vulpes*) feces in mice. *Behav. Neurosci.* 121, 1063–1072. doi: 10.1037/0735-7044.121.5.1063

Busquets-Garcia, A., Gomis-González, M., Guegan, T., Agustín-Pavón, C., Pastor, A., Mato, S., et al. (2013). Targeting the endocannabinoid system in the treatment of fragile X syndrome. *Nat. Med.* 19, 603–607. doi: 10.1038/nm.3127

Cansler, H. L., Wright, K. N., Stetzik, L. A., and Wesson, D. W. (2020). Neurochemical organization of the ventral striatum's olfactory tubercle. *J. Neurochem.* 152, 425–448. doi: 10.1111/jnc.14919

Chu, H.-Y. (2020). Synaptic and cellular plasticity in Parkinson's disease. *Acta Pharmacol. Sin.* 41, 447–452. doi: 10.1038/s41401-020-0371-0

Cicchetti, F., Prensa, L., Wu, Y., and Parent, A. (2000). Chemical anatomy of striatal interneurons in normal individuals and in patients with Huntington's disease. *Brain Res. Brain Res. Rev.* 34, 80–101. doi: 10.1016/s0165-0173(00)00039-4

Ehrlich, M. E. (2012). Huntington's disease and the striatal medium spiny neuron: cell-autonomous and non-cell-autonomous mechanisms of disease. *Neurotherapeutics* 9, 270–284. doi: 10.1007/s13311-012-0112-2

Fitzgerald, B. J., Richardson, K., and Wesson, D. W. (2014). Olfactory tubercle stimulation alters odor preference behavior and recruits forebrain reward and motivational centers. *Front. Behav. Neurosci.* 8:81. doi: 10.3389/fnbeh.2014.00081

Foster, K. G., and Fingar, D. C. (2010). Mammalian target of rapamycin (mTOR): conducting the cellular signaling symphony. *J. Biol. Chem.* 285, 14071–14077. doi: 10.1074/jbc.R109.094003

Fu, C., Cawthon, B., Clinkscales, W., Bruce, A., Winzenburger, P., and Ess, K. C. (2012). GABAergic interneuron development and function is modulated by the Tsc1 gene. *Cereb. Cortex* 22, 2111–2119. doi: 10.1093/cercor/bhr300

Ikemoto, S. (2007). Dopamine reward circuitry: two projection systems from the ventral midbrain to the nucleus accumbens-olfactory tubercle complex. *Brain Res. Rev.* 56, 27–78. doi: 10.1016/j.brainresrev.2007.05.004

Jaworski, J., and Sheng, M. (2006). The growing role of mTOR in neuronal development and plasticity. *Mol. Neurobiol.* 34, 205–219. doi: 10.1385/MN:34:3:205

Kassai, H., Sugaya, Y., Noda, S., Nakao, K., Maeda, T., Kano, M., et al. (2014). Selective activation of mTORC1 signaling recapitulates microcephaly, tuberous sclerosis, and neurodegenerative diseases. *Cell Rep.* 7, 1626–1639. doi: 10.1016/j.celrep.2014.04.048

Laplante, M., and Sabatini, D. M. (2012). mTOR signaling in growth control and disease. *Cell* 149, 274–293. doi: 10.1016/j.cell.2012.03.017

Liang, B., Zhang, L., Zhang, Y., Werner, C. T., Beacher, N. J., Denman, A. J., et al. (2022). Striatal direct pathway neurons play leading roles in accelerating rotarod motor skill learning. *iScience.* 25:104245. doi: 10.1016/j.isci.2022.104245

Machado, C. F., Reis-Silva, T. M., Lyra, C. S., Felicio, L. F., and Malnic, B. (2018). Buried food-seeking test for the assessment of olfactory detection in mice. *Bio. Protoc.* 8:e2897. doi: 10.21769/BioProtoc.2897

Malik, R., Pai, E. L.-L., Rubin, A. N., Stafford, A. M., Angara, K., Minasi, P., et al. (2019). Tsc1 represses parvalbumin expression and fast-spiking properties in somatostatin lineage cortical interneurons. *Nat. Commun.* 10:4994. doi: 10.1038/s41467-019-12962-4

McKenna, J. T., Yang, C., Franciosi, S., Winston, S., Abarr, K. K., Rigby, M. S., et al. (2013). Distribution and intrinsic membrane properties of basal forebrain GABAergic and parvalbumin neurons in the mouse. *J. Comp. Neurol.* 521, 1225–1250. doi: 10.1002/cne.23290

Murata, K., Kanno, M., Ieki, N., Mori, K., and Yamaguchi, M. (2015). Mapping of learned odor-induced motivated behaviors in the mouse olfactory tubercle. *J. Neurosci.* 35, 10581–10599. doi: 10.1523/JNEUROSCI.0073-15.2015

Murata, K. (2020). Hypothetical roles of the olfactory tubercle in odor-guided eating behavior. *Front. Neural. Circuits.* 14:577880. doi: 10.3389/fncir.2020.577880

Nakamura, T., Sato, A., Kitsukawa, T., Momiyama, T., Yamamori, T., and Sasaoka, T. (2014). Distinct motor impairments of dopamine D1 and D2 receptor knockout mice revealed by three types of motor behavior. *Front. Integr. Neurosci.* 8:56. doi: 10.3389/fnint.2014.00056

Ohne, Y., Takahara, T., Hatakeyama, R., Matsuzaki, T., Noda, M., Mizushima, N., et al. (2008). Isolation of hyperactive mutants of mammalian target of rapamycin. *J. Biol. Chem.* 283, 31861–31870. doi: 10.1074/jbc.M801546200

Orlova, K. A., and Crino, P. B. (2010). The tuberous sclerosis complex. *Ann. N. Y. Acad. Sci.* 1184, 87–105. doi: 10.1111/j.1749-6632.2009.05117.x

Paxinos, G., and Franklin, K. B. J. (2001). The mouse brain in stereotaxic coordinates. *2nd* Edn. Cambridge, MA: Academic Press.

Pryor, W. M., Biagioli, M., Shahani, N., Swarnkar, S., Huang, W.-C., Page, D. T., et al. (2014). Huntingtin promotes mTORC1 signaling in the pathogenesis of Huntington's disease. *Sci. Signal.* 7:ra103. doi: 10.1126/scisignal.2005633

Saito, R., Koebis, M., Nagai, T., Shimizu, K., Liao, J., Wulaer, B., et al. (2020). Comprehensive analysis of a novel mouse model of the 22q11.2 deletion syndrome: a model with the most common 3.0-Mb deletion at the human 22q11.2 locus. *Transl. Psychiatry* 10:35. doi: 10.1038/s41398-020-0723-z

Saito, R., Miyoshi, C., Koebis, M., Kushima, I., Nakao, K., Mori, D., et al. (2021). Two novel mouse models mimicking minor deletions in 22q11.2 deletion syndrome revealed the contribution of each deleted region to psychiatric disorders. *Mol. Brain* 14:68. doi: 10.1186/s13041-021-00778-7

Sakai, Y., Kassai, H., Nakayama, H., Fukaya, M., Maeda, T., Nakao, K., et al. (2019). Hyperactivation of mTORC1 disrupts cellular homeostasis in cerebellar Purkinje cells. *Sci. Rep.* 9:2799. doi: 10.1038/s41598-019-38730-4

Santini, E., Heiman, M., Greengard, P., Valjent, E., and Fisone, G. (2009). Inhibition of mTOR signaling in Parkinson's disease prevents L-DOPA-induced dyskinesia. *Sci. Signal.* 2:ra36. doi: 10.1126/scisignal.2000308

Sato, A., Kasai, S., Kobayashi, T., Takamatsu, Y., Hino, O., Ikeda, K., et al. (2012). Rapamycin reverses impaired social interaction in mouse models of tuberous sclerosis complex. *Nat. Commun.* 3:1292. doi: 10.1038/ncomms2295

Shin, S., Santi, A., and Huang, S. (2021). Conditional Pten knockout in parvalbumin- or somatostatin-positive neurons sufficiently leads to autism-related behavioral phenotypes. *Mol. Brain* 14:24. doi: 10.1186/s13041-021-00731-8

Soriano, P. (1999). Generalized lacZ expression with the ROSA26 Cre reporter strain. *Nat. Genet.* 21, 70–71. doi: 10.1038/5007

Stephens, B., Mueller, A. J., Shering, A. F., Hood, S. H., Taggart, P., Arbuthnott, G. W., et al. (2005). Evidence of a breakdown of corticostriatal connections in Parkinson's disease. *Neuroscience* 132, 741–754. doi: 10.1016/j.neuroscience.2005.01.007

Taniguchi, H., He, M., Wu, P., Kim, S., Paik, R., Sugino, K., et al. (2011). A resource of Cre driver lines for genetic targeting of GABAergic neurons in cerebral cortex. *Neuron* 71, 995–1013. doi: 10.1016/j.neuron.2011.07.026

Wang, L., Zhang, Z., Chen, J., Manyande, A., Haddad, R., Liu, Q., et al. (2020). Cell-type-specific whole-brain direct inputs to the anterior and posterior piriform cortex. *Front. Neural. Circuits.* 14:4. doi: 10.3389/fncir.2020.00004

Wesson, D. W., and Wilson, D. A. (2011). Sniffing out the contributions of the olfactory tubercle to the sense of smell: hedonics, sensory integration, and more? *Neurosci. Biobehav. Rev.* 35, 655–668. doi: 10.1016/j.neubiorev.2010.08.004

Yager, L. M., Garcia, A. F., Wunsch, A. M., and Ferguson, S. M. (2015). The ins and outs of the striatum: role in drug addiction. *Neuroscience* 301, 529–541. doi: 10.1016/j.neuroscience.2015.06.033

Yamasaki, M., Matsui, M., and Watanabe, M. (2010). Preferential localization of muscarinic M1 receptor on dendritic shaft and spine of cortical pyramidal cells and its anatomical evidence for volume transmission. *J. Neurosci.* 30, 4408–4418. doi: 10.1523/JNEUROSCI.5719-09.2010

Yang, M., and Crawley, J. N. (2009). Simple behavioral assessment of mouse olfaction. *Curr. Protoc. Neurosci.* 8, Unit 8.24–Unit 8.12. doi: 10.1002/0471142301.ns0824s48

Zhang, Z., Zhang, H., Wen, P., Zhu, X., Wang, L., Liu, Q., et al. (2017). Whole-brain mapping of the inputs and outputs of the medial part of the olfactory tubercle. *Front. Neural. Circuits* 11:52. doi: 10.3389/fncir.2017.00052

frontiers | Frontiers in Molecular Neuroscience

TYPE Original Research
PUBLISHED 14 October 2024
DOI 10.3389/fnmol.2024.1483238

OPEN ACCESS

EDITED BY
Nicola Simola,
University of Cagliari, Italy

REVIEWED BY
Roberto Henzi,
Temuco Catholic University, Chile
Amanda Alves Marcelino Da Silva,
Universidade de Pernambuco, Brazil

*CORRESPONDENCE
Mohammad Naderi
✉ naderimohd@gmail.com

RECEIVED 19 August 2024
ACCEPTED 26 September 2024
PUBLISHED 14 October 2024

CITATION
Naderi M, Nguyen TMN, Pompili C and Kwong RWM (2024) Unraveling the socio-cognitive consequences of KCC2 disruption in zebrafish: implications for neurodevelopmental disorders and therapeutic interventions.
Front. Mol. Neurosci. 17:1483238.
doi: 10.3389/fnmol.2024.1483238

Unraveling the socio-cognitive consequences of KCC2 disruption in zebrafish: implications for neurodevelopmental disorders and therapeutic interventions

Mohammad Naderi*, Thi My Nhi Nguyen, Christopher Pompili and Raymond W. M. Kwong

Department of Biology, York University, Toronto, ON, Canada

During postnatal brain development, maintaining a delicate balance between excitation and inhibition (E/I) is essential for the precise formation of neuronal circuits. The K+/cl– cotransporter 2 (KCC2) is instrumental in this process, and its dysregulation is implicated in various neurological disorders. This study utilized zebrafish (*Danio rerio*) to investigate the socio-cognitive consequences of KCC2 disruption. Through CRISPR-Cas9 technology, biallelic *kcc2a* knockout zebrafish larvae were generated, revealing behavioral abnormalities, including impaired social interactions and memory deficits. Molecular analyses unveiled alterations in key genes associated with the GABAergic and glutamatergic systems, potentially contributing to E/I imbalance. Additionally, KCC2 disruption influenced the expression of oxytocin and BDNF, crucial regulators of social behaviors, synaptic plasticity, and memory formation. The study also explored the therapeutic potential of KCC2 modulation using pharmaceuticals, showing the rescuing effects of CLP-290 and LIT-001 on social abnormalities. However, the selective impact of LIT-001 on social behaviors, not memory, highlights the complexity of neurobehavioral modulation. In summary, this study sheds light on the pivotal role of KCC2 in shaping socio-cognitive functions and suggests potential therapeutic avenues for KCC2-related neurological disorders.

KEYWORDS

K^+/Cl^- cotransporter 2, zebrafish (*Danio rerio*), memory, oxytocin, excitation inhibition balance

1 Introduction

A delicate equilibrium between excitation and inhibition (E/I) of neurons and neuronal networks is crucial for the normal functioning of the central nervous system (CNS), ensuring precise neural communication and information processing (Buzsáki et al., 2007; Sohal and Rubenstein, 2019). The K^+/Cl^- cotransporter 2 (KCC2/SLC12A5) is an evolutionarily conserved neuron-specific cation-chloride cotransporter that plays a vital role in establishing and maintaining this balance. KCC2 maintains neuronal chloride homeostasis and determines the hyperpolarizing activity of γ-aminobutyric acid A ($GABA_A$) receptors. GABA exhibits an excitatory role during early brain development, transitioning to an inhibitory neurotransmitter in the mature brain. This dynamic nature of GABAergic transmission arises from alterations

in the chloride (Cl^-) gradient (Kaila et al., 2014). During the initial stages of brain development, the Na^+–K^+– Cl^- cotransporter 1 (NKCC1) predominates, facilitating the intracellular accumulation of chloride ions. Subsequently, the activation of $GABA_A$Rs triggers the efflux of Cl^- ions, thereby inducing membrane depolarization. As the nervous system matures, up-regulation of the neuronal chloride extruder KCC2 and down-regulation of NKCC1 cause a progressive reduction of intracellular Cl^- concentration in neurons, resulting in a hyperpolarizing shift of Cl^- reversal potential and an excitation-to-inhibition switch of GABAergic action (Ben-Ari et al., 2007). Besides the chloride extrusion function, KCC2 promotes functional maintenance and plasticity of glutamatergic synapses (Li et al., 2007; Gauvain et al., 2011; Chevy et al., 2015). In line with its pivotal role in regulating inhibitory and excitatory neurotransmission, alterations in KCC2 expression and function have emerged as a common mechanism underlying a range of human brain disorders, including epilepsy (Puskarjov et al., 2014), schizophrenia (Hyde et al., 2011), Rett syndrome (Banerjee et al., 2016; Hinz et al., 2019), and autism spectrum disorders (ASD) (Merner et al., 2015). Likewise, studies on rodent models have revealed that alterations in KCC2 function are associated with Downs syndrome, fragile X syndrome (Tyzio et al., 2014), Rett syndromes (El-Khoury et al., 2014), and ASD (Anacker et al., 2019). The critical role of KCC2 in early brain development underscores its potential as a target for innovative therapeutic strategies. Consequently, there has been a surge of research on therapeutic strategies to safely upregulate KCC2 expression to promote neural inhibition (Duy et al., 2020; Tang, 2020).

KCC2 exists in two isoforms, KCC2a and KCC2b, differing by their N-terminal sequences but possessing comparable ion transport activity. The mRNA levels of the two isoforms are similar during the neonatal period. While KCC2b expression increases steeply across postnatal development, the overall expression of KCC2a remains relatively constant and then decreases to contribute only a part of the total KCC2 in the mature brain. This points to overlapping roles of KCC2a and KCC2b in neonatal neurons but presumably different roles in mature neurons (Uvarov et al., 2007; Markkanen et al., 2014). There is a growing body of evidence pointing to the multifaceted impact of KCC2 in the brain and its significance in shaping complex behaviors and social interactions. Rodent studies have shown that partial reduction and/or conditional deletion of KCC2 (both isoforms) led to spatial and nonspatial memory impairments, intracellular chloride accumulation, increased anxiety-like behaviors, seizure susceptibility, and hyposensitivity to thermal and mechanical stimuli but normal locomotor activity and motor coordination (Delpire and Mount, 2002; Tornberg et al., 2005; Kreis et al., 2023). KCC2b heterozygous knockout mice also exhibit altered social dominance behaviors and increased amplitude of spontaneous postsynaptic currents in the medial prefrontal cortex (PFC) (Anacker et al., 2019). While these studies have provided valuable insights into the functional roles of KCC2 and its impact on neural development and behavior, there is still a need for further investigation into the specific contributions of KCC2a and KCC2b isoforms in sociocognitive functions. Particularly, the precise role of KCC2a in regulating neurobehavioral functions remains elusive and warrants additional research.

The zebrafish (*Danio rerio*) has emerged as a promising model for unraveling the complexities of brain disorders, including attention-deficit/hyperactivity disorder (ADHD), schizophrenia, and particularly ASD. Its genetic manipulability and inherent neurodevelopmental traits, which resemble those found in humans, offers a refreshing departure from the conventional reliance on rodent models (Norton, 2013; De Abreu et al., 2020). By leveraging these traits, zebrafish provide a valuable tool for studying the complexities and dynamics of human brain disorders. In recent years, the combined utilization of zebrafish, along with state-of-the-art genomic editing technologies like the CRISPR/Cas9 (Clustered regularly interspaced short palindromic repeats (CRISPR)/CRISPR-associated protein 9) system, has emerged as a highly promising and efficient approach to accelerate the development of disease-relevant models, validate novel drug targets, and explore potential therapeutic interventions with significant clinical implications (Cornet et al., 2018). The KCC2-mediated GABA switch in zebrafish retinal neurons occurs at around 2.5 days post-fertilization (dpf) (Zhang et al., 2010; Zhang et al., 2013). Moreover, dysregulation of KCC2 expression impairs neural development and locomotor behaviors in zebrafish embryos (Reynolds et al., 2008), revealing a structural role of KCC2 in brain development. In spite of this, the potential long-term pathophysiological effects of embryonic KCC2 dysregulation on social behaviors and memory in zebrafish have yet to be studied. Thus, this study aimed to characterize the behavioral phenotype of CRISPR-Cas9/pharmacological induced-KCC2-deficient zebrafish as well as to determine the therapeutic potential of KCC2 modulation in biallelic F0 *kcc2a* knockout (KO) animals (hereafter referred to as crispants).

2 Materials and methods

Adult zebrafish (Tübingen Longfin strain) were reared at the York University aquatic facility in a recirculating system (Aquaneering, USA) under a 14:10 h light/dark cycle. Temperature was maintained at 28 ± 1°C, conductivity between 650 and 750 μS, pH at 7.4, and hardness (as CaCO3) at 150 mg/L. The zebrafish were fed twice daily with a combination of a commercial zebrafish diet (Zeigler, USA) and nutritious brine shrimp (*Artemia salina*). For breeding, females and males were paired in a 2:1 ratio in breeding tanks overnight. The following morning, eggs were collected and transferred to 90 mm Petri dishes.

2.1 Generation of KCC2a crispants

In this study, F0 knockout larvae for a single gene were generated using a protocol based on Kroll et al. (2021). The method involved the use of synthetic gRNAs, targeting three loci per gene, and adjusting the concentrations of total gRNA and Cas9 for injections. Specific crRNAs (Alt-R™ CRISPR-Cas9 crRNA, 1 μL) were selected from the Integrated DNA Technologies (IDT) database based on predicted efficiency, and then annealed with tracrRNA (Alt-R CRISPR-Cas9 tracrRNA, 1 μL) at 95°°C for 5 min to form the gRNA. In this study, we designed 3 distinct crRNAs targeting either exon 2, 3, or 4 on *slc12a5a* (*kcc2a*). The crRNA selection prioritized distinct exons, and the ranking followed the best predicted crRNA from the IDT database. The gRNA/Cas9 ribonucleoprotein (RNPs) complex was then prepared by incubating Cas9 protein (Alt-R S.p. Cas9 Nuclease V3, 57 mM, IDT) with equal volumes of gRNA at 37°°C for 5 min. The

three RNP solutions were pooled in equal amounts before injections, and approximately 1 nL (~ 28.5 fmol of RNP per gene) of the pool was injected into the yolk at the single-cell stage using a Pneumatic PicoPump (SYS-PV830; World Precision Instruments, USA). To account for possible influence from the microinjection procedure, pooled RNP complexes were prepared from three scrambled crRNAs (IDT: Alt-R CRISPR-Cas9 Negative Control crRNA #1, 1072544; #2, 1072545; #3, 1072546) and were injected as described above. These embryos were used as controls for comparison with the KO mutants. This method provided a highly efficient approach for rapidly screening the functional involvement of *kcc2a* in zebrafish behavior and other complex phenotypes in the F0 generation. The details of the selected crRNAs (sgRNAs) and targeted loci can be found in Supplementary Table S1. Injected embryos were collected at 1 dpf and genomic DNA was extracted by incubating each embryo with 50 µL of 50 mM NaOH at 95°C for 10 min. After cooling to 4°C, 5 µL of 1 M Tris–HCl (pH 8) was added for neutralization. The PCR reaction mixture contained 10 µL of 5X buffer, 1 µL of 10 mM dNTP, 1 µL of 10 µM forward and reverse primer each, 0.25 µL of Tag Polymerase, and 36.5 µL of H_2O. The PCR program was: 95°C for 3 min; then 40 cycles of: 95°C for 30 s, 60°C for 30 s, 72°C for 30 s; then 72°C for 5 min; 4°C hold. After PCR, the PCR products were run on a 3% (w/v) agarose gel to confirm the correct amplification of the target region. The PCR amplicons were purified using a DNA purification kit (Qiagen, Santa Clarita, CA) as per instructions. The clean PCR products were sent for Sanger sequencing (The Centre for Applied Genomics, the Hospital for Sick Children, Toronto). The sequence chromatograms and results were analyzed using SnapGene software (Supplementary Figure S1). The primer sets used for genotyping are listed in Supplementary Table S2.

2.2 Chemical exposure

A multifaceted validation strategy was undertaken to substantiate the efficacy of KCC2 gene deletion/disruption and comprehensively assess resulting phenotypic alterations. To this end, a group of wild-type zebrafish embryos was subjected to exposure to a KCC2 inhibitor VU0240551 (Cayman Chemical, USA). This pharmacological exposure sought to elicit effects similar to those expected in KCC2-mutant animals, thereby corroborating the functional impact of KCC2 disruption. In a complementary approach, another group featured wild-type zebrafish embryos was exposed to valproic acid (VPA, Sigma–Aldrich, USA), an anti-epileptic drug that is commonly used to induce ASD-like traits in various animal models, including zebrafish (Mabunga et al., 2015). This group served as a critical reference point, facilitating a comprehensive evaluation of whether *kcc2a* gene deletion effects were akin to those observed in established models of ASD. The stock solutions of VU0240551 and VPA were prepared by dissolving them in dimethyl sulfoxide (DMSO; Sigma-Aldrich, USA) and stored at −20°C until use. The working solutions of these chemicals were subsequently prepared by diluting the stock solution in embryo water to achieve the desired concentration. At 8 h post-fertilization (hpf), embryos were randomly distributed in wells (30 embryos per well) of a 6-well plate containing either VPA (10 µM), VU0240551 (500 nM), or DMSO (from 8 hpf to 5dpf). Exposure concentrations were chosen based on a preliminary range-finding test, with VPA ranging from 1 µM to 50 µM and VU0240551 ranging from 250 nM to 5 µM. The EC50 values were determined via behavioral and morphological assessments at 6 dpf, ensuring low mortality and minimal morphological abnormalities (data not shown).

In another scenario and in order to assess KCC2 as a potential therapeutic target in neurodevelopmental disorders, *kcc2a* crispants were treated with either CLP-290 or LIT-001 through bath immersion. CLP-290 is a novel KCC2-selective activator which effectively restores KCC2 expression in various pathological conditions (Gagnon et al., 2013; Lam et al., 2023). LIT-001 is a novel characterized nonpeptide oxytocin receptor (OXTR) agonist that improves social interaction in neurodevelopmental models of ASD and schizophrenia (Frantz et al., 2018; Piotrowska et al., 2024). Oxytocin (OXT) directly modulates KCC2 expression/stabilization at the plasma membrane during early windows of development (Leonzino et al., 2016). Therefore, by utilizing LIT-001, this study aimed to capitalize on oxytocin's direct modulation of KCC2, exploring its therapeutic potential for neurobehavioral abnormalities. To this end, zebrafish larvae were subjected to either synthetic CLP-290 (25 µM) or LIT-001 (5 µM), in beakers containing 25 mL of each solution for 48 h (1 h/2 times per day). The control group was treated with 0.01% DMSO. Subsequently, larval zebrafish were washed 3 times with system water for 15 min before engaging in behavioral paradigms. CLP-290 and LIT-001 concentrations and exposure durations were selected based on prior research demonstrating a positive impact of two-day exposure to KCC2-enhancing drugs on ASD-like behaviors in zebrafish (Rahmati-Holasoo et al., 2023). The chosen concentrations were determined to prevent abnormal locomotor patterns and erratic swimming behavior.

2.3 Behavioral paradigms

2.3.1 Social behaviors

Social deficits are core symptoms of ASD. Shoaling and social preference tests are two robust measures of social behaviors in zebrafish. Shoaling test was carried out at 21 dpf in a white custom made square shaped arena (15 cm × 15 cm) for 8 min (8 larvae per arena, 3 replicates per group, n = 4–7). The shoaling parameters included time spent in proximity (within 0.5 cm of another subject) and the inter-individual distance among a group of zebrafish. Social preference test in 21 dpf larvae was performed in custom-built behavioral setups as described elsewhere (Naderi et al., 2022). The arena consisted of three parts: a center area, an empty side, and a conspecific side (16 cm L × 6 cm W × 6 cm H). Adjacent to the conspecific side was a chamber (4 cm L × 6 cm W) with 5 stimulus zebrafish larvae matched in size to the focal fish. Zebrafish were allowed to explore the arena for 10 min. Social preference was measured as the percentage of total time spent in the conspecific zone (n = 29–30).

2.3.2 Object recognition memory

Object-recognition memory in zebrafish larvae (21 dpf) was assessed based on their tendency to explore novel objects as described previously (Naderi et al., 2022). Zebrafish larvae were first habituated to an empty apparatus (square-shaped maze: 9 cm L × 9 cm W × 6 cm H) for 5 min twice daily over 5 consecutive days, spanning from 16 to 20 dpf. At 21 dpf, the subjects explored two identical objects for 8 min (two red round-shaped LEGO®). After a 1.5-h interval, one of the objects was replaced with a new item (a green round-shaped LEGO®),

and the fish was allowed to explore the objects for another 8 min. The exploration ratio, calculated as time spent with the novel object divided by the total exploration time, determined the preference (n = 25–28). A score greater than 0.5 indicated a preference for the novel object.

2.3.3 Whole-brain mRNA expression analysis by digital droplet PCR

Total RNA was extracted from whole-brains of zebrafish larvae (n = 5–7, with each replicate comprising a pool of 5 brains) using the RNeasy Mini Kit (Qiagen, Canada), followed by assessing RNA quality using a plate spectrophotometer (Take3, Biotek Synergy LX, USA). Subsequently, cDNA was synthesized from 1 µg of total RNA using the iScript cDNA synthesis kit (Bio-Rad, USA). Droplet digital PCR (ddPCR) was performed using EvaGreenTM supermix (Bio-Rad, USA) on the QX200 Droplet Digital PCR system (Bio-Rad, USA) to determine the absolute mRNA expression levels of target genes. After amplification, droplets were analyzed using the QX200 droplet reader and QuantaSoftTM software (Bio-Rad, USA). The mRNA expression of each target gene was normalized to the transcript levels of ribosomal protein L13a (*rpl13a*) and ribosomal protein S18 (*rps18*). Specific primers used in this study are listed in Table S3.

2.3.4 Enzyme-linked immunosorbent assay

Zebrafish isotocin (IT) exhibits a significant resemblance to mammalian oxytocin. Consequently, IT levels in the brains of zebrafish larvae were quantified using the DetectX® Oxytocin Enzyme Immunoassay Kit (K048-H1, Assay Designs, Ann Arbor, USA), following the manufacturer's guidelines. Each assay utilized a pooled sample of 6–8 brains (n = 4–6) that had been pre-treated with a protease inhibitor (Thermo Scientific, USA).

2.3.5 Western blotting

Total proteins were extracted from a pool of 10 larval zebrafish brains in RIPA buffer (Thermo Fisher Scientific, USA). After 30 min of incubation at 4°C, homogenization was performed using TissueLyser II (Qiagen, USA) and cell debris was removed by centrifugation at 14,000 g for 20 min. The supernatant was collected and protein concentrations were quantified using a BCA protein assay kit (Thermo Scientific, USA). Protein samples (30 µg) were then heated at 95°C for 10 min and separated on a 12% polyacrylamide gel through SDS-PAGE. The proteins were then transferred to a polyvinylidene difluoride (PVDF) membrane using a BioRad Trans Blot Turbo (Bio-Rad, USA). After transfer, the membranes were stained with 0.1% Ponceau S (dissolved in 5% acetic acid) and visualized on an iBright Imaging System (Invitrogen, USA) for subsequent normalization to total protein. Following this, the membrane was blocked with 5% non-fat milk in TBST (10 mM Tris pH 8.0, 150 mM NaCl, 0.5% Tween 20) for 2 h at room temperature followed by overnight incubation with anti-BDNF antibody (1,400, Invitrogen, USA) at 4°C. After washing with TBST for 20 min, the membranes were further incubated with a goat anti-rabbit IgG-HRP conjugate secondary antibody (1,1,000) for 2 h at room temperature. Protein bands were detected following incubation with a chemiluminescence substrate (PierceTM ECL Western Blotting Substrate; ThermoFisher Scientific, USA). The membranes were then scanned on the iBright imager, and band intensities were normalized to total protein levels using ImageJ software (NIH, Bethesda, ML, USA).

2.3.6 Immunostaining and confocal microscopy

Brain tissues were extracted and immersed in a 4% paraformaldehyde (PFA) solution in phosphate-buffered saline (PBS), undergoing fixation at 4°C for 24 h. The tissues were then equilibrated with 10% sucrose/20% EDTA and 20% sucrose/20% EDTA for 48 h, and subsequently embedded in optimal cutting temperature compound (OCT, Fisher HealthCare, USA). The whole brain was cut into 10-micron sections on a cryotome (Leica, Germany) and mounted onto poly-L-lysine pre-coated glass slides (Superfrost Plus; Thermo Fisher). Slides were rehydrated in PBS and washed three times with PBTD (1X PBS with 0.1% Tween-20 and 1% DMSO). Subsequently, sections were blocked for 3 h in 5% normal goat serum (NGS) in PBTD (e.g., blocking buffer) followed by overnight incubation with rabbit anti-PSD-95 (1:300, Abcam, USA) or rabbit anti-gephyrin (1:800, Abcam, USA) antibody at 4°C in a humid chamber. On the next day, sections were washed three times with PBTD and incubated with Alexa Fluor® 488 secondary antibody (Thermo Fisher Scientific, USA) in PBTD for 2 h at room temperature. Optic tectum and telencephalon regions were imaged using a Zeiss Cell Observer Spinning disk inverted microscope equipped with a Yokogawa CSU-x1 confocal scanner and a Plan-Apochromat 63x/1.4 NA oil objective. PSD-95 and gephyrin puncta were quantified using the "Analyze Particles" function in ImageJ/Fiji, with puncta size ranging between 0.012 µm^2 and 3.2 µm^2. The density of PSD-95 and gephyrin signal in the optic tectum and telencephalon was calculated by dividing the total number of PSD-95 or gephyrin puncta by the surface area of the corresponding regions.

2.3.7 Statistical analysis

Statistical analyses utilized SPSS software (version 23.0, IBM SPSS Inc., USA), and data were presented as mean ± S.E.M. unless stated otherwise. Normality and homogeneity of variances were assessed using the Kolmogorov–Smirnov one-sample test and Levene's test, respectively. The potential impact of *kcc2a* KO on zebrafish behavior was assessed through an Independent Sample t-test, aiming to compare the responses between the control and mutant zebrafish groups. Variations in behavioral outcomes, mRNA abundance, and biochemical parameters among groups treated with pharmaceuticals were assessed using one-way ANOVA, followed by Tukey's *post hoc* test for pairwise comparisons. Gene expression data underwent log transformation for variance stabilization. In cases of severe heteroscedasticity, Welch's test with the Games–Howell *post hoc* test was employed. The arcsine square root transformation was performed on percentage data, where appropriate. The alpha level was set at 0.05.

3 Results

3.1 KCC2 dysregulation and socio-cognitive abnormalities in zebrafish larvae

Previous studies in rodents showed that homozygous KCC2$^{-/-}$ mice and mice lacking *kcc2b* die after birth (Woo et al., 2002). To avoid this perinatal lethality, we decided to target *kcc2a* which is the dominant KCC2 isoform in the immature nervous system and possess similar levels of Cl^- transport function compared to KCC2b (Uvarov et al., 2007). To elucidate the molecular function of KCC2a in the zebrafish brain, we simultaneously targeted three exons of *kcc2a* using

a novel CRISPR/Cas9-mediated genome editing strategy. The Sanger sequencing results revealed a disrupted nucleotide sequence in exon 2 of *kcc2a* in the F0 generation (Supplementary Figure S1), suggesting possible impairment of its gene function.

CRISPR-injected F0 embryos (so-called *kcc2a* crispants) and zebrafish larvae treated with the selective KCC2 inhibitor VU0240551 and VPA exhibited grossly a normal phenotype and locomotion, remained viable, and survived into adulthood. However, *Kcc2a* crispants displayed altered social behaviors. As shown in Figure 1A,B, time spent in proximity and the inter-individual distance were significantly reduced and increased, respectively (both $p \leq 0.001$). Interestingly, the same scenario was observed in fish exposed to VPA (Figures 1E,F; $p \leq 0.001$ and $p \leq 0.005$). While there was a significant decrease in time spent in proximity in larvae exposed to KCC2 blocker ($p \leq 0.002$), the change in inter-individual distance among subjects was statistically indistinguishable from the control group ($p = 0.063$). The results also revealed significant changes in social preference in *Kcc2a* crispants and treated fish (Figure 1C). F0 *kcc2a* KO fish exhibited a reduced social preference as shown by a decrease in the percentage of total time spent in the conspecific side ($p \leq 0.001$). Likewise, a significant decrease in the total time spent in conspecific zone was observed in zebrafish larvae exposed to VPA and VU0240551 (Figure 1G; both $p \leq 0.001$). In addition to social behaviors, cognitive performance in zebrafish larvae was assessed employing a widely used object recognition task. Our results revealed that F0 *kcc2a* KO zebrafish spent significantly less time exploring the novel object compared to the control group (i.e., decreases in exploration ratio) (Figure 1D; $p \leq 0.001$) indicating memory impairment in *kcc2a* crispants. Likewise, embryonic exposure to VU0240551 and VPA recapitulated the memory deficits observed in F0 *kcc2a* knockouts (Figure 1H; both $p \leq 0.001$).

3.2 Alterations in transcription of molecular markers of excitation/inhibition balance

Our results further revealed an alteration in expression of several genes crucial for establishment and maintenance of E/I balance in the CNS. As shown in Figures 2A,B, there was a significant decrease in the mRNA expression level of *kcc2a* (*slc12a5a*, $p \leq 0.014$), while the levels of *kcc2b* (*slc12a5b*) showed a slight increase compared to the control fish, although the difference was not statistically significant ($p = 0.052$). There was also a significant increase in the mRNA expression levels of *nkcc1* (*slc12a2*) in *kcc2a* crispants compared to the control fish (Figure 2C; $p \leq 0.001$). Although there was an apparent decline in the expression levels of glutamate decarboxylase 1b (*gad1b*), this difference was not statistically significant compared to the control (Figure 2D; $p = 0.08$). Furthermore, CRISPR-Cas9-mediated knockout of *kcc2a* gene led a significant decrease in the transcript levels of glutamate decarboxylase 2 (*gad2*, $p \leq 0.007$), GABA transporter 1 (*gat1*, *slc6a1a*, $p = 0.018$), and vesicular glutamate transporter 1 (*vglut1*, *slc17a7a*, $p = 0.004$), known as molecular markers of GABAergic and glutamatergic systems (Figures 2E–G). A significant decrease in the transcript levels of both oxytocin receptor (*oxtra* and *oxtrb*, also known as isotocin receptor) was observed in *kcc2a* crispants (Figures 2I,J; $p \leq 0.003$ and $p = 0.022$), while the mRNA levels of *oxt* gene remained unchanged compared to the control fish (Figure 2H; $p = 0.13$).

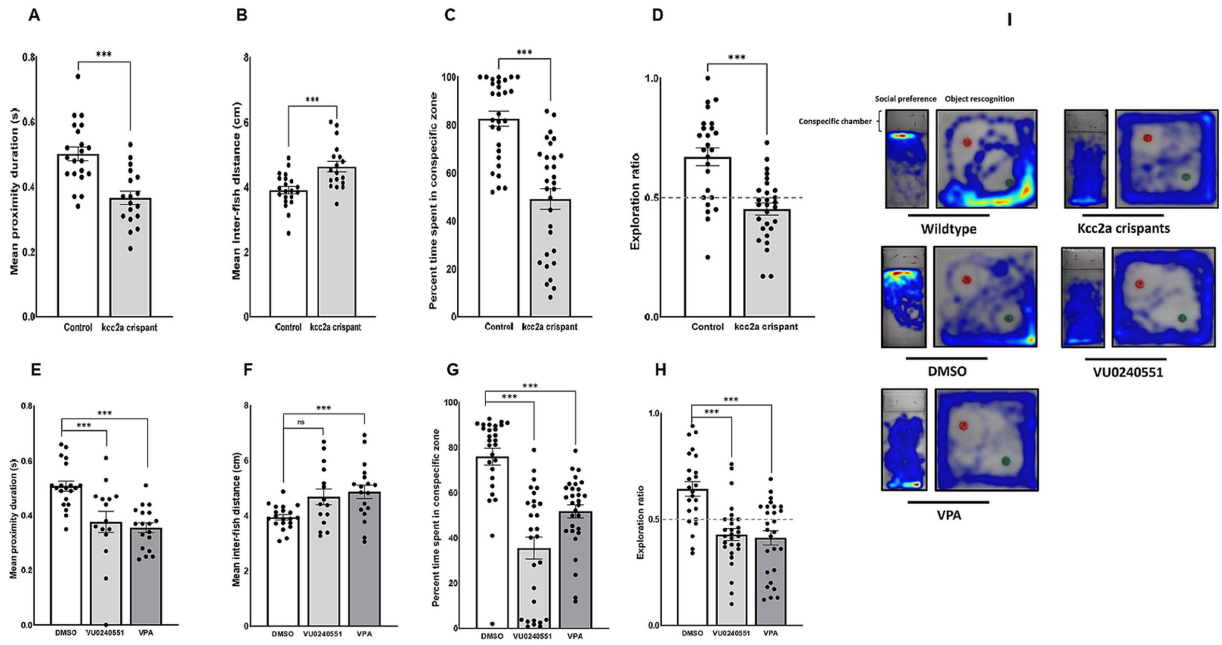

FIGURE 1
Alterations in social behaviors and cognitive performance in *kcc2a* crispants. Changes in shoaling behavior is shown as **(A)** mean proximity duration and **(B)** mean inter-fish distance ($n = 4–7$). Social preference is shown as **(C)** the percentage of time spent in the conspecific zone ($n = 29–30$), and **(D)** object recognition memory represented by exploration ratio ($n = 25–28$). The figure also depicts changes in (**E,F**) shoaling behavior ($n = 15–20$), **(G)** social preference (28–30), and **(H)** object recognition memory ($n = 24–28$) in fish exposed to VU 0240551 (a KCC2 blocker) and valproic acid (VPA). **(I)** Representative heat map of zebrafish larvae in social preference and object recognition tasks. The asterisks above data bars represent a significant difference vs. the control group at * $p < 0.05$, ** $p < 0.01$, and *** 0.001. "ns" indicates not significant ($p > 0.05$).

10.3389/fnmol.2024.1483238

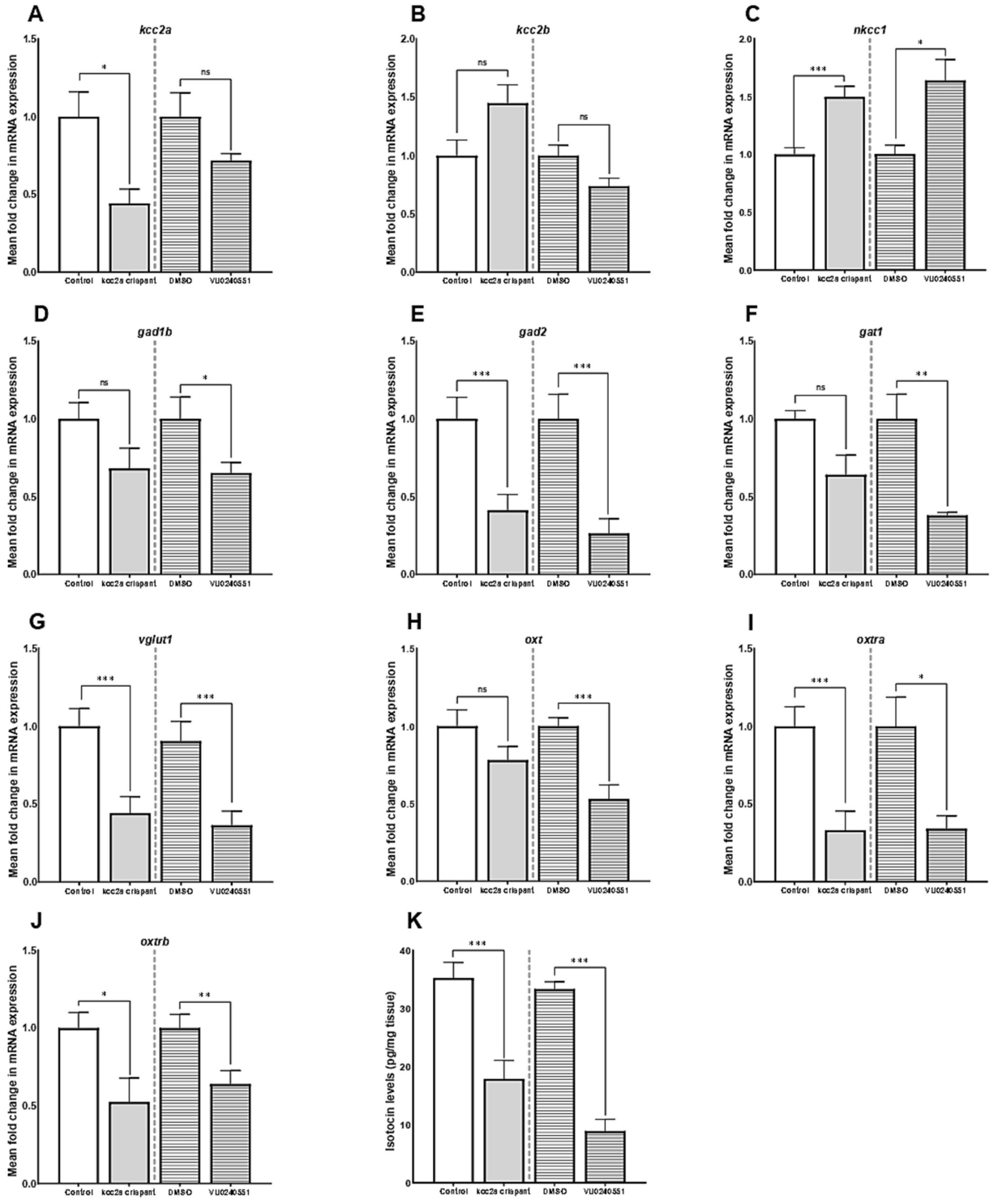

FIGURE 2
The mean fold change in the mRNA expression level of **(A)** *kcc2a* (*slc12a5a*), **(B)** *kcc2b* (*slc12a5b*), **(C)** *nkcc1* (*slc12a2*), **(D)** *gad1b* (glutamate decarboxylase 1b), **(E)** *gad2* (glutamate decarboxylase 2), **(F)** *gat1* (GABA transporter 1, *slc6a1a*), **(G)** *vglut1* (vesicular glutamate transporter 1, *slc17a7a*), **(H)** *oxt,* **(I)** *oxtra,* and **(J)** *oxtrb* genes ($n = 5–7$). **(K)** The whole-brain oxytocin (isotocin) levels between different experimental conditions (control vs. *kcc2a* crispants and DMSO-treated fish vs. KCC2 blocker VU 0240551, $n = 4–6$). The asterisks above data bars represent a significant difference vs. the control group at $*p < 0.05$, $**p < 0.01$, and $***p < 0.001$. "ns" indicates not significant ($p > 0.05$).

Embryonic exposure to the KCC2 blocker (VU0240551) also brought about changes in the transcript levels of several genes in the zebrafish brain. Our results depict a significant increase in the mRNA levels *nkcc1* (*slc12a2*, $p = 0.024$), while the transcript levels of both KCC2 isoforms (*slc12a5a* and *slc12a5b*) remained unchanged (Figures 2A–C; $p = 0.53$ and $p = 0.12$). Administration

of the KCC2 blocker significantly decreased the mRNA levels of *gad1b* (Figure 2D; $p = 0.04$), *gad2* (Figure 2E; $p = 0.007$), *gat1* (Figure 2F; $p = 0.003$), and *vglut1* (Figure 2G; $p = 0.004$) in the brain of zebrafish larvae. In the same vein, we found a significant reduction in the transcript abundance of *oxt* ($p \leq 0.003$) and its receptors *oxtra* ($p = 0.022$) and *oxtrb* ($p \leq 0.001$) compared to the control group (Figures 2H–J).

As Figure 2K depicts, there was a significant reduction in whole-brain OXT protein levels (isotocin) in *kcc2a* crispants compared to the control fish ($p \leq 0.003$). Likewise, a marked decrease in whole-brain OXT protein levels was observed in zebrafish larva embryonically exposed to the KCC2 blocker (VU0240551) compared to controls (DMSO, $p \leq 0.001$).

3.3 Inhibitory/excitatory synaptic balance in KCC2a KO larvae

As shown in Figure 3, quantification of the two post-synaptic populations showed a marked decrease in gephyrin labeling ($p \leq 0.009$, Figures 3A–C), while PSD-95 puncta density remained unchanged ($p = 0.35$, Figures 3D–F). This led to a significant increase in the ratio of excitatory to inhibitory neurons compared to the control (i.e., an increase in PSD-95/gephyrin puncta density ratio, Figure 3G; $p \leq 0.035$).

3.4 BDNF expression in KCC2a KO larvae

The lack of a dependable antibody precluded the possibility of validating KCC2 protein levels in mutant zebrafish through western blot analysis. Therefore, we sought an alternative approach by utilizing a specific antibody targeting BDNF in our study. BDNF is the most well-studied modulator of KCC2 activation in immature neurons. In the developing brain, BDNF can increase KCC2 activation by regulating its localization at the membrane (Khirug et al., 2010; Puskarjov et al., 2014). Western blot analysis of brain samples from control and *Kcc2a* crispants revealed a significant change in BDNF expression (Figure 4). This change was attributed to a significant decrease ($p = 0.005$) in the expression of BDNF in *Kcc2a* crispants compared to the control. Likewise, there was a significant reduction ($p = 0.009$) in BDNF expression in the brain of zebrafish larvae embryonically exposed to the KCC2 blocker VU0240551.

3.5 Pharmacological rescue of behavioral abnormalities induced by KCC2 knockout

We then explored the therapeutic potential of postnatal exposure to several novel compounds aimed at mitigating ASD-like behaviors in F0 *kcc2a* knockout zebrafish at 21 dpf. Our results demonstrated that a 48-h exposure to CLP-290 and LIT-001

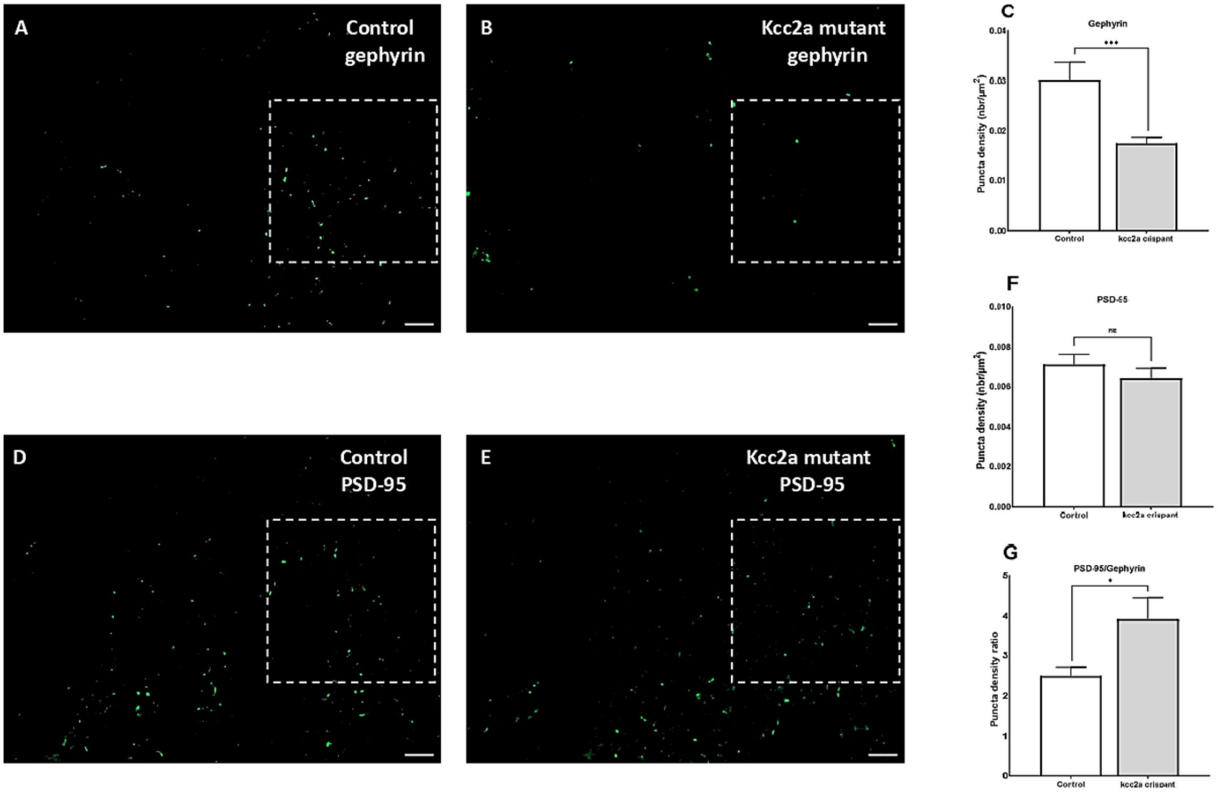

FIGURE 3
Defects of excitatory/inhibitory balance in the *kcc2a* KO larvae. 10 µm coronal sections of 21 dpf **(A)** control ($N = 4$, $n = 12$), **(B)** *kcc2a* crispants ($N = 3$, $n = 9$) stained with gephyrin, an inhibitory post-synaptic scaffolding protein and **(C)** quantification of gephyrin puncta density. **(D)** Coronal sections of 21 dpf control ($N = 3$, $n = 9$) larvae and **(E)** *kcc2a* crispants stained with PSD-95, an excitatory post-synaptic scaffolding protein and **(F)** quantification of PSD-95 puncta density. **(G)** PSD-95/gephyrin puncta density ratio. Scale bar 10 µm. N, number of larvae; n, number of sections. The asterisks above data bars represent a significant difference vs. the control group at $*p < 0.05$, $**p < 0.01$, and $***p < 0.001$. "ns" indicates not significant ($p > 0.05$).

successfully alleviated social abnormalities in F0 *kcc2a* KO zebrafish larvae (Figures 5A,B). This was evident in the comparison of time spent in proximity ($p = 0.25$ and $p = 0.12$) and inter-individual distance with DMSO-treated fish ($p = 0.9$ and $p = 0.2$). However, F0 *kcc2a* KO zebrafish larvae exposed to KCC2 blocker (VU0240551) showed decreased and increased time spent in proximity and inter-individual distance compared to the fish exposed to DMSO (Figures 5A,B; both $p \leq 0.001$). Likewise, the postnatal administration of CLP-290 and LIT-001 restored diminished social preference in F0 *kcc2*a KO zebrafish larvae (all $p \leq 0.86$, Figure 5C). Conversely, mutants exposed to the KCC2 antagonist (VU0240551) exhibited a significant decrease in the time spent with shoalmates compared to DMSO fish ($p \leq 0.003$). Furthermore, postnatal administration of CLP-290 alleviated memory deficits in F0 *kcc2* KO zebrafish larvae when compared to DMSO-treated fish (Figure 5D; both $p \leq 0.84$). However, postnatal exposure to either oxytocin receptor agonist (LIT-001) or KCC2 blocker (VU0240551) failed to rescue cognitive performance in *Kcc2a* crispants in the object recognition task compared to DMSO control treatment (both $p \leq 0.001$).

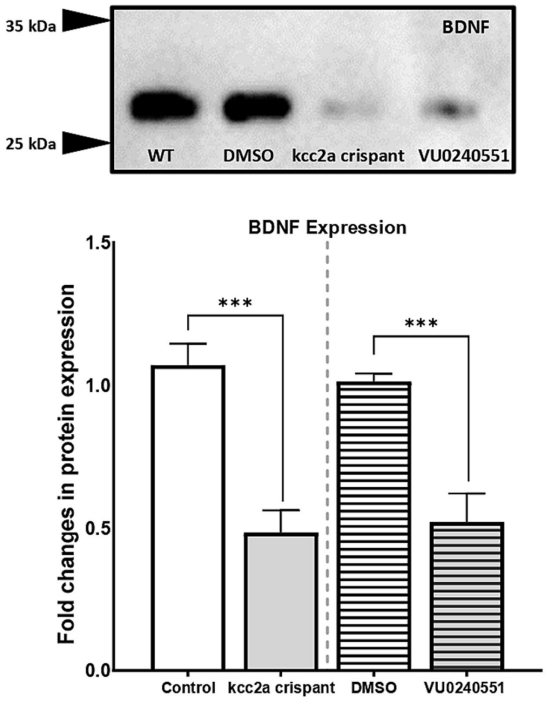

FIGURE 4
(A) Western blot analysis and **(B)** quantification of brain-derived neurotrophic factor (BDNF) protein levels in the zebrafish whole-brain ($n = 3$). Protein band intensities were normalized to total protein levels obtained via Ponceau staining represented as relative difference between experimental groups. The asterisks above data bars represent a significant difference vs. the control group at $*p < 0.05$, $**p < 0.01$, and $***p < 0.001$. "ns" indicates not significant ($p > 0.05$).

4 Discussion

KCC2 is a vital neuron-specific K^+/Cl^- cotransporter that sets the strength and polarity of GABAergic currents during neuronal maturation. Dysregulation in its expression and function has been linked to the pathogenesis of various neurological disorders, including epilepsy, Rett Syndrome, schizophrenia, and ASD (Hyde et al., 2011; Merner et al., 2015; Tomita et al., 2023). In this study, we employed a novel synthetic CRISPR-Cas9-based mutagenesis approach for generating biallelic F0 zebrafish knockouts to study the functional importance of the *kcc2a* gene in the development of socio-cognitive functions in the zebrafish larvae. The *kcc2a* crispants displayed normal morphology, body length, and motor function and survived into adulthood as reported previously (Stödberg et al., 2015). However, the results of behavioral assessment revealed marked socio-cognitive deficits in F0 mutants. The F0 *kcc2a* KO zebrafish larvae displayed abnormal social behaviors which was evidenced by a reduction in shoaling behavior and social preference. Moreover, *kcc2a* KO fish exhibited impaired object recognition memory, as documented by a decrease in novel object exploration ratio. Embryonic administration of the KCC2 blocker VU0240551 also reduced shoaling behavior, social preference, and compromised recognition memory in 21 dpf zebrafish larvae. This suggests a shared mechanistic pathway affected by both genetic and pharmacological perturbations, reinforcing the critical involvement of KCC2 in shaping fundamental aspects of socio-cognitive functions in zebrafish larvae. Our findings align with prior studies indicating that mutations or premature onset of KCC2 function during early developmental stages lead to enduring abnormalities in social behavior and memory. For example, disrupting the phosphorylation process impeded the postnatal establishment of KCC2 function, consequently yielding enduring abnormalities in social behavior and memory retention in mice (Moore et al., 2019). Tamoxifen-induced conditional deletion of KCC2 in the glutamatergic neurons resulted in spatial and nonspatial learning impairments in 3 months old mice (Kreis et al., 2023). In another study, however, KCC2b heterozygous knockout mice ($KCC2^{+/-}$) demonstrated enhanced social dominance behaviors and elevated amplitude of spontaneous postsynaptic currents within the medial prefrontal cortex (PFC), a crucial region implicated in governing social hierarchy and dominance behaviors (Anacker et al., 2019). These suggest that any departure from a precise balance between excitation and inhibition may contribute to aberrant behavioral manifestations. Intriguingly, these behavioral abnormalities mirrored those observed in zebrafish larvae embryonically exposed to VPA, a well-established inducer of ASD-like traits, suggesting a parallel between KCC2 dysfunction and established models of ASD. Prenatal exposure to VPA also decreased protein levels of KCC2 and resulted in impaired spatial memory, limited exploration, increased anxiety, and reduced sociability in the model group (Li et al., 2017). In a more recent study, Haratizadeh et al. (2023) have shown that prenatal VPA exposure increased repetitive/stereotyped movements and impaired object recognition memory and social behaviors in adult rats. These deficits were linked to the reduction of KCC2, causing subsequent disruption in E/I balance. Taken together, these findings underscore the pivotal role of KCC2 in socio-cognitive functions, where genetic or pharmacological disruptions induce lasting abnormalities resembling ASD models, emphasizing the significance of excitation-inhibition balance.

Transcriptomic analyses using ddPCR unveiled marked changes in the expression levels of key genes involved in maintaining E/I balance. CRISPR-Cas9-mediated knockout of *kcc2a* led to a reduction in the transcript abundance of the *kcc2a* gene, with a concurrent

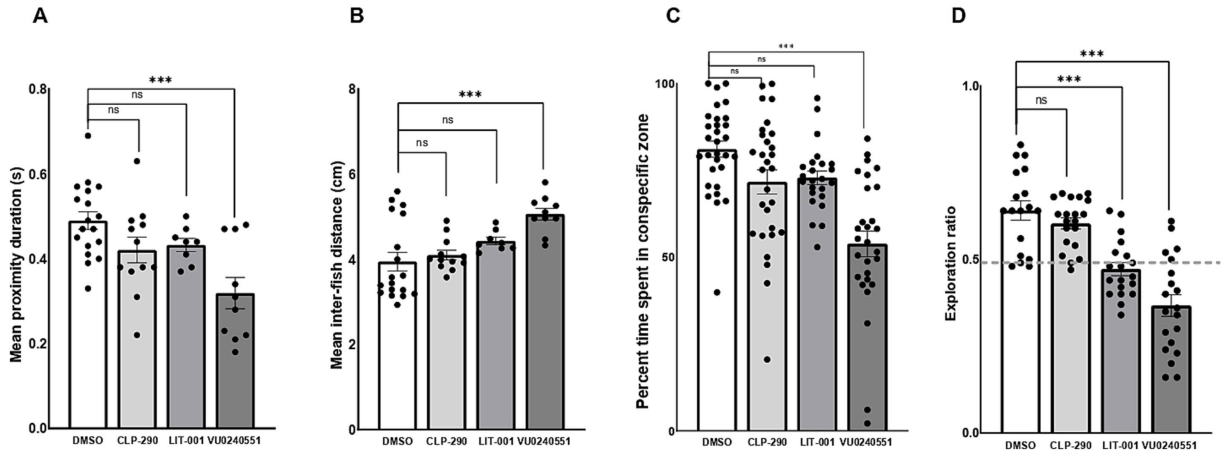

FIGURE 5
Effects of CLP-290, LIT-001, and VU 0240551 on social deficits, measured by time spent in proximity to shoal members **(A)**, inter-individual distance **(B)**, time spent in the conspecific zone **(C)**, and memory impairment **(D)** in kcc2a crispants. Asterisks above the data bars indicate significant differences compared to the control group: $*p < 0.05$, $**p < 0.01$, and $***p < 0.001$. "ns" indicates not significant ($p > 0.05$).

elevation in *kcc2b* mRNA levels. Given the abundant expression of both *kcc2a* and *kcc2b* isoforms with their shared ability for chloride extrusion in neonatal animals, the absence of one isoform seems to be partially compensated for by the other as suggested previously (Markkanen et al., 2014). Moreover, the downregulation of *kcc2a* was accompanied by an upregulation in the expression of *nkcc1*, indicating a possible disruption in chloride homeostasis. This *nkcc1* upregulation might be attributed to the imperative need for maintaining a low intracellular chloride concentration ($[Cl^-]i$) within neurons, coupled with extracellular potassium ($[K^+]o$) accumulation, likely stemming from prolonged downregulation of *kcc2a*. The *Kcc2a* KO also caused a marked reduction in the mRNA expression of key molecular markers associated with the GABAergic (*gad2* and *gat1*) and glutamatergic (VGLUT1) systems. The attenuated *gad2* expression, responsible for GABA synthesis, suggests a potential decline in inhibitory signaling, while the reduced VGLUT1 levels indicate compromised excitatory neurotransmission due to decreased glutamate release. Additionally, the decreased expression of *gat1* implies a potential prolongation of inhibitory signals. Collectively, these molecular alterations may contribute to an aberrant E/I balance and perturbed neural circuitry. Consistent observations in zebrafish larvae treated with the KCC2 blocker VU0240551 during embryonic development further substantiate the association between KCC2 dysfunction and E/I imbalance. Our findings are in agreement with previous studies in rodents reporting that KCC2 mutation and/or inhibition contributes to E/I imbalance in mice and rats (Gauvain et al., 2011; Engberink et al., 2018; Raol et al., 2020). Moreover, KCC2 deficits in mouse models of Rett syndrome and ASD have been linked to the altered the polarity of GABAergic inhibition in cortical neurons (Banerjee et al., 2016). Using KCC2-mutant mice, Pisella et al. (2019) have also reported an altered GABAergic inhibition and increased glutamate/GABA synaptic ratio in cortical and hippocampal pyramidal neurons, reinforcing the role of KCC2 in regulating E/I balance across different neurological contexts.

The E/I imbalance in ASD is associated with increased excitation or reduced inhibition, leading to a higher excitatory-to-inhibitory ratio. Individuals with ASD often show decreased GABAergic signaling, which is theorized to contribute to cognitive deficits, repetitive behaviors, and abnormal social behaviors (Rubenstein and Merzenich, 2003). The measurement of PSD-95 and gephyrin serves as crucial indicators of synaptic function, particularly at excitatory and inhibitory synapses, respectively. PSD-95, located at post-synaptic density of excitatory synapses, plays a vital role in stabilizing synaptic contacts and in synaptic maturation for glutamate receptors. On the other hand, gephyrin, a critical component at inhibitory synapses, interacts with $GABA_A$ and glycine receptors, facilitating inhibitory neurotransmission (Chen et al., 2014). In this study, we illustrated that the knockout or inhibition of *kcc2a* resulted in a reduction of inhibitory post-synaptic terminals, consequently leading to an increased ratio of excitatory to inhibitory neurons. Gephyrin directly interacts with KCC2 to regulate its surface expression and function in cortical neurons. KCC2 knockdown has been shown to reduce gephyrin protein in primary cultures of spinal cord neurons (Schwale et al., 2016). Moreover, the reduction in gephyrin may be a consequence of disrupted inhibitory neurotransmission due to the absence or reduction of functional *kcc2a* transporter. On the other hand, the unchanged levels of PSD-95 could be a result of homeostatic mechanisms attempting to stabilize excitatory synapses in response to the disruption of inhibitory synapses. Overall, these findings reveal that early life disruption of *kcc2a* may reduce the efficacy of inhibitory neurotransmission and increase neuronal excitability in the brain of zebrafish larvae.

There is conclusive evidence that E/I imbalance affects the function of neural circuits involved in social cognition and emotional regulation leading to altered information processing and transmission in the brain (Yizhar et al., 2011). Disruptions in inhibitory signaling, particularly in the GABAergic system, may also contribute to aberrant neural responses to social stimuli, leading to difficulties in interpreting social cues and engaging in appropriate social behaviors. On the other hand, excitatory dysfunction involves irregularities in the functioning of excitatory neurotransmitters such as glutamate leading to abnormal neuronal activation. This disruption can result in hyperactivity or hypoactivity within neural networks associated with social cognition and memory, ultimately affecting the encoding, consolidation, and

retrieval of social information. Deleterious effects of E/I imbalance on neural processes extends to the modulation of key neuromodulators, notably OXT. Oxytocin, a hypothalamic neuropeptide, stands as a pivotal regulator of diverse social behaviors across various species. During early brain development, oxytocin and its receptor play fundamental roles in orchestrating the postnatal shift of neuronal GABA neurotransmission from an excitatory to an inhibitory state. Leonzino et al. (2016) has illustrated that the oxytocinergic signaling actively influences the functional dynamics of KCC2 by facilitating its phosphorylation and subsequent insertion/stabilization in the plasma membrane. Gigliucci et al. (2022) also reported a concomitant reduction in the KCC2 and OXTR expression in a mouse model of Rett syndrome. Additionally, it has been demonstrated that the down-regulation of KCC2 induced by lipopolysaccharide (LPS) led to a reduction in OXTR mRNA levels, highlighting a mutual relationship between oxytocin and chloride homeostasis (Tomita et al., 2022). The results of the present study also demonstrated a decrease in the mRNA expression of OXTR genes and whole-brain OXT levels, a finding that was further corroborated through the administration of the KCC2 blocker VU0240551. Together, these findings suggest that the absence of physiological upregulation of the chloride transporter KCC2 during early brain development can result in aberrant E/I balance, which in turn, compromises the firing rates of OXT-producing neurons, the dynamics of OXT release, and the responsiveness of OXTRs, collectively contributing to a decrease in oxytocin expression levels.

Signaling via BDNF and its receptor, tropomycin receptor kinase B (TrkB) is one of the most critical regulators of glutamatergic and GABAergic synapse development (Cohen-Cory et al., 2010). On the other hand, KCC2 regulates dendritic spine formation in hippocampal and cortical neurons in a BDNF-dependent manner (Awad et al., 2018). KCC2 has also been shown to play a key role in the regulation of BDNF–TrkB in rats (Zhang et al., 2023). The deficiency of MECP2 in Rett syndrome has also been associated with the downregulation of BDNF, while the overexpression of KCC2 ameliorated the phenotype (Abuhatzira et al., 2007; Tang et al., 2016). In this study, we found that either genetic or pharmacological disruption of *kcc2a* resulted in a marked decrease in BDNF levels in the zebrafish brain, reinforcing the compelling connection between KCC2 and BDNF. It is plausible that the loss of KCC2 function disrupts the balance between excitatory and inhibitory signaling, leading to depolarizing GABAergic responses and heightened neuronal excitability, which impairs activity-dependent BDNF transcription (Porcher et al., 2018). KCC2 dysfunction may also alter intracellular calcium homeostasis, which is critical for the regulation of BDNF expression via calcium-dependent transcription factors such as cAMP-response element binding protein CREB (Shieh and Ghosh, 1999). Disruption of calcium signaling can, therefore, reduce BDNF expression and impair synaptic plasticity. Furthermore, the loss of KCC2 function may compromise the integrity of BDNF/TrkB signaling pathways, thereby diminishing BDNF-mediated neurotrophic support and synaptic efficacy (Rivera et al., 2002). While these mechanisms offer plausible explanations, the precise molecular pathways linking KCC2 disruption to decreased BDNF expression remain unclear and warrant further investigation. BDNF plays a critical role in synaptic plasticity and neurotransmitter release (Lu et al., 2014). Decreased BDNF expression has been associated with a range of neurological disorders, including schizophrenia (Nieto et al., 2013), Alzheimer's disease (Lee et al., 2005), and ASD (Ricci et al., 2013). In zebrafish, CRISPR/Cas9-mediated knockout of the BDNF gene resulted in learning deficits and abnormal social behaviors (Lucon-Xiccato et al., 2022; Lucon-Xiccato et al., 2023). Therefore, the observed reduction in BDNF levels following *kcc2a* knockout is likely to contribute to synaptic dysfunction, thereby affecting signal transmission in brain regions essential for memory and social behavior.

While the behavioral and molecular consequences of KCC2a disruption were profound, our study went a step further to explore the therapeutic potential of pharmaceuticals that affect the expression and function of KCC2. In recent years, enhancing KCC2 function has emerged as a promising therapeutic target for the treatment of a wide range of neurological disorders (Lam et al., 2023; Tomita et al., 2023). For example, restoring KCC2 using short-term CLP-290 treatment, successfully alleviated spatial memory deficits and improved social function in a mouse model of Alzheimer's disease (Keramidis et al., 2023). Likewise, we found that 2 days of exposure to CLP-290 rescued both recognition memory and social abnormalities in *kcc2a* KO zebrafish. Intranasal OXT has long been known as a potential treatment for addressing socio-cognitive dysfunctions in various brain disorders, such as ASD (Keech et al., 2018). The potential therapeutic benefits of oxytocinergic drugs have recently been correlated with their capacity to boost the expression and activity of KCC2. For instance, OXT treatment has been shown to restore KCC2 expression and E/I balance in a mouse model of Rett syndrome (Gigliucci et al., 2022). Neonatal subcutaneous OXT administration improved social memory deficits and reversed KCC2 dysfunction in hippocampal GABAergic activity in a mouse model of ASD (Bertoni et al., 2021). In another study, 3 days continuous intrathecal infusion of OXT restored the expression levels of KCC2 in the spinal dorsal horn caused by nerve injury (Ba et al., 2022). Furthermore, Rahmati-Holasoo et al. (2023) have recently shown that 48 h OXT treatment during the larval stage improved ASD-like behaviors in a VPA zebrafish model. The findings of this study align with previous research, affirming that the administration of LIT-001 rescued social behaviors in *kcc2a* crispants. However, the lack of LIT-001's effect on object recognition memory indicates that LIT-001 may modulate neural circuits or pathways associated with social behaviors, while its influence on cognitive functions, particularly memory, may be limited or absent. These observations underscore the intricate nature of neurobehavioral modulation and highlight the importance of delineating specific cognitive domains when evaluating the effects of pharmacological interventions. Further investigations into the molecular and neural mechanisms targeted by LIT-001 can provide deeper insights into its functional profile and potential therapeutic applications.

In conclusion, our study, for the first time, shed light on the critical role of KCC2 in shaping socio-cognitive functions in zebrafish larvae, with disruptions leading to long-lasting behavioral abnormalities. The observed abnormalities in behavioral outcomes, shared between genetic knockout and pharmacological perturbations, underscore the pivotal involvement of KCC2 in the developmental regulation of socio-cognitive functions. Molecular analyses demonstrated altered expression of key genes associated with the GABAergic and glutamatergic systems, contributing to an aberrant E/I balance and perturbed neural circuitry. Notably, these disruptions mirrored the behavioral abnormalities observed in established models of ASD (VPA-induced ASD), emphasizing the significance of excitation-inhibition balance in socio-cognitive functions. Furthermore, our

exploration of therapeutic interventions targeting KCC2, such as CLP290 and LIT-001, demonstrated promising outcomes in rescuing memory and social abnormalities. However, the selective effects of LIT-001 on social behaviors, not memory, underscore the complexity of neurobehavioral modulation. These findings underscore the potential therapeutic avenues for KCC2-related neurological disorders, emphasizing the need for further investigations into the molecular and neural mechanisms underlying these effects.

Data availability statement

The datasets presented in this study can be found in online repositories. The names of the repository/repositories and accession number(s) can be found in the article/Supplementary material.

Ethics statement

The animal study was approved by York University Animal Care Committee (YUACC). The study was conducted in accordance with the local legislation and institutional requirements.

Author contributions

MN: Conceptualization, Data curation, Formal analysis, Investigation, Methodology, Project administration, Software, Validation, Visualization, Writing – original draft, Writing – review & editing. TN: Formal analysis, Methodology, Writing – review & editing. CP: Investigation, Methodology, Writing – review & editing. RK: Resources, Supervision, Writing – review & editing.

Funding

The author(s) declare that financial support was received for the research, authorship, and/or publication of this article. MN was supported by the Banting Postdoctoral Fellowship from the Natural Sciences and Engineering Research Council of Canada (NSERC). TN was supported by the Ontario Graduate Scholarship (OGS). RK was supported by a Discovery Grant (05984) from NSERC and the Canada Research Chairs Program. The research was also supported by the Canada Foundation for Innovation John R. Evans Leaders Fund and an Ontario Research Fund.

Acknowledgments

The authors thank Janet Fleites Medina and Veronica Scavo for their support in zebrafish husbandry, as well as Magdalena Jaklewicz for her assistance with confocal microscopy.

Conflict of interest

The authors declare that the research was conducted in the absence of any commercial or financial relationships that could be construed as a potential conflict of interest.

Publisher's note

Supplementary material

The Supplementary material for this article can be found online at: https://www.frontiersin.org/articles/10.3389/fnmol.2024.1483238/full#supplementary-material

References

Abuhatzira, L., Makedonski, K., Kaufman, Y., Razin, A., and Shemer, R. (2007). Mecp2 deficiency in the brain decreases BDNF levels by REST/CoREST-mediated repression and increases TRKB production. *Epigenetics* 2, 214–222. doi: 10.4161/epi.2.4.5212

Anacker, A. M., Moran, J. T., Santarelli, S., Forsberg, C. G., Rogers, T. D., Stanwood, G. D., et al. (2019). Enhanced social dominance and altered neuronal excitability in the prefrontal cortex of male KCC2b mutant mice. *Autism Res.* 12, 732–743. doi: 10.1002/aur.2098

Awad, P. N., Amegandjin, C. A., Szczurkowska, J., Carriço, J. N., Fernandes do Nascimento, A. S., Baho, E., et al. (2018). Kcc2 regulates dendritic spine formation in a brain-region specific and BDNF dependent manner. *Cereb. Cortex* 28, 4049–4062. doi: 10.1093/cercor/bhy198

Ba, X., Ran, C., Guo, W., Guo, J., Zeng, Q., Liu, T., et al. (2022). Three-day continuous oxytocin infusion attenuates thermal and mechanical nociception by rescuing neuronal chloride homeostasis via upregulation KCC2 expression and function. *Front. Pharmacol.* 13:845018. doi: 10.3389/fphar.2022.845018

Banerjee, A., Rikhye, R. V., Breton-Provencher, V., Tang, X., Li, C., Li, K., et al. (2016). Jointly reduced inhibition and excitation underlies circuit-wide changes in cortical processing in Rett syndrome. *Proc. Natl. Acad. Sci.* 113, E7287–E7296. doi: 10.1073/pnas.1615330113

Ben-Ari, Y., Gaiarsa, J.-L., Tyzio, R., and Khazipov, R. (2007). GABA: a pioneer transmitter that excites immature neurons and generates primitive oscillations. *Physiol. Rev.* 87, 1215–1284. doi: 10.1152/physrev.00017.2006

Bertoni, A., Schaller, F., Tyzio, R., Gaillard, S., Santini, F., Xolin, M., et al. (2021). Oxytocin administration in neonates shapes hippocampal circuitry and restores social behavior in a mouse model of autism. *Mol. Psychiatry* 26, 7582–7595. doi: 10.1038/s41380-021-01227-6

Buzsáki, G., Kaila, K., and Raichle, M. (2007). Inhibition and brain work. *Neuron* 56, 771–783. doi: 10.1016/j.neuron.2007.11.008

Chen, J., Yu, S., Fu, Y., and Li, X. (2014). Synaptic proteins and receptors defects in autism spectrum disorders. *Front. Cell. Neurosci.* 8:276. doi: 10.3389/fncel.2014.00276

Chevy, Q., Heubl, M., Goutierre, M., Backer, S., Moutkine, I., Eugène, E., et al. (2015). KCC2 gates activity-driven AMPA receptor traffic through cofilin phosphorylation. *J. Neurosci.* 35, 15772–15786. doi: 10.1523/JNEUROSCI.1735-15.2015

Cohen-Cory, S., Kidane, A. H., Shirkey, N. J., and Marshak, S. (2010). Brain-derived neurotrophic factor and the development of structural neuronal connectivity. *Dev. Neurobiol.* 70, 271–288. doi: 10.1002/dneu.20774

Cornet, C., Di Donato, V., and Terriente, J. (2018). Combining zebrafish and CRISPR/Cas9: toward a more efficient drug discovery pipeline. *Front. Pharmacol.* 9:703. doi: 10.3389/fphar.2018.00703

De Abreu, M. S., Genario, R., Giacomini, A. C., Demin, K. A., Lakstygal, A. M., Amstislavskaya, T. G., et al. (2020). Zebrafish as a model of neurodevelopmental disorders. *Neuroscience* 445, 3–11. doi: 10.1016/j.neuroscience.2019.08.034

Delpire, E., and Mount, D. B. (2002). Human and murine phenotypes associated with defects in cation-chloride cotransport. *Annu. Rev. Physiol.* 64, 803–843. doi: 10.1146/annurev.physiol.64.081501.155847

Duy, P. Q., He, M., He, Z., and Kahle, K. T. (2020). Preclinical insights into therapeutic targeting of KCC2 for disorders of neuronal hyperexcitability. *Expert Opin. Ther. Targets* 24, 629–637. doi: 10.1080/14728222.2020.1762174

El-Khoury, R., Panayotis, N., Matagne, V., Ghata, A., Villard, L., and Roux, J.-C. (2014). GABA and glutamate pathways are spatially and developmentally affected in the brain of Mecp2-deficient mice. *PLoS One* 9:e92169. doi: 10.1371/journal.pone.0092169

Engberink, A. O., Meijer, J., and Michel, S. (2018). Chloride cotransporter KCC2 is essential for GABAergic inhibition in the SCN. *Neuropharmacology* 138, 80–86. doi: 10.1016/j.neuropharm.2018.05.023

Frantz, M.-C., Pellissier, L. P., Pflimlin, E., Loison, S., Gandía, J., Marsol, C., et al. (2018). Lit-001, the first nonpeptide oxytocin receptor agonist that improves social interaction in a mouse model of autism. *J. Med. Chem.* 61, 8670–8692. doi: 10.1021/acs.jmedchem.8b00697

Gagnon, M., Bergeron, M. J., Lavertu, G., Castonguay, A., Tripathy, S., Bonin, R. P., et al. (2013). Chloride extrusion enhancers as novel therapeutics for neurological diseases. *Nat. Med.* 19, 1524–1528. doi: 10.1038/nm.3356

Gauvain, G., Chamma, I., Chevy, Q., Cabezas, C., Irinopoulou, T., Bodrug, N., et al. (2011). The neuronal K-Cl cotransporter KCC2 influences postsynaptic AMPA receptor content and lateral diffusion in dendritic spines. *Proc. Natl. Acad. Sci.* 108, 15474–15479. doi: 10.1073/pnas.1107893108

Gigliucci, V., Teutsch, J., Woodbury-Smith, M., Luoni, M., Busnelli, M., Chini, B., et al. (2022). Region-specific KCC2 rescue by rhIGF-1 and oxytocin in a mouse model of Rett syndrome. *Cereb. Cortex* 32, 2885–2894. doi: 10.1093/cercor/bhab388

Haratizadeh, S., Ranjbar, M., Darvishzadeh-Mahani, F., Basiri, M., and Nozari, M. (2023). The effects of postnatal erythropoietin and nano-erythropoietin on behavioral alterations by mediating K-Cl co-transporter 2 in the valproic acid-induced rat model of autism. *Dev. Psychobiol.* 65:e22353. doi: 10.1002/dev.22353

Hinz, L., Torrella Barrufet, J., and Heine, V. M. (2019). Kcc2 expression levels are reduced in post mortem brain tissue of Rett syndrome patients. *Acta Neuropathol. Commun.* 7, 1–6. doi: 10.1186/s40478-019-0852-x

Hyde, T. M., Lipska, B. K., Ali, T., Mathew, S. V., Law, A. J., Metitiri, O. E., et al. (2011). Expression of GABA signaling molecules KCC2, NKCC1, and Gad1 in cortical development and schizophrenia. *J. Neurosci.* 31, 11088–11095. doi: 10.1523/JNEUROSCI.1234-11.2011

Kaila, K., Price, T. J., Payne, J. A., Puskarjov, M., and Voipio, J. (2014). Cation-chloride cotransporters in neuronal development, plasticity and disease. *Nat. Rev. Neurosci.* 15, 637–654. doi: 10.1038/nrn3819

Keech, B., Crowe, S., and Hocking, D. R. (2018). Intranasal oxytocin, social cognition and neurodevelopmental disorders: a meta-analysis. *Psychoneuroendocrinology* 87, 9–19. doi: 10.1016/j.psyneuen.2017.09.022

Keramidis, I., Mcallister, B. B., Bourbonnais, J., Wang, F., Isabel, D., Rezaei, E., et al. (2023). Restoring neuronal chloride extrusion reverses cognitive decline linked to Alzheimer's disease mutations. *Brain* 146, 4903–4915. doi: 10.1093/brain/awad250

Khirug, S., Ahmad, F., Puskarjov, M., Afzalov, R., Kaila, K., and Blaesse, P. (2010). A single seizure episode leads to rapid functional activation of KCC2 in the neonatal rat hippocampus. *J. Neurosci.* 30, 12028–12035. doi: 10.1523/JNEUROSCI.3154-10.2010

Kreis, A., Issa, F., Yerna, X., Jabbour, C., Schakman, O., De Clippele, M., et al. (2023). Conditional deletion of KCC2 impairs synaptic plasticity and both spatial and nonspatial memory. *Front. Mol. Neurosci.* 16:1081657. doi: 10.3389/fnmol.2023.1081657

Kroll, F., Powell, G. T., Ghosh, M., Gestri, G., Antinucci, P., Hearn, T. J., et al. (2021). A simple and effective F0 knockout method for rapid screening of behaviour and other complex phenotypes. *eLife* 10:e59683. doi: 10.7554/eLife.59683

Lam, P., Newland, J., Faull, R. L., and Kwakowsky, A. (2023). Cation-chloride cotransporters KCC2 and NKCC1 as therapeutic targets in neurological and neuropsychiatric disorders. *Molecules* 28:1344. doi: 10.3390/molecules28031344

Lee, J., Fukumoto, H., Orne, J., Klucken, J., Raju, S., Vanderburg, C. R., et al. (2005). Decreased levels of BDNF protein in Alzheimer temporal cortex are independent of BDNF polymorphisms. *Exp. Neurol.* 194, 91–96. doi: 10.1016/j.expneurol.2005.01.026

Leonzino, M., Busnelli, M., Antonucci, F., Verderio, C., Mazzanti, M., and Chini, B. (2016). The timing of the excitatory-to-inhibitory GABA switch is regulated by the oxytocin receptor via KCC2. *Cell Rep.* 15, 96–103. doi: 10.1016/j.celrep.2016.03.013

Li, H., Khirug, S., Cai, C., Ludwig, A., Blaesse, P., Kolikova, J., et al. (2007). KCC2 interacts with the dendritic cytoskeleton to promote spine development. *Neuron* 56, 1019–1033. doi: 10.1016/j.neuron.2007.10.039

Li, Y., Zhou, Y., Peng, L., and Zhao, Y. (2017). Reduced protein expressions of cytomembrane GABAARβ3 at different postnatal developmental stages of rats exposed prenatally to valproic acid. *Brain Res.* 1671, 33–42. doi: 10.1016/j.brainres.2017.06.018

Lu, B., Nagappan, G., and Lu, Y. (2014). Bdnf and synaptic plasticity, cognitive function, and dysfunction. *Handb. Exp. Pharmacol.* 220, 223–250. doi: 10.1007/978-3-642-45106-5_9

Lucon-Xiccato, T., Montalbano, G., Gatto, E., Frigato, E., D'aniello, S., and Bertolucci, C. (2022). Individual differences and knockout in zebrafish reveal similar cognitive effects of BDNF between teleosts and mammals. *Proc. R. Soc. B* 289:20222036. doi: 10.1098/rspb.2022.2036

Lucon-Xiccato, T., Tomain, M., D'aniello, S., and Bertolucci, C. (2023). BDNF loss affects activity, sociability, and anxiety-like behaviour in zebrafish. *Behav. Brain Res.* 436:114115. doi: 10.1016/j.bbr.2022.114115

Mabunga, D. F. N., Gonzales, E. L. T., Kim, J.-W., Kim, K. C., and Shin, C. Y. (2015). Exploring the validity of valproic acid animal model of autism. *Experimental neurobiology* 24, 285–300. doi: 10.5607/en.2015.24.4.285

Markkanen, M., Karhunen, T., Llano, O., Ludwig, A., Rivera, C., Uvarov, P., et al. (2014). Distribution of neuronal KCC2a and KCC2b isoforms in mouse CNS. *J. Comp. Neurol.* 522, 1897–1914. doi: 10.1002/cne.23510

Merner, N. D., Chandler, M. R., Bourassa, C., Liang, B., Khanna, A. R., Dion, P., et al. (2015). Regulatory domain or CpG site variation in Slc12A5, encoding the chloride transporter KCC2, in human autism and schizophrenia. *Front. Cell. Neurosci.* 9:386. doi: 10.3389/fncel.2015.00386

Moore, Y. E., Conway, L. C., Wobst, H. J., Brandon, N. J., Deeb, T. Z., and Moss, S. J. (2019). Developmental regulation of KCC2 phosphorylation has long-term impacts on cognitive function. *Front. Mol. Neurosci.* 12:173. doi: 10.3389/fnmol.2019.00173

Naderi, M., Puar, P., Javadiesfahani, R., and Kwong, R. W. (2022). Early developmental exposure to bisphenol a and bisphenol S disrupts socio-cognitive function, isotocin equilibrium, and excitation-inhibition balance in developing zebrafish. *Neurotoxicology* 88, 144–154. doi: 10.1016/j.neuro.2021.11.009

Nieto, R., Kukuljan, M., and Silva, H. (2013). BDNF and schizophrenia: from neurodevelopment to neuronal plasticity, learning, and memory. *Front. Psych.* 4:45. doi: 10.3389/fpsyt.2013.00045

Norton, W. H. (2013). Toward developmental models of psychiatric disorders in zebrafish. *Front. Neural Circuits* 7:79. doi: 10.3389/fncir.2013.00079

Piotrowska, D., Potasiewicz, A., Popik, P., and Nikiforuk, A. (2024). Pro-social and pro-cognitive effects of lit-001, a novel oxytocin receptor agonist in a neurodevelopmental model of schizophrenia. *Eur. Neuropsychopharmacol.* 78, 30–42. doi: 10.1016/j.euroneuro.2023.09.005

Pisella, L. I., Gaiarsa, J.-L., Diabira, D., Zhang, J., Khalilov, I., Duan, J., et al. (2019). Impaired regulation of KCC2 phosphorylation leads to neuronal network dysfunction and neurodevelopmental pathology. *Sci. Signal.* 12:eaay0300. doi: 10.1126/scisignal.aay0300

Porcher, C., Medina, I., and Gaiarsa, J.-L. (2018). Mechanism of BDNF modulation in GABAergic synaptic transmission in healthy and disease brains. *Front. Cell. Neurosci.* 12:273. doi: 10.3389/fncel.2018.00273

Puskarjov, M., Seja, P., Heron, S. E., Williams, T. C., Ahmad, F., Iona, X., et al. (2014). A variant of KCC2 from patients with febrile seizures impairs neuronal cl− extrusion and dendritic spine formation. *EMBO Rep.* 15, 723–729. doi: 10.1002/embr.201438749

Rahmati-Holasoo, H., Maghsoudi, A. S., Akbarzade, M., Gholami, M., Shadboorestan, A., Vakhshiteh, F., et al. (2023). Oxytocin protective effects on zebrafish larvae models of autism-like spectrum disorder. *Iran. J. Basic Med. Sci.* 26:316. doi: 10.22038/IJBMS.2023.68165.14889

Raol, Y. H., Joksimovic, S. M., Sampath, D., Matter, B. A., Lam, P. M., Kompella, U. B., et al. (2020). The role of Kcc2 in hyperexcitability of the neonatal brain. *Neurosci. Lett.* 738:135324. doi: 10.1016/j.neulet.2020.135324

Reynolds, A., Brustein, E., Liao, M., Mercado, A., Babilonia, E., Mount, D. B., et al. (2008). Neurogenic role of the depolarizing chloride gradient revealed by global overexpression of KCC2 from the onset of development. *J. Neurosci.* 28, 1588–1597. doi: 10.1523/JNEUROSCI.3791-07.2008

Ricci, S., Businaro, R., Ippoliti, F., Lo Vasco, V. R., Massoni, F., Onofri, E., et al. (2013). Altered cytokine and BDNF levels in autism spectrum disorder. *Neurotox. Res.* 24, 491–501. doi: 10.1007/s12640-013-9393-4

Rivera, C., Li, H., Thomas-Crusells, J., Lahtinen, H., Viitanen, T., Nanobashvili, A., et al. (2002). BDNF-induced TrkB activation down-regulates the K+–cl− cotransporter KCC2 and impairs neuronal Cl− extrusion. *J. Cell Biol.* 159, 747–752. doi: 10.1083/jcb.200209011

Rubenstein, J., and Merzenich, M. M. (2003). Model of autism: increased ratio of excitation/inhibition in key neural systems. *Genes Brain Behav.* 2, 255–267. doi: 10.1034/j.1601-183X.2003.00037.x

Schwale, C., Schumacher, S., Bruehl, C., Titz, S., Schlicksupp, A., Kokocinska, M., et al. (2016). Kcc2 knockdown impairs glycinergic synapse maturation in cultured spinal cord neurons. *Histochem. Cell Biol.* 145, 637–646. doi: 10.1007/s00418-015-1397-0

Shieh, P. B., and Ghosh, A. (1999). Molecular mechanisms underlying activity-dependent regulation of Bdnf expression. *J. Neurobiol.* 41, 127–134. doi: 10.1002/(SICI)1097-4695(199910)41:1<127::AID-NEU16>3.0.CO;2-J

Sohal, V. S., and Rubenstein, J. L. (2019). Excitation-inhibition balance as a framework for investigating mechanisms in neuropsychiatric disorders. *Mol. Psychiatry* 24, 1248–1257. doi: 10.1038/s41380-019-0426-0

Stödberg, T., Mctague, A., Ruiz, A. J., Hirata, H., Zhen, J., Long, P., et al. (2015). Mutations in Slc12A5 in epilepsy of infancy with migrating focal seizures. *Nat. Commun.* 6:8038. doi: 10.1038/ncomms9038

Tang, B. L. (2020). The expanding therapeutic potential of neuronal Kcc2. *Cells* 9:240. doi: 10.3390/cells9010240

Tang, X., Kim, J., Zhou, L., Wengert, E., Zhang, L., Wu, Z., et al. (2016). Kcc2 rescues functional deficits in human neurons derived from patients with Rett syndrome. *Proc. Natl. Acad. Sci.* 113, 751–756. doi: 10.1073/pnas.1524013113

Tomita, K., Kuwahara, Y., Igarashi, K., Kitanaka, J., Kitanaka, N., Takashi, Y., et al. (2023). Therapeutic potential for KCC2-targeted neurological diseases. *Japan. Dental Sci. Rev.* 59, 431–438. doi: 10.1016/j.jdsr.2023.11.001

Tomita, K., Yamanishi-Taira, S., Igarashi, K., Oogai, Y., Kuwahara, Y., Roudkenar, M. H., et al. (2022). Oxytocin ameliorates KCC2 decrease induced by oral bacteria-derived LPS that affect rat primary cultured cells and Pc-12 cells. *Peptides* 150:170734. doi: 10.1016/j.peptides.2021.170734

Tornberg, J., Voikar, V., Savilahti, H., Rauvala, H., and Airaksinen, M. S. (2005). Behavioural phenotypes of hypomorphic KCC2-deficient mice. *Eur. J. Neurosci.* 21, 1327–1337. doi: 10.1111/j.1460-9568.2005.03959.x

Tyzio, R., Nardou, R., Ferrari, D. C., Tsintsadze, T., Shahrokhi, A., Eftekhari, S., et al. (2014). Oxytocin-mediated GABA inhibition during delivery attenuates autism pathogenesis in rodent offspring. *Science* 343, 675–679. doi: 10.1126/science.1247190

Uvarov, P., Ludwig, A., Markkanen, M., Pruunsild, P., Kaila, K., Delpire, E., et al. (2007). A novel N-terminal isoform of the neuron-specific K-Cl cotransporter KCC2. *J. Biol. Chem.* 282, 30570–30576. doi: 10.1074/jbc.M705095200

Woo, N. S., Lu, J., England, R., Mcclellan, R., Dufour, S., Mount, D. B., et al. (2002). Hyperexcitability and epilepsy associated with disruption of the mouse neuronal-specific K–Cl cotransporter gene. *Hippocampus* 12, 258–268. doi: 10.1002/hipo.10014

Yizhar, O., Fenno, L. E., Prigge, M., Schneider, F., Davidson, T. J., O'shea, D. J., et al. (2011). Neocortical excitation/inhibition balance in information processing and social dysfunction. *Nature* 477, 171–178. doi: 10.1038/nature10360

Zhang, R. W., Wei, H. P., Xia, Y. M., and Du, J. L. (2010). Development of light response and Gabaergic excitation-to-inhibition switch in zebrafish retinal ganglion cells. *J. Physiol.* 588, 2557–2569. doi: 10.1113/jphysiol.2010.187088

Zhang, H., Xu, L., Xiong, J., Li, X., Yang, Y., Liu, Y., et al. (2023). Role of Kcc2 in the regulation of brain-derived neurotrophic factor on ethanol consumption in rats. *Mol. Neurobiol.* 60, 1040–1049. doi: 10.1007/s12035-022-03126-5

Zhang, R.-W., Zhang, S.-Y., and Du, J.-L. (2013). KCC2-dependent subcellular ECL difference of on-off retinal ganglion cells in larval zebrafish. *Front. Neural Circuits* 7:103. doi: 10.3389/fncir.2013.00103

frontiers | Frontiers in Neuroscience

TYPE Original Research
PUBLISHED 20 December 2024
DOI 10.3389/fnins.2024.1520710

OPEN ACCESS

EDITED BY
Ferdinando Di Cunto,
University of Turin, Italy

REVIEWED BY
Samir Ranjan Panda,
University of California San Francisco, United States
Hongmei Yang,
Harvard Medical School, United States

*CORRESPONDENCE
Dan Fan
✉ fandan1976@163.com

†These authors have contributed equally to this work and share first authorship

RECEIVED 31 October 2024
ACCEPTED 06 December 2024
PUBLISHED 20 December 2024

CITATION
Yao Y, Hu L, Li D, Wang Y, Pan J and Fan D (2024) Perioperative enriched environment attenuates postoperative cognitive dysfunction by upregulating microglia TREM2 via PI3K/Akt pathway in mouse model of ischemic stroke. *Front. Neurosci.* 18:1520710. doi: 10.3389/fnins.2024.1520710

Perioperative enriched environment attenuates postoperative cognitive dysfunction by upregulating microglia TREM2 via PI3K/Akt pathway in mouse model of ischemic stroke

Yuchen Yao[1†], Liru Hu[2†], Danni Li[1], Yuhao Wang[2], Jian Pan[2] and Dan Fan[1*]

[1]Department of Anesthesiology, Sichuan Provincial People's Hospital, School of Medicine, University of Electronic Science and Technology of China, Chengdu, China, [2]State Key Laboratory of Oral Diseases, Department of Oral and Maxillofacial Surgery, National Center for Stomatology and National Clinical Research Center for Oral Diseases, West China Hospital of Stomatology, Sichuan University, Chengdu, China

Postoperative cognitive dysfunction (POCD) is a prevalent complication that significantly affects the quality of life. Notably, patients who have experienced ischemic stroke are at an increased risk of developing POCD. Exploring the underlying mechanisms of POCD is crucial for its management. Numerous studies have established neuroinflammation as an independent risk factor in POCD pathogenesis, with TREM2 emerging as a key neuroprotective factor that modulates neuroinflammatory responses through the PI3K/Akt signaling pathway. In this study, we aimed to investigate the effect of TREM2 on POCD in a mouse model of ischemic stroke, with a focus on the mechanisms involving TREM2 and the PI3K/Akt signaling pathway. Our findings indicated that mice with ischemic stroke exhibited severe cognitive impairment after surgical trauma. However, we observed that an enriched environment (EE) could ameliorate this cognitive impairment by upregulating microglia TREM2 expression in the hippocampus and suppressing neuroinflammation. Additionally, the PI3K/AKT signaling pathway was activated in the hippocampal tissue of the mice housed in EE. Importantly, the beneficial neuroprotective and anti-inflammatory effects of EE were abolished when TREM2 was knocked down, underscoring the essential role of TREM2 in mediating the effects of EE on neuroinflammation and cognitive function after ischemic stroke and surgical trauma. In general, our study has confirmed a potential molecular mechanism that led to the occurrence of POCD in individuals with ischemic stroke and provided new strategies to treat POCD.

KEYWORDS

enriched environment, POCD, ischemic stroke, microglia, TREM2

Introduction

Ischemic stroke, characterized by a sudden occurrence of focal neurological deficits due to reduced blood supply to a particular region of the brain, is intimately linked to cognitive impairment, memory deterioration, and dementia. This condition places a substantial strain on global public health systems (Mozaffarian et al., 2015; GBD 2019 Stroke Collaborators, 2021). Against the backdrop of a growing aging population, the incidence of ischemic stroke among patients in the perioperative period is on the rise annually. These patients are particularly vulnerable to postoperative cognitive dysfunction (POCD), which significantly hampers postoperative recovery and diminishes the quality of life (NeuroVISION Investigators, 2019; Messé et al., 2024).

The pathophysiological changes associated with the combination of POCD and ischemic stroke are intricate, encompassing neuroinflammation, blood–brain barrier disruption, epigenetic modifications, amyloid-beta accumulation, and excessive tau phosphorylation (He et al., 2024). Although considerable research has been conducted, the precise mechanisms underlying stroke-induced damage remain not entirely elucidated. Normal brain function is critically reliant on a steady supply of oxygen and nutrients, and proinflammatory cytokines unleashed during ischemic and anoxic episodes can trigger neuroinflammation, which may be localized or systemic, leading to neuronal damage in the hippocampus (Zhang et al., 2016, 2018). Consequently, neuroinflammation within the central nervous system (CNS) remains a paramount mechanism that merits further investigation for POCD in patients who have experienced ischemic stroke.

Microglia, critical immune cells within the CNS, are instrumental in preserving brain homeostasis through the mediation of immune responses, phagocytosis of pathogens, and the modulation of neuronal activity (Borst et al., 2021). A study by Thiel A et al. noted a significant activation of microglia following ischemic stroke in mice, which triggers chronic CNS inflammation and subsequent neuronal damage, particularly in the hippocampal dentate gyrus region (Thiel et al., 2010). Additionally, general anesthesia and surgical trauma have been shown to disrupt the homeostasis of CNS and exacerbate cognitive impairment by affecting microglial function (Jin et al., 2023; Sheu et al., 2023). TREM2 is an immune regulatory receptor predominantly found in microglia. It associates with DAP12 to form transmembrane receptor signaling complexes, which play a role in anti-inflammatory processes (Wang et al., 2015, 2022). Research has indicated that TREM2 deficiency can severely compromise microglial activation, inflammatory response, and phagocytic capabilities. Moreover, the absence of TREM2 has been associated with increased infarct size and hindered neurological recovery in mice post-ischemia due to reduced microglial activation (Cantoni et al., 2015). These findings underscore the pivotal role of TREM2 in the regulation of brain tissue repair and the recovery of neurological function, highlighting its significance as a key receptor in microglia.

The PI3K/Akt signaling pathway is integral to various cellular functions, including the regulation of neurogenesis, synaptic plasticity, and neuronal metabolism within the nervous system (Chen et al., 2022; Vasconcelos de Matos et al., 2023). TREM2 has been identified to play a neuroprotective role by engaging the PI3K/Akt signaling pathway to regulate neuroinflammatory responses (Wang et al., 2020). Besides, this regulatory mechanism is crucial for maintaining CNS homeostasis and promoting recovery after neurological insults following ischemic injury (Chen et al., 2020).

The concept of an enriched environment (EE) was first introduced in 1947, defining it as a living space designed with cognitive, physical, and social stimuli, in contrast to a standard environment (SE) (Alwis and Rajan, 2014). Research by Wang et al. has demonstrated that 4 weeks of enriched environmental training can significantly ameliorate learning and memory deficits in mice (He et al., 2017). In our previous study, it has been observed that EE training can mitigate the inflammatory responses triggered by surgical stress and enhance cognitive function postoperatively (Fan et al., 2016).

In the present study, we hypothesized that activation of TREM2 by EE could improve neurological deficits and attenuate neuroinflammation triggered by surgical trauma via the PI3K/Akt signaling pathway in a mouse model of ischemic stroke.

Materials and methods

Animal experiments

Eight-week-old male C57BL/6 mice weighing 20–23 g were obtained from Dashuo Experimental Animal Limited Company (Chengdu, China). As gender differences were not the primary focus of our study, female mice were not used in this experiment. The animals were housed in a temperature-controlled environment with a 12-h light/dark cycle, with free access to laboratory food and water. The animal studies were registered and approved by the Ethics Committees of Sichuan Provincial People's Hospital Research Ethics Committee. The study was conducted in compliance with the ARRIVE guidelines. For the experimental procedures, the mice were anesthetized by inhalation of 5% isoflurane (RWD Life Technology, Shenzhen, China). Throughout the surgical interventions, anesthesia was sustained with 2% isoflurane to ensure the animals remained unconscious.

The mice were divided into the following groups: (1) Sham+SE, Sham+EE, PT + SE, and PT + EE groups; (2) SE + vehicle, SE + shRNA, EE+ vehicle, and EE + shRNA groups.

To induce ischemic stroke models, photothrombotic (PT) stroke induction was conducted as previously described (Labat-gest and Tomasi, 2013). Following anesthesia, the mice were firmly secured in a stereotaxic frame (RWD Life Science). Their body temperature was maintained at 37.0°C throughout the surgical procedure using a temperature-controlled heating pad.

A 1-cm midline incision was made from the level of the eyes, and a skin retractor was used to maintain exposure of the skull. The frontal area was targeted for infarction, with the bregma serving as a reference point (coordinates: anterior/posterior: 1.5 mm, medial/lateral: 2 mm). Rose Bengal solution (Sigma-Aldrich, United States) at a dosage of

Abbreviations: POCD, Postoperative cognitive dysfunction; CNS, Central nervous system; EE, Enriched environment; SE, Standard environment; PT, Photothrombotic; AAV, Adeno-associated virus; MRI, Magnetic resonance imaging; TTC, 2,3,5-Triphenyl tetrazolium chloride; mNSS, Modified neurological severity score; SAB, Spontaneous alternation behavior; ELISA, Enzyme-linked immunosorbent assay; PBS, Phosphate-buffered solution; DAPI, 4′,6-diamidino-2-phenylindole; PCC, Pearson correlation coefficient; PVDF, poly- (vinylidene fluoride); RT-PCR, Reverse transcription polymerase chain reaction.

125 mg/kg was administered via slow subcutaneous injection. After a five-minute interval, the designated area was exposed to yellow-green laser light (532 nm, 40 mW/cm^2) for a duration of 10 min, with other areas shielded from the light. The incision was then closed with sutures. Schematic diagrams are presented in Figure 1A. Immediately post-irradiation, the ischemic penumbra in the PT animals was visualized using laser speckle contrast imaging, as depicted in Figures 1B–E. The animals were closely monitored until they regained full consciousness. For the control group, sham animals underwent an identical procedure except for the omission of the subcutaneous Rose Bengal injection, thus serving as a baseline for comparison in the experiment.

To induce POCD models, all animals underwent left nephrectomy on day 46 following PT stroke induction. Briefly, mice were anesthetized and then fixed in the supine position. A midline abdominal incision was made to expose the left kidney. Blunt forceps were then used to dissect and separate the perirenal fat and connective tissue. The left kidney was subsequently extirpated after ligating the artery, vein, and ureter. The abdominal muscle layer and skin were sutured closed. Throughout the procedure, animals received continuous inhalation anesthesia, which was maintained for a total duration of 2 h to cover the entire surgical period. A schematic of the entire experimental timeline is displayed in Figure 1F.

Stereotaxic injection of adeno-associated virus

AAV vectors encoding the mouse TREM2 gene (NCBI ID: NM_031254.4) and control AAV vectors were purchased from Hanbio (Shanghai, China). TREM2-shRNA (shRNA) or vehicle-shRNA (vehicle) with AAV vector was stereotactically injected into the bilateral hippocampi of mice with photothrombotic lesions on day 24 before left nephrectomy. Briefly, mice were anesthetized, and then these vectors were injected bilaterally into the hippocampus with the following coordinates relative to bregma: −2.3 mm anteroposterior, ±1.8 mm mediolateral, and − 2 mm dorsoventral. Each site was injected with 1 μL (4×10^9 vg/site) of diluted AAV vectors over a 10-min period. The efficacy of AAV-mediated TREM2 silencing was verified on day 21 after injection.

Enriched environment housing

Following the induction of PT stroke, mice were randomly assigned to either EE or SE housing without stratification. The EE was composed of larger cages measuring 43.1 cm × 22.8 cm × 19.5 cm, equipped with a variety of stimulating objects such as climbing ladders, running wheels, mazes, seesaws, and balls. The toys and bedding were refreshed every 3 days to maintain a dynamic and engaging environment. In contrast, smaller cages measuring 27.9 cm × 15.2 cm × 11.4 cm, devoid of any additional toys, were set as SE. All animals had free access to water and food.

Measurement of infarct volume

The formation of the infarct focus was preliminarily evaluated using magnetic resonance imaging (MRI, Bruker BioSpec 70/30USR, Germany). For a quantitative calculation of the infarct volume, the brain sections were incubated in 2% 2,3,5-Triphenyltetrazolium chloride (TTC, Sigma-Aldrich) for 20 min at 37°C. The infarcted and non-infarcted areas were then analyzed using Image J software (National Institutes of Health, United States). The percentage of infarct volume was calculated as the total volume of white infraction / total volume of brain section × 100%.

Rota-rod test

The mice were tested using the rota-rod test to assess their motor coordination abilities. The animals were placed on a rotating rod that accelerated smoothly from 4 to 40 rpm per min over a 5-min period. The length of time taken for the mice to fall off the rod was recorded, with a maximum cutoff time of 300 s. Prior to the establishment of the ischemic stroke model, the initial drop latency time was documented as the baseline measurement.

Modified neurological severity score

The mNSS test, which consisted of five tasks including motor, sensory, balance, and reflex functions, was performed to assess their neurological functions. The scores were graded from 0 to 18 (0 = normal function; 1–7 = mild deficit; 8–12 = moderate deficit; 13–18 = severe deficit), and higher scores reflected greater neurological injury.

Y-maze test

Short-term cognitive memory and exploratory behavior were measured using a Y-maze apparatus (25 cm long × 8 cm wide × 15 cm high, oriented at 120°, BrainScience Idea, Osaka, Japan). Mice were placed at the center of the Y-maze and allowed to freely explore the three arms for a duration of 5 min. The spontaneous alternation behavior (SAB) was calculated as the percentage of spontaneous alternation: (the number of spontaneous alternations) / (total number of arms crossed – 2) × 100%.

In the Y-maze novel arm test, the three arms were randomly assigned to be the novel arm, the start arm, and the other arm. During the free-exploration phase, mice were allowed to explore the start arm and the other arm for a 10-min session while the novel arm was blocked. After this, the mice were returned to their cages for a 1-h interval. In the test phase, the mice were placed back in the start arm with access to the novel arm for a 5-min session. The time spent in each arm was recorded, and the novel arm entries were calculated as follows: time spent in the novel arm / total time× 100%.

Fear conditioning test

The fear conditioning test, comprising both contextual and tone tests, was designed to assess hippocampal-dependent and non-hippocampal-dependent cognitive functions, respectively. Before conditioning, the testing chamber (Ugo Basilie, Italy) was sanitized with 75% ethyl alcohol. The mice were gently put into the chamber to adapt

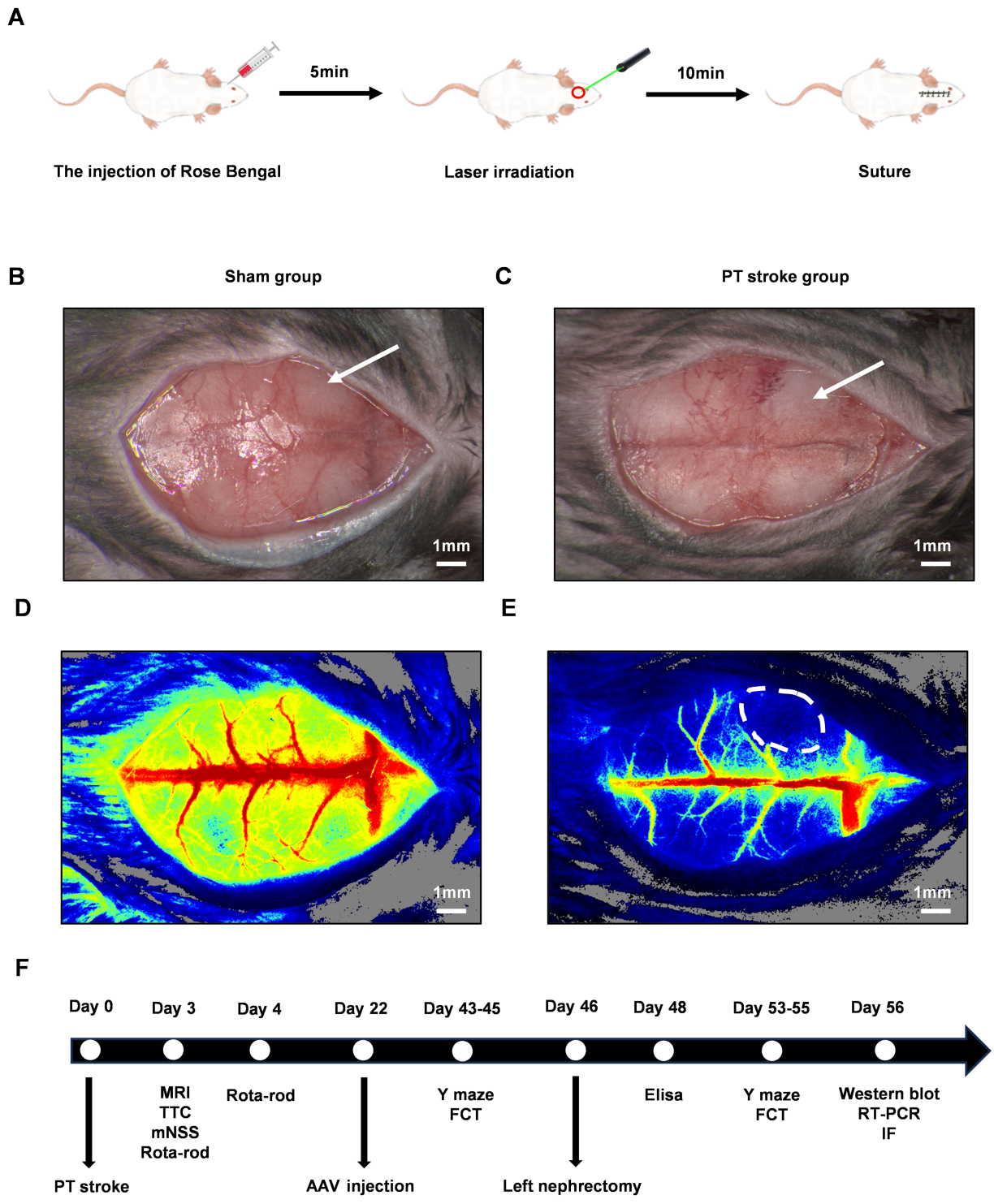

FIGURE 1
The experimental design and the verification of the cerebellar infarct region following PT stroke. The schematic diagrams of PT stroke for focal ischemic stroke model in mice were shown in **(A)**. The gross pictures after the PT stroke were shown for the sham group **(B)** and the PT group **(C)**. The white arrow indicated the target infarct site. **(D,E)** Were the pseudo-color maps of ischemic regions following PT stroke in the sham group and PT group, respectively. The white dot circled area indicated the ischemic lesion. Scale bars represented 1 mm. A Schematic of the entire experimental timeline is shown in **(F)**. PT, photothrombotic; MRI, magnetic resonance imaging; TTC, 2,3,5-Triphenyltetrazolium chloride; mNSS, modified neurological severity score; AAV, adeno-associated virus; FCT, fear conditioning test; RT-PCR, reverse transcription polymerase chain reaction; IF, immunofluorescence staining.

to the surroundings for 2 min. Subsequently, they were subjected to two pairings of tone and foot shock (tone at 2,000 Hz, 85 dB, for 30 s; foot shock at 0.8 mA, for 2 s) with a 60-s intertrial interval. After a 24-h interval, mice were randomly assigned to either the contextual test or the tone test, and their freezing behavior was recorded. In the contextual test, mice were returned to the same test chamber without any shock for a

duration of 8 min. For the tone test, mice were placed in a differently lit chamber, which had been wiped with white vinegar to provide a distinct olfactory context. Following a 3-min adaptation period to the test box, the sound stimulation (2,000 Hz, 85 dB, for 30 s) was administered for 4.5 min. The entire test, including the adaptation period, lasted 8 min.

Enzyme-linked immunosorbent assay

The levels of inflammation-associated cytokines in the hippocampi, including IL-1β, IL-6, TNF-α, IL-4, and IL-10, were quantified using specific ELISA kits (R&D systems, United States). All experimental procedures were performed following the manufacturer's instructions.

Immunofluorescence staining

The hippocampi were fixed in 4% paraformaldehyde and embedded in paraffin for immunofluorescence staining. After antigen retrieval with EDTA, the paraffin sections were washed with phosphate-buffered solution (PBS) and then blocked with 5% bovine serum albumin at room temperature for 1 h. Following this, the sections were incubated with a mouse anti-TREM2 primary antibody (1:1,000, 68723-1-Ig, Proteintech) overnight at 4°C. The next day, sections were incubated with a goat anti-mouse secondary antibody (1:500, RGAM004, Proteintech) for 1 h at room temperature after being washed with PBS. For immunofluorescence double staining, these sections were then incubated with the following primary antibodies overnight at 4°C: rabbit anti-Iba-1 (1:400, 26177-1-AP, Proteintech), rabbit anti-GFAP (1:2500, 16825-1-AP, Proteintech), and rabbit anti-MAP2 (1:2,500, 17490-1-AP, Proteintech) overnight at 4°C, respectively. After being washed with PBS, sections were incubated with a goat anti-rabbit secondary antibody (1:500, RGAR002, Proteintech) for 1 h at room temperature. Finally, the sections were stained with 4′,6-diamidino-2-phenylindole (DAPI) to locate the nucleus for 5 min and then immediately sealed with an anti-fluorescence quenching agent. Stained images were obtained through the LSM700 confocal microscopy system (ZEISS, Germany). The co-localization of TREM2 with Iba-1, GFAP, and MAP2 was quantified using the Pearson correlation coefficient (PCC). The PCC measures the linear correlation between the fluorescence signals of the two markers, where a PCC of 1 indicates a perfect positive correlation, 0 indicates no correlation, and −1 indicates a perfect negative correlation. To determine if the PCC was significantly greater than 0 (which would indicate no correlation), a one-sample, one-tailed student's *t*-test was employed (Paul et al., 2021).

Western blotting analysis

The total proteins of the hippocampi were extracted by using a tissue protein extraction kit (BC3711, Solarbio, Beijing, China) according to the manufacturer's instructions. Equal amounts of proteins were separated by sodium dodecyl sulfate-polyacrylamide gel electrophoresis (SDS-PAGE) followed by transfer to polyvinylidene fluoride (PVDF) membranes. After being blocked with 5% milk for 60 min at room temperature, PVDF membranes were incubated at 4°C overnight with the following primary antibodies: rabbit anti-TREM2 antibody (1:1,000, 27599-1-AP, Proteintech), mouse anti-PI3K antibody (1:5,000, 60225-1-Ig, Proteintech), rabbit anti-phosphor-PI3K antibody (1:1000, HA721672, Huabio), rabbit anti-AKT antibody (1:2,000, 10176-2-AP, Proteintech), rabbit anti-phospho-AKT antibody (1:5,000, 80455-1-RR, Proteintech), rabbit anti-DAP12 antibody (1:1,000, EPR24244-76, Abcam), rabbit anti-BDNF antibody (1:600 dilution, 25699-1-AP, Proteintech), and mouse anti-*β*-actin antibody (1:20,000 dilution, 66009-1-Ig, Proteintech). PVDF membranes were washed with TBST buffer three times and then incubated with secondary antibodies for 1 h at room temperature on the next day. The bands on PVDF membranes were visualized in a chemiluminescence machine (Bio-Rad, United States) using an enhanced chemiluminescence kit (Solarbio, China). The relative density of the protein images was analyzed using ImageJ software.

Reverse transcription polymerase chain reaction

The total RNA of hippocampi was collected with Trizol reagent (Sigma-Aldrich) according to the operation instructions. The reverse transcription of the total RNA was completed by using the HiScript II Q RT SuperMix for the qPCR kit (Vazyme Biotech, China). The synthesized cDNA templates were used to do quantitative PCR by using SYBR Green PCR reagents (Bio-Rad). The ΔΔCt (the threshold cycle) values were calculated, and the results were expressed as the ratio of the mRNA copies of the TREM2, DAP12, and BDNF genes to that of the *β*-actin genes (reference gene). All data was presented in the fold change compared to the control group.

The primers involved in our study were shown as follows: 5′-ACTGGCTTGGTCATCTCTTTTCT-3′ (forward) and 5′-GTG TTGAGGGCTTGGGACA-3′ (reverse) for TREM2; 5′-CCTCCTG GTGCCTTCTGTTC-3′ (forward) and 5′-AGTCGCATCTTGGGA AAGTGT-3′ (reverse) for DAP12; 5′-TATTAGCGAGTGGGTC ACAGC-3′ (forward) and 5′-ATTGCGAGTTCCAGTGCCTT-3′ (reverse) for BDNF; 5′-GGCTGTATTCCCCTCCATCG-3′ (forward) and 5′-CCAGTTGGTAACAATGCCATGT-3′ (reverse) for β-actin.

Statistical analyses

The sample size was based on previous pilot studies and literature. All data were shown as the mean and standard deviation (mean ± SD). Statistical evaluation of the data was performed by one-way analysis of variance (ANOVA), followed by Tukey multiple-comparison *post hoc* analysis. Statistical significance was defined as $p < 0.05$. All statistical graphs were performed with Graph Pad Prism (Graph Pad Software 6.0, San Diego, CA, United States).

Results

EE protected against neurological dysfunctions induced by ischemic stroke in mice

To determine the neuroprotective effects of EE *in vivo*, the rota-rod test and mNSS were applied to evaluate the neurological functions of mice after PT stroke. On days 3 and 4 after ischemic stroke, the latency to fall was calculated 8 times from 4 consecutive measurements with an interval

of 1 h a day. As presented in Figure 2A, mice in all PT groups maintained their balance on the rota-rod apparatus for a shorter time than the sham groups. Mice in the PT + EE group had longer latency times compared with the PT + SE group. Similarly, mice in the Sham+EE group had longer latency times than mice in the Sham +SE group. In the mNSS test, mice in the PT + SE group showed higher scores when compared with the PT + EE group ($p < 0.05$) and the Sham+SE group ($p < 0.0001$) on day 3 after PT stroke (Figure 2B).

Meanwhile, we performed a whole-brain MRI to detect the ischemic foci on day 3 after the ischemic stroke. The T2-weighted images characterized by increased signal intensity compared to the surrounding brain tissue could be observed in the PT + SE group and PT + EE group (Figure 2C). In TTC staining, a white area was observed in the PT + SE group and PT + EE group, which represented cerebral infarction (Figure 2D). However, infarct volume had no significant difference between the PT + SE group and PT + EE group according to the TTC staining ($p > 0.05$, Figure 2E). The results indicated that EE ameliorated neurological dysfunctions induced by ischemic brain injury and promoted motor coordination ability in mice without brain damage.

EE improved neurological impairment exacerbated by ischemic stroke after surgical trauma

To investigate the effect of EE on surgery-induced cognitive dysfunctions in mice with ischemic stroke, the Y-maze test was used

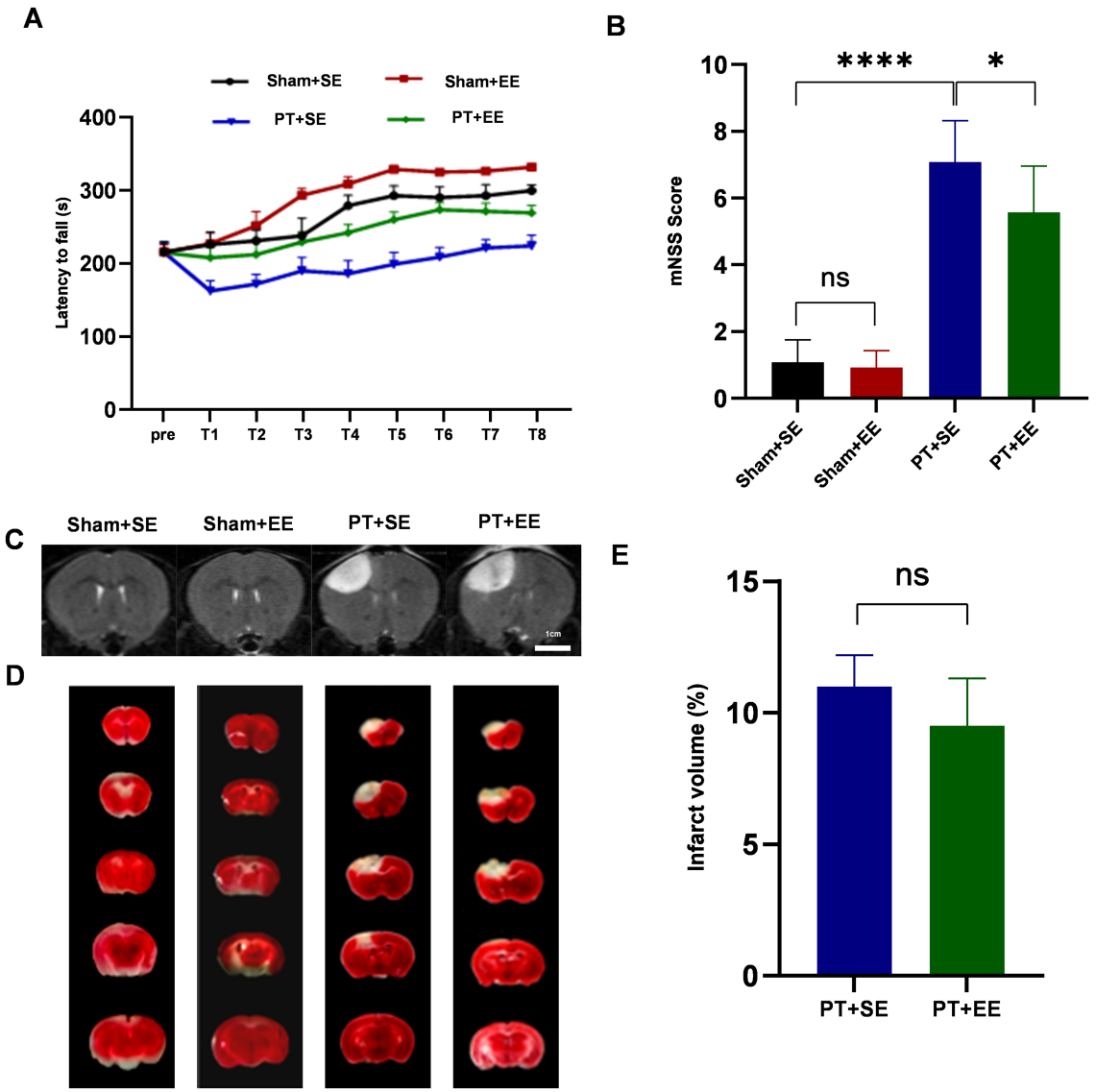

FIGURE 2
EE protects against brain damage after an ischemic stroke. **(A)** The time of latency to fall in the rota-rod test during the 2-day training ($n = 18$). **(B)** The brain damage was evaluated by mNSS scores ($n = 12$). **(C)** The T2-weighted images of whole-brain MRI on day 3 after the PT stroke showed the infarct area (increased signal intensity). **(D)** 2,3,5-Triphenyltetrazolium chloride (TTC) staining of brain slices 3 days after PT stroke showed the infarct area (white). **(E)** The relative proportion and quantification of infarct volume by TTC staining ($n = 3$). ns: no significant, *$p < 0.05$, ***$p < 0.001$, ****$p < 0.0001$. Error bars were represented as mean ± SD.

to assess the memory functions and spatial learning abilities of mice on days 7–10 after left nephrectomy. As shown in Figure 3A, the SAB ratio showed a significant decrease in the PT + SE group when compared to the Sham+SE ($p < 0.05$) group and PT + EE group ($p < 0.05$) before surgery. And surgical trauma enlarged their difference ($p < 0.0001$ for Sham+SE vs. PT + SE, $p < 0.01$ for PT + SE vs. PT + EE, Figure 3B). The decreased SAB ratio was higher in the PT + SE when compared to the Sham+SE group ($p < 0.0001$) and PT + EE ($p < 0.0001$, Figure 3C). These data indicated that surgical trauma exacerbated the existing memory impairment in mice with ischemic stroke, and EE improved their memory functions. Meanwhile, the decreased SAB ratio was lower in the Sham+EE when compared to the Sham+SE group ($p < 0.05$), which indicated that EE was also helpful for improving memory in mice without brain damage. Similar to the memory functions, the Y-maze novel arm test showed the positive effects of EE on the spatial learning abilities of mice with ischemic stroke. As shown in Figure 3D, the novel arm entries showed a significant decrease in the PT + SE group when compared to the Sham+SE ($p < 0.05$) group and PT + EE group ($p < 0.05$) before surgery. And a larger decrease could be observed after surgery ($p < 0.01$ for Sham+SE vs. PT + SE, $p < 0.001$ for PT + SE vs. PT + EE, Figure 3E). The decreased novel arm entries were higher in the PT + SE when compared to the Sham+SE group ($p < 0.05$) and PT + EE ($p < 0.05$, Figure 3F). The above findings indicated that surgical trauma exacerbated cognitive dysfunctions induced by ischemic stroke, while EE played a role in attenuating learning and memory impairment.

To explore whether the hippocampus was involved in regulating cognitive functions, the mice were tested by the contextual test and tone test on days 7–10 after left nephrectomy. In the contextual test, the freezing time was shorter in the PT + SE group when compared with the Sham+SE group ($p < 0.01$ for preoperation, $p < 0.001$ for postoperation) and PT + EE ($p < 0.05$ for preoperation, $p < 0.05$ for postoperation, Figures 3G,H). Figure 3I showed that the PT + SE group exhibited the greatest change ratio in freezing time among all groups. However, there was no significant difference among all groups in the tone-related fear test (Figures 3J–K). It indicated that both the ischemic stroke-induced impairment and surgery-induced impairment were hippocampus-dependent.

EE suppressed neuroinflammation in the hippocampus after surgery

Twenty-four hours after surgery, the expression level of inflammation-associated factors in the hippocampus was significantly higher in the PT + SE group when compared to the Sham+SE group and PT + EE group (IL-1β: $p < 0.001$ for sham+SE *vs.* PT + SE, $p < 0.05$ for PT + SE *vs.* PT + EE; IL-6: $p < 0.01$ for sham+SE *vs.* PT + SE, $p < 0.01$ for PT + SE *vs.* PT + EE; TNF-α: $p < 0.01$ for sham+SE *vs.* PT + SE, $p < 0.001$ for PT + SE *vs.* PT + EE; Figures 4A–C). And compared with the Sham+SE group, the concentrations of IL-6 ($p < 0.001$) and TNF-α ($p < 0.0001$) were significantly decreased in the Sham+EE group (Figures 4A–C). However, opposite changing trends were observed in the expressions of proinflammatory factors, including IL-4 and IL-10 (Figures 4D,E). These results indicated that the development of POCD had a strong correlation with high-grade inflammation in the hippocampus, and EE inhibited the inflammatory reaction to improve neurological dysfunctions induced by cerebral injury and surgery.

EE upregulated the expression of TREM2 after surgical trauma

To explore the effect of EE on the endogenous expression level of TREM2 in the hippocampus, we performed RT-PCR and the western blot analysis on day 10 after surgery. The results of the western blot showed that ischemic stroke downregulated the expression of TREM2 at the protein level in the hippocampus while EE reversed its effect ($p < 0.05$ for Sham+SE *vs.* PT + SE; $p < 0.05$ for Sham+SE *vs.* Sham+EE; $p < 0.01$ for PT + SE *vs.* PT + EE; Figures 5A,B). DAP12, as the obligate adaptor of TREM2, its expression level at the protein level showed a similar trend coinciding with that of TREM2 (Figures 5C,D). Meanwhile, the results of RT-PCR further confirmed the changing trend of TREM2 and DAP12 at the mRNA level (Figures 5E,F).

It is reported that TREM2 is primarily expressed by microglia in the CNS, with expression levels significantly higher than in neurons or other cells (Deczkowska et al., 2020). Therefore, double immunofluorescence staining was performed to determine the cellular localization of TREM2 in the hippocampus of mice in the Sham+EE group on day 10 after surgery.

The results showed that the fluorescence signal of TREM2 was highly colocalized with that of Iba-1 (microglia), whereas no significant overlapping fluorescence signals were observed between TREM2 and GFAP (astrocytes) or between TREM2 and MAP2 (neurons) in the dentate gyrus (DG) (Figures 5G,H). These results indicated that the upregulation of TREM2 on microglia in the hippocampus played an important role in neuroprotection against surgical trauma.

EE activated the PI3K/Akt signaling pathway

To explore the possible mechanism of how EE improved POCD in mice with ischemic stroke, we focused on the PI3K/Akt signaling pathway, which is important in regulating the inflammatory reaction. We observed that after surgery, the p-PI3K / PI3K ratio in the EE groups was significantly higher than that in the SE groups ($p < 0.01$ for sham+SE *vs.* sham+EE; $p < 0.0001$ for PT + SE *vs.* PT + EE; Figures 6A,B). Additionally, the downregulation of the p-PI3K / PI3K ratio was found in the hippocampus of mice with ischemic stroke ($p < 0.05$ for sham+SE *vs.* PT + SE, Figures 6A,B). The same trend was found in the protein p-Akt /Akt ratio, as shown in Figures 6C,D. The above data demonstrated that EE reversed the development of POCD via activating the PI3K/Akt signaling pathway, and ischemic stroke aggravated neurologic impairment by inhibiting the phosphorylation of key proteins.

The knockdown of TREM2 abolished the neuroprotective effects of EE in mice with ischemic stroke

In this study, AAV-TREM2-shRNA was injected in C57BL/6 mice to knock down the expression of TREM2 in the hippocampal tissue.

10.3389/fnins.2024.1520710

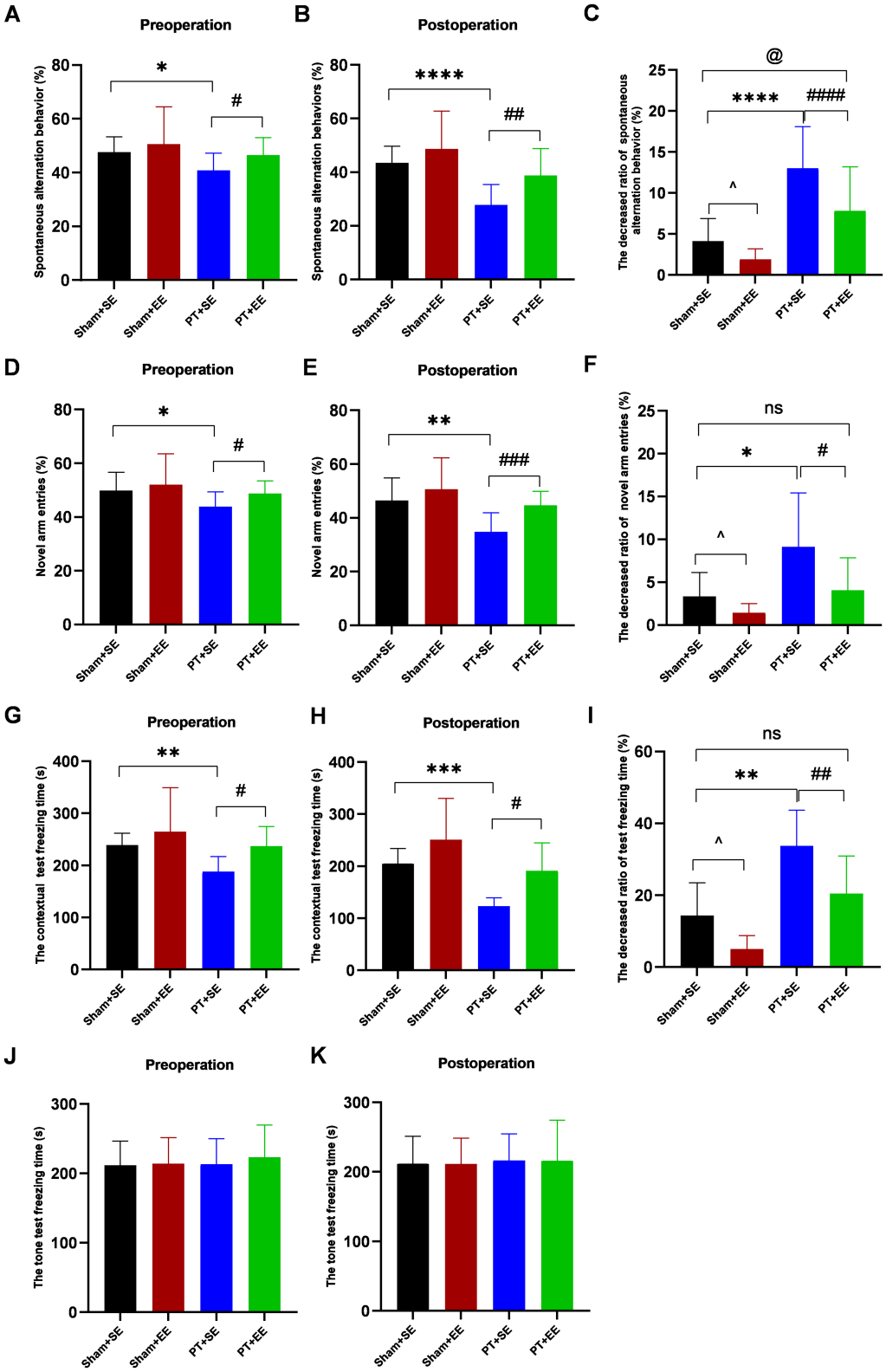

FIGURE 3
The results of behavioral tests before and after surgery in mice with ischemic stroke. **(A–C)** The percentage of spontaneous alteration in the Y maze test (n = 12). **(D–F)** The percentage of novel arm entries in the Y maze test (n = 12). **(G–I)** The freezing time in contextual test (n = 6). **(J–K)** The freezing time in tone test (n = 6). ns: no significant; *p < 0.05, **p < 0.01, ***p < 0.001, ****p < 0.0001, the Sham+SE group vs. the PT + SE group; #p < 0.05, ##p < 0.01, ###p < 0.001, the PT + SE group vs. the PT + EE group; ^p < 0.05, the Sham+SE group vs. the Sham+EE group; @p < 0.05, Sham+SE group vs. the PT + EE group. Error bars were represented as mean ± SD.

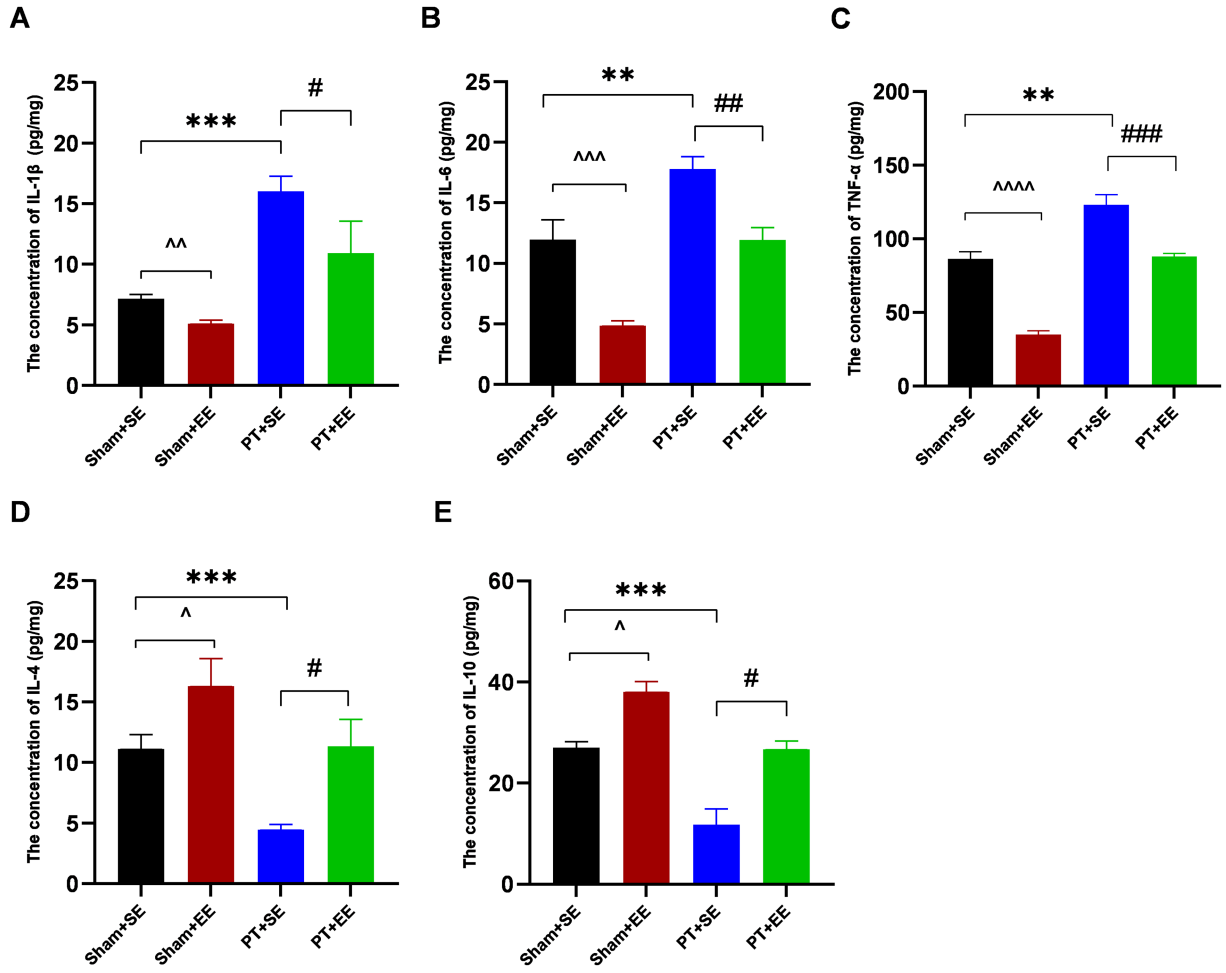

FIGURE 4
The inflammation level in the hippocampus after surgery in mice with ischemic stroke. **(A–E)** The concentrations of inflammation-associated factors in the hippocampus in mice with ischemic stroke at 24 h after surgery (n = 3). $^{**}p < 0.01$, $^{***}p < 0.001$, the Sham+SE group vs. the PT + SE group; $\#p < 0.05$, $\#\#p < 0.01$, $\#\#\#p < 0.001$, the PT + SE group vs. the PT + EE group; $\hat{}p < 0.05$, $\hat{}\hat{}p < 0.01$, $\hat{}\hat{}\hat{}p < 0.001$, $\hat{}\hat{}\hat{}\hat{}p < 0.0001$, the Sham+SE group vs. the Sham+EE group. Error bars were represented as mean ± SD.

To determine the knockdown efficiency of AAV-TREM2-shRNA in each group, the expression of TREM2 in the hippocampal tissue was detected by western blot analysis and RT-PCR on day 21 after the stereotaxic injection of AAV-TREM2-shRNA.

The results of the western blot showed that the expression of TREM2 at the protein level showed a significant decrease in the hippocampus after the administration of TREM2-shRNA ($p < 0.05$ for SE+ vehicle *vs.* SE+ shRNA and $p < 0.01$ for EE+ vehicle *vs.* EE+ shRNA, Figures 7A,B). Moreover, the expression level of the TREM2 protein showed no significant difference between the SE+ shRNA group and the EE+ shRNA group ($p > 0.05$, Figures 7A,B). The same trend was found in the expression level of the DAP12 protein, as Figures 7C,D shows. The results of RT-PCR further confirmed the knockdown of TREM2 at the mRNA level (Figures 7E,F).

The knockdown of TREM2 in the hippocampus induced severe neurological deficits assessed by the Y-maze spontaneous alternation test ($p < 0.05$ for SE+ vehicle *vs.* SE+ shRNA, $p < 0.0001$ for EE+ vehicle *vs.* EE+ shRNA, Figure 8A), Y-maze novel arm test ($p < 0.001$ for SE+ vehicle *vs.* SE+ shRNA, $p < 0.0001$ for EE+ vehicle *vs.* EE+ shRNA, Figure 8B), and contextual test ($p < 0.05$ for SE+ vehicle *vs.* SE+ shRNA, $p < 0.01$ for EE+ vehicle *vs.* EE+ shRNA, Figure 8C). Meanwhile, mice in the SE+ shRNA group had similar performance in behavioral tests compared with mice in the EE + shRNA group ($p > 0.05$, Figures 8A–C). These data indicated that the TREM2-knockdown in the hippocampus abolished the neuroprotective effects of EE after surgery.

The TREM2-knockdown with TREM2-shRNA significantly decreased the phosphorylation level of PI3K and Akt in shRNA groups compared with vehicle groups (p-PI3K/PI3K: $p < 0.05$ for SE+ vehicle *vs.* SE+ shRNA, $p < 0.01$ for EE+ vehicle *vs.* EE+ shRNA; p-AKT/AKT: $p < 0.05$ for SE+ vehicle *vs.* SE+ shRNA, $p < 0.01$ for EE+ vehicle *vs.* EE+ shRNA, Figures 8D–G). Meanwhile, the expression level of p-PI3K and p-AKT showed no difference between the SE+ shRNA group and the EE+ shRNA group ($p > 0.05$, Figures 8D–G). Similar expression levels of IL-1β, IL-6, TNF-α, IL-4, and IL-10 were observed in the two groups ($p > 0.05$, Supplementary Figures S1A–E). According to the above data, it could be speculated that the TREM2-knockdown inhibited the activation of the PI3K/Akt signaling pathway to abolish the neuroinflammation inhibitory effects of EE in the development of POCD.

10.3389/fnins.2024.1520710

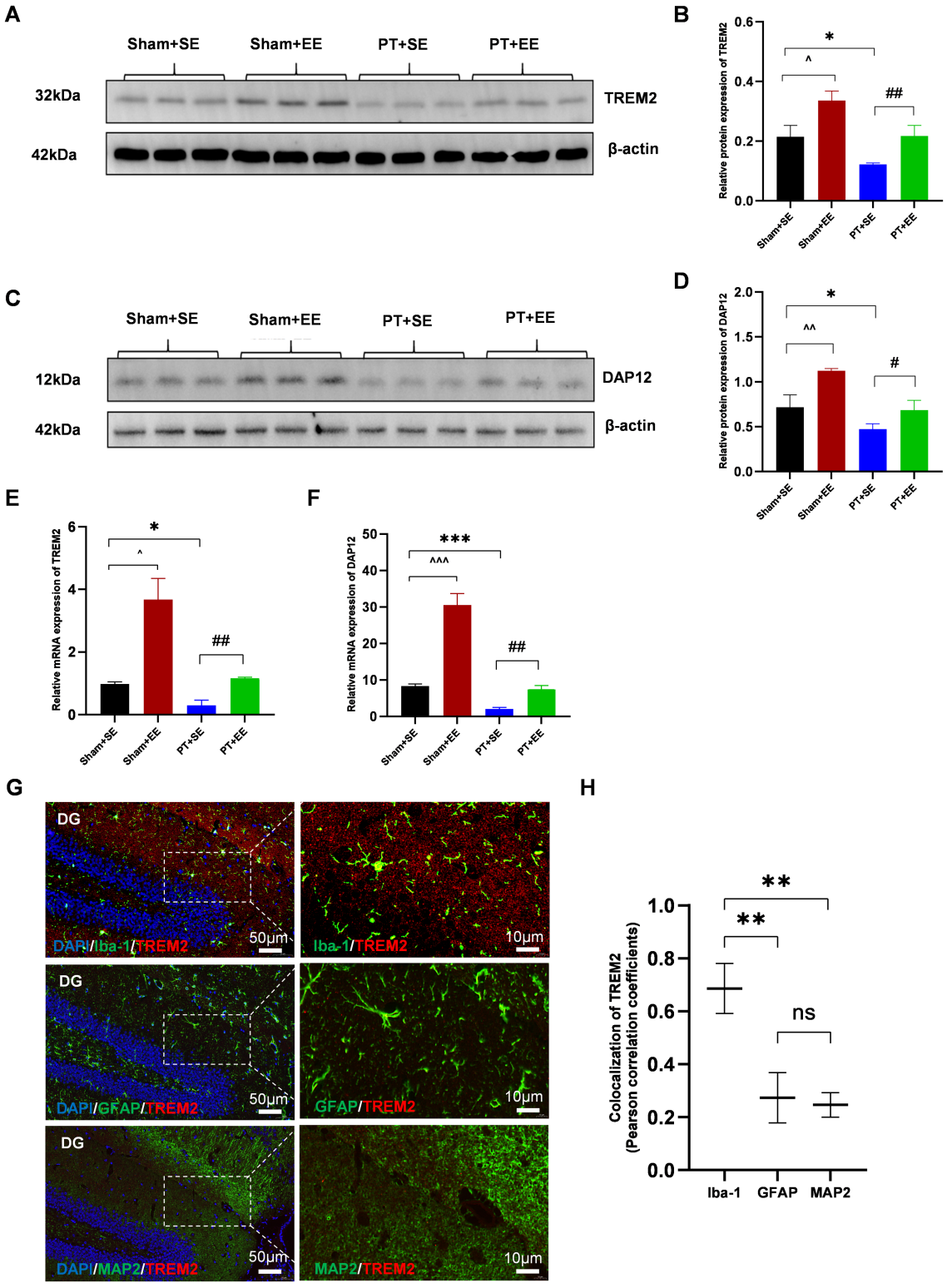

FIGURE 5
EE upregulated the expression of TREM2 in the hippocampus after surgery in mice with ischemic stroke. **(A,B)** The expression of TREM2 protein in the hippocampus on day 10 after surgery (n = 3). **(C,D)** The expression of DAP12 protein in the hippocampus on day 10 after surgery (n = 3). **(E)** The expression of TREM2 mRNA in the hippocampus on day 10 after surgery (n = 3). **(F)** The expression of DAP12 mRNA in the hippocampus on day 10 after surgery (n = 3). **(G)** The immunofluorescence of the cellular localization of TREM2 in the hippocampus of mice in the Sham+EE group on day 10 after surgery (n = 3). DG: dentate gyrus. Scale bars represented 10 μm and 50 μm. ns: no significant; *p < 0.05, ***p < 0.001, the Sham+SE group vs. the PT + SE group; #p < 0.05, ##p < 0.01, the PT + SE group vs. the PT + EE group; ^p < 0.05, ^^^p < 0.001, the Sham+SE group vs. the Sham+EE group. Error bars were represented as mean ± SD.

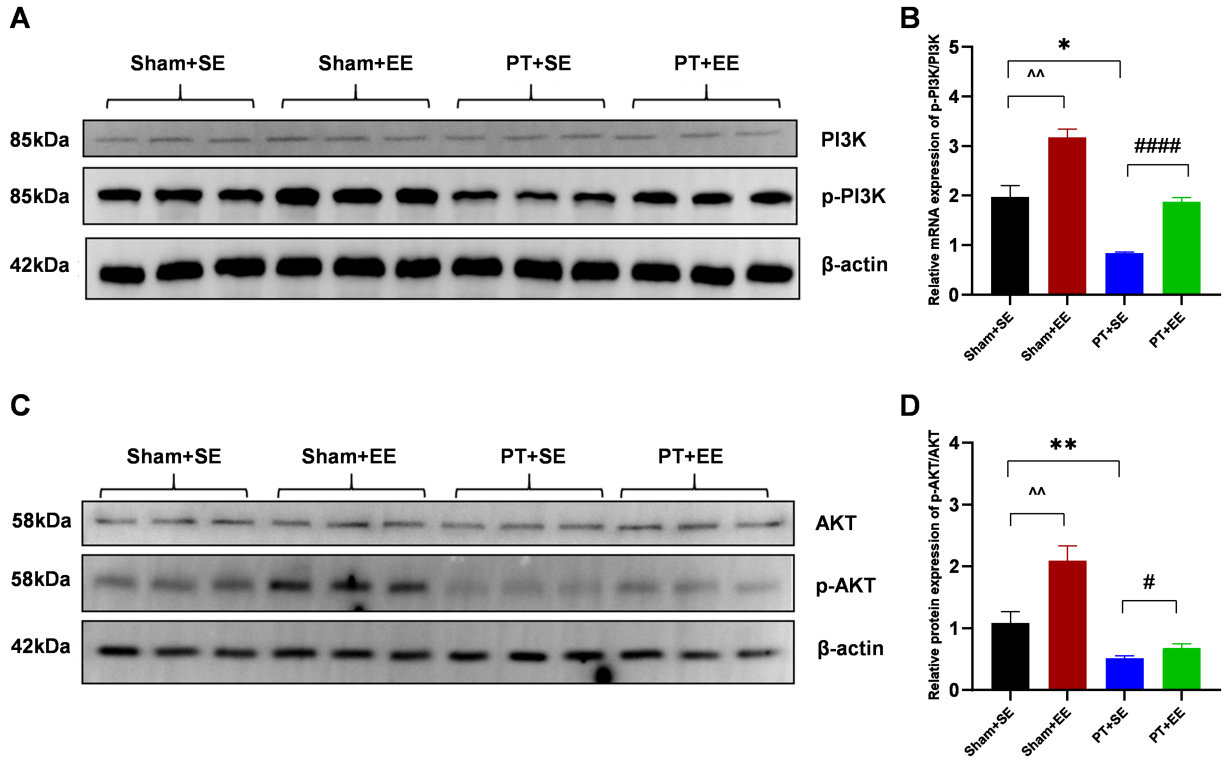

FIGURE 6
EE activated the PI3K/Akt signaling pathway in the hippocampus after surgery in mice with ischemic stroke. **(A)** The results of the western blot of p-PI3K and PI3K. **(B)** The protein p-PI3K / PI3K ratio in the hippocampus on day 10 after surgery (n = 3). **(C)** Western bolt results of p-AKT and AKT. **(D)** The protein p-AKT/ AKT ratio in the hippocampus on day 10 after surgery (n = 3). *p < 0.05, **p < 0.01, the Sham+SE group vs. the PT + SE group; #p < 0.05, ####p < 0.0001, the PT + SE group vs. the PT + EE group; ^^p < 0.01, the Sham+SE group vs. the Sham+EE group. Error bars were represented as mean ± SD.

Discussion

Neuroinflammation plays a significant role in neurodegenerative diseases and has been established as an independent risk factor for the development of POCD (Li et al., 2022; Qin et al., 2022; Yang et al., 2022). In our experiment, the post-surgical assessment of proinflammatory cytokines, including IL-1β, IL-6, and TNF-α in the hippocampal tissue, revealed that the inflammatory response in the CNS of mice with stroke was markedly higher than that in mice undergoing sham operations. During cerebral ischemia, alterations in endothelial shear stress and hemorheological changes due to vascular occlusion rapidly initiate an inflammatory cascade (Jurcau and Simion, 2021). The sustained inflammatory response following an infarct may disrupt the blood–brain barrier's integrity, permitting peripheral inflammatory cells and factors activated by surgical stress to infiltrate the CNS and exacerbate the inflammatory response (Liu et al., 2023). Based on this perspective, interventions that target neuroinflammatory responses, including the direct administration of anti-inflammatory medications, the blockade of inflammatory signaling pathways, and the modulation of microglial activity, have attracted increased attention in the prevention and treatment of POCD (Huang et al., 2020; Li et al., 2020; Cho et al., 2021).

TREM2 is pivotal in modulating immune responses, inflammation, and neuroprotection, positioning it as a promising therapeutic target for neurodegenerative diseases such as Alzheimer's, Parkinson's, and multiple sclerosis (Cignarella et al., 2020; Zhang et al., 2023; Huang et al., 2024). The activation of TREM2 can mitigate inflammatory responses and enhance microglial phagocytosis, thereby ameliorating neurological function and reducing neuroinflammation and neuronal apoptosis (Liu et al., 2022). Our research corroborates these effects, as mice in EE demonstrated superior behavioral performance post-stroke and post-surgical stimulation compared to those in SE, with concurrent elevated TREM2 expression in their hippocampal tissue. The activated PI3K/Akt signaling pathway induced by TREM2 mediates the shift of microglia from the M1 to the M2 phenotype in response to CNS inflammation, thereby improving cognitive impairment (Wang et al., 2020). Our study further identified the activation of the PI3K/Akt signaling pathway, with the expression levels of phosphorylated proteins being positively correlated with TREM2 expression levels. Additionally, the knockdown of endogenous TREM2 by TREM2 shRNA exacerbated neurological deficits and reduced TREM2 expression in ischemic stroke mice. Moreover, TREM2 knockdown reversed the beneficial effects of EE on the expression of proinflammatory factors and key proteins within the PI3K/Akt signaling pathway. Ultimately, our findings suggest that TREM2 activation induced by EE mitigated neuroinflammation and POCD in ischemic stroke mice, an effect that was, at least in part, mediated by the activation of the PI3K/Akt signaling pathway.

Microglia are essential in hippocampal neuroinflammation following aseptic trauma, where they influence cognitive function by

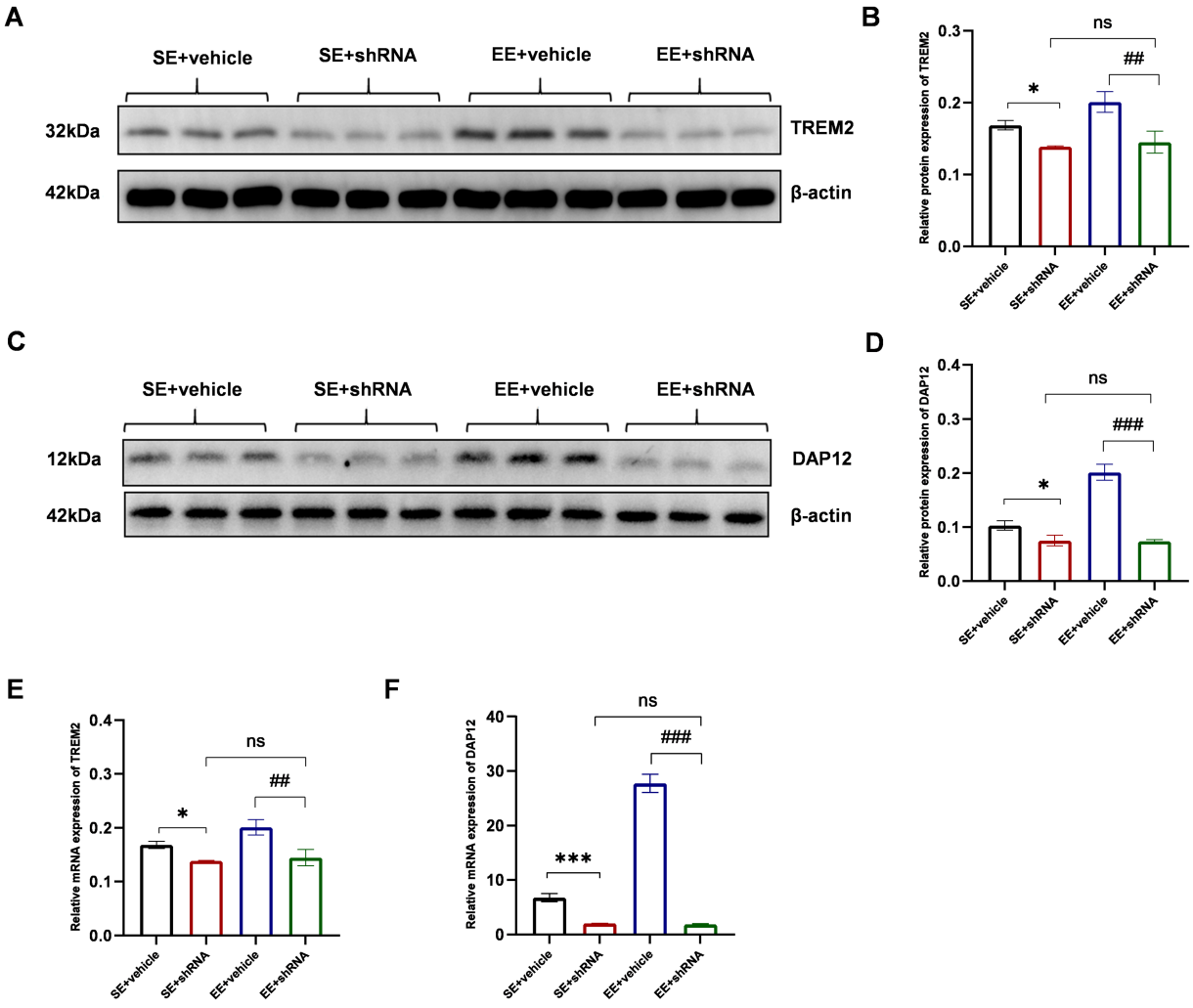

FIGURE 7
TREM2 shRNA successfully decreased the expression of TREM2 in the hippocampus on day 21 after the injection of TREM2 shRNA. **(A,B)** The expression of TREM2 protein in the hippocampus (n = 3). **(C,D)** The expression of DAP12 protein in the hippocampus (n = 3). **(E)** The expression of TREM2 mRNA in the hippocampus (n = 3). **(F)** The expression of DAP12 mRNA in the hippocampus. ns: no significant; *p < 0.05, ***p < 0.001, the SE + vehicle group vs. the SE + shRNA group; ##p < 0.01, ###p < 0.001, the EE+ vehicle group vs. the EE+ shRNA group. Error bars were represented as mean ± SD.

modulating neural activity and synaptic plasticity through the release of various cytokines (Feng et al., 2017; Lecca et al., 2022). It was reported that TREM2 was expressed not only on microglia but also on astrocytes and neurons in a mouse model of intracerebral hemorrhage (Chen et al., 2020). DG is an important site for neurogenesis and plays a significant role in the function of the hippocampus, particularly in the formation of memory and spatial navigation (Anacker et al., 2018; Li et al., 2023). Consequently, it is an important research subject in the study of cognitive disorders (Le et al., 2014; Kong et al., 2024). However, our results showed that the colocalization correlation of TREM2 on astrocytes and neurons was not significant in DG, possibly due to distinct pathological changes between hemorrhagic and ischemic conditions.

TREM2 agonists and inhibitors of the PI3K/AKT signaling pathway are being explored as potential therapeutic strategies for neurological disorders (Zhang et al., 2019; Rodriguez et al., 2020; Singh et al., 2024). However, the clinical application of these drugs faces several challenges, including the need for precise molecular targeting, effective drug delivery systems, and the minimization of potential side effects. In our study, we selected EE as a non-pharmacological TREM2 agonist, with the goal of mitigating POCD by exposing mice with ischemic stroke to enriched environmental stimuli during the perioperative period. Our results align with previous studies in this regard (Yang et al., 2021). Cognitive neuroscience research suggests that cognitive processes can influence neural structures and functions. An enriched environment offers additional stimuli that promote neuronal growth and development. Concurrently, the brain's adaptive capacity works to counteract increasing damage through the dynamics of neural networks (Gabriel et al., 2020; Yu and Wei, 2021; Di Castro et al., 2022).

Several limitations need to be mentioned in this study. Firstly, our assessment was confined to short-term neurofunctional outcomes in mice, necessitating further research to elucidate the

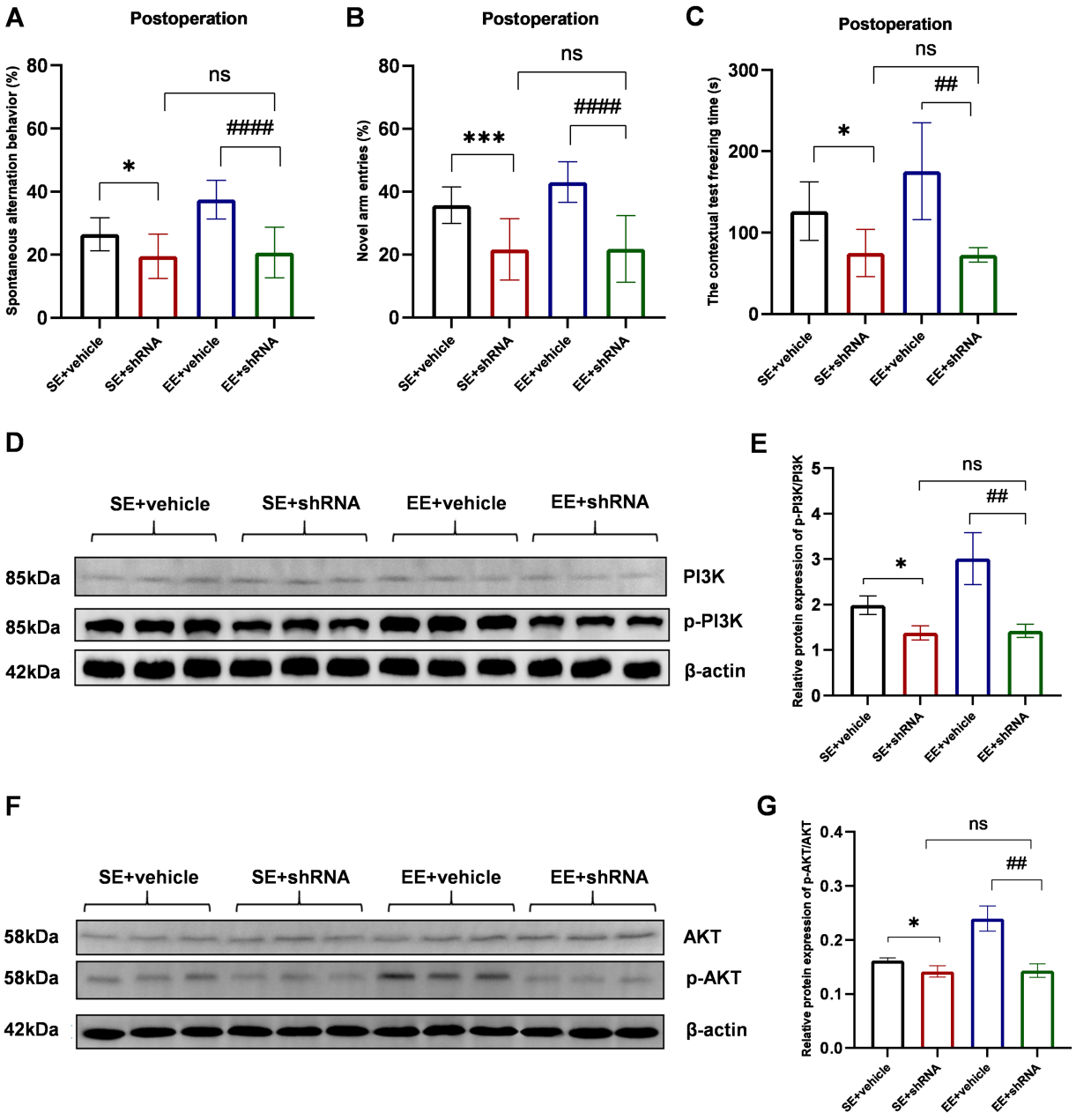

FIGURE 8
The knockdown of TREM2 abolished the neuroprotective effects of EE and inhibited the PI3K/Akt signaling pathway in the hippocampus of mice with ischemic stroke after surgery. **(A–C)** The behavioral tests of each group (n = 6). **(D)** Western bolt results of p-PI3K and PI3K. **(E)** The protein p-PI3K / PI3K ratio in the hippocampus on day 10 after surgery (n = 3). **(F)** Western bolt results of p-AKT and AKT. **(G)** The protein p-AKT/AKT ratio in the hippocampus on day 10 after surgery (n = 3). ns: no significant; *p < 0.05, ***p < 0.001, the SE + vehicle group vs. the SE + shRNA group; ##p < 0.01, ####p < 0.0001, the EE+ vehicle group vs. the EE+ shRNA group. Error bars were represented as mean ± SD.

long-term therapeutic effects of EE. Secondly, given that TREM2 expression was diminished by chronic ischemic stroke, it is imperative to investigate how acute ischemic stroke impacts TREM2 levels. Additionally, the activation and polarization state of microglia are pivotal in the progression of neural damage following ischemic stroke (Jiang et al., 2020). Our study did not focus on the differentiation of microglial subtypes; hence, relying solely on inflammatory cytokine results might not provide an accurate depiction of inflammation levels.

In this study, we initially established an ischemic stroke model by PT stroke to investigate the impact of EE on POCD. Our focus was on the potential neuroprotective role of TREM2 and its relationship with the PI3K/Akt signaling pathway. We observed that ischemic stroke resulted in neurological functional impairment, which was exacerbated by surgical trauma. However, exposure to EE could ameliorate these neurofunctional deficits. The improvement in neurofunctional impairment was associated with a reduction in inflammatory status and an upregulation of

TREM2 in the hippocampus, along with the activation of the PI3K/AKT signaling pathway. We believe that our findings can contribute to the development of a safe perioperative prevention and treatment strategy for improving POCD in patients with stroke. Furthermore, our research may provide valuable insights for future investigations into the mechanisms underlying the combination of stroke and POCD.

Data availability statement

The datasets presented in this study can be found in online repositories. The names of the repository/repositories and accession number(s) can be found in the article/supplementary material.

Ethics statement

The animal study was approved by the Sichuan Provincial People's Hospital Research Ethics Committee. The study was conducted in accordance with the local legislation and institutional requirements.

Author contributions

YY: Conceptualization, Formal analysis, Investigation, Methodology, Writing – original draft. LH: Conceptualization, Methodology, Writing – original draft. DL: Investigation, Visualization, Writing – review & editing. YW: Formal analysis, Investigation, Visualization, Writing – review & editing. JP: Conceptualization, Funding acquisition, Supervision, Writing – review & editing. DF: Conceptualization, Funding acquisition, Project administration, Supervision, Writing – review & editing.

Funding

The author(s) declare that financial support was received for the research, authorship, and/or publication of this article. This study was supported by grants from the Sichuan Science and Technology Support Program (2022YFS0302).

Acknowledgments

We acknowledge the colleagues of Sichuan Provincial People's Hospital, Chengdu, PR China, and the colleagues of West China Hospital of Stomatology, Sichuan University, Chengdu, PR China.

Conflict of interest

The authors declare that the research was conducted in the absence of any commercial or financial relationships that could be construed as a potential conflict of interest.

Generative AI statement

The author(s) declare that no Generative AI was used in the creation of this manuscript.

Publisher's note

All claims expressed in this article are solely those of the authors and do not necessarily represent those of their affiliated organizations, or those of the publisher, the editors and the reviewers. Any product that may be evaluated in this article, or claim that may be made by its manufacturer, is not guaranteed or endorsed by the publisher.

Supplementary material

The Supplementary material for this article can be found online at: https://www.frontiersin.org/articles/10.3389/fnins.2024.1520710/full#supplementary-material

FIGURE S1
The knockdown of TREM2 aggravated neuroinflammation in hippocampus of mice with ischemic stroke after surgery. **(A–E)** The concentrations of inflammation-associated factors in hippocampus at 24 h after surgery (n = 3). ns: no significant; *p < 0.05, ***p < 0.001, the SE+vehicle group vs. the SE +shRNA group; ##p < 0.01, ###p < 0.001, ####p < 0.0001, the EE+ vehicle group vs. the EE+ shRNA group. Error bars were represented as mean ± SD.

References

Alwis, D. S., and Rajan, R. (2014). Environmental enrichment and the sensory brain: the role of enrichment in remediating brain injury. *Front. Syst. Neurosci.* 8:156. doi: 10.3389/fnsys.2014.00156

Anacker, C., Luna, V. M., Stevens, G. S., Millette, A., Shores, R., Jimenez, J. C., et al. (2018). Hippocampal neurogenesis confers stress resilience by inhibiting the ventral dentate gyrus. *Nature* 559, 98–102. doi: 10.1038/s41586-018-0262-4

Borst, K., Dumas, A. A., and Prinz, M. (2021). Microglia: Immune and non-immune functions. *Immunity* 54, 2194–2208. doi: 10.1016/j.immuni.2021.09.014

Cantoni, C., Bollman, B., Licastro, D., Xie, M., Mikesell, R., Schmidt, R., et al. (2015). TREM2 regulates microglial cell activation in response to demyelination *in vivo*. *Acta Neuropathol.* 129, 429–447. doi: 10.1007/s00401-015-1388-1

Chen, K., Li, Y., Zhang, X., Ullah, R., Tong, J., and Shen, Y. (2022). The role of the PI3K/AKT signalling pathway in the corneal epithelium: recent updates. *Cell Death Dis.* 13:513. doi: 10.1038/s41419-022-04963-x

Chen, S., Peng, J., Sherchan, P., Ma, Y., Xiang, S., Yan, F., et al. (2020). TREM2 activation attenuates neuroinflammation and neuronal apoptosis via PI3K/Akt pathway after intracerebral hemorrhage in mice. *J. Neuroinflammation* 17:168. doi: 10.1186/s12974-020-01853-x

Cho, I., Kim, J. M., Kim, E. J., Kim, S. Y., Kam, E. H., Cheong, E., et al. (2021). Orthopedic surgery-induced cognitive dysfunction is mediated by CX3CL1/R1 signaling. *J. Neuroinflammation* 18:93. doi: 10.1186/s12974-021-02150-x

Cignarella, F., Filipello, F., Bollman, B., Cantoni, C., Locca, A., Mikesell, R., et al. (2020). TREM2 activation on microglia promotes myelin debris clearance and remyelination in a model of multiple sclerosis. *Acta Neuropathol.* 140, 513–534. doi: 10.1007/s00401-020-02193-z

Deczkowska, A., Weiner, A., and Amit, I. (2020). The physiology, pathology, and potential therapeutic applications of the TREM2 signaling pathway. *Cell* 181, 1207–1217. doi: 10.1016/j.cell.2020.05.003

Di Castro, M. A., Garofalo, S., De Felice, E., Meneghetti, N., Di Pietro, E., Mormino, A., et al. (2022). Environmental enrichment counteracts the effects of glioma in primary visual cortex. *Neurobiol. Dis.* 174:105894. doi: 10.1016/j.nbd.2022.105894

Fan, D., Li, J., Zheng, B., Hua, L., and Zuo, Z. (2016). Enriched environment attenuates surgery-induced impairment of learning, memory, and neurogenesis possibly by preserving BDNF expression. *Mol. Neurobiol.* 53, 344–354. doi: 10.1007/s12035-014-9013-1

Feng, X., Valdearcos, M., Uchida, Y., Lutrin, D., Maze, M., and Koliwad, S. K. (2017). Microglia mediate postoperative hippocampal inflammation and cognitive decline in mice. *JCI Insight* 2:e91229. doi: 10.1172/jci.insight.91229

Gabriel, P., Mastracchio, T.-A., Bordner, K., and Jeffrey, R. (2020). Impact of enriched environment during adolescence on adult social behavior, hippocampal synaptic density and dopamine D2 receptor expression in rats. *Physiol. Behav.* 226:113133. doi: 10.1016/j.physbeh.2020.113133

GBD 2019 Stroke Collaborators (2021). Global, regional, and national burden of stroke and its risk factors, 1990-2019: a systematic analysis for the global burden of disease study 2019. *Lancet Neurol.* 20, 795–820. doi: 10.1016/S1474-4422(21)00252-0

He, L., Duan, X., Li, S., Zhang, R., Dai, X., and Lu, M. (2024). Unveiling the role of astrocytes in postoperative cognitive dysfunction. *Ageing Res. Rev.* 95:102223. doi: 10.1016/j.arr.2024.102223

He, X.-F., Liu, D.-X., Zhang, Q., Liang, F.-Y., Dai, G.-Y., Zeng, J.-S., et al. (2017). Voluntary exercise promotes Glymphatic clearance of amyloid Beta and Reduces the activation of astrocytes and microglia in aged mice. *Front. Mol. Neurosci.* 10:144. doi: 10.3389/fnmol.2017.00144

Huang, J.-M., Lv, Z.-T., Zhang, B., Jiang, W.-X., and Nie, M.-B. (2020). Intravenous parecoxib for early postoperative cognitive dysfunction in elderly patients: evidence from a meta-analysis. *Expert. Rev. Clin. Pharmacol.* 13, 451–460. doi: 10.1080/17512433.2020.1732815

Huang, P., Zhang, Z., Zhang, P., Feng, J., Xie, J., Zheng, Y., et al. (2024). TREM2 deficiency aggravates NLRP3 Inflammasome activation and Pyroptosis in MPTP-induced Parkinson's disease mice and LPS-induced BV2 cells. *Mol. Neurobiol.* 61, 2590–2605. doi: 10.1007/s12035-023-03713-0

Jiang, C.-T., Wu, W.-F., Deng, Y.-H., and Ge, J.-W. (2020). Modulators of microglia activation and polarization in ischemic stroke (review). *Mol. Med. Rep.* 21, 2006–2018. doi: 10.3892/mmr.2020.11003

Jin, L., Zhu, Z., Hong, L., Qian, Z., Wang, F., and Mao, Z. (2023). ROS-responsive 18β-glycyrrhetic acid-conjugated polymeric nanoparticles mediate neuroprotection in ischemic stroke through HMGB1 inhibition and microglia polarization regulation. *Bioact Mater* 19, 38–49. doi: 10.1016/j.bioactmat.2022.03.040

Jurcau, A., and Simion, A. (2021). Neuroinflammation in cerebral ischemia and ischemia/reperfusion injuries: from pathophysiology to therapeutic strategies. *Int. J. Mol. Sci.* 23:14. doi: 10.3390/ijms23010014

Kong, X., Lyu, W., Lin, X., Lin, C., Feng, H., Xu, L., et al. (2024). Itaconate alleviates anesthesia/surgery-induced cognitive impairment by activating a Nrf2-dependent anti-neuroinflammation and neurogenesis via gut-brain axis. *J. Neuroinflammation* 21:104. doi: 10.1186/s12974-024-03103-w

Labat-gest, V., and Tomasi, S. (2013). Photothrombotic ischemia: a minimally invasive and reproducible photochemical cortical lesion model for mouse stroke studies. *J. Vis. Exp.* 9:50370. doi: 10.3791/50370

le, Y., Liu, S., Peng, M., Tan, C., Liao, Q., Duan, K., et al. (2014). Aging differentially affects the loss of neuronal dendritic spine, neuroinflammation and memory impairment at rats after surgery. *PLoS One* 9:e106837:e106837. doi: 10.1371/journal.pone.0106837

Lecca, D., Jung, Y. J., Scerba, M. T., Hwang, I., Kim, Y. K., Kim, S., et al. (2022). Role of chronic neuroinflammation in neuroplasticity and cognitive function: a hypothesis. *Alzheimers Dement.* 18, 2327–2340. doi: 10.1002/alz.12610

Li, H.-H., Liu, Y., Chen, H.-S., Wang, J., Li, Y.-K., Zhao, Y., et al. (2023). PDGF-BB-dependent neurogenesis buffers depressive-like behaviors by inhibition of GABAergic projection from medial septum to dentate gyrus. *Adv. Sci. (Weinh.)* 10:e2301110. doi: 10.1002/advs.202301110

Li, J., Shi, C., Ding, Z., and Jin, W. (2020). Glycogen synthase kinase 3β promotes postoperative cognitive dysfunction by inducing the M1 polarization and migration of microglia. *Mediat. Inflamm.* 2020, 1–10. doi: 10.1155/2020/7860829

Li, Z., Zhu, Y., Kang, Y., Qin, S., and Chai, J. (2022). Neuroinflammation as the underlying mechanism of postoperative cognitive dysfunction and therapeutic strategies. *Front. Cell. Neurosci.* 16:843069. doi: 10.3389/fncel.2022.843069

Liu, S., Cao, X., Wu, Z., Deng, S., Fu, H., Wang, Y., et al. (2022). TREM2 improves neurological dysfunction and attenuates neuroinflammation, TLR signaling and neuronal apoptosis in the acute phase of intracerebral hemorrhage. *Front. Aging Neurosci.* 14:967825. doi: 10.3389/fnagi.2022.967825

Liu, Y., Yang, W., Xue, J., Chen, J., Liu, S., Zhang, S., et al. (2023). Neuroinflammation: the central enabler of postoperative cognitive dysfunction. *Biomed. Pharmacother.* 167:115582. doi: 10.1016/j.biopha.2023.115582

Messé, S. R., Overbey, J. R., Thourani, V. H., Moskowitz, A. J., Gelijns, A. C., Groh, M. A., et al. (2024). The impact of perioperative stroke and delirium on outcomes after surgical aortic valve replacement. *J. Thorac. Cardiovasc. Surg.* 167, 624–633.e4. doi: 10.1016/j.jtcvs.2022.01.053

Mozaffarian, D., Benjamin, E. J., Go, A. S., Arnett, D. K., Blaha, M. J., Cushman, M., et al. (2015). Heart disease and stroke statistics--2015 update: a report from the American Heart Association. *Circulation* 131, e29–e322. doi: 10.1161/CIR.0000000000000152

NeuroVISION Investigators (2019). Perioperative covert stroke in patients undergoing non-cardiac surgery (NeuroVISION): a prospective cohort study. *Lancet* 394, 1022–1029. doi: 10.1016/S0140-6736(19)31795-7

Paul, N., Raymond, J., Lumbreras, S., Bartsch, D., Weber, T., and Lau, T. (2021). Activation of the glucocorticoid receptor rapidly triggers calcium-dependent serotonin release *in vitro*. *CNS Neurosci. Ther.* 27, 753–764. doi: 10.1111/cns.13634

Qin, C., Yang, S., Chu, Y.-H., Zhang, H., Pang, X.-W., Chen, L., et al. (2022). Signaling pathways involved in ischemic stroke: molecular mechanisms and therapeutic interventions. *Signal Transduct. Target. Ther.* 7:215. doi: 10.1038/s41392-022-01064-1

Rodriguez, A., Von Salzen, D., Holguin, B. A., and Bernal, R. A. (2020). Complex destabilization in the mitochondrial chaperonin Hsp60 leads to disease. *Front. Mol. Biosci.* 7:159. doi: 10.3389/fmolb.2020.00159

Sheu, M.-L., Pan, L.-Y., Yang, C.-N., Sheehan, J., Pan, L.-Y., You, W.-C., et al. (2023). Neuronal death caused by HMGB1-evoked via Inflammasomes from thrombin-activated microglia cells. *Int. J. Mol. Sci.* 24:12664. doi: 10.3390/ijms241612664

Singh, M. K., Shin, Y., Han, S., Ha, J., Tiwari, P. K., Kim, S. S., et al. (2024). Molecular chaperonin HSP60: current understanding and future prospects. *Int. J. Mol. Sci.* 25:5483. doi: 10.3390/ijms25105483

Thiel, A., Radlinska, B. A., Paquette, C., Sidel, M., Soucy, J.-P., Schirrmacher, R., et al. (2010). The temporal dynamics of poststroke neuroinflammation: a longitudinal diffusion tensor imaging-guided PET study with 11C-PK11195 in acute subcortical stroke. *J. Nucl. Med.* 51, 1404–1412. doi: 10.2967/jnumed.110.076612

Vasconcelos de Matos, L., Volovat, S., Debiasi, M., and Cardoso, F. (2023). Unfolding the role of the PI3K/AKT/MTOR pathway in male breast cancer: a pragmatic appraisal. *Breast* 72:103576. doi: 10.1016/j.breast.2023.103576

Wang, Y., Cella, M., Mallinson, K., Ulrich, J. D., Young, K. L., Robinette, M. L., et al. (2015). TREM2 lipid sensing sustains the microglial response in an Alzheimer's disease model. *Cell* 160, 1061–1071. doi: 10.1016/j.cell.2015.01.049

Wang, Y., Lin, Y., Wang, L., Zhan, H., Luo, X., Zeng, Y., et al. (2020). TREM2 ameliorates neuroinflammatory response and cognitive impairment via PI3K/AKT/FoxO3a signaling pathway in Alzheimer's disease mice. *Aging (Albany NY)* 12, 20862–20879. doi: 10.18632/aging.104104

Wang, S., Sudan, R., Peng, V., Zhou, Y., du, S., Yuede, C. M., et al. (2022). TREM2 drives microglia response to amyloid-β via SYK-dependent and -independent pathways. *Cell* 185, 4153–4169.e19. doi: 10.1016/j.cell.2022.09.033

Yang, Y., Liu, Y., Zhu, J., Song, S., Huang, Y., Zhang, W., et al. (2022). Neuroinflammation-mediated mitochondrial dysregulation involved in postoperative cognitive dysfunction. *Free Radic. Biol. Med.* 178, 134–146. doi: 10.1016/j.freeradbiomed.2021.12.004

Yang, S., Zhang, S., Tang, W., Fang, S., Zhang, H., Zheng, J., et al. (2021). Enriched environment prevents surgery-induced persistent neural inhibition and cognitive dysfunction. *Front. Aging Neurosci.* 13:744719. doi: 10.3389/fnagi.2021.744719

Yu, S., and Wei, M. (2021). The influences of community-enriched environment on the cognitive trajectories of elderly people. *Int. J. Environ. Res. Public Health* 18:8866. doi: 10.3390/ijerph18168866

Zhang, Z., Li, X., Li, F., and An, L. (2016). Berberine alleviates postoperative cognitive dysfunction by suppressing neuroinflammation in aged mice. *Int. Immunopharmacol.* 38, 426–433. doi: 10.1016/j.intimp.2016.06.031

Zhang, X., Tang, L., Yang, J., Meng, L., Chen, J., Zhou, L., et al. (2023). Soluble TREM2 ameliorates tau phosphorylation and cognitive deficits through activating transgelin-2 in Alzheimer's disease. *Nat. Commun.* 14:6670. doi: 10.1038/s41467-023-42505-x

Zhang, K., Wang, H., Xu, M., Frank, J. A., and Luo, J. (2018). Role of MCP-1 and CCR2 in ethanol-induced neuroinflammation and neurodegeneration in the developing brain. *J. Neuroinflammation* 15:197. doi: 10.1186/s12974-018-1241-2

Zhang, Y., Yan, H., Xu, Z., Yang, B., Luo, P., and He, Q. (2019). Molecular basis for class side effects associated with PI3K/AKT/mTOR pathway inhibitors. *Expert Opin. Drug Metab. Toxicol.* 15, 767–774. doi: 10.1080/17425255.2019.1663169

Frontiers in Neuroscience

Provides a holistic understanding of brain function from genes to behavior

Part of the most cited neuroscience journal series which explores the brain - from the new eras of causation and anatomical neurosciences to neuroeconomics and neuroenergetics.

Discover the latest Research Topics

See more →

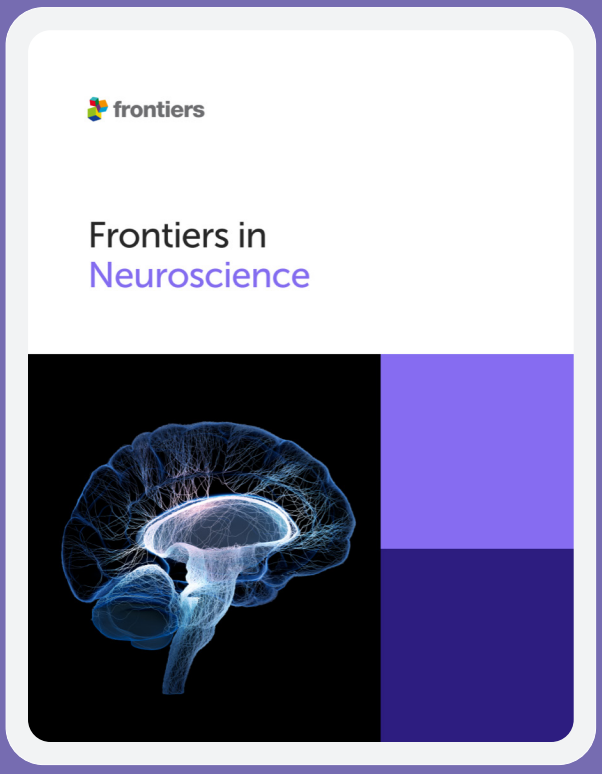

Frontiers

Avenue du Tribunal-Fédéral 34
1005 Lausanne, Switzerland
frontiersin.org

Contact us

+41 (0)21 510 17 00
frontiersin.org/about/contact